Models of Generalization in Motor Control

by

Yoky Matsuoka

B.S., University of California, Berkeley (1993)
S.M., Massachusetts Institute of Technology (1995)

Submitted to the Department of Electrical Engineering and Computer Science
in partial fulfillment of the requirements for the degree of

Doctor of Philosophy
in Artificial Intelligence and Computational Neuroscience

at the

MASSACHUSETTS INSTITUTE OF TECHNOLOGY

September 1998

Signature of Author ....
Department of Electrical Engineering and
Computer Science
July 21, 1998

Certified by ....
Emilio Bizzi
Professor, Department of Brain and Cognitive Sciences
Thesis Supervisor

Certified by ....
Rodney Brooks
Professor, Department of Electrical Engineering and Computer Science
Thesis Supervisor

Accepted by ....
A. C. Smith
Chairman, Departmental Committee on Graduate Students

Models of Generalization in Motor Control

by

Yoky Matsuoka

Revised version of a thesis submitted to the
Department of Electrical Engineering and
Computer Science
on July 21, 1998, in partial fulfillment of the
requirements for the degree of
Doctor of Philosophy
in Artificial Intelligence and Computational Neuroscience

Abstract

Motor learning for humans is based on the capacity of the central nervous system (CNS) to perform computation and build an internal model for a task.

This thesis investigates the CNS's ability to generalize a learned motor skill throughout neighboring spatial locations, its ability to divide the spatial generalization with variation of context, and proposes models of how these generalizations might be implemented.

The investigation involved human psychophysics and simulations. The experimental paradigm was to study human neuromuscular adaptation to viscous force perturbation. When external perturbations were applied to the hand during a reaching task, the movement became distorted. This distortion motivated the CNS to produce counterbalancing forces, which resulted in the modification of the internal model for the task.

Experimental results indicated that the introduction of interfering perturbations near the trained location disturbed the learned skill. In addition, if the same movement was perturbed in two opposite directions in sequence, neither of the forces are learned.

Conversely, the adaptation to two opposite forces was possible within the same space when the forces were applied to two contextually distinguished movements. This was possible only when these movements were interleaved fairly regularly.

During the adaptation to a difficult task, such as contextual distinction in the same spatial location, humans often used other strategies to avoid learning the actual paradigm. These strategies allowed subjects to perform the task without changing their internal models appropriately, and thus this was also investigated as a part of the learning process.

Finally, a multiple function model was constructed which allowed multiple contextually dependent functions to co-exist within one state space. The sensory feedback affected all functions, however, only one function was active to output a motor command. This model supported the experimental data presented.

The results of the psychophysical experiments as well as an explanation of the simulations and models that were developed will be presented in this thesis.

Thesis Supervisor: Emilio Bizzi
Title: Professor, Department of Brain and Cognitive Sciences

Thesis Supervisor: Rodney Brooks
Title: Professor, Department of Electrical Engineering and Computer Science

Acknowledgments

First of all, I would like to thank my advisors, Emilio Bizzi and Rodney Brooks. Emilio taught me not only the approach to science but the patience it requires. In addition, Rod gave me the support I needed for every step of the way. Thank you so much for believing in me. I could not have made it without either of them.

Eric Grimson's guidance throughout the graduate career allowed much flexibility: working full time for a company, switching the field, and finishing quickly.

Gill Pratt somehow got unlucky and was assigned as my committee for all the quals. He has stood by me and gave me unique advice which nobody else could.

Francesca Gandolfo initiated me in psychophysical experiments.
Emo Todorov gave me much advice and ideas in experiments.
Javid Sadr actually read the entire thesis in a rough form.

I also would like to thank the rest of Bizzi Lab especially: James for being distracting, Andrea for being intense, and Brian for balancing everything out.

I cannot thank enough for Barrett Technology's immense support and understanding. Especially, Bill Townsend let me go back to school and finish my degree by putting himself second. Thank you, Bill.

In addition, there were many people who stood by me: Cathy was there to listen when I was at the lowest; Art was more helpful about everything and anything than any friend I have had; And Glen slowed me down to experience life again.

Last but not least, I would like to thank Okasama and Otosama for always being there for me for all these years.

Contents

List of Figures

List of Tables

Chapter 1

Introduction

Human motor production has been analyzed and modeled for many years [Woodworth, 1899, Bernstein,1967, Adams, 1971, Schmidt, 1975]. Various insightful models have been hypothesized [Flash and Hogan, 1985, Bizzi, et al., 1991, Mazzoni, et al., 1991, Kawato and Gomi, 1992, Contreras-Vidal, et al., 1997], but the depth of our biologically derived control of movement is still not well captured. As a consequence, non-biologically driven strategies have been implemented in robots designed to perform movements in specific environments. With these strategies, robots' performance can be far more accurate, faster, and repeatable than humans' capabilities. However, the development of a general purpose robot is still at a very primitive stage [Brooks and Stein, 1994].

In order to enhance the usability of automated systems and to build a general purpose robot, they must be designed to be more versatile. Humans are capable of generalizing movements. When one specific movement execution is learned, the acquired information transfers to movements that are similar to the one trained. Due to this generalization phenomenon, repeated movements do not have to be performed exactly the same, allowing the freedom to execute movements with versatility. Thus, it is crucial to understand biological systems which can learn and execute a great variety of movements in order to allow the implementation of a highly versatile artificial system.

In this thesis, I investigate the properties of human movement generalization, and a model for it is proposed. Movements are shown to be generalized within the space where they are executed [Shadmehr and Mussa-Ivaldi, 1994b, Gandolfo, 1996]. Furthermore, with specific contextual training, multiple generalization modules can be introduced within one spatial coordinate system.

1.1 Motor Control and Adaptation

Due to our complex and redundant musculo-skeletal system, investigating motor control and learning become mathematically unmanageable if every potential degree of freedom was considered. In order to model the behavior, the majority of motor learning studies are conducted by observing arm movements in a planar workspace and by assuming the arm to have only two degrees of freedom. This simplification allows one to concentrate more on the complexity of the behavior without losing the core components of the investigation.

Humans are constantly adapting to the interacting environment. In order to quantify learning, Held [1962] coined the word "aftereffect" signifying the effect observed when a learned perturbation was removed. For example, the authors had subjects wear prism eye glasses and asked them to point to a target. Initially subjects pointed in the wrong direction, but with training, they learned to point toward the perceived object direction. When the prisms were removed, subjects pointed in the opposite direction of the prism distortion. This counter-directional correction is the aftereffect demonstrated in this experiment.

In another experiment, Wolpert, et al. [1995] demonstrated the effects of adaptation to visual perturbations during movements. Human subjects were asked to make a planar reaching movement to a target while being given visual feedback of the hand location. While the target location did not change, the cursor movement was perturbed from the actual hand trajectory to make subjects visually perceive that the movement was curving outward. This indicated that subjects distorted their arm movements to straighten the visual feedback. When the visual perturbation was removed, distorted mirror image movements were observed.

Furthermore, many other investigations suggest that various motor perturbations can be adapted to. Flash and Gurevich [1991] showed that humans can adapt to different loads on their limbs. In addition, it was shown that humans can adapt to differing viscous loads [Shadmehr and Mussa-Ivaldi, 1994b], Coriolis forces [Lackner and Dizio, 1994], and inertial perturbations [Sainburg, et al., 1995] during reaching movements.

The experiments conducted for this thesis specifically addressed the issue of adaptation and generalization. Viscous force perturbation was employed during planar reaching movement, as used for Shadmehr and Mussa-Ivaldi. Viscous perturbation is chosen for its stability at low velocity and its strong resistance to compensation. While it takes time on the order of minutes for viscous perturbations to be learned and compensated for, elastic perturbations would be be learned almost instantaneously in comparison.

1.2 Central Nervous System and its Model

The above experiments were conducted to develop and test hypotheses regarding the motor structure of the central nervous system. The central nervous system has been shown to be subdivided structurally and functionally. This concept has received much attention from neuroscientists earlier in this century. Penfield [1950] stimulated different areas of the brain and discovered that the brain is not a homogeneous structure. While stimulating various sections of the brain, he also identified that the primary somatosensory cortex is topographically organized. This topographic organization is not exclusive to the somatosensory cortex. Jackson [1932] indicated that the primary motor cortex is also topologically organized by observing the seizures and the corresponding stimulated locations.

More recently, the organization of the motor cortex has been investigated at its functional level. Georgopoulos, et al. [1982] indicated that the motor areas of the CNS are organized by direction of motion. They have suggested that cells in the motor cortex have a preferred direction of movement. When monkeys executed a reaching task in a specific direction, for some cells, the firing rate was higher than when the movement was made to other directions. These directions are specified in extrinsic coordinates. In contrast, some researchers debate that the mapping uses multiple coordinates transferring from an extrinsic coordinate representation to an intrinsic coordinate representation [Scott and Kalaska 1995]. Furthermore, there is some evidence indicating that movement dynamics are also encoded by the motor cortex.

System-level models of motor control are often designed from behavior observed during psychophysical experiments. Experiments are conducted in a specific environment and with specific instructions regarding movement execution. In order to execute a movement, a motor command to the muscles must be signaled from the CNS. Thus an inverse model is proposed as a way to calculate a motor command from knowledge of a desired movement. The inverse model requires full knowledge of the kinematics of the limbs, and the calculation is complex. Some researchers have proposed that the inverse model exists in the cerebellum [Kawato and Gomi, 1992].

The inverse model alone cannot explain some of the behavior observed during a movement execution. Movements are observed to contain corrections before sensory information is available. Thus, there must be a system that predicts future sensory feedback information from knowledge of efferent signals. Such a model would be referred to as a forward model [Jordan and Rumelhart, 1992].

When a movement is learned, an internal model of the task is built within the motor system of the CNS [Jordan and Rumelhart, 1991]. In this thesis, such internal model is investigated and modeled. The hypotheses proposed in this thesis do not discuss the actual details of the inverse or forward models. Instead, they assume that there is a mechanism that allows such calculation, and concentrate instead on the adaptation and generalization of motor control.

1.3 Overview of Thesis

In this thesis, experimental results are presented which display evidence of the spatial and contextual generalization of arm movement adaptation. Movements are generalized within the spatial coordinates and tuned within local areas. However, with training, spatial generalization can be further divided by contextual variation.

This thesis is of two parts. Part One discusses the issue of spatial generalization during a reaching task. Past investigations have shown that the human CNS has the ability to generalize a learned motor skill within a restricted region around the location where specific training has been experienced. This part has three chapters.

The first chapter (Chapter 2) discusses the organization of spatial generalization qualitatively and quantitatively. Experiments are conducted to define the spatial primitives for spatial generalization.

The second chapter (Chapter 3) explores spatial generalization within one continuous movement. This analysis is conducted by applying spatially high frequency perturbations. Due to the size of the primitives defined in Chapter 2, if the frequency of the perturbation exceeds the frequency of the primitives, the dynamics of the environment become unlearnable. This limitation of learnability is compared to the limitation of perception. In addition, the limitation enhancement is investigated with an exposure to an easier task a priori. From these experimental results, a simulation of a two link human arm is constructed.

Chapter 4 investigates the temporal processes of learning and unlearning for spatial generalization. In the first half of the chapter, various features are analyzed as a way to quantify adaptation. Using these features, models are constructed for learning and unlearning processes. For example, using the simulation of an arm from Chapter 3, the size of the primitive is investigated for generalization between movements

(Chapter 2).

Part Two of the thesis discusses the issue of context-level generalization. In Part One, I have hypothesized that if two movements are identical directionally and spatially, they are generalized together and cannot be distinguished. This part contains three chapters, first arguing that spatial generalization can be separated, and then exploring the properties of contextual generalization.

Chapter 5 reveals how movements initially generalized spatially can be separated and generalized contextually with training. Experiments are presented to show that such separations are possible by varying components such as location of the targets, velocity of the movement, sequence of the movements, and the amount of a priori knowledge given about the movements.

Chapter 6 explores how these different models are created, modified or selected within one state space. As discussed in Chapter 5, when two interfering environments are presented interleaved, multiple models can be acquired. However, when these environments are introduced separately, without consolidation over time, the internal models for both environments cannot be learned simultaneously due to the interference effect. Therefore, the sequence of exposure to multiple environments is critical. This chapter explores the process of retaining multiple models, and the model is simulated.

Finally, Chapter 7 investigates various strategies used in the learning of context-dependent movements. When the task is particularly challenging, a strategy is often utilized to cope with the environment rather than to actually adapt to the situation. However, such simplifying strategies are utilized frequently, giving subjects the perception of having mastered the task, thus strategies should be considered as a part of the learning process.

All the experiments for this thesis were force-perturbation psychophysical studies, and employed a robot manipulandum. The setup and procedures of the experiments are described in the next section.

1.4 Methods of Psychophysical Experiments

1.4.1 Setup

Subjects were 18 to 38 years old, right-handed, and reported no known neurological disease. Most Subjects were MIT students or staff, and they were paid $10 an hour for their participation. Subjects were asked to sit on a chair in front of a manipulandum,

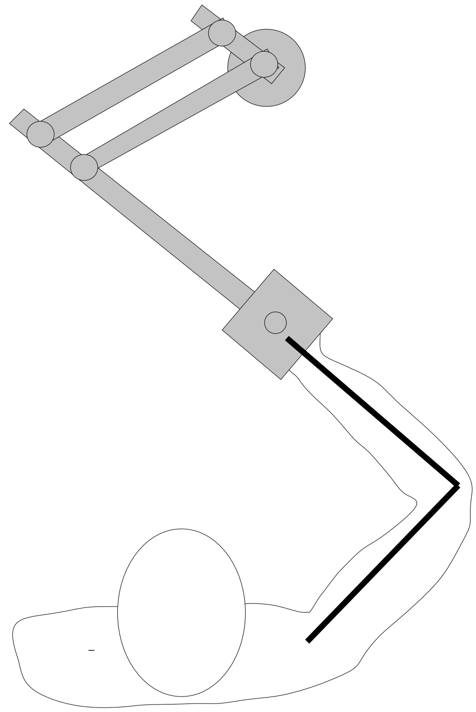

Figure 1-1: The setup of psychophysical experiments. The two jointed robotic arm (manipulandum) is coupled with a human arm operating in a planar workspace. The manipulandum applies the perturbing forces to the subjects' arm.

shown schematically in Figure 1-1. They wore a seat belt to keep their shoulder at a fixed location and wore a sling hanging from the ceiling to keep the arm movement as planar as possible. The manipulandum has two links and operates on a plane parallel to the floor. It has a handle at the end of the arm links, and subjects were asked to hold the handle with their right hand. The link lengths are 35.7 cm and 33.7 cm and their moment of inertia is estimated as 0.0195 and 0.0037 $Kg.m^2$ [Mussa-Ivaldi, et al., 1985]. The joints are operated by JR16M4CH DC torque motor and optical encoders and tachometers are used for sensing and feedback. The robot is controlled by a Gateway 2000 90MHz Pentium computer, and the status of the movement is recorded at 100 Hz. A monitor was set up in front of the subject, displaying targets and a moving cursor corresponding to the subjects' hand position (the handle of the manipulandum).

1.4.2 Procedure

One session of an experiment consisted of a series of reaching tasks executed by one subject. The task was to perform point to point reaching movements. On a given trial, a target appeared on the screen and the subject was asked to make one continuous movement to place the cursor within the target, within a specified interval. The next target appeared after the subject held the cursor at the prior target for one second. This procedure was repeated thereafter. Subjects were given feedback if they moved faster or slower than the allowed time interval, and the optimal timing was pre-specified for each experiment. When they reached the target more than 50 msec faster than the assigned speed, the target turned red, and if the target was reached more than 50 msec slower than the optimal speed, the target turned blue. When the target was reached within the interval of +/- 50 msec of the assigned timing, subjects received a loud quacky sound as the reward. These color assignments allowed subjects to calibrate their speed to the optimal speed and to achieve a consistent speed for all trajectories. Some experiments displayed the total number of targets acquired within the given time to help motivate the subjects to perform well. Various components of the setup were varied for different experiments. The components included the length, direction, speed, and starting position of the movements, target size, and target color.

One epoch of an experiment consisted of 192 reaching movements. A baseline epoch was always conducted first. Forces were not used during the baseline epoch in order to assess the typical performance of each subject. This epoch also allowed the subjects to learn the dynamics of the manipulandum.

Following the baseline epoch, there were force epochs in which the subject performed movements while the torque motors exerted forces on the arm. The perturbations used for the experiments were of a magnitude proportional to the velocity of the hand (i.e. forces were viscous), and the direction of the force was a function of the workspace location. Given the subject's end-point velocity, $\vec{v}$, the manipulandum produces the end point force, $\vec{F}$,

$$\vec{F} = \overline{B}\vec{v}, \tag{1.1}$$

where $\overline{B}$ is a viscosity matrix assigning the angular dependence of the force direction specific to the current hand location. Because no force was applied to the arm unless some motion was detected, subjects could not determine the existence of the force prior to the movement. The force assignments were varied depending on the experiments and they are described within each chapter.

1.4.3 Paradigm

The normal paradigm of the experiments applies viscous force perturbation while subjects made planar reaching movements. During initial exposure, the forces distorted the subjects' movements significantly. However, with practice, the subjects' reaching movements changed back to the non-distorted trajectories, as if they were moving in a null field (without the forces, but holding onto the manipulandum). In order to observe the aftereffects of adaptation to the perturbing forces, the last part of the force epoch usually incorporated interleaved trials with no forces, called catch trials. During catch trials, the hand trajectories were distorted to the mirror image of the movements made when the forces were introduced for the first time. The presence of aftereffects indicates that the internal model for the dynamics system had been changed.

Part I

Spatial Generalization

Overview

While learning a motor skill at a specific region in a workspace the central nervous system generalizes the acquired skill to the areas close to where the training occurred [Shadmehr and Mussa-Ivaldi, 1994b, Gandolfo, et al., 1996]. This restricted spatial generalization is an important ability in order to avoid the need to train for all possible situations, which could take an infinite amount of time. In Part One of this thesis, our unique spatial generalization capability is investigated.

The first chapter (Chapter 2) discusses the organization of spatial generalization qualitatively and quantitatively. Experiments are described to define the spatial primitives for spatial generalization.

The second chapter (Chapter 3) explores spatial generalization within one continuous movement. This analysis is conducted by applying spatially high frequency perturbations. Due to the size of the primitives defined in Chapter 2, if the frequency of the perturbation exceeds the frequency of the primitives, the dynamics of the environment become unlearnable. This limitation of learnability is compared to the limitation of perception. In addition, the enhancement of the limitation is investigated with an exposure to an easier task a priori. From these experimental results, a simulation of a two link human arm is constructed.

The last chapter (Chapter 4) investigates the temporal processes of learning and unlearning for spatial generalization. In the first half of the chapter, various features are analyzed as a way to quantify adaptation. Using these features, models are constructed for learning and unlearning processes. For an example, the size of the primitive is investigated for generalization between movements (Chapter 2) using the simulation of an arm from Chapter 3.

Chapter 2

Spatial Learning Properties

2.1 Introduction

When the control of limb movements is learned, the acquired knowledge about the environment and the intrinsic limb parameters must be encoded in the nervous system. The learned information is not restricted only to the specific movement but is generalized for other movements that are similar. The transfer of learned information is called generalization and it has been shown to be organized spatially [Shadmehr and Mussa-Ivaldi, 1994b]. In addition, it is shown to be restricted within the neighborhood areas of the workspace [Gandolfo, et al., 1996].

This transfer of knowledge to neighboring areas allows the flexibility to achieve the same end position without producing exactly the same movement every time. When a robot receives a command to reach for an object, it makes stereotyped movements. However, if the course of movement is interrupted, the end position is never reached. Inflexibility can be an advantage for repetitive operations, however the robots cannot make versatile movements as humans do without specific programming.

Thus, in this chapter, kinematic perturbation experiments are conducted with human subjects to identify the organization and the characteristics of such spatial generalization.

2.2 Background

Spatial locality has been identified in many adaptation schemes. In visual adaptation, learning to discriminate gratings of different waveforms [Fiorentini and Berardi, 1980] and hyperacuity towards stimuli [Poggio, et al., 1992] are reported to be not only limited to the trained retinal area but also the areas that are spatially close.

This finding of spatial generalization in adaptation is also observed for motor adaptation. During visuo-motor adaptation of reaching movements with prisms, subjects distorted their movement to compensate for the perturbation. This distortion effect was transferred to the locations near where the training took place [Ghahramani, et al., 1996, Roby-Brami and Burnod, 1995]. The spatial decay of adaptation was observed to be smooth.

To investigate the locality of generalization under motor perturbation, Shadmehr and Mussa-Ivaldi introduced force perturbation only in a small region of the workspace [Shadmehr and Mussa-Ivaldi, 1994b]. Their results showed the adaptation to be broadly tuned: i.e. the subjects retained aftereffects matching the perturbation in the neighboring areas. The decay of the effect observed during force perturbation is qualitatively similar to the decay seen for visuo-motor adaptation experiments.

Shadmehr and Mussa-Ivaldi's experiment utilized the manipulandum described in Chapter 1. Subjects held onto the end-effector of the manipulandum, which is a two-link planar robotic arm, while the force perturbations were applied to distort subjects' arm movements. Six directional movements were tested as shown in Figure 2-1. Before the perturbation was applied, the hand trajectories were straight toward the targets (Fig. 2-1.A). When the force field was turned on, the movements were distorted according to the direction of the forces (Fig. 2-1.B). With training, the subjects were able to produce straight movements again (Fig. 2-1.C). When the perturbation was removed, the movements displayed aftereffects (Fig. 2-1.D).

Using the same setup as Shadmehr and Mussa-Ivaldi, Gandolfo tested seven directional movements every 22.5 degrees as shown in Figure 2-2. During training with forces, only the 90 and 45 degree movements were trained (highlighted in Fig. 2-2.A). As shown in Figure 2-2.B, both movements were distorted to the direction of the perturbation. As the previous experiment by Shadmehr and Mussa-Ivaldi, the trajectories became straight again with training (Fig. 2-2.C). At the end of the training, catch trials were conducted to examine the five movements that were not trained under forces. As shown in Figure 2-2.D, the movements that were never trained under the force perturbation exhibited distortions matching the effect of the trained movements. In addition, the aftereffects decayed smoothly with increasing distance from the trained trajectories.

From the experiment, the coordinate system in which the generalization is mapped in the CNS could be hypothesized as extrinsic or intrinsic. If it is encoded in the extrinsic coordinate system, the kinematics of the arm are completely ignored, building the map purely based on the hand position in the workspace. Alternately, if it is encoded in the intrinsic coordinates, the CNS must organize the learned skill with

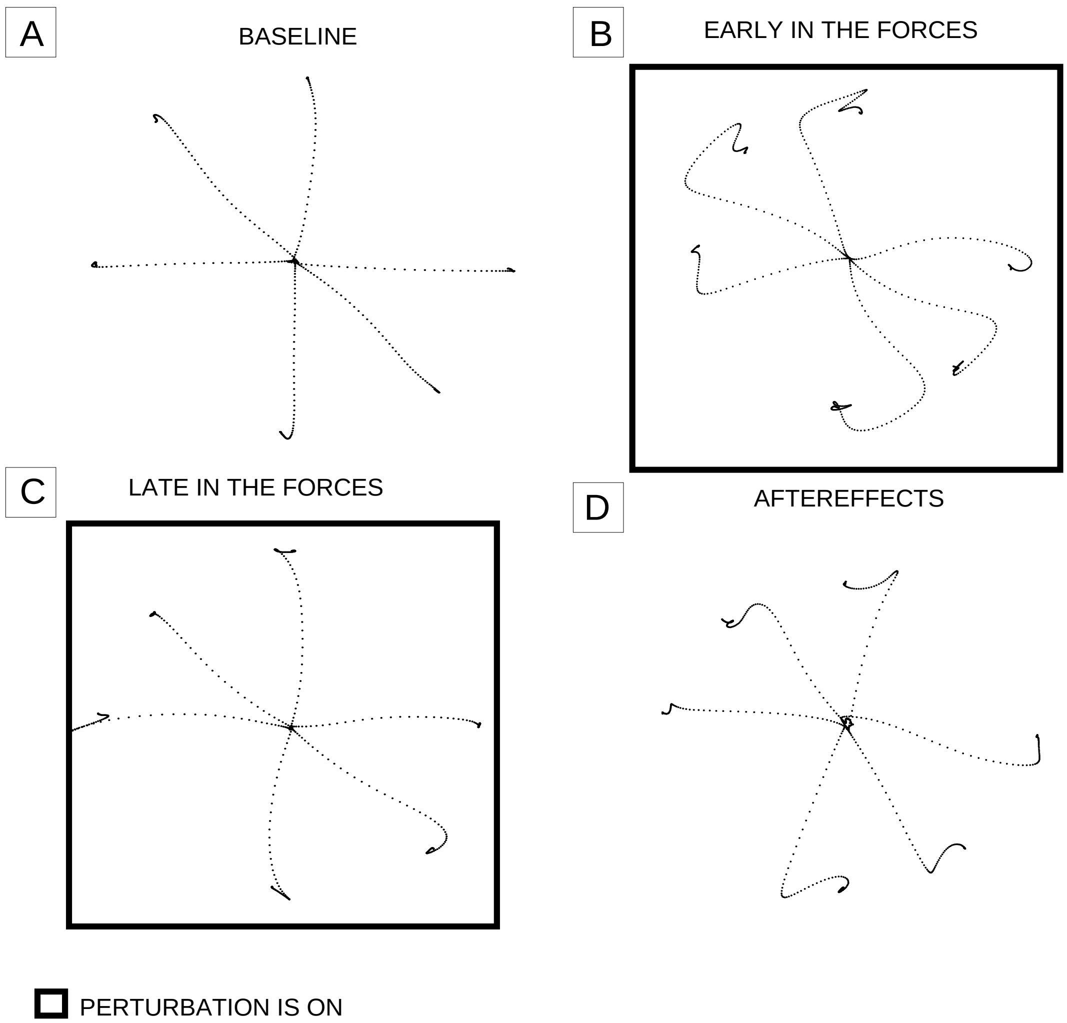

Figure 2-1: From Gandolfo et al. [1996]. Six directional movements were tested with the manipulandum described in Chapter 1. Without any perturbation, the executed movements were normally straight toward the targets (A). The counter clock-wise perturbation was applied during training. When the perturbation was initially applied, the movements were distorted to the direction of the forces (B). However, with training, the subjects were able to produce straight movements again (C). When the forces were removed, the hand trajectories were distorted to the mirror image direction of the forces applied (D).

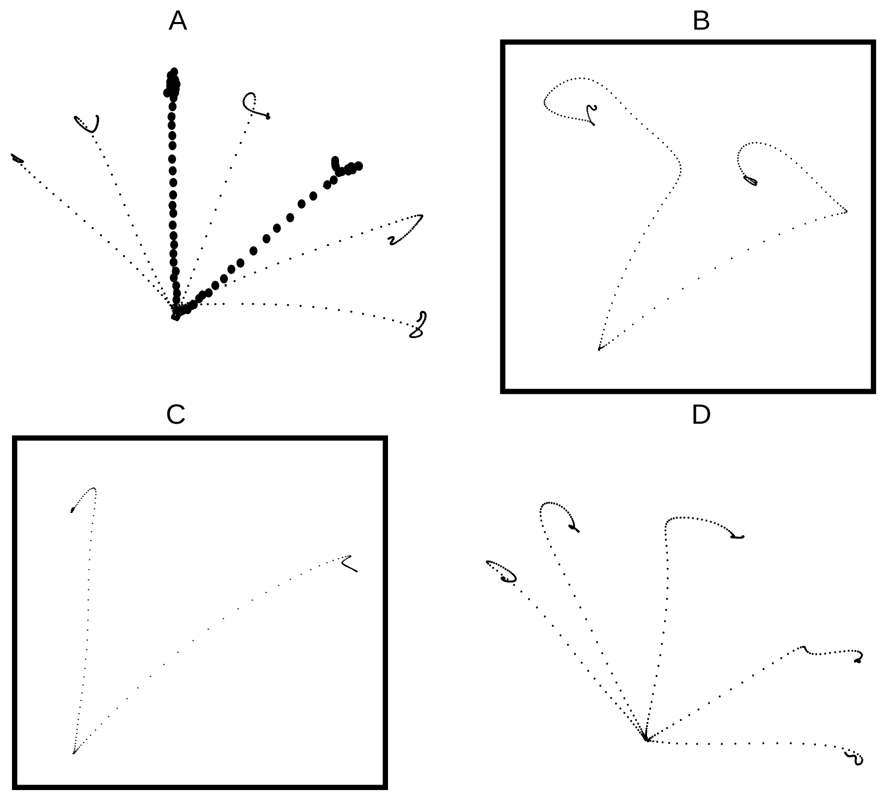

Figure 2-2: From Gandolfo et al. [1996]. A clock wise force field was used as the perturbation. A:baseline trajectories are almost straight. The dark dots show the directional movements that are used for training with force perturbation. B:Trajectories when force perturbation was introduced. C:The same target reaching task as B under perturbation after training. D:Aftereffects of trajectories that were not trained.

the structure of the arm, such as the position, velocity, and the activation levels of the muscles.

To investigate the hypothesis, Gandolfo, et al. [1996] tested two different arm postures while keeping the task identical in extrinsic coordinates. They trained subjects with force perturbation for only one of the postures and observed both postures during catch trials. The results indicated aftereffects for only the posture trained under forces. Even though the other postural movement was identical in extrinsic coordinates, the learned information did not transfer. Thus the mapping must occur in the intrinsic coordinate system.

Gandolfo [1996] simulated the local adaptation effect by setting up an internal model of compensation torque. The learned model was set up in Cartesian coordinates and the effect was eventually generalized in the neighborhood areas in a cosine-like manner as shown in Figure 2-3.

To explain the mechanism of limited spatial generalization, one hypothesis is that such learning is made possible by the modularity of spatial generalization primitives. A primitive can be defined as a spatial bin that has a certain size and shape, and the general shape of one primitive is plotted in Figure 2-4. It is a Gaussian-like shaped learning effect plotted over space.

By definition, one primitive cannot obtain multiple perturbation effects. To identify the size and the shape of one primitive, neighboring primitives can be brought closer as shown in Figure 2-5. This effect can be simulated by applying two opposite forces in the neighboring locations. The distance between them can be changed to test the spatial characteristics of primitives.

2.3 Overview of Experiments

In this chapter, I first identify the existence of such modularity and then investigate the properties of the primitives using interfering forces in neighboring training areas. Tables 2.1 and 2.2 summarize the experiments discussed in this chapter.

All the movements executed were 10 cm long. The target size was 8 x 8 mm and the hand cursor was 2 x 2 mm. Subjects were told to make all movements within a desired time interval of 0.5 +/- 0.05 seconds. One session of training consisted of two to four epochs: one baseline epoch without perturbation and one to three epochs of training with forces. Each epoch consisted of 192 reaching movements or trials, and the last epoch contained catch trials to observe aftereffects.

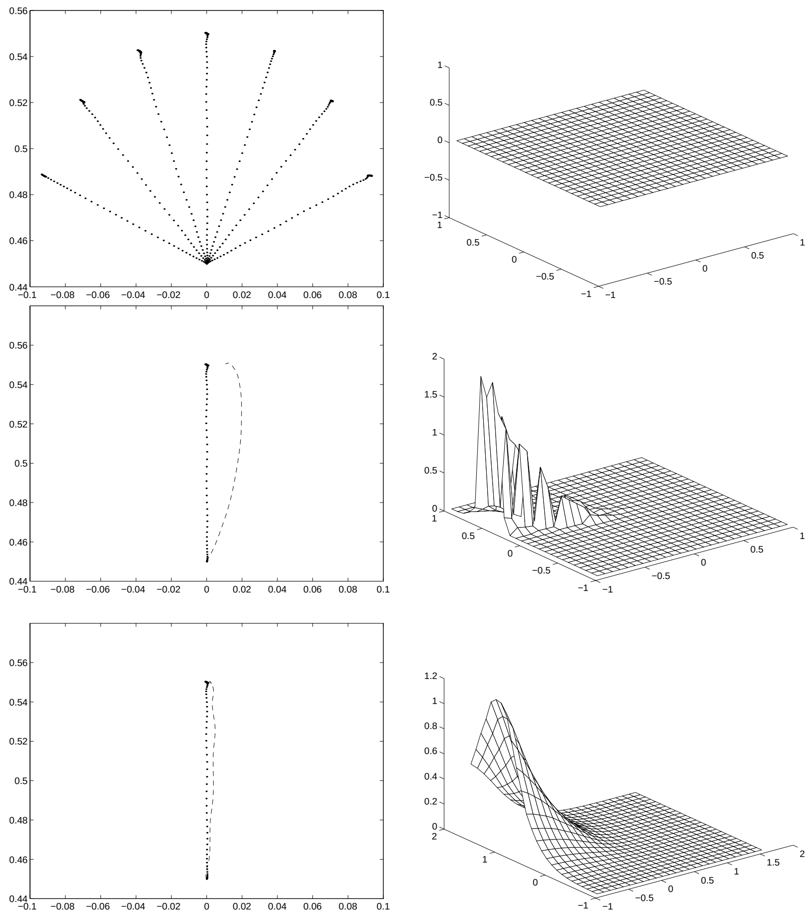

Figure 2-3: From Gandolfo et al [1996]. A model of local adaptation effect by setting up an internal model of compensation torque applied by the subjects. The map of the model is set up in the Cartesian coordinates and the map eventually generalized the effect in the neighborhood areas.

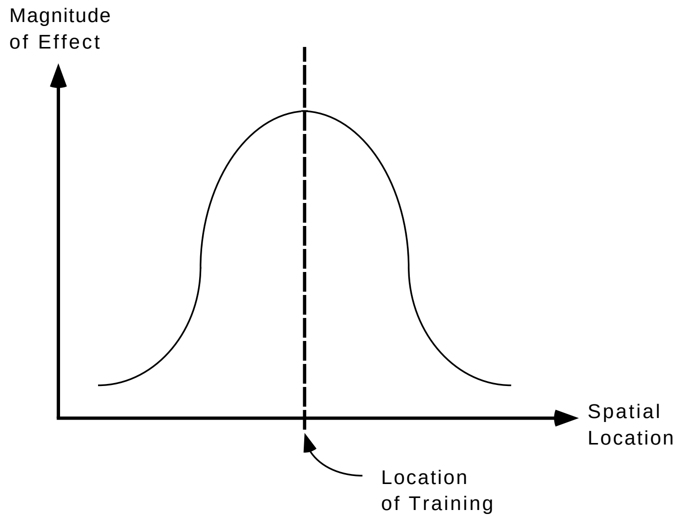

Figure 2-4: A plot of one spatial generalization primitive. A primitive can be defined as a Gaussian-like shaped learned effect plotted over space.

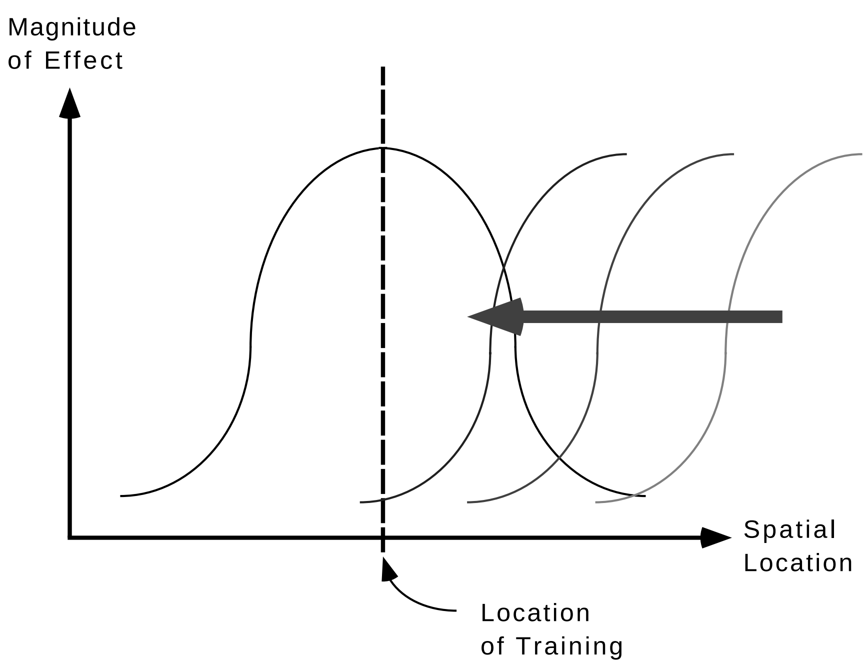

Figure 2-5: An illustration showing how to bring neighboring primitives closer.

Exp.	*#*	*Movement* (*deg*)	(*cm*)	*Perturbation* (*degrees*)	*Investigate:*
DOM	1	90	0	0	Gen. of opposite directional movements at same location.
		-90	v10	no force	
	3	90	0	0	Gen. of same directional movements at different locations.
		90	h10,h20	no training	
DG-A	1	90	0	0	Directional tuning with angle variations.
		45, 135	0	180	
	2	90	0	0	
		67.5, 112.5	0	180	
	3	90	0	0	
		82.5, 97.5	0	180	
DG-SA	1	sequence of exp's 1, 2, and 3. from Exp. DG-A.			Primitive's tuning effect.
	2	sequence of exp's 1, and 2 from Exp. DG-A.			
DG-V	1	90 w/ 5cm vis. channel	0	0	Directional tuning with visual channel.
		0,22.5,45,67.5,112.5	0	no training	
	2	90 w/ 3cm vis. channel	0	0	
		0,22.5,45,67.5,112.5	0	no training	
	3	90 w/ 1cm vis. channel	0	0	
		0,22.5,45,67.5,112.5	0	no training	

Table 2.1: The road map for experiments in Chapter 2. Two numbers in "Movement" column are direction of the movement and the starting point displacement from the first movement listed. For example, if two 90 degree movements are executed 10cm horizontally away from each other, the entries would be: 90, 0; 90, h10. For "Perturbation" column, if the entry is "no training", the movement is not trained during training session, but the movements were included within catch trials to observe the aftereffects. All movements were 10 cm long and the reward was given to the subjects only when the movements were completed within 0.5 +/- 0.05 seconds.

Exp.	#	*Movement* *(deg)*	*(cm)*	*Perturbation* *(degrees)*	*Investigate:*
ST-1	1	90	0	0	Spatial tuning: one dimension.
		90	h10,h20	180	
	2	90	0,h20	0	
		90	h10	180	
	3	90	0	180	
		90	v10	no training	
	4	90	0	180	
		90	v10	0	
ST-2	1	90	0	0	Spatial tuning: two dimensions.
		90	h10,h20,v10,v10h10,v10h20	no training	
	2	90	0,h10,h20,v10h10	0	
		90	v10,v10h20	180	
	3	90	0,h10,h20,v10,v10h20	0	
		90	v10h10	180	

Table 2.2: The continuation of Table 2.1. Two numbers in "Movement" column are direction of the movement and the starting point displacement from the first movement listed. For example, if two 90 degree movements are executed 10cm horizontally away from each other, the entries would be: 90, 0; 90, h10. For "Perturbation" column, if the entry is "no training", the movement is not trained during training session, but the movements were included within catch trials to observe the aftereffects. All movements were 10 cm long and the reward was given to the subjects only when the movements were completed within 0.5 +/- 0.05 seconds.

2.4 Experiment DOM: Domains of Generalization

Before the analysis of the primitives, two simple experiments are introduced to explore the domains of spatial generalization.

Two Movements in the Same Location

There were only two movements trained for this experiment; the 90 and -90 degree reaching movements. These two movements had the same hand path in the space, except that the direction of the movements was opposite. Thus the movements were executed in the same Cartesian spatial location. During the baseline epoch, both movements were practiced, whereas only the 90 degree movements were trained during the force epoch. The -90 degree movements were never trained while the force field was on. If the spatial primitives are indeed organized purely in the workspace coordinates, the learned effect for the 90 degree movements would transfer to the -90 degree movements.

Figure 2-6 illustrates the movements made during the training session. For convenience, the 90 and -90 degree movements are illustrated at the separate locations, but the movements were in fact made at the same spatial location though in opposite directions. During the force epoch, the perturbed movements displayed distortions in the direction of the forces. With training, the distortions diminished over time. During catch trials, the 90 degree movements showed aftereffects in the opposite direction of the forces, whereas the -90 degree movements showed no training effect. Thus movements made in the same spatial location but in the opposite direction were not affected.

This result is consistent with previous results showing that the CNS generalizes movements intrinsically [Gandolfo, et al., 1996]. Even though two movements executed in this experiment are executed in the same workspace, the intrinsic properties of the movements are very different. Therefore, the generalization of movements should not be simulated in the Cartesian coordinate system as suggested previously [Gandolfo, 1996].

Three Movements in the Same Direction

If the direction of the movements are used as the coordinate system of generalization, all movements executed in the same direction would generalize together. An experiment was designed in which subjects executed three 10 cm movements that were

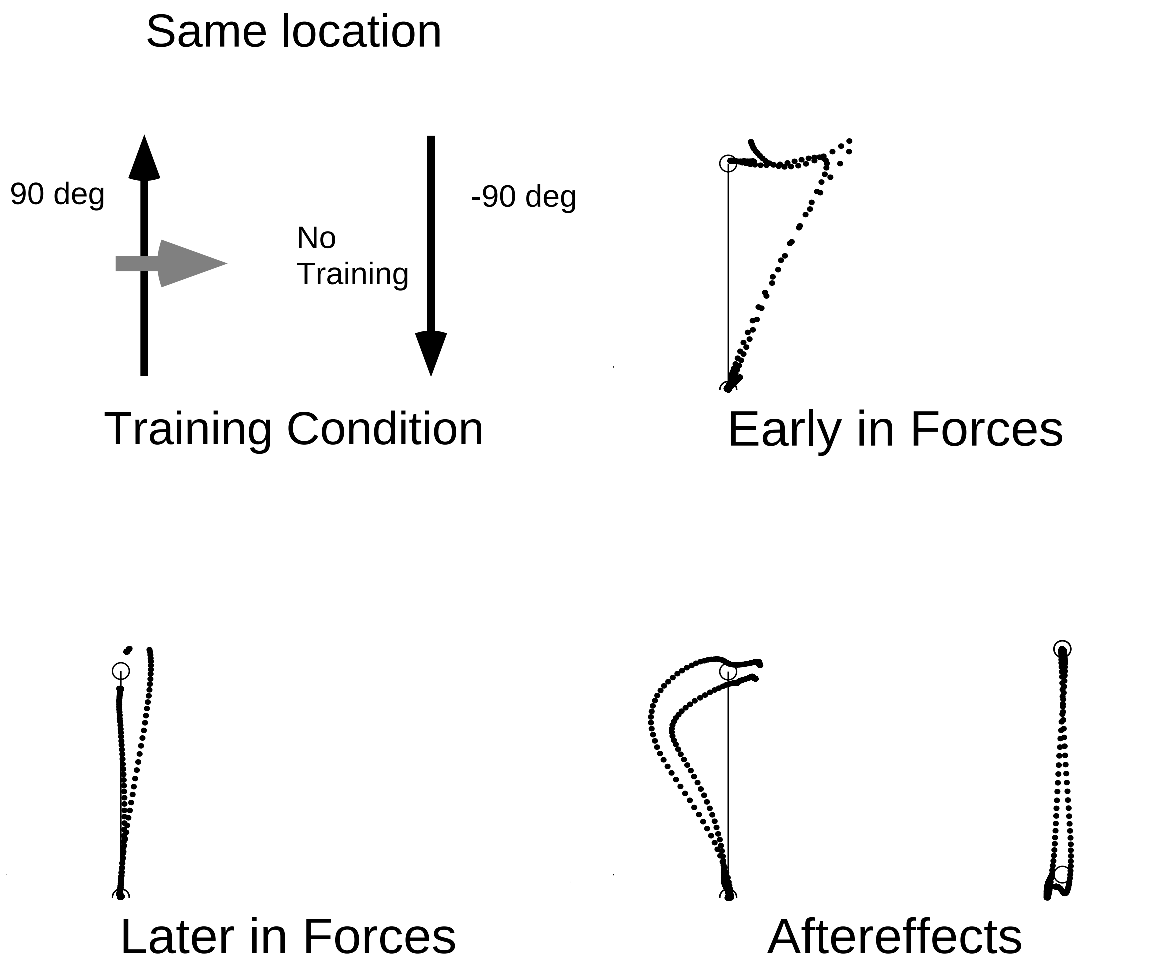

Figure 2-6: The movements were made at the same spatial location but the directions were opposites of each other. Only the 90 degree movements were trained under the force perturbation. First exposure in the perturbation distorted the 90 degree movements to the direction of the force. The distortion disappeared toward the end of training. The aftereffects showed distortion to the opposite direction of the forces for the 90 degree movements but no distortion was observed for the -90 degree movements.

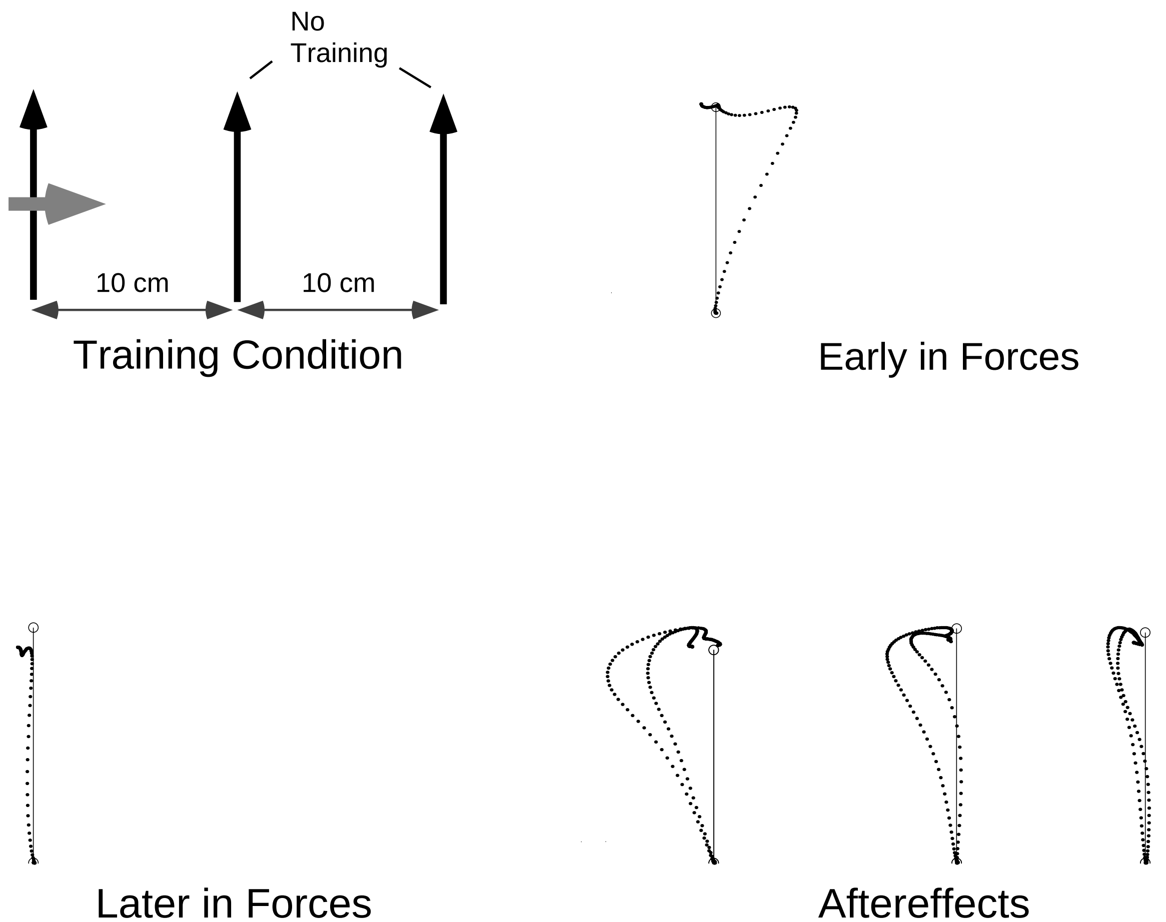

Figure 2-7: The same directional movements are made at different spatial locations. The left movement was perturbed in the 0 degree direction. As the aftereffects show, the learned effect transferred significantly to movements made in the same direction but at different locations. As the distance from the trained location increased, the influence decreased.

directionally identical but 10 cm apart from each other. The subjects were trained first for all three movements without perturbation. During the force epoch, only the left movement was perturbed to the 0 degree direction. The other movements were never executed while the forces were turned on.

The observed hand movements are shown in Figure 2-7. All catch trial movements including the ones that were not trained under force perturbations were distorted in the direction opposite to the forces. The movements made to the same direction are generalized together even if they are executed at a different location in the workspace. However, as it is apparent in the aftereffects, the movements made in the right part of the workspace are not as distorted as those in the middle. Thus as the distance increases from the trained location, the effect of generalization decays.

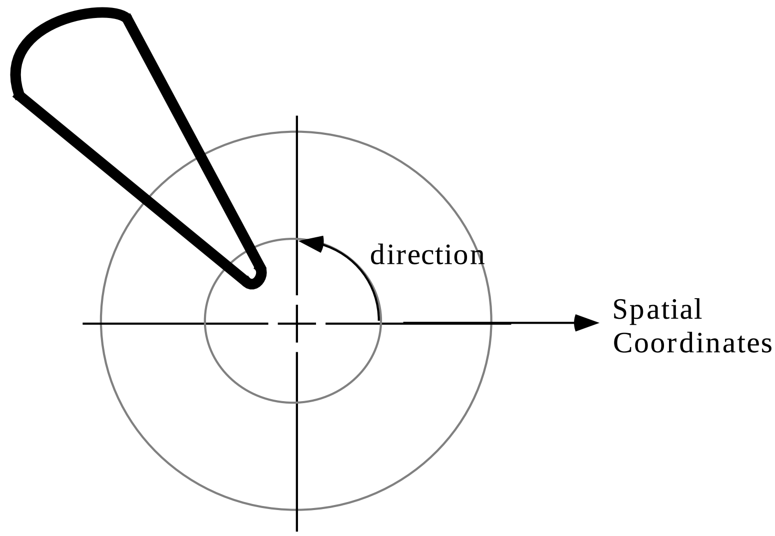

Figure 2-8: The domain of spatial generalization. The marked area represents the general shape of a spatial generalization primitive. The effect of learning transfers more easily to movements with the same direction executed at different locations than for different directional movements.

These experimental results suggest that the spatial generalization is strongly constrained by the direction of the movements. When two movements are executed along the same path, but in opposite directions, the movements are not generalized together at all. Furthermore, when two movements in the same direction are executed some distance apart, the effects learned for one movement transfer greatly to the other movements. However, for movements executed in the same direction, the effects still decay with distance. Using these results, the domain of spatial generalization can be mapped in the coordinates shown in Figure 2-8. The marked area represents the general shape of spatial primitives that are used to learn movements. The influence of the primitive is larger for the movements executed at different locations than for movements that are executed in different directions.

2.5 Experiment DG-A: Directional Generalization with Angle Variations

In the previous section, the general size and the shape of the spatial generalization primitive were defined. In Experiment DG-A, the tuning effect of each primitive was

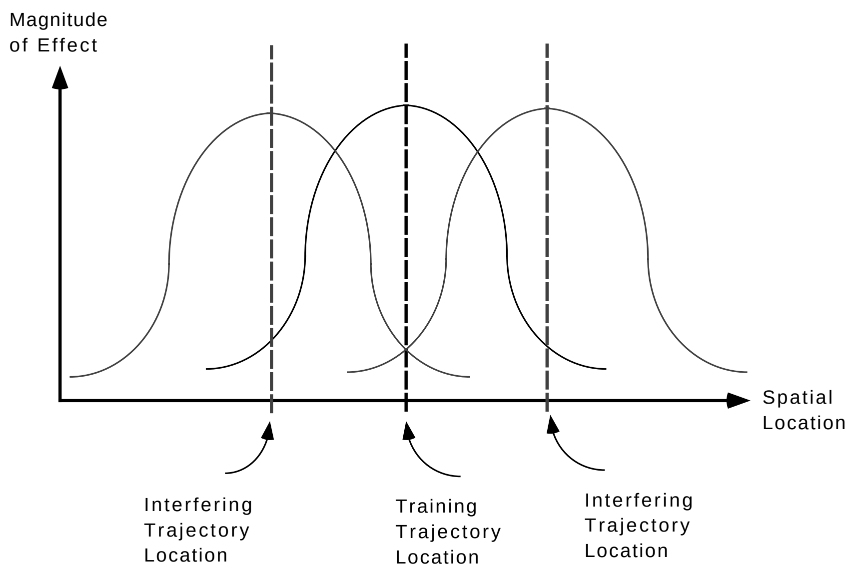

Figure 2-9: The first hypothesis of how the primitives are brought closer. Primitives overlap and do not change the shape.

investigated. There are two hypotheses of how primitives may be brought closer. The first is that primitives overlap in the workspace without changing one another's shape, as shown in Figure 2-9. The effect observed would be a sum of the influence from all the primitives that reside in a given location. Another hypothesis is to imagine that the primitives change shape and fit closer together in the workspace with training, as shown in Figure 2-10. If this is true, then the effect for multiple primitives would not have an additive effect for a particular spatial location.

To investigate these hypotheses, two interfering movements were introduced surrounding the 90 degree movement. During training with force perturbations, the 90 degree movements were always perturbed to 0 degree, pushing the hand to the right. The 90 degree movement is designated as the "training" trajectory. Other movements were all considered as "interfering" trajectories and were perturbed to 180 degrees, pushing the hand to the left.

The interfering movements were trained at +/- 45, 22.5 and 7.5 degrees away from the "training" movement. Four subjects were tested for each angle of interference. They were tested over three force epochs and the aftereffects were recorded during catch trials at the end of the last epoch.

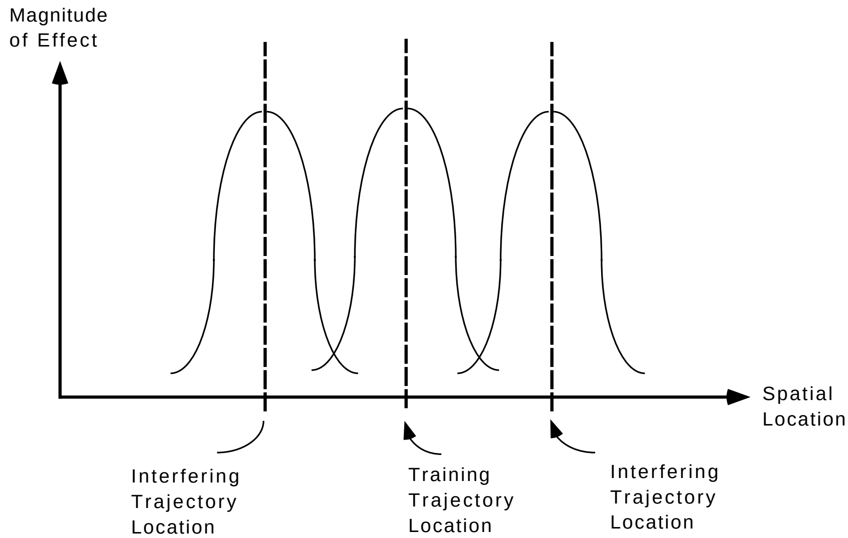

Figure 2-10: The second hypothesis of how the primitives are brought closer. Primitives shrink and fit without overlaps.

+/- 45 degrees

The first group was trained with interfering trajectories at 45 degrees away from the 90 degree movement as shown in Figure 2-11. The initial movements in the first force epoch were distorted in the direction of the forces. After three epochs of forces, some distortions were still observed for all movements, but the magnitude of distortions were smaller for all subjects. When the force field was removed during catch trials, all movements contained aftereffects that were the mirror image of the forces experienced specific to that movement. Thus it is evident that the training and the interfering forces can be learned separately when the movements with opposite force perturbations are 45 degrees apart.

+/- 22.5 degrees

The second group of subjects was tested with interfering trajectories 22.5 degrees away from the "training" trajectory. The results are shown in Figure 2-12. The magnitude of distortions observed later in forces did not change significantly as shown for the experiment with the 45 degree interfering movements. When the forces were removed during catch trials, the 90 degree movements did not display aftereffects matching the forces experienced, demonstrating the interfering effect.

These effects were not identical among subjects. While some subjects displayed some effects matching the training forces, most did not. The trajectories illustrated in

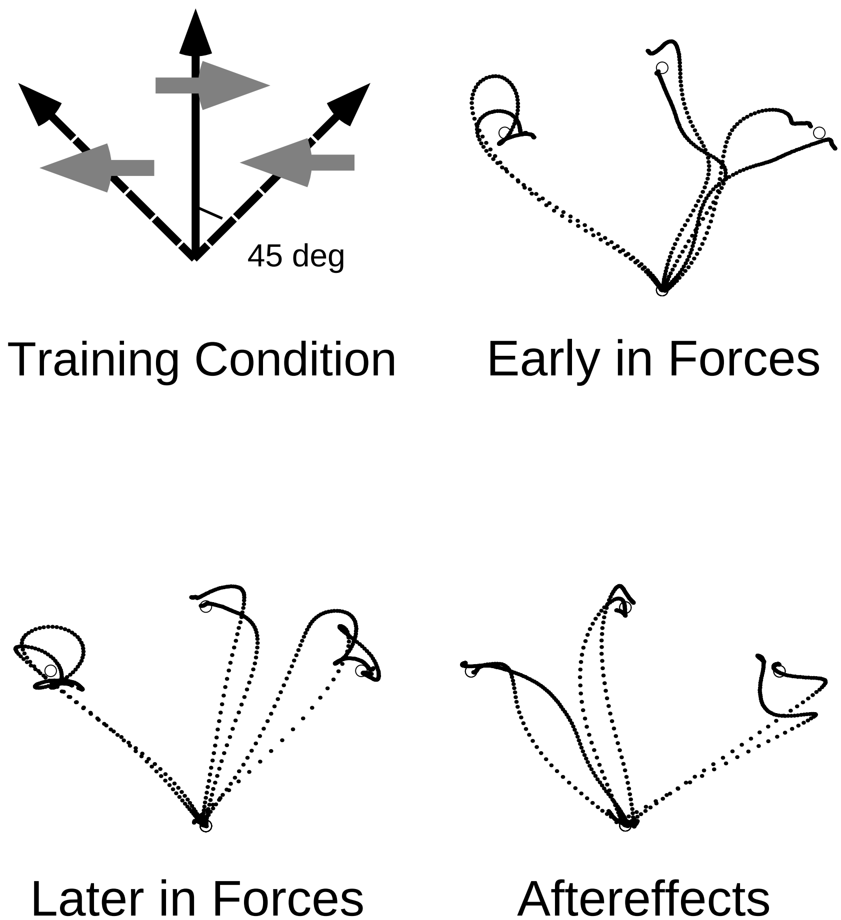

Figure 2-11: Experiment DG-A with interfering trajectories 45 degrees away from the "training" trajectory. Trajectories are initially distorted, learned over time, and the aftereffects show the distortion in the opposite direction of the forces experienced. The effects for the 90 degree movement and the surrounding interfering movements are clearly distinguished.

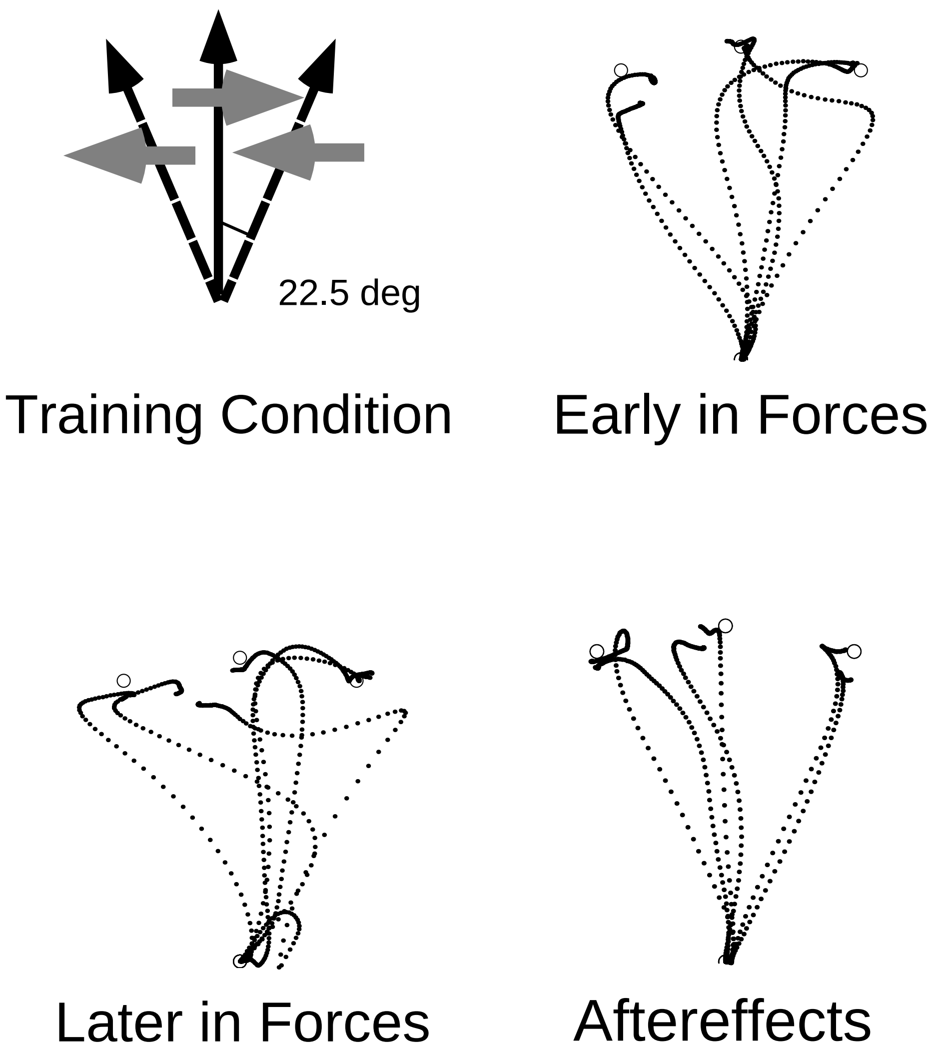

Figure 2-12: Experiment DG-A with interfering trajectories 22.5 degrees away from the training trajectory. Trajectories for initial exposure to the forces, end of training, and during catch trials are shown. The effect learned for the 90 degree movement does not match the force perturbation experienced, showing the interference effect.

the figure are the typical movements observed, and individual differences are discussed later in this section.

+/- 7.5 degrees

The last group was tested with interfering trajectories 7.5 degrees away from the "training" trajectory, and Figure 2-13 shows the results. As shown, the aftereffects of the interfering trajectories matched the direction of the forces. However, the aftereffects of the 90 degree trajectories also matched the interfering forces. Aftereffects demonstrating learning of the forces applied to the 90 degree movements was not observed.

2.5.1 Analysis

The experiments described above displayed different results. When the interfering angles were +/- 45 degrees, the corresponding forces were learned for all movements. At +/- 22.5 degrees, the aftereffects for the training movements varied from one subject to another. However, the effects observed were consistently less than those which were observed when the interfering angles were 45 degrees away. Furthermore, when the interference angles were 7.5 degrees, all the subjects learned the interfering forces for all the movements, including the 90 degree movement.

These results can be interpreted by using the overlapping hypothesis proposed. Figure 2-14 shows the effects for all the conditions. When the interfering angles were 45 degrees, the primitives did not overlap very much. When the angles were 22.5 degrees, the primitives did not change shape, but rather, the outer primitives moved closer to the middle primitive and the effects overlapped. Where the primitives were overlapped, the effects summed. For the results shown in Figure 2-12, the 90 degree trajectory hardly contained any aftereffects. Thus when the effects of the three primitives were added at the location of training movements, the sum was close to zero.

When the interfering angles were 7.5 degrees, the primitives overlapped further as shown in Figure 2-14. At the location where the 90 degree trajectory was trained, when the three primitives are summed, the effect is dominated by the interfering forces. This result matches the experimental data.

After these experiments, it is natural to ask what the exact size of the primitive may be. This question was addressed by running experiments with various angles between 45 and 7.5 degrees: angles 35, 25, and 15 were tested. From this investigation,

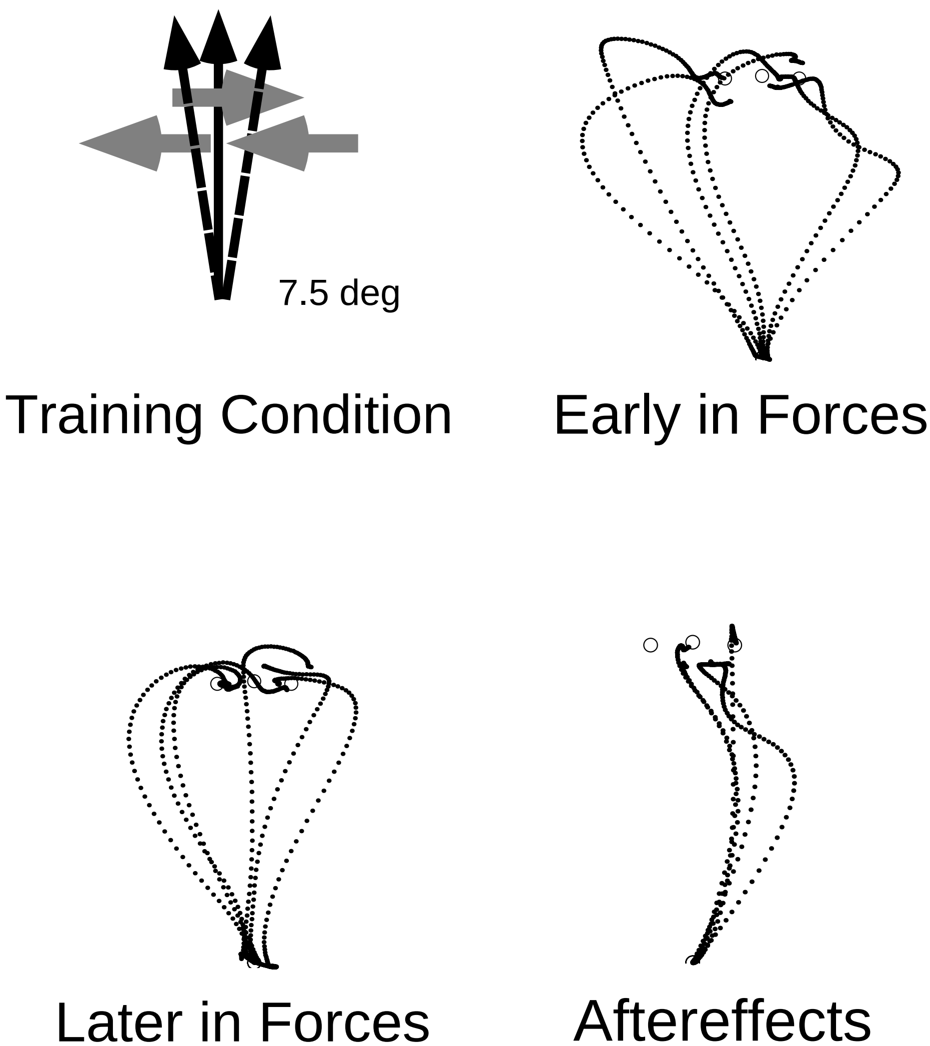

Figure 2-13: Experiment DG-A with interfering trajectories 7.5 degrees away from the training trajectory. The aftereffects for the 90 degree movements showed that there was no learning for the force perturbations experienced, but the movements adapted the effects from interfering forces.

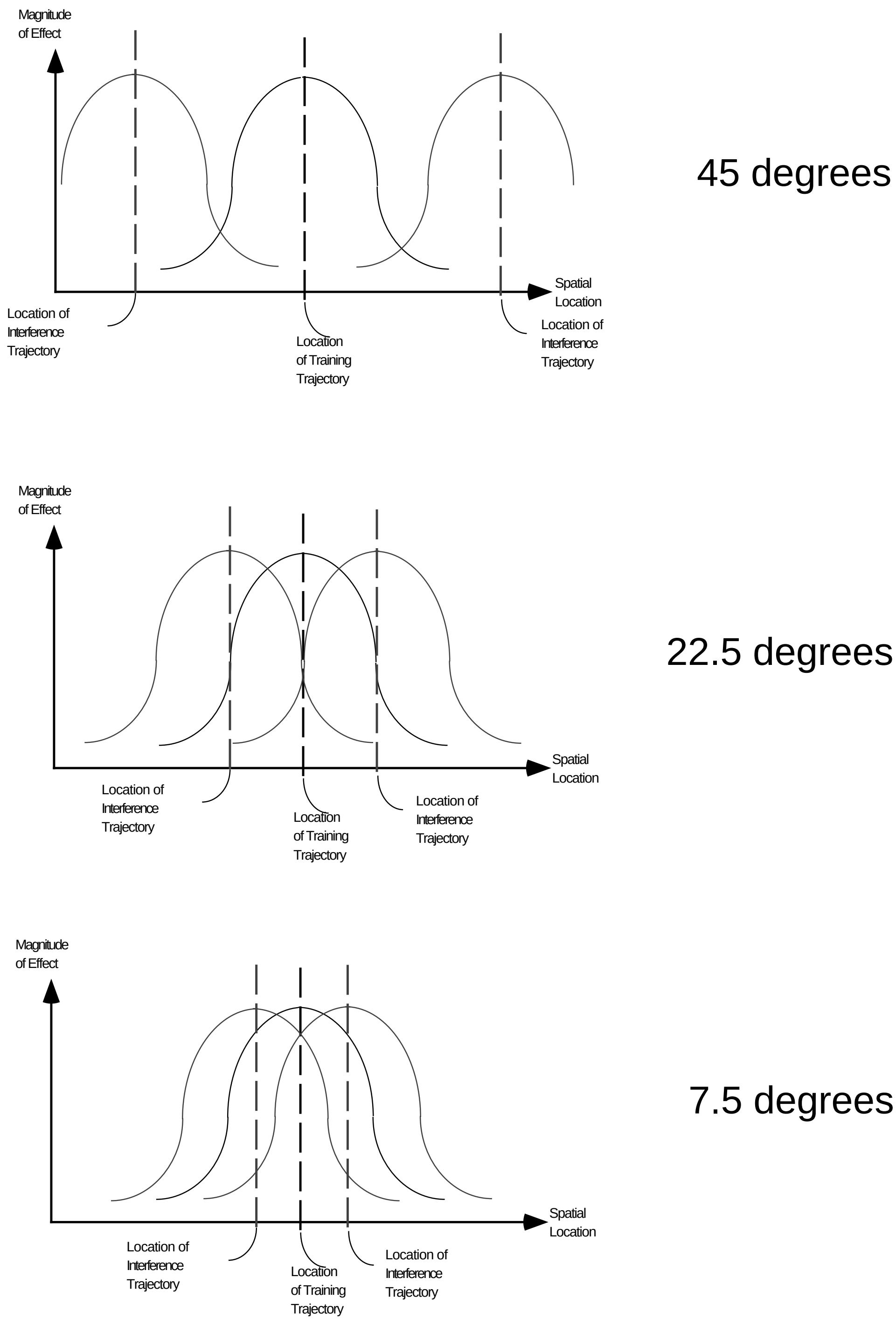

Figure 2-14: Overlapping hypothesis for 45, 22.5, and 7.5 degrees. At 45 degrees, the middle primitive dominates at the training location. However, as the interference angle shrunk, the other primitives effected the training location. At 7.5 degrees, the sum of all three primitives is biased to the interfering forces rather than the training forces at the location of training trajectory.

a large range of individual difference was observed. Some subjects were not able to learn the training forces when the interfering forces where present at 35 degrees away. In contrast, some subjects were able to learn the training forces even when the interfering trajectories were introduced at 15 degrees away. These differences are illustrated in Figure 2-15.

For a subject with small primitives, both 35 and 15 degree interfering trajectories do not overpower the effect of the middle primitive. However, for a subject with large primitives, the primitives overlap significantly more, and learning with even the 35 degree interference interference becomes difficult. These primitive size differences may be a result of the arm kinematics and/or the training approach. It is reasonable to assume that the primitives would be smaller for a shorter and lighter arm.

Furthermore, if the specific environment was presented in the order of difficulties, it may be easier to learn. If so, the primitives may indeed shrink in size adapting to the new situations. In the next section, the interfering angle variations are temporally sequenced to address this issue.

2.6 Experiment DG-SA: Directional Generalization with Sequential Angle Variations

From the previous experiment, it is evident that the primitives overlap and the effects are summed. However, it is still not clear if the primitives can also change their shape, or be tuned, through training. If the primitives are tunable, prior exposure to the easier and learnable environment should help in learning more difficult environments.

Karni and Ahissar have paid attention to the effect of practice for visual tasks [Karni and Sagi, 1993, Ahissar and Hochstein, 1997]. Specifically, Ahissar and Hochstein showed that for perceptual visual learning, learning easy conditions guide the learning of hard ones. They have shown that subjects generalize over spatial dimensions and become increasingly specific to the complex dimensions of the stimulus.

There is much evidence to support that motor skill improves over time [Shadmehr and Mussa-Ivaldi, 1993]. However, exposure of easier tasks before a harder task to improve adaptation has not been discussed. For example, when someone is trying to learn how to play tennis for the first time, it is not productive to play against Pete Sampras. However, by having trained easier tasks first, playing with Pete Sampras becomes more beneficial.

To investigate this theory, the interfering angles were slowly reduced during train-

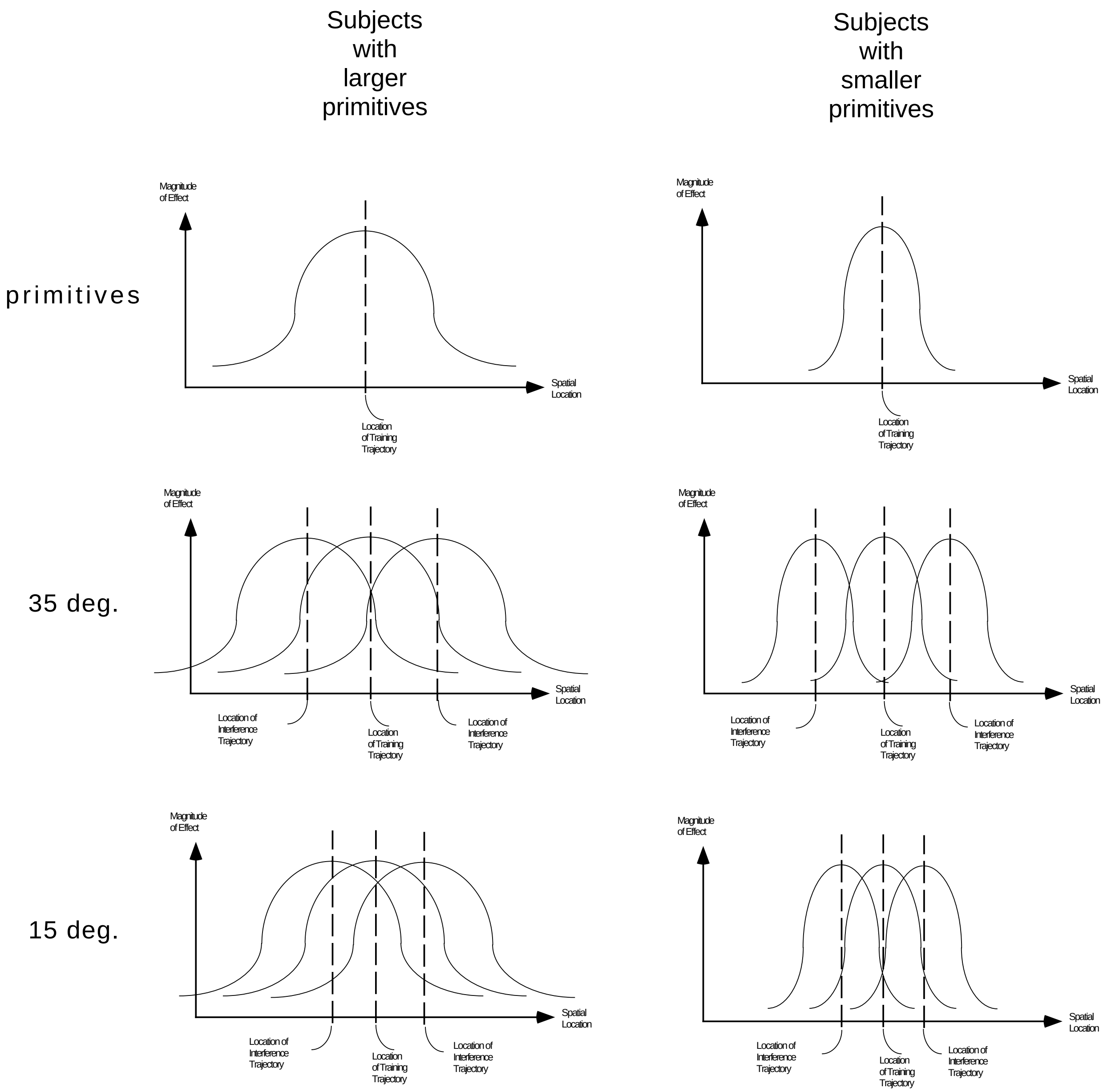

Figure 2-15: Individual differences in the primitive size. When the primitive is large, it is even difficult to learn the training forces with 35 degree interference. However, with the smaller primitive, the training forces are almost learnable even with 15 degree interference trajectories.

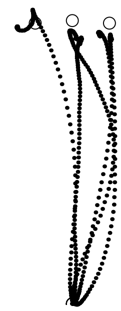

Figure 2-16: The results of Experiment DG-SA. The aftereffects observed at the end of fourth session when the angle difference was 7.5 degrees. Compare these trajectories with Figure 2-13.

ing, starting from a learnable angle, 45 degrees, to observe variations in learnability.

45 → 22.5 → 7.5 degrees

Three subjects were tested for three epochs with force fields. During training with force perturbations, the 90 degree movements were always perturbed to 0 degree, pushing the hand to the right. Other movements were all considered as interfering trajectories and were perturbed to 180 degrees, pushing the hand to the left. The first epoch had interfering trajectories at 45 degrees away from the 90 degree training trajectory, the second epoch at 22.5 degrees away, and the third epoch at 7.5 degrees away. Interleaved catch trials at the end of the third epoch were used to detect any learning effects.

The aftereffects observed at the end of the third epoch are shown in Figure 2-16. Comparing the results from non-sequential experiments shown in Figure 2-13, even though the training was sequenced in the order of difficulty, this training sequence did not seem to help the subjects learn the perturbations when the interfering trajectories are at 7.5 degrees away.

Because 7.5 degree interference was originally very difficult to learn, it may be the case that it is beyond the limit of tunability. Thus another experiment was conducted with the final interfering angle at 22.5 degrees.

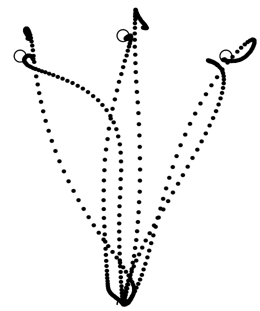

Figure 2-17: The aftereffects observed at the end of fourth session when the angle difference was 22.5 degrees. Compare these trajectories with Figure 2-12.

45 → 22.5 degrees

As the last experiment, three subjects were tested under this condition and three epochs were trained with force perturbations. The first force epoch and the first half of the second epoch were trained with 45 degree interfering angle, while the last half of the second epoch and the third epoch were trained with 22.5 degree interfering trajectories. The end of the third epoch contained interleaved catch trials, and the results are shown in Figure 2-17. The effects observed at the end of the sequential training session are compared to the results from Figure 2-12 by analyzing the initial moving directions. The results showed no statistical difference between sequential and non-sequential experiments. Thus the primitives do not seem to be tunable by prior exposure to an easier environment.

2.7 Experiment DG-V: Directional Tuning with Visual Channel

Experiment DG-A imposed kinematic interference in an attempt to tune the primitives, but no evidence of tuning was observed. Thus another experiment that imposes a different constraint, namely a visual channel, was carried out to further investigate the tuning of primitives. A visual channel, drawn with yellow lines, was established around the 90 degree movement, as shown in Figure 2-18. The channel width was varied between 5cm, 3cm and 1cm. Subjects received a reward sound only if the movements were executed within the given time interval and if the movement did not leave the visual channel.

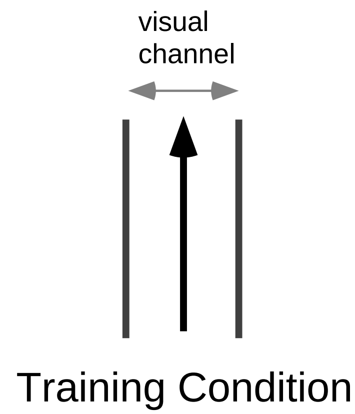

Figure 2-18: The visual channel imposed for Experiment DG-V. The channel width was varied between 5cm, 3cm, and 1cm while the movement was always 10cm long and to the 90 degrees.

For all conditions, one force epoch was conducted and only the 90 degree movements were trained. At the end of the force epoch, movements at 0, 22.5, 45, 67.5 and 112.5 degrees were examined for aftereffects. Three subjects were tested for each condition and the results for all conditions are shown in Figure 2-19. As these typical trajectories show, the effect of visual constraint did not change the tuning of the primitives.

2.8 Experiment ST-1: One Dimensional Spatial Tuning with Interference Force Variations

So far, the experiments discussed in this chapter explored the directional dimension of the spatial generalization domain. In the next two sections, the spatial dimension for the same directional movements are considered.

Horizontal Dimension Interference

All the movements tested were 90 degree movements and the starting point for three 90 degree movements were 10 cm apart horizontally. The left-most movement was designated as the "training" trajectory and the other two movements were designated as the "interfering" trajectories. When only the left movements were trained with forces, the effects transferred to other movements as shown in Figure 2-7. This section describes two additional experiments with interfering force perturbations.

When both interfering movements were trained with the opposite forces from

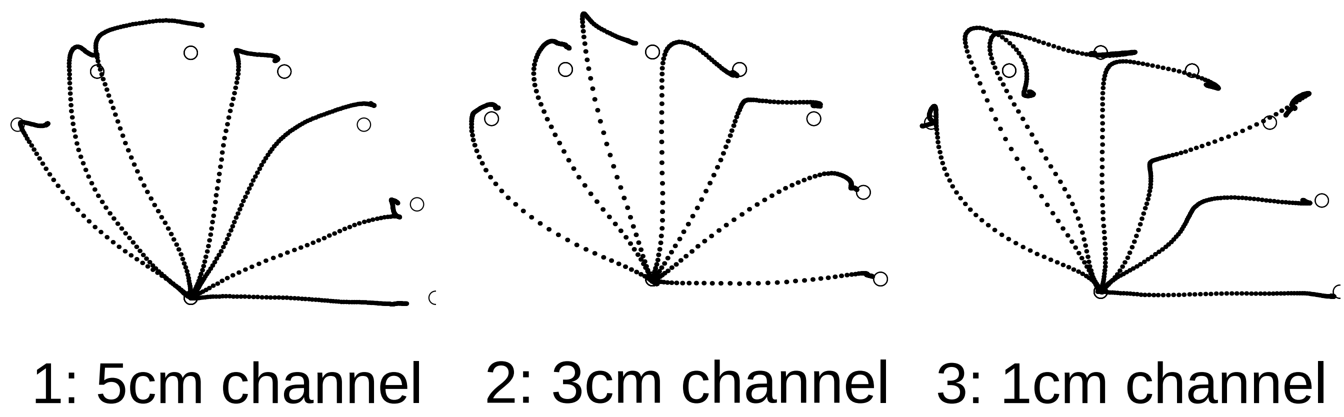

Figure 2-19: The aftereffects observed at the end of the training session for Experiment DG-V. 1: 5cm visual channel, 2: 3cm visual channel, and 3: 1cm visual channel. All the effects are qualitatively the same showing no tuning for spatial generalization primitives.

the training forces as shown in Figure 2-20, the training and the middle movements did not retain any learned effects. However, the right movements contained slight distortion to the left. Conversely, if the right interfering trajectory was perturbed to the right as for the training trajectory, none of the trajectory retain any effects as shown in Figure 2-21. These experiments indicate strong generalization for the same directional movements with horizontal displacement in the workspace.

Vertical Dimension Interference

Another one dimensional displacement in space was examined by training two trajectories in the same direction with starting points 10cm away from each other vertically. Effectively, the bottom movement ends at the starting point of the upper movement. When only the bottom trajectory was trained with the 180 degree forces, the learned effect transferred to the upper trajectory as shown in Figure 2-22.

When these two movements where perturbed in the opposite direction as shown in Figure 2-23, the aftereffects corresponded to the perturbations applied for each movement. This is surprising since two movements that were also displaced for 10cm but in the horizontal direction could not be separated as shown in Figure 2-20. In the following experiment, displacement for both horizontal and vertical directions were investigated together.

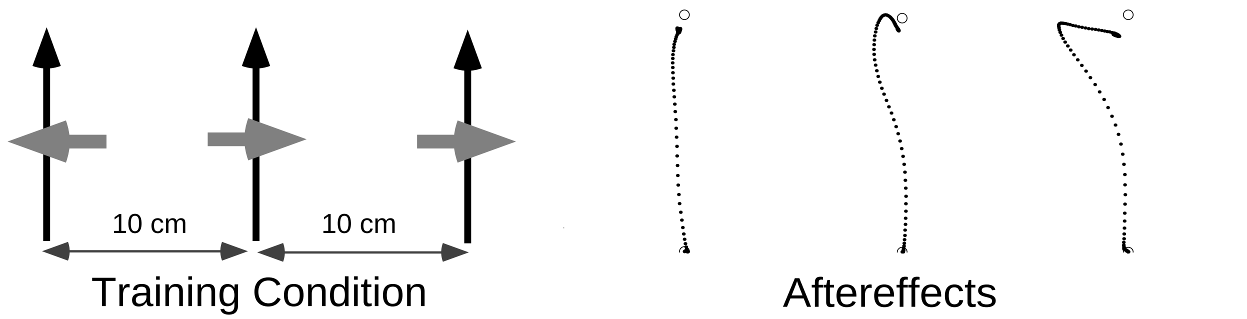

Figure 2-20: The right force perturbation was applied to the training trajectory and the left forces were applied to the interfering trajectories. Aftereffects were observed during catch trials. Only the right interfering trajectory retained significant effect from training.

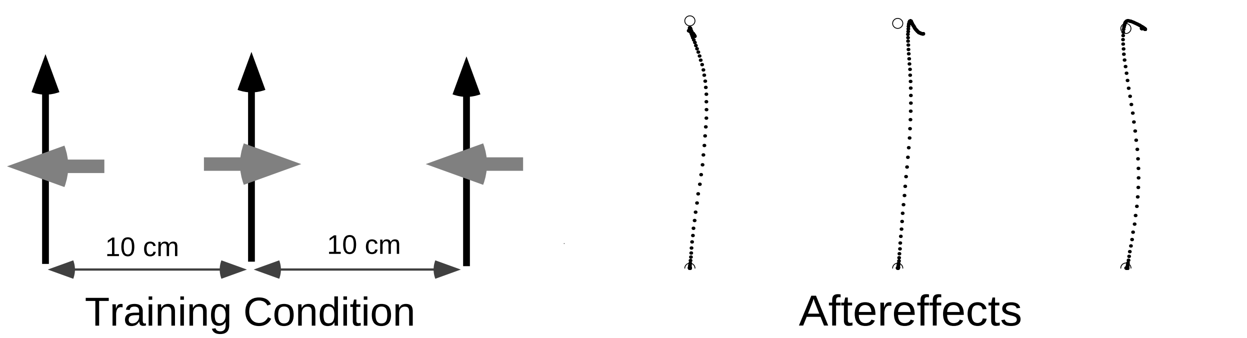

Figure 2-21: The right force perturbation was applied to the training trajectory and the right interfering trajectories, and left forces were applied to the middle trajectory. Aftereffects were observed during catch trials. No effects were learned for any trajectories.

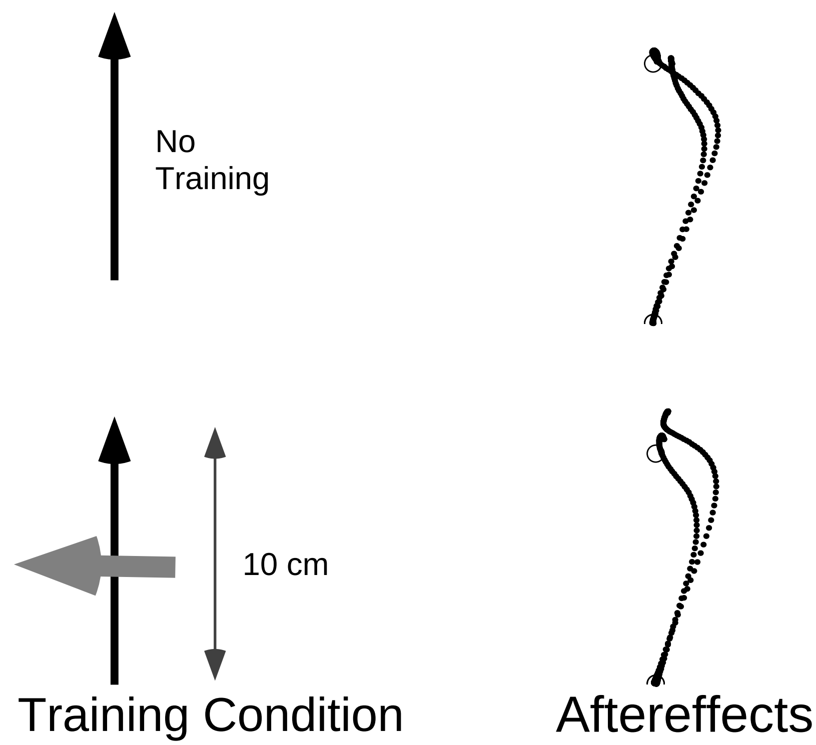

Figure 2-22: Only the bottom movements were perturbed. The learned effect was transferred to a movement that is 10cm displaced vertically.

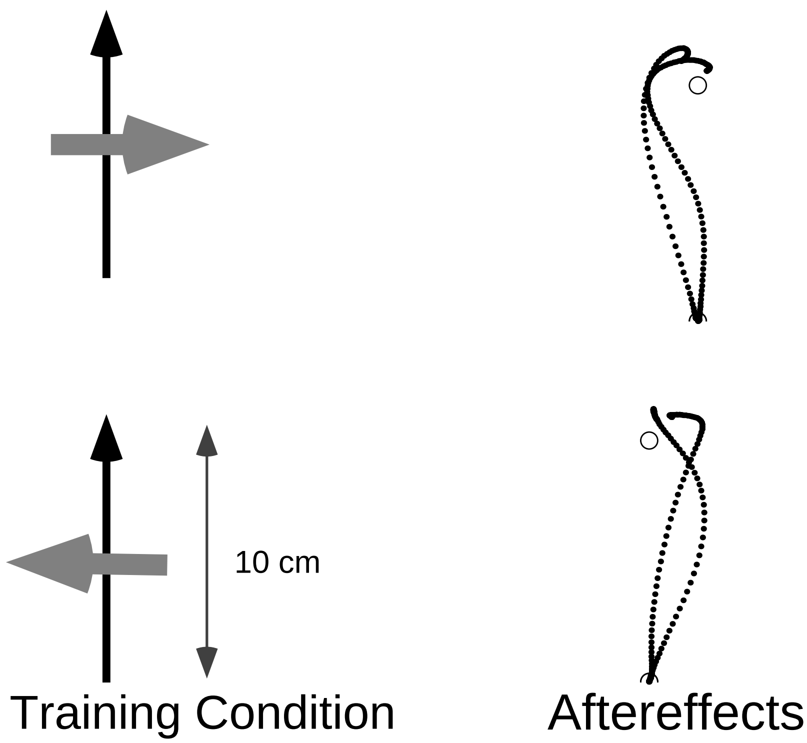

Figure 2-23: The bottom trajectory was perturbed to the left and the upper trajectory was perturbed to the right. Both trajectories retained separate aftereffects corresponding to the direction of the forces applied.

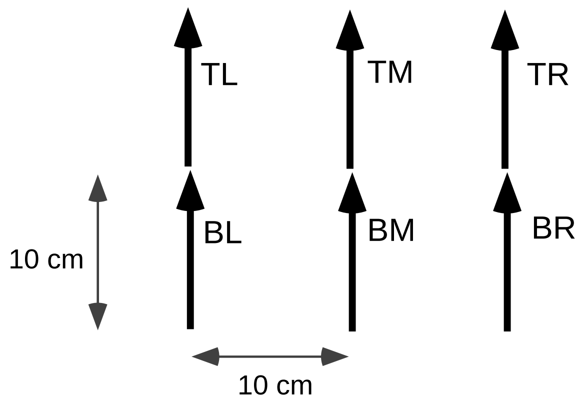

Figure 2-24: Six movements that are used to analyze the shape of primitives in a two dimensional workspace. The movements are labeled as BL (bottom left), BM (bottom middle), BR (bottom right), TL (top left), TM (top middle), and TR (top right).

Group #	*BL*	*BM*	*BR*	*TL*	*TM*	*TR*
1	0	NT	NT	NT	NT	NT
2	0	0	0	180	0	180
3	0	0	0	0	180	0

Table 2.3: Three scenarios investigated for six movements in the same direction. BL = bottom left; BM = bottom middle; BR = bottom right; TL = top left; TM = top middle; TR = top right. All entries stand for F_d. NT = no training.

2.9 Experiment ST-2: Two Dimensional Spatial Tuning with Interference Force Variations

In this experiment, six movements were recorded to analyze the shape of the generalization primitives in the two dimensional workspace as shown in Figure 2-24 . Three scenarios were investigated, and they are tabulated in Table 2.3. For each condition, three subjects were tested.

No Interference Training

For the first condition, only the bottom left movements were trained. The results are shown in Figure 2-25. The aftereffects observed during catch trials displayed that the information learned for the bottom left trajectory transferred to all other movements. In particular, the effect was noticeably stronger for the movements on the bottom row. This finding is consistent with the one dimensional experiments.

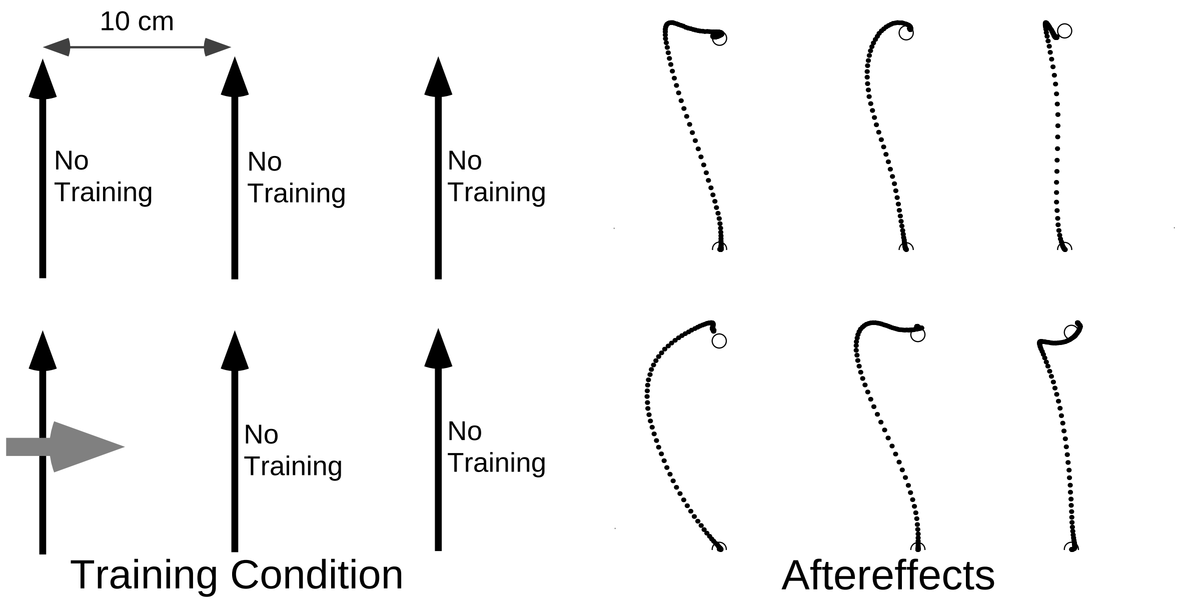

Figure 2-25: The forces assigned and the aftereffects recorded during catch trials for Experiment ST-2, group 1. The learned effect transferred significantly to other movements, especially the movements on the bottom.

Two Interfering Trajectories on Corners

In the second condition, two upper outer movements were perturbed by interfering forces and the results are shown in Figure 2-26. The effects of the interference forces were spread out radially. The bottom middle movements, which were surrounded by movements perturbed in the same direction, exhibited the most significant aftereffects.

Surrounded by Interfering Trajectories

Finally, all the trajectories surrounding the top middle trajectory were assigned interfering force perturbations, as shown in Figure 2-27. The aftereffects for the top middle movements contained the aftereffects corresponding to the surrounding interfering force rather than the forces experienced for the top middle trajectory itself.

Analysis

Unfortunately, the workspace of the manipulandum can only fit the six movements made in this section. When no interference was imposed, the generalization effect

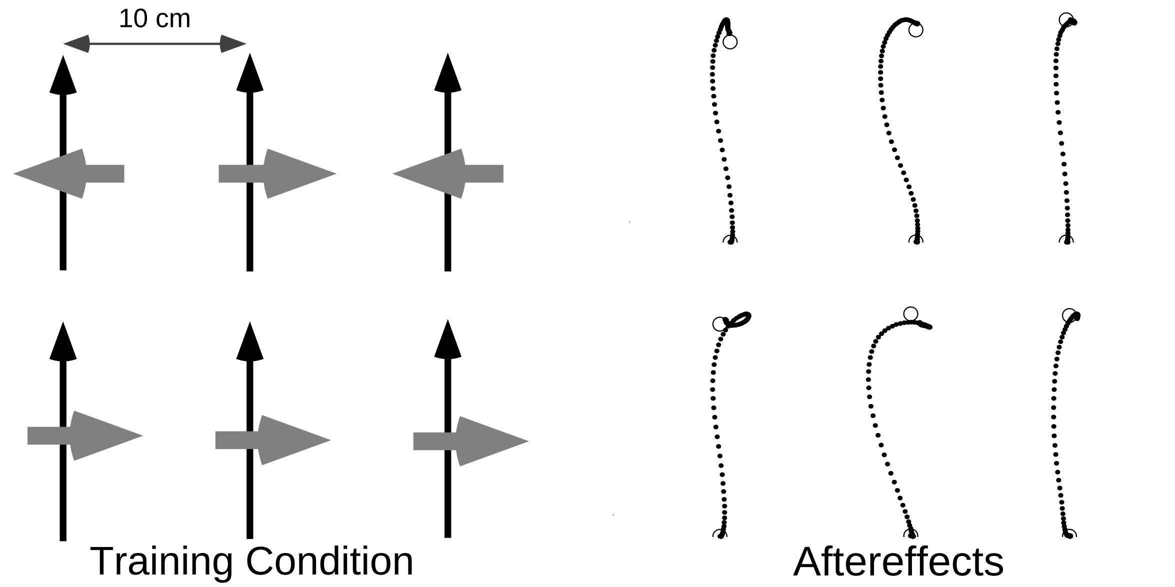

Figure 2-26: The forces assigned and the aftereffects recorded during catch trials for Experiment ST-2, group 2. The further away from the interfering forces the more effect retained.

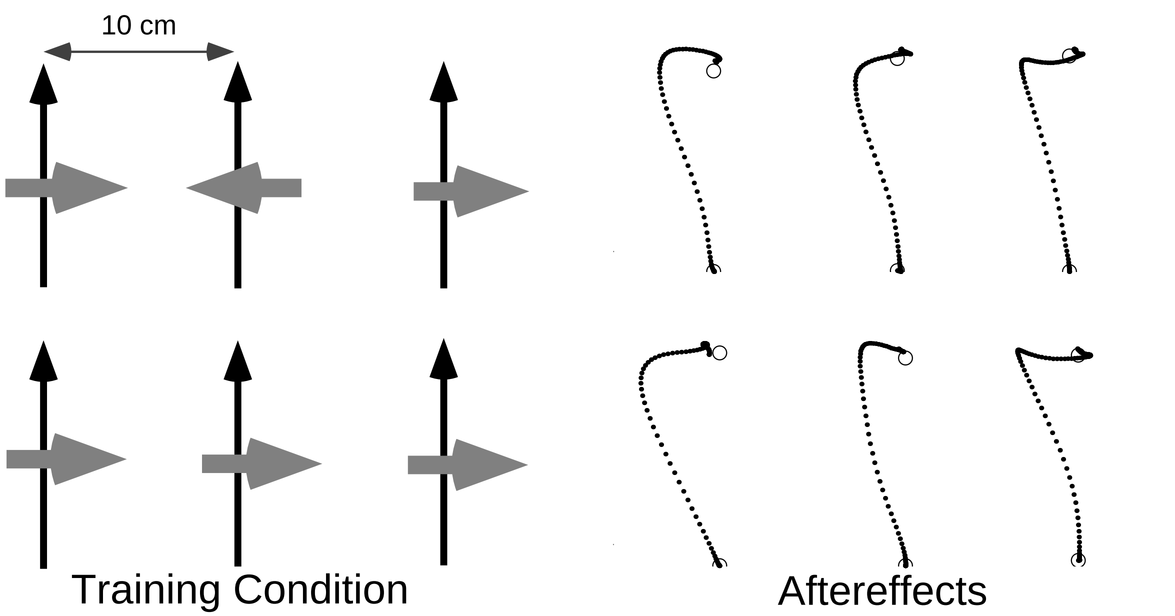

Figure 2-27: The forces assigned and the aftereffects recorded during catch trials for Experiment ST-2, group 3. The upper middle trajectory retained the aftereffect from the surrounding interfering forces instead of its own perturbation forces.

was larger than the workspace, as shown in Figure 2-25. Thus the interference experiments had to be conducted to identify the extent of the influence of one primitive. When the trajectory that was 10 cm horizontally apart was under perturbation with opposite forces, neither of them showed any aftereffects after the training session. Conversely, if the trajectories were 10cm apart vertically, subjects could learn opposite perturbations simultaneously.

As observed for the upper middle trajectory in Figure 2-26, even if two trajectories that were 10 cm apart horizontally were perturbed with opposite forces, the correct perturbation was learnable if the movements that were vertically near were perturbed with the same forces. Moreover, if the forces that were vertically near are perturbed to the opposite direction instead, the effect for the upper middle trajectory was overwhelmed by the opposite forces as shown in Figure 2-27. Therefore, the primitive effects multiple dimensions within the workspace. It can be inferred that the transfer of learned information and its decay can be observed along the z-axis.

There is another factor that may contribute to the effects observed besides the pure effects from spatial primitives. When many movements in the same direction are presented, it is not a bad strategy to pick the force perturbations that are applied for the majority of the trajectories and only adapt to it by ignoring the others. The effect observed in Figure 2-27 may have been influenced by this factor. This strategy is called "winner-take-all" strategy and it is discussed further in Chapter 7.

The results from the experiments in this chapter suggest that the influence of such force perturbations is local. It is local in both extrinsic and intrinsic coordinates: when the movement is identical but 10 centimeters away in extrinsic coordinates the influence of the interference is much larger than when the interference was experienced 20 centimeters away.

2.10 Quantification of the Spatial Primitives

Spatial primitives are finite in size and have a certain shape that exists in the domains of the direction of the movement and the location where the movement is made. Tuning effects have not been apparent from the experiments so far. Thus primitives can be hypothesized to have a fixed size and shape, and the peak of the primitives shift throughout the workspace depending on the environment. When two conflicting environments are presented next to each other, two primitives approach close to each other to a limit. When two primitives are at the closest position, there is a point where the primitives overlap. This point is called the "overlap point", and it is shown

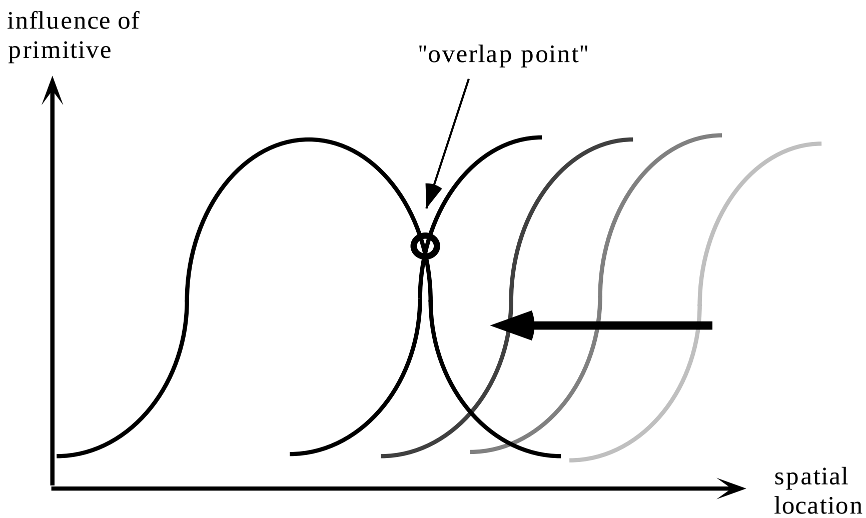

Figure 2-28: When spatial primitives with containing different information are spatially close, they overlap and interfere with each other. The primitives do not change the shape and move around in the workspace depending on the environment. There is a limit in distance that two primitives can reside. When they are at the closest position and the point where the overlap occurs is called the "overlap point."

in Figure 2-28.

Using the overlap point as the border of the primitives, they can be plotted in the domain of movement direction and the location of movement execution. By separating out the location coordinates to x-position (horizontal) and y-position (vertical), the primitive can be plotted as shown in Figure 2-29. As observed in the experiments, the primitive is wider in the horizontal direction than the vertical direction. In addition, the direction of the movement has a larger radius than the horizontal or vertical directions.

2.11 Conclusion

In this chapter, the spatial locality in motor adaptation and generalization was investigated. Experiments conducted were discussed to define the spatial primitives to quantify the effect. Having these finite spatial primitives is an advantage in learning complex tasks which require piece-wise learning. In the next chapter, the spatial primitives within one continuous movement are investigated using high frequency force perturbations.

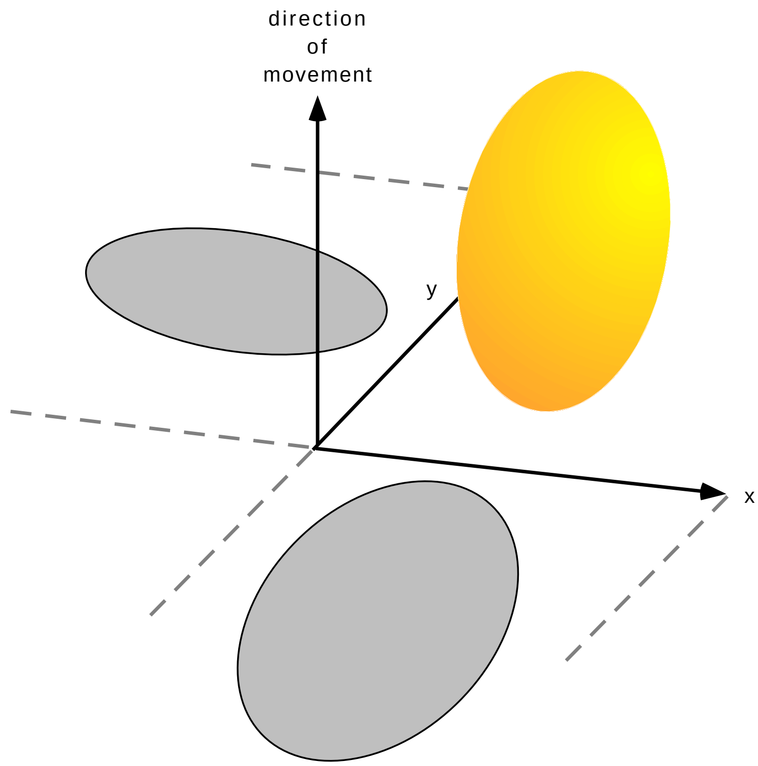

Figure 2-29: A spatial primitive is plotted in the three dimensional domain.

Chapter 3

Spatial Generalization during Execution of One Movement

3.1 Introduction

In the previous chapter, generalization of motor learning was shown to be spatially organized, and the spatial generalization primitives were defined and quantified. The analysis was movement-based: the perturbation force direction was consistent within one 10 cm movement, and the effects among different movements were compared. According to the sequential movement-based analysis, primitives were hypothesized to be fixed in size and shape.

Instead of movement-based analysis, the generalization effect for one continuous movement is investigated in this chapter. One continuous movement is defined as a movement whose velocity profile is bell-shaped and unimodal. According to this definition, even if the hand movement does not come to a stop, it is not a continuous movement when the velocity profile contains multiple peaks.

In order to assess the spatial properties of one movement, smooth high frequency force fields were designed to apply disturbance to one continuous movement. When the spatial frequency of the perturbation forces exceeds the frequency of the primitives, the forces should become non-learnable. However, if a high frequency force field is filtered to a low enough frequency, subjects should be able to learn and develop an internal model of this filtered field. Furthermore, the tuning property of the primitives are investigated again by sequentially introducing low to high frequency force fields that are related. They are related in the sense that the lower frequency fields are filtered versions of the high frequency field.

Even if the primitives are shown to be tunable from the sequential exposure to related fields, there is a limitation for such adaptation. This raises a question whether the spatial limitation in motor adaptation differs from the limitation of perception.

To perceive means to become aware of (or to achieve understanding of), directly through any of the senses. To learn is to gain knowledge, comprehension, or mastery of through experience or study. Speaking in terms of the nervous system, specifically the motor system, sensory inputs are used to create internal models of the world. When a limb interacts with the world, it collects sensory information from the external world. This sensory information is mediated by perception and the next action is planned accordingly. In parallel, these sensory inputs are also used for learning. The internal model is *affected* when the afferent information is perceived and the model is *changed* when the information is learned. Although they are distinguished in definition, they are often treated together without adequate clarification. Thus, the difference between these two are discussed along with the experimental data.

In addition, I constructed dynamic models of the arm and the manipulandum to simulate the movements under high frequency perturbation. Following the calibration of these parameters, the process of adaptation and generalization was simulated using the primitives defined in the previous chapter.

3.2 Overview of Experiments

If a viscous force perturbation is applied during a reaching movement, the hand movement is distorted in the direction of the force. After being exposed to the force for a period of time, the nervous system builds a model to counterbalance it [Shadmehr and Mussa-Ivaldi, 1993]. This effect can be observed when the force is removed and the trajectory is distorted in the opposite direction of the perturbation force. This is defined as aftereffect. Moreover, this counterbalance model acts like a local map which is spatially organized [Gandolfo, et al., 1996] and can be expressed as a superposition of primitives whose learning effects decay smoothly with distance from the perturbed locations. This superposition results in the size of the primitives dictating what spatial frequency of perturbation can be learned.

To explore the size of spatial generalization primitives within one movement, the spatial frequency of the perturbation forces be altered. The simplified idea is shown in Figure 3-1. Assume an experimental setup where subjects are asked to make one continuous movement from the origin (x) to a target (o). Without any external forces, the hand trajectories are normally straight. If the force field A, shown in Figure 3-1, is presented in the workspace, the initial reaching movement is distorted in the direction of the forces. With practice, the trajectory becomes straight within the force field. When the forces are removed from the workspace, an aftereffect is present

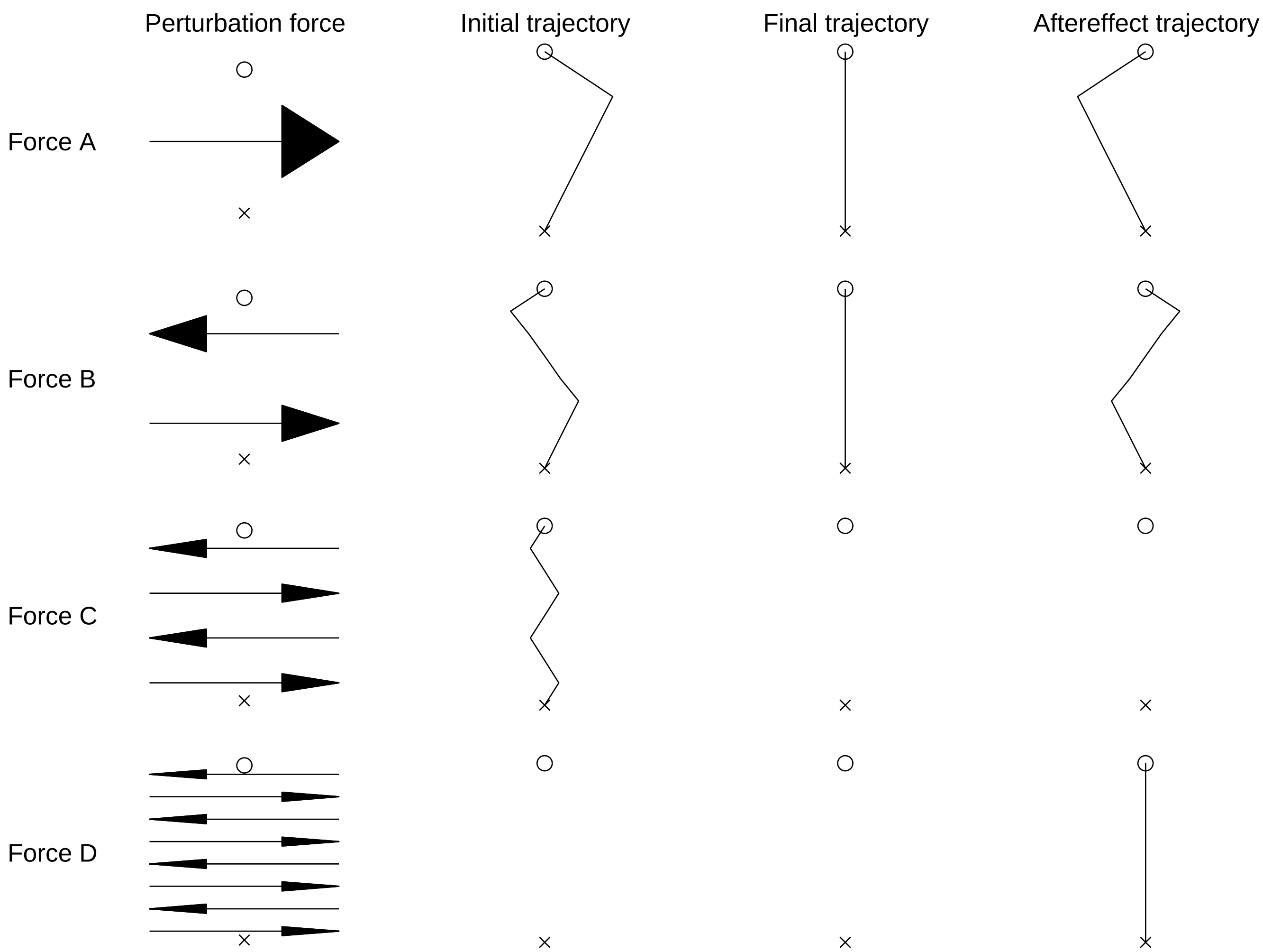

Figure 3-1: Perturbation forces and the theoretical reaching movements made in various forces. Columns (from the left): force perturbation conditions, initial trajectories under perturbation, trained final trajectories under perturbation, and aftereffect trajectories when the forces are removed. Rows (from the top): Force fields A, B, C, and D where the spatial frequency of the force is doubled at each step. Wherever the outcome was not predictable theoretically, the entry is left blank.

as shown in the catch trial trajectory. This result is apparent from the previous chapter. Next, if force field B is presented and assuming that multiple primitives exist within one movement, the results can be hypothesized to reflect both force directions as shown in Figure 3-1. Now, what kind of result is expected if force field C is applied? It is not clear whether it is possible to adapt to the granulation of the external forces presented for force field C. Furthermore, when the perturbation is of very high frequency, it should become impossible to learn as shown for the force field D. When there is no learning, the hand trajectory should not exhibit any distortion when the forces are removed.

The setup illustrated in Figure 3-1 is ideal for presenting the idea, but there is a problem with running it on subjects. Humans do not seem to learn a perturbation force field that contains discontinuity. When the force direction is changed to the opposite direction with a clear dividing line as shown in Figure 3-1, the fields are not continuous. Therefore a different technique is proposed to create various continuous force fields. These techniques are described in section 3.4.

The summary of all the experiments conducted in this chapter are tabulated in Table 3.1. The set of numbers in the "Movement" column are the directions and the lengths of the movements. All the movements started from the same point. The target size was 8 x 8 mm and the hand cursor was 2 x 2 mm. Subjects were told to make all movements within +/- 0.05 seconds of the desired time interval, specified in the table. One session of training consisted of two to four epochs: one baseline epoch without perturbation and one to three epochs of training with forces. One epoch consisted of 192 reaching movements or trials, and the last epoch contained catch trials to observe aftereffects.

3.3 Experiment TDP: Two Different Perturba -tions in One Movement

In order to answer the question whether multiple primitives can encode separate aftereffect information within one movement, the workspace was divided into two regions, and each region was perturbed with differing interference forces.

Partial Perturbations

According to the spatial encoding hypothesis that has been discussed in this thesis, if the perturbation were applied to only a small region within one movement, the

Exp.	*#*	*Movement (deg)*	*(cm)*	*Perturbation*	*Interval (+/- 0.05 sec)*	*Investigate:*
TDP	1	90	20	180deg partial	0.65	Generalization within one movement.
	2	90	10, 10	no force, 180deg	0.95	
	3	90	20	0deg, 180deg	0.65	
HF-COM	1	0,45,90,135	10	Field 0	0.50	Components learned with high frequency force fields.
	2	0,45,90,135	10	Field 2	0.50	
	3	0,45,90,135	10	Field 5	0.50	
	4	0,45,90,135	10	Field 8	0.50	
	5	0,45,90,135	10	Field 13	0.50	
	6	0,45,90,135	10	Field 18	0.50	
HF-SEQ	1	0,45,90,135	10	Fields 18, 5, 0	0.50	Sequential learning of high frequency force fields.
	2	0,45,90,135	10	Fields 18, 5, 2	0.50	
	3	0,45,90,135	10	Fields 18, 9, 5	0.50	
HF-PER	1	0,45,90,135	10	HFF, HFF, HFF	0.50	Perception and learning under high frequency force fields.
	2	0,45,90,135	10	LFF, LFF, LFF	0.50	
	3	0,45,90,135	10	LFF, MFF, HFF	0.50	
	4	0,45,90,135	10	LFF, MFF, null	0.50	
	5	0,45,90,135	10	LFF, MFF, OHFF	0.50	
	6	0,45,90,135	10	LFF, MFF, IHFF	0.50	

Table 3.1: The road map for experiments in Chapter 3. The set of numbers in the "Movement" column are the directions and the lengths of the movements. For the "Perturbation" column, the field number assigned signifies the amount of filtration. HFF = high frequency field, MFF = medium frequency field, LFF = low frequency field, OHFF = opposite high frequency field, IHFF = integrated high frequency field, and null = no forces. All the field names are defined in detail within each of the experimental sections. The "Interval" column specifies the time interval that the movements had to be completed in to receive a reward. The intervals are +/- 0.05 seconds from the specified time. All the movements start from the same point. 8 x 8 mm targets and 2 x 2 mm hand cursors are used.

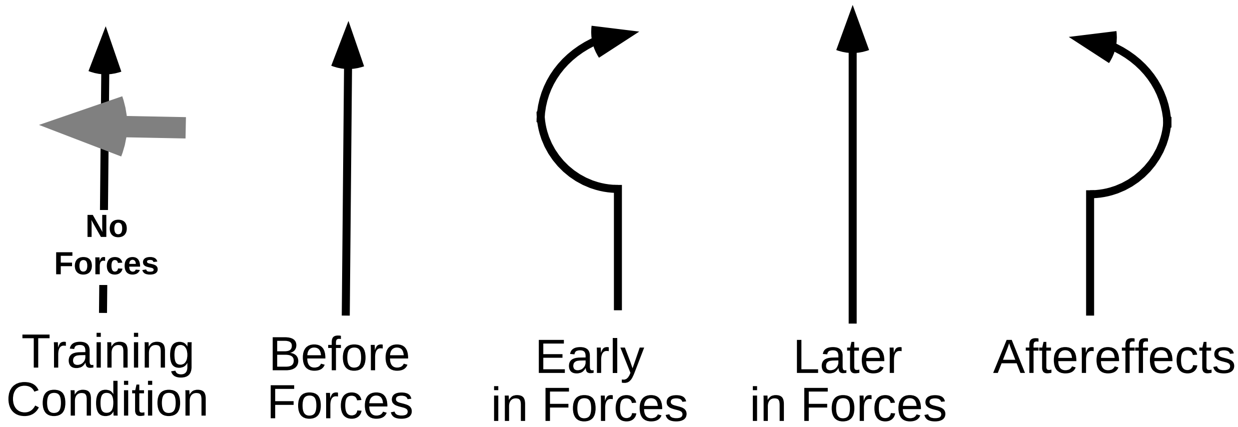

Figure 3-2: Theoretical trajectories under partial perturbations during executing one movement. Before the perturbations were imposed, the hand trajectory should be straight. The initial trajectory is perturbed in the location where the perturbation was applied. After training, the trajectory becomes straight as previously observed. The aftereffect trajectory is distorted in the local area where the forces were experienced.

adaptation should take place locally. For example, Figure 3-2 displays the theoretically plausible trajectories in a condition in which only the last half of the movement was perturbed. The trajectory without force perturbation should be straight towards the target. As soon as the perturbations are applied the trajectory is distorted locally where the forces are experienced. With training, the movement of the hand should return to a straight trajectory, as shown in previous experiments. When the forces are removed, the aftereffect should exhibit the counter balancing forces, thus the distortion should be present locally where the forces were experienced.

Another hypothesis is that, due to the information transfer among neighboring primitives, the effect will be evident for the whole movement as shown in Figure 3-3.

An experiment was conducted to observe the learning and generalization effects seen under the training circumstances discussed above. The force field was designed to apply perturbations to the last 12cm of a 20cm long movement. The viscosity of the perturbation was gradually increased but also proportional to the velocity. The viscosity matrix was set to

$$\vec{B} = \begin{bmatrix} x_p \times g & 0 \\ 0 & (y_p - 120) \times g \end{bmatrix}, \text{for } y_p \geq 120 \tag{3.1}$$

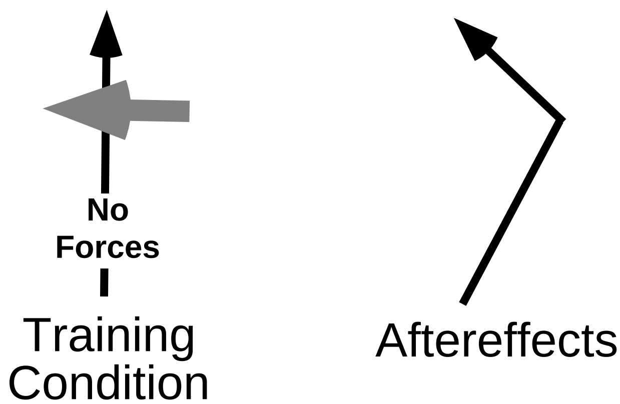

Figure 3-3: Another theoretical aftereffect trajectory under partial perturbations during executing one movement. With an assumption that the learned information transfers to the neighborhood primitives, the whole trajectory should contain the information of the partial perturbation.

for x-position, x_p, and y-position, y_p, in millimeters, assuming the coordinate of the starting point is $[0, 0]$. This design allowed the force field to be continuous, eliminating the problem discussed in the previous section. However, this design can work only when the frequency of the force direction change is low. An examination of how perturbation frequency relates to aftereffects is explored later in this chapter.

All movements executed during training were identical: 20cm long movements in the 90 degree direction. The interval of movement time was 0.65 +/- 0.05 seconds. After one epoch of baseline training, one partial perturbation epoch was conducted. The last 20 movements of the force epoch were interleaved with catch trials.

Three subjects were trained with the partial forces, and the results are shown in Figure 3-4. When the forces were initially introduced, the hand movements were distorted locally at the place where the force was experienced. Contrary to the prediction, after a period of exposure to the forces, the trajectory did not become straight, but rather arc-shaped. This behavior was consistently observed for all subjects. The typical velocity profiles for this task are shown in Figure 3-5. The velocity profiles are unimodal before exposure to the perturbation. However, when the forces are introduced for the first time, the profile contained multiple peaks. With training, the velocity profile returned to contain only one peak.

In agreement with the second hypothesis, when the forces were removed the movements were globally distorted, not restricted to the location of the perturbation. Instead of making a local correction where the forces were experienced, the correction was made at the beginning of the movement. The initial moving directions were the

Figure 3-4: The force is assigned to perturb the last 12 cm of a 20 cm long movement. When the perturbation was imposed initially, the hand trajectory was distorted only at the location where the forces were experienced. However, with training, the movement became arc-shaped and never returned to the straight movements observed prior to training. When the perturbation was removed, the distortion in the movement existed for the whole movement instead of the local distortion.

same during catch trials and at the end of training in forces. The difference was that the expected forces that had previously pushed the hand toward the target during training were not present in the catch trials, and thus the subjects' movements overshot straight according to the starting direction of movement.

These results are not unusual considering that, as seen in the previous chapter, learned effects transfer to neighboring primitives.

Decomposing into Two Movements

In the previous experiment, subjects were asked to execute one continuous movement between targets. If this movement was decomposed into two movements with the same force setup, does the first half of the movement retain the aftereffects as seen in the last experiment? If a different behavior can be observed for this experiment, the primitives must have different size for making one continuous movement than from the ones defined in Chapter 2. To test this, a via-point was placed where the force direction changed.

Two subjects were tested under this condition and they were asked to make two continuous movements through the via point. They were also told that there was no need to stop completely at the via point. Subjects received the reward sound only if the via point was crossed with their hand trajectories and the target was reached within the interval 0.95 +/- 0.05 seconds.

Figure 3-6 shows the typical velocity profile for this movement during the baseline

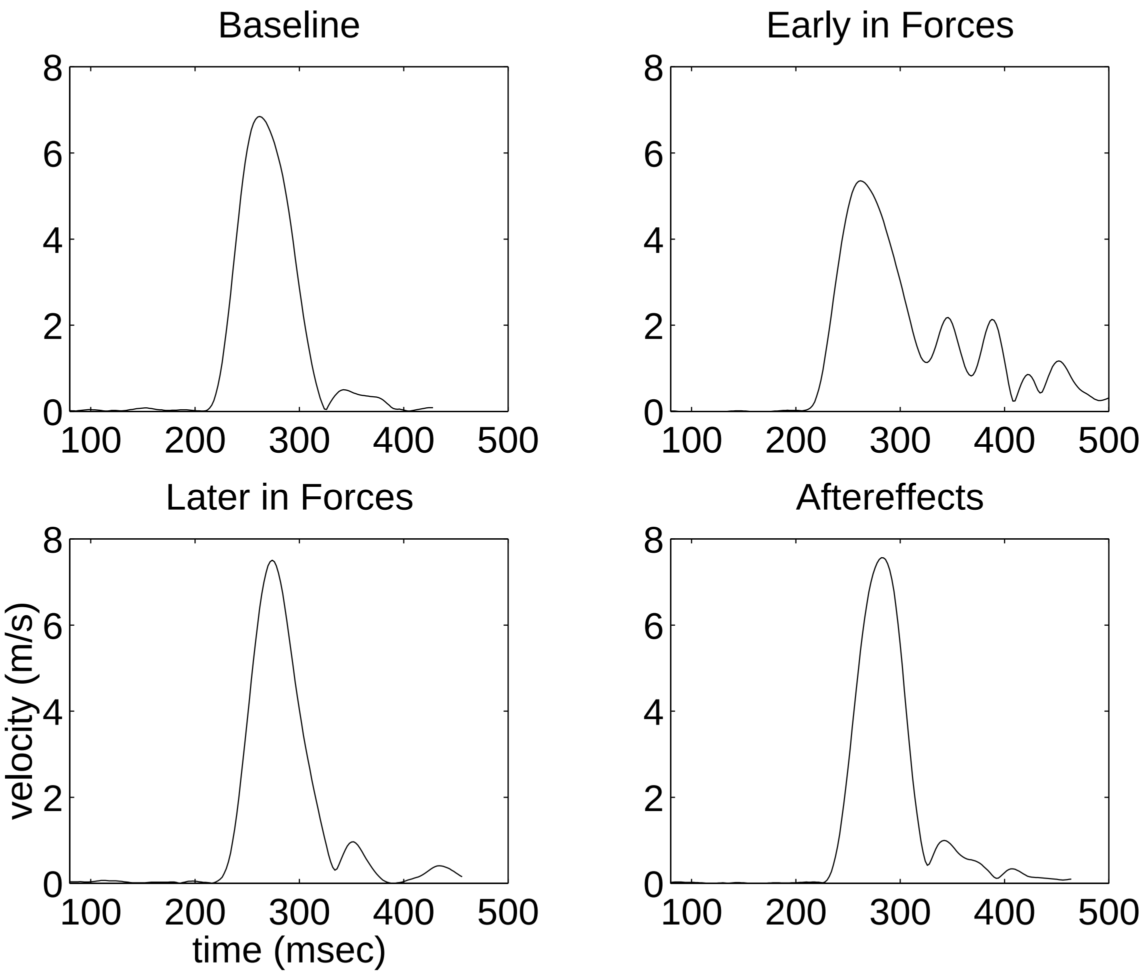

Figure 3-5: Typical velocity profiles when only the latter half of the movement was perturbed. Without perturbations, the velocity profile was a smooth unimodal curve. The initial trajectory under forces contained multiple peaks, but with training it transformed back to the curve that was observed without perturbation.

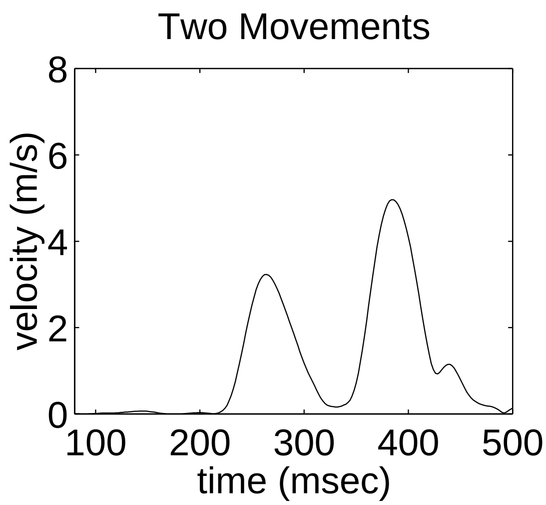

Figure 3-6: The typical velocity profile when two continuous movements are executed (left). It is compared to the profile when one continuous movement was executed for the same space (right).

epoch as compared to the previous experiment. One training epoch was conducted with interleaved catch trials, and the results are shown in Figure 3-7. With the via-point, the first half of the aftereffect trajectories contained no distortions. When these trajectories are compared to the ones from Figure 3-4, it is clear that the effects transfer more significantly within one movement for the same force condition. Thus the size of the general primitive is different depending on how the movements are executed. In the following experiment, two opposite forces were introduced within one movement to determine whether two opposite forces could be learned within one continuous movement.

Two Opposite Perturbations

By perturbing part of a movement, one continuous movement was globally affected. To investigate whether two different perturbations can be learned separately within one movement, two regions of the workspace were assigned with opposite force perturbation directions as shown in Figure 3-8. The first 8 cm of the movement was exposed to the force to the right and the last 12 cm of the movement was exposed to the force to the left. The viscosity matrix was set to allow smooth transition between two force directions. As in the previous experiment, one epoch of perturbation training was conducted following a baseline epoch, and the results are shown in Figure 3-9. Initially, exposure to the forces caused two opposite directional distortions. As the training went on, the movement became more continuous. When the perturbation

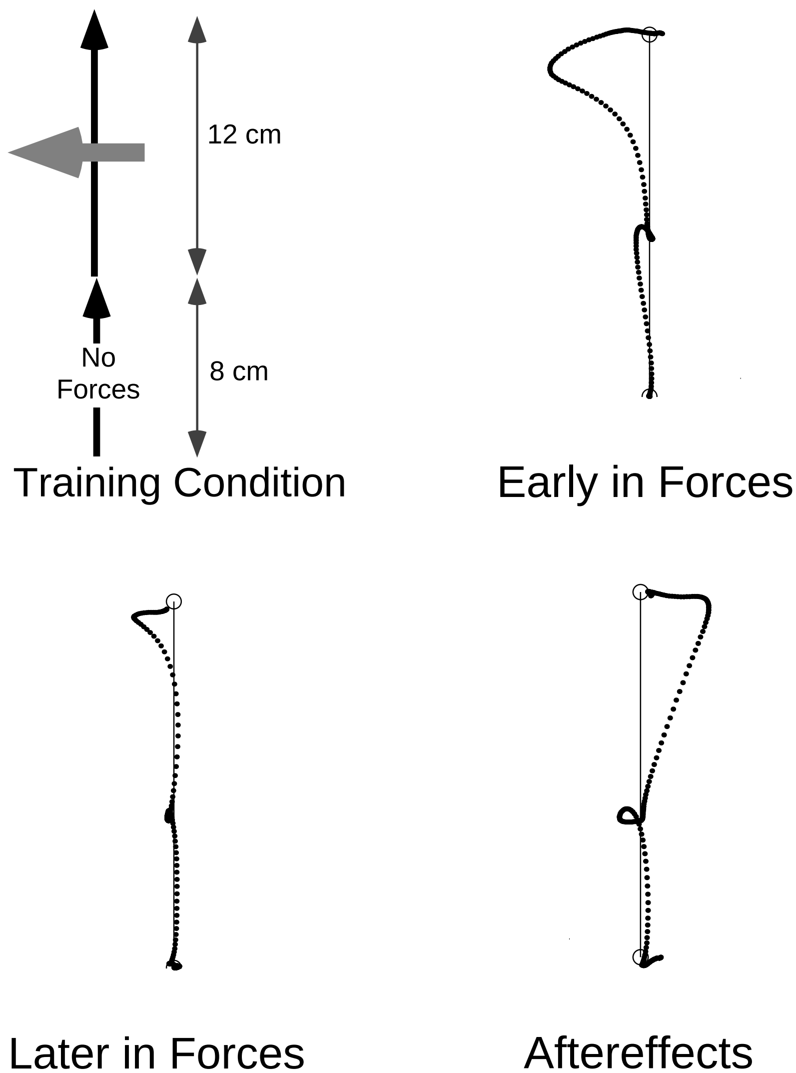

Figure 3-7: The perturbation forces are applied only above the via-point. The initial trajectories were distorted toward the direction of the force, and the aftereffect trajectories showed the mirror image of the initial trajectories. The bottom half of the aftereffect trajectories did not contain any distortions.

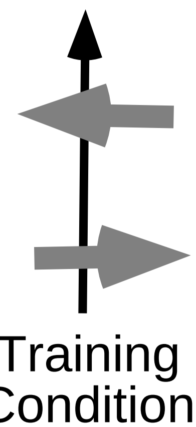

Figure 3-8: The forces are assigned to perturb the first 8 cm of the movement to the right and the last 12 cm to the left. The gain was adjusted to have a smooth transition between two force directions.

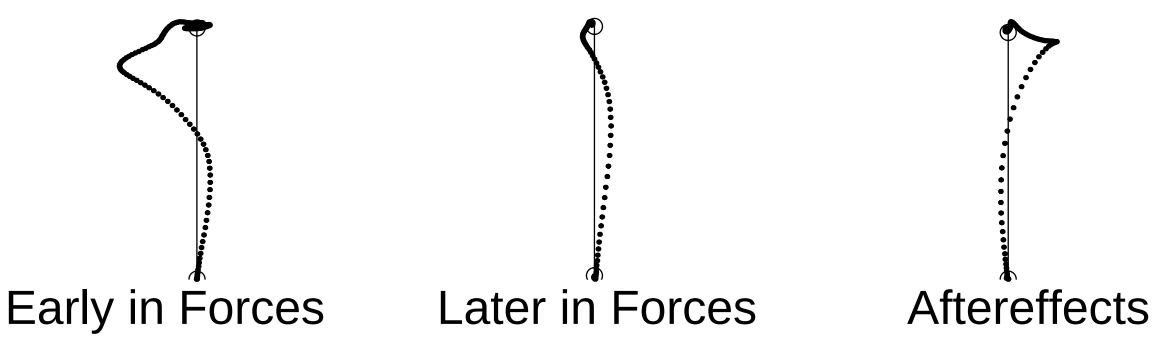

Figure 3-9: The initial exposure to the forces affected the movement to distort to the right and then to the left matching the direction of the perturbation. With training, the movement became somewhat arc-shaped but more straight. The aftereffects contained the opposite force directions of the two directional distortions.

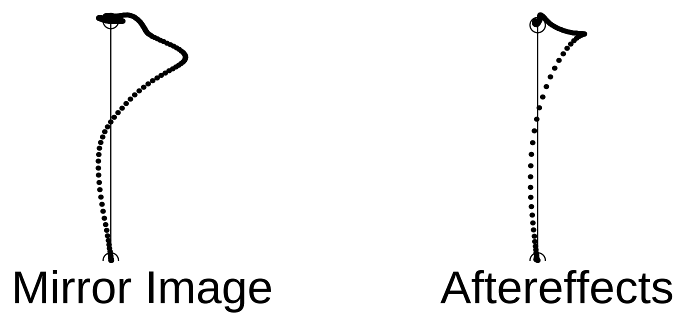

Figure 3-10: The mirror image of the initial trajectory under perturbation compared with the aftereffect trajectory.

was removed, the movements seemed to have two directional aftereffects, matching the opposites of the force directions experienced. The mirror image of the trajectory early in forces is plotted in Figure 3-10 to compare with the aftereffects. Their general shapes were similar. Thus the arm produced the correct torques to compensate for the external perturbations, showing that two different forces can indeed be learned within one continuous movement.

3.4 Experiment HF-COM: Components Learned during Exposure to High Frequency Perturbation

The experiments in the previous section demonstrated that it is possible to learn multiple disturbances within one continuous movement. If the spatial frequency of the perturbation forces is increased, the frequency exceeds the frequency of the spatial primitives and the environment should become not learnable.

For a continuous movement, the influence of inertia must be accounted for. With the inclusion of the inertial factor, the size of the primitive must become dependent on other factors such as velocity of the movement and mass of the arm. Therefore, the exact size of the primitives during one continuous movement is more complex to identify. Thus, instead of quantification of the primitives, experiments were conducted to understand the characteristics of spatial generalization under high frequency force perturbation. Specifically, the properties of movement under non-learnable conditions were investigated. When the perturbation is not learnable, the arm must produce different sets of torques to cope with the situation. Can an internal model of the non-learnable environment be built?

There are a few possibilities of ways to cope with an environment that is not learnable. First, the nervous system may allow the arm to passively respond to the high frequency field, yet retain absolutely no information about the field. If this is true, when the frequency of the force perturbation exceeds the primitive frequency there should be no aftereffects observed.

Second, it may be that the nervous system can produce torques to respond to the high frequency perturbations but cannot retain the information as an internal model. If this is true, the aftereffects should not contain any distortion, but the movement should become straight with training. This scenario is unlikely to occur because if the torques are produced in response to each perturbation, then the response has to be stored somewhere in the nervous system.

Finally, it may be that the nervous system can perceive the high frequency perturbations and extract information that does not necessarily match the perturbation. The extracted information would be useful in coping with the situation, and it should there by build an internal model of the simplified or altered environment. In this case, the aftereffect observed should contain distortion matching the internal model, not necessarily the environment.

3.4.1 High Frequency Field Setup

The setup described in Figure 3-1 could not be used for high frequency perturbation as discussed. Therefore, the force field setup was not trivial. The force field must be able to produce smooth and continuous but high frequency disturbance to the hand.

To make the perturbation force direction independent from the hand location, the force direction was fixed to the spatial location while the force amplitude remained proportional to the hand velocity. The highest frequency field was designed to be not learnable, and its force directions were assigned to be completely random and uniformly distributed throughout the workspace. Random force directions were assigned with some separation within the workspace and were linearly interpolated. This strategy allowed the perturbation fields to be smooth and continuous but with high frequency components still preserved in the force directions.

The workspace of the manipulandum was 30 cm x 24 cm and the force direction was assigned every 2 cm in both a vertical and horizontal direction, creating 16 x 13 force assignments and 180 interpolation squares. Within one square, four force directions from each corner were linearly interpolated. The initial random directions were created with MATLAB between -180 to 179 degrees. To create related but lower frequency fields, the field was low-pass filtered. The field was filtered multiple times, using a filter of size 6 cm x 6 cm, to create fields with different frequencies. The filtering can be visualized using Figure 3-11. Force directions assigned in Figure 3-11 are plotted onto the workspace, and the force fields are shown in Figure 3-12. The top field was the one which has not been filtered and was the highest frequency field used for the experiment. This random field was filtered 19 times to create 19 different force fields. Including the non-filtered field, all the force fields are labeled with the number of times that they were filtered. For example, the field that was filtered 5 times is called Field 5. The non-filtered field is called Field 0. In Figure 3-11, the middle field was filtered 5 times, and the bottom field was filtered 18 times.

All the filtered fields' frequencies are plotted in Figure 3-13. Because the filtration causes all the directions to merge to the half way point, which is 0 degrees, the low frequency field is almost equivalent to the force field shown as the force field A in Figure 3-1.

3.4.2 Experiments

Six groups of subjects were tested for Fields 0, 2, 5, 8, 13 and 18, where the numbers represent the number of times the random field is filtered. Eight right-handed individuals, ranging in age from 18 to 38 years, were tested for each field. Subjects were asked to make one continuous reaching movement to a target that flashed on the screen. They were given 0.5 +/- 0.05 seconds to make a movement, and the distance from the origin to the target was 10 centimeters. There were a total of 4 reaching directions to 0, 45, 90, and 135 degrees from the origin located in the middle of the workspace.

One epoch of training consisted of 192 trajectories and the subjects were trained for a total of four epochs within one training session. In order to assess baseline performance, the movements in the first epoch were not perturbed, and the subjects were consecutively exposed to the force fields for the next three epochs. The last force epoch contained catch trials. In order to observe the difference between the presence and absence of visual feedback, half of the catch trials did not have hand cursors displayed on the screen.

The hand trajectories of the subjects were illustrated in Figures 3-14, 3-15, 3-16, 3-17, 3-18 and 3-19. All trajectories were distorted when the perturbation was initially introduced and the distortions matched the force directions. When the fre-

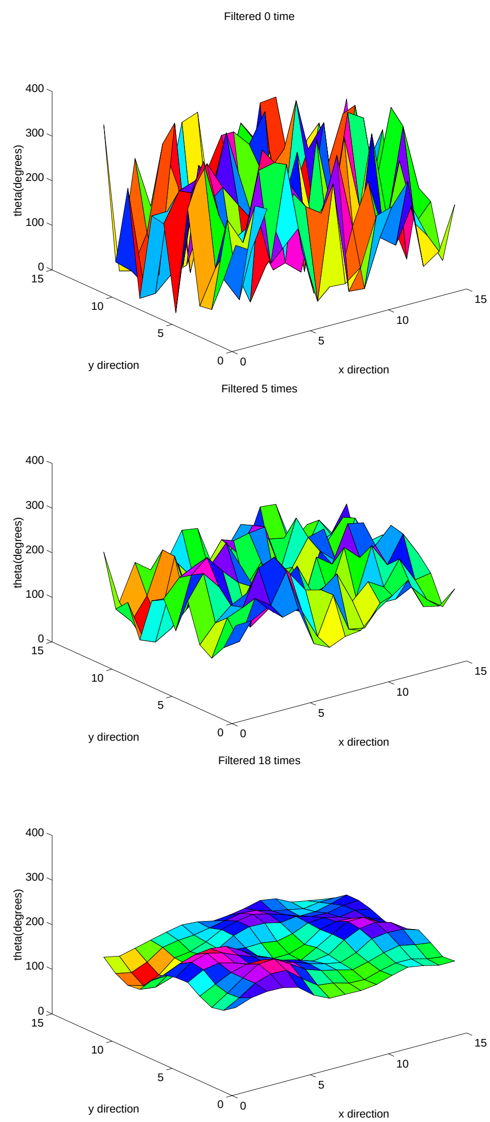

Figure 3-11: Filtration of force directions using low pass filter. Top Figure: uniformly distributed random values from 0 to 359 degrees. These values are shifted down for 180 degrees to get the mean value at 0 degrees. Middle Figure: low pass filtered version of the top figure. It has been filtered 5 times. Bottom Figure: low pass filtered 18 times.

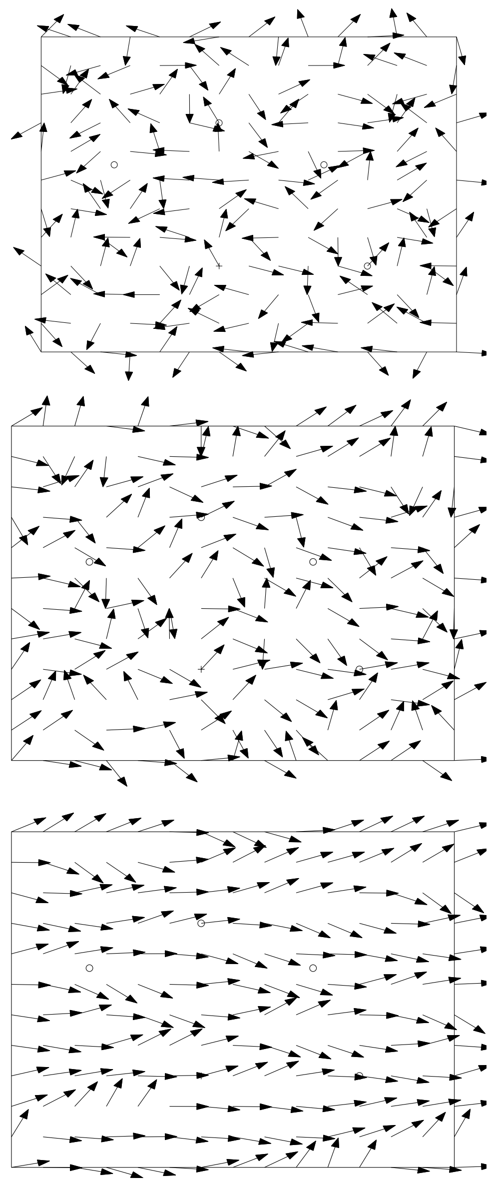

Figure 3-12: Filtration of force directions using a low pass filter. Top Figure: uniformly distributed random values from -180 to 179 degrees. This is the high frequency field (HFF). Middle Figure: low pass filtered version of the top figure. It has been filtered 5 times (MFF). Bottom Figure: low pass filtered 18 times. This is the low frequency field (LFF).

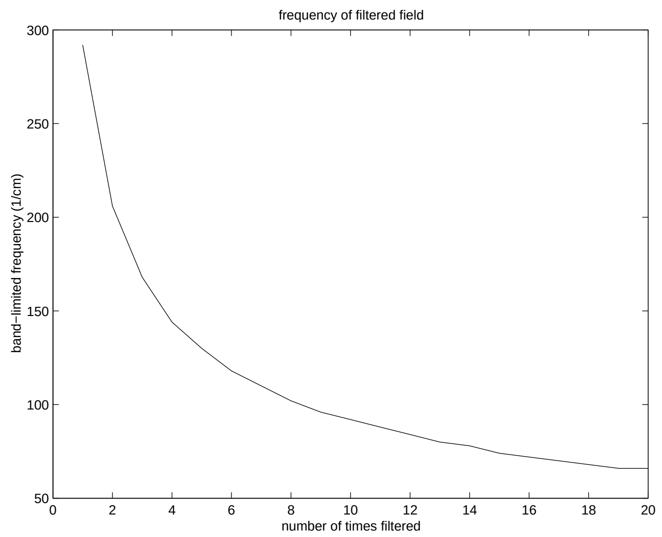

Figure 3-13: Filtered fields' spatial frequency was plotted.

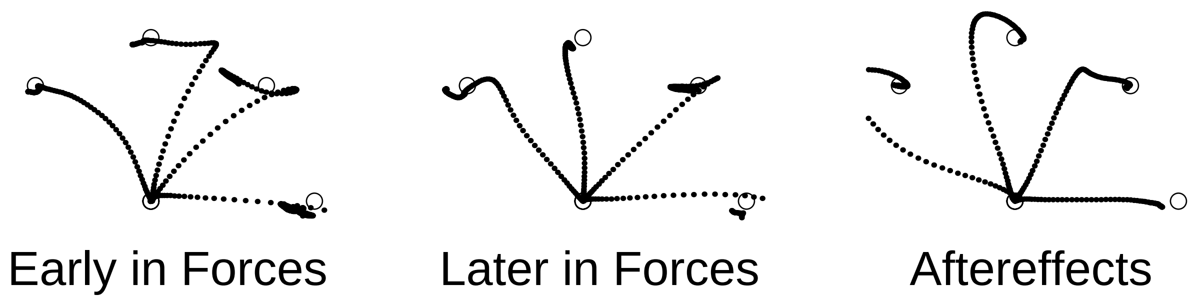

Figure 3-14: Hand trajectories for Field 18. Left to right: initial trajectories under perturbation, later trajectories under perturbation, and aftereffect trajectories during catch trials. The aftereffect is the mirror image of the initial trajectory showing that the field is learnable.

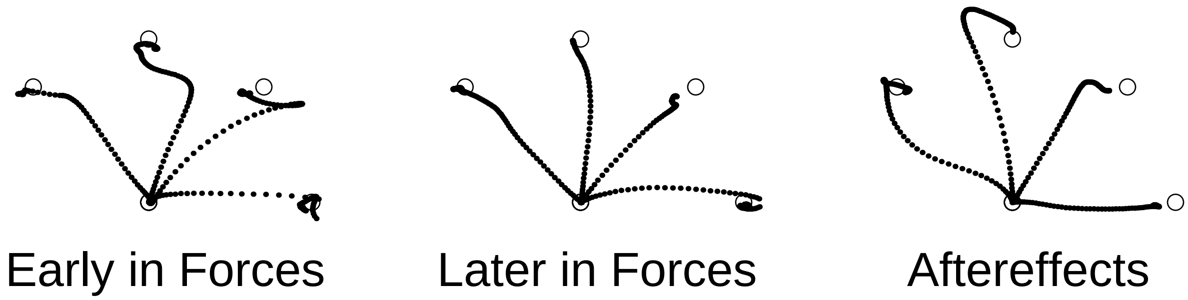

Figure 3-15: Hand trajectories for Field 13. Left to right: initial trajectories under perturbation, later trajectories under perturbation, and aftereffect trajectories during catch trials. The trajectories are similar to the response seen for Field 18. The frequency of Field 13 is not very different from Field 18 shown in Figure 3-13.

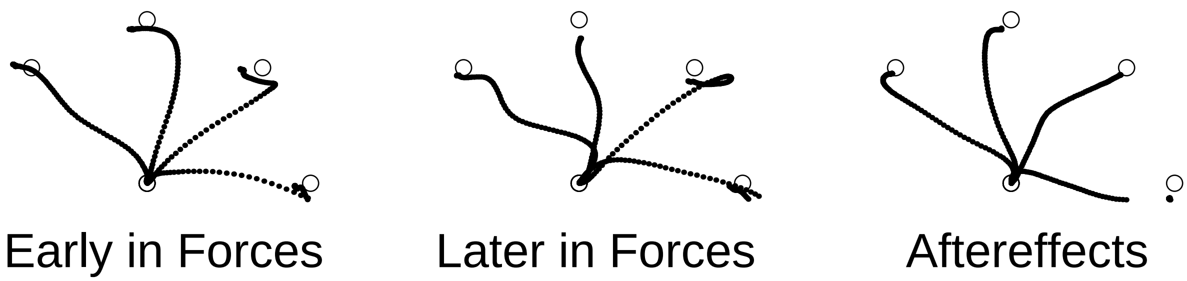

Figure 3-16: Hand trajectories for Field 8. Left to right: initial trajectories under perturbation, later trajectories under perturbation, and aftereffect trajectories during catch trials. The effect is rather smooth to 180 degree direction, but the magnitude of distortions is smaller than for Figure 3-15.

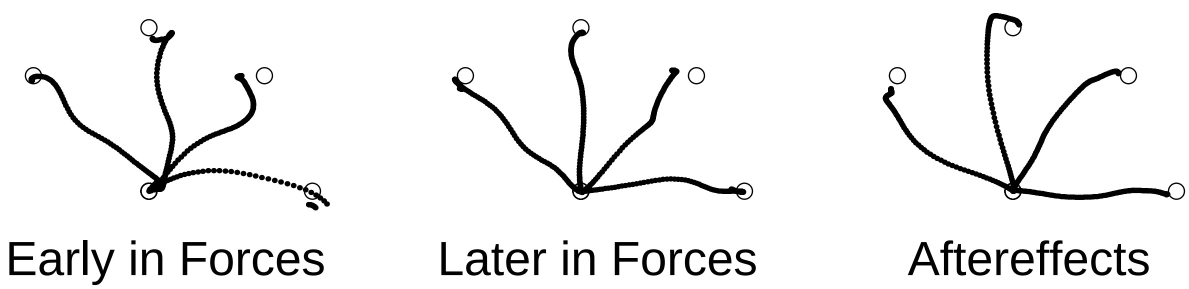

Figure 3-17: Hand trajectories for Field 5. Left to right: initial trajectories under perturbation, later trajectories under perturbation, and aftereffect trajectories during catch trials. Initial trajectories show bumpiness corresponding to the force directions. However, the aftereffect trajectories do not contain any of the bumps.

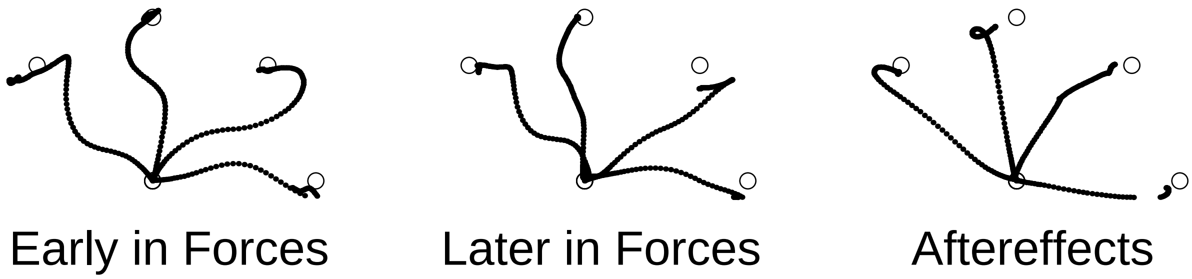

Figure 3-18: Hand trajectories for Field 2. Left to right: initial trajectories under perturbation, later trajectories under perturbation, and aftereffect trajectories during catch trials. The initial trajectories contain bumpy distortions. The aftereffects toward 180 degree direction are still observable and the trajectories are smooth.

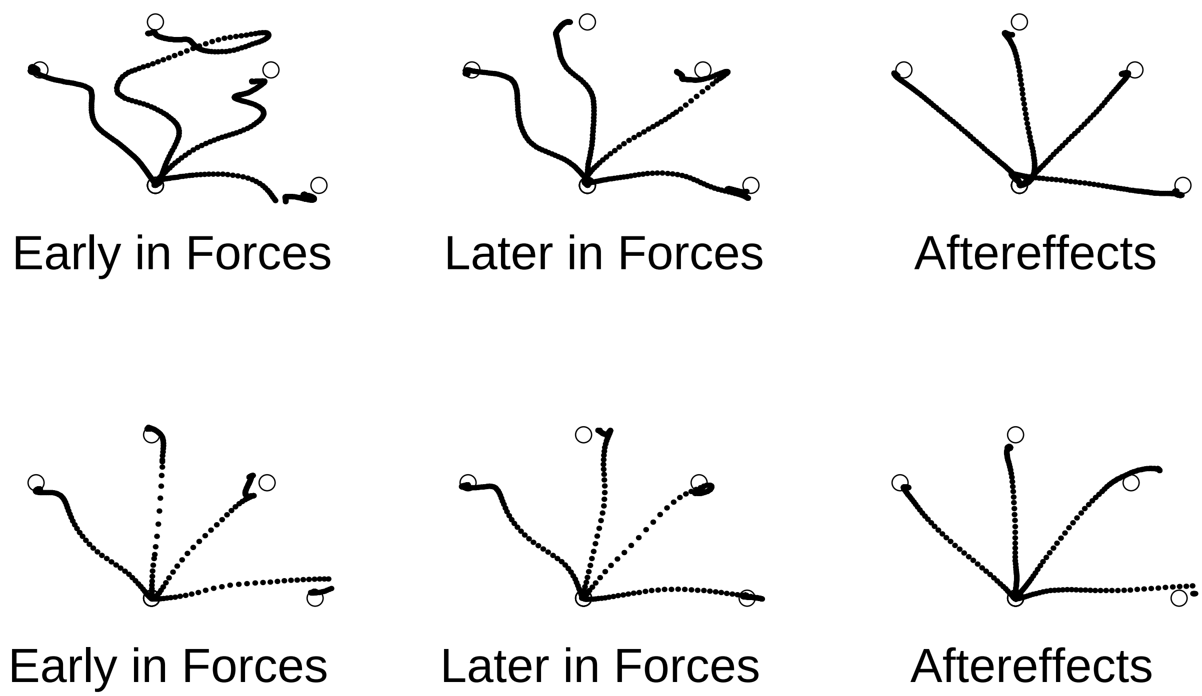

Figure 3-19: The trajectories for Field 0. The top row shows the trajectories for subject 1; The bottom row shows the trajectories for subject 2. From the left, initial trajectories under perturbation, later trajectories under perturbation, and aftereffect trajectories during catch trials. Subject 1's trajectories later in training are still quite distorted and the aftereffect trajectories did not show any distortions or bias toward any directions. Subject 2's trajectories were close to being straight through out the training, but aftereffect trajectories still did not show any sign of learning.

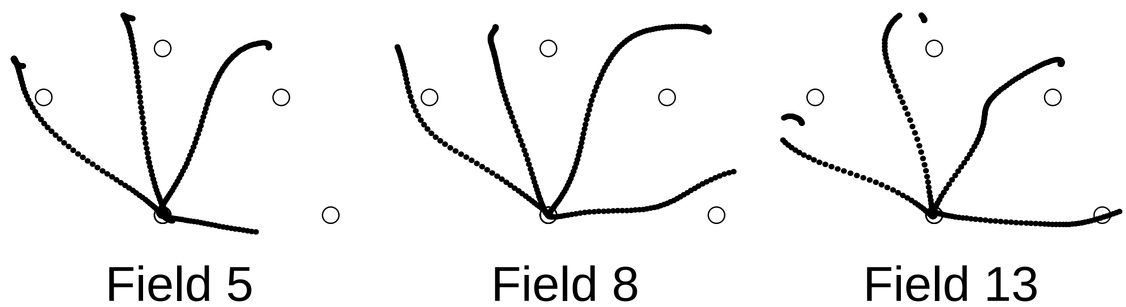

Figure 3-20: Hand trajectories during catch trials without visual feedback of the hand location. From left to right: for Fields 5, 8, and 13. The trajectories did not contain the hook at the end of the movement most of the time. When the distortion is so large that the arm movement is obviously off, the correction is made again at the end of the movement.

quency was low enough, the force field was learned and catch trials showed aftereffects that were mirror images of the initial trajectories. As the frequency increased, the initial trajectories were affected more by small disturbances or bumps. As training progressed, the trajectories became straighter, showing that the perturbations may have been learned. However, the aftereffects did not correspond to the bumps observed during initial exposure to the perturbations, but instead the distortions were to the 180 degree direction for all filtered fields. These distortions decreased in magnitude as the frequency of the force field increased. For the un-filtered field, the distortion was not observed in the catch trial trajectories.

When the visual feedback of the subjects hand location was removed from the computer screen during catch trials, the trajectory shapes changed as shown in Figure 3-20. Most of the trajectories did not contain the hook at the end of the movement. However, some hooking motions were observed for lower frequency fields where the aftereffect trajectories contained more distortions. When the distortion was large enough, subjects seemed to use the proprioceptive sensory information or visually located their arm position to determine if the movement was severely off in one direction, and made a hooking correction movement. This correction was always made when visual feedback was present informing the amount and direction of the distortion in their movements.

For very high frequencies, some subjects co-contracted their arm muscles to execute nearly straight movements during the training sessions, as shown in the bottom row of Figure 3-19. This co-contraction was obvious in the way the subjects held the manipulandum. Concurrently, their peak velocities was significantly higher than

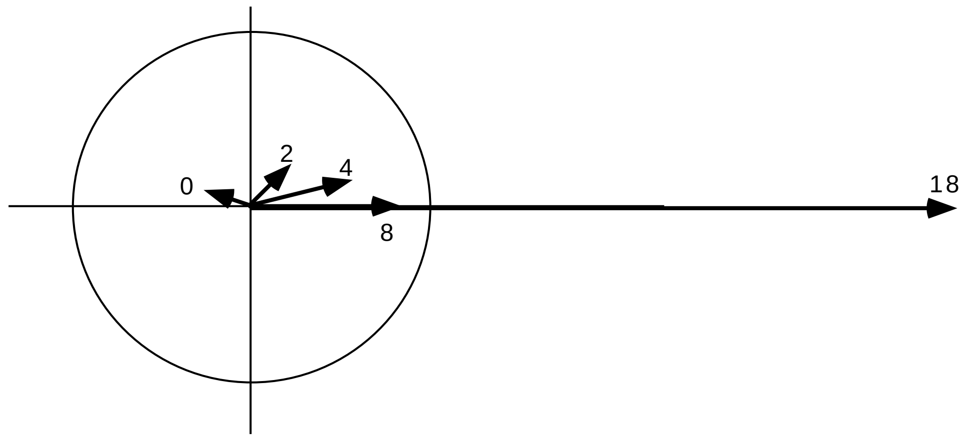

Figure 3-21: When all the forces at corners of interpolation squares are integrated, the forces add up to the 0 degree direction because of the filtering process. The numbers on the arrows are the field numbers. The magnitude of the integrated arrow toward the 0 degree direction increases as the frequency of the field gets lower.

the baseline trajectory velocities. The subjects who did not co-contract their muscles were greatly affected by the forces and their trajectories were severely distorted, as shown in the top row of Figure 3-19. In either case, the high frequency force field was not learned.

What do the distortions observed during catch trials represent? The amount of distortions decreased with increase in frequency. There are two hypotheses to explain this behavior. First, the increase in frequency disturbs the amount of learning that could take place. The second hypothesis is that learning occurs fully, but the magnitude of the component being learned decreases. As described above, the most filtered fields contain bias directions to 0 degrees. Figure 3-21 shows the result direction and the magnitude when all forces assigned at corners of interpolation squares are integrated together. As the frequency decreased, the magnitude of the integrated forces toward 0 degrees increased. This finding matches the results observed during catch trials for all the fields.

When the frequency of the perturbation forces were increased below the size of the primitives, the field became not learnable. When the environment could not be learned, instead of ignoring the sensory inputs completely, the nervous system seemed to have learned information of the environment as if the field was integrated.

Group #	*First Field*	*Second Field*	*Third Field*
1	18	5	0
compared with	0	0	0
2	18	5	2
compared with	2	2	2
3	18	9	5
compared with	5	5	5

Table 3.2: The three different sequential conditions evaluated. The numbers correspond to the field numbers. The numbers correspond to the number of times the field was filtered. The results at the end of the third field are compared to the results from non-sequential experiments.

3.5 Experiment HF-SEQ: Sequential Learning of High Frequency Perturbation

In the last set of experiments, the results indicated that when the unlearnable high frequency force perturbation was presented, the nervous system learned the forces that corresponded to the integrated version of the high frequency field. Thus the internal model was built not specifically matching the environment, but contained useful information to cope with the situation and still allow the task to be completed.

If these fields were introduced in sequence such that low and related frequency fields were imposed prior to the more difficult or non-learnable force fields, could the grain size of the responses become smaller? In other words, can the bumps present in the hand trajectories during the initial exposure to the forces be learned instead of being integrated?

Three sequential conditions are compared with the results from learning Fields 0, 2, and 5 without prior exposure to the lower frequency fields. The sequences that were tested are tabulated in Table 3.2. The catch trial trajectories for Fields 0, 2 and 5 after sequential exposure to related lower frequency fields are shown in Figure 3-22. Despite such sequential exposures, none of the catch trial trajectories displayed any components indicating responses to smaller force direction changes.

Sequential learning did not increase the spatial precision of the movement response to force perturbation. However the catch trial trajectories exhibited more aftereffect distortions than did the catch trials from non-sequential learning. In the next section, this difference is analyzed further to determine whether perturbations that are beyond our ability to learn can still be perceived.

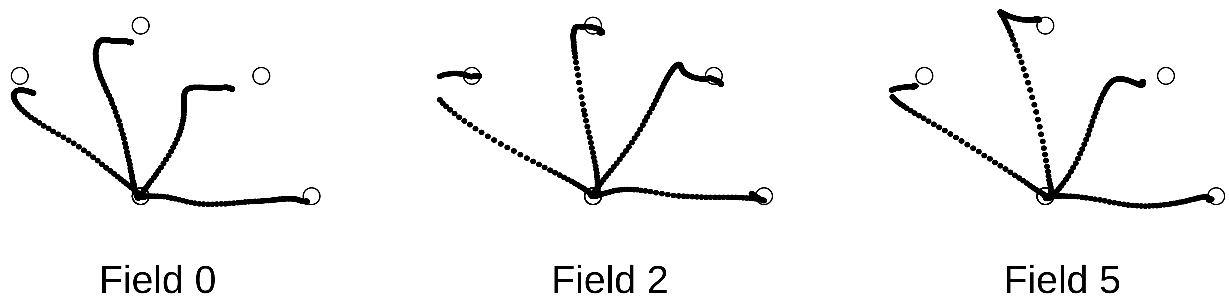

Figure 3-22: The catch trial trajectories for Fields 0, 2 and 5. Despite the exposure to the sequence of fields that are related, the aftereffect trajectories did not contain any bumps corresponding to individual force directions.

3.6 Experiment HF-PER: Perception and Learning under High Frequency Perturbation

When the afferent information is *learned* the internal model is transformed to match the external stimuli. In contrast, if the information is *perceived*, the internal model is affected but not necessarily changed. The assumption normally made is

$$P \leftrightarrow L \tag{3.2}$$

where P is the perceivable information and L is the learnable information. However, it is possible that

$$L \subset P \tag{3.3}$$

that if the information is learnable it is perceivable, but it being perceivable does not imply learnability. In this experiment, an environment already known as non-learnable is presented to determine if there is a non-empty

$$P \cap \overline{L}. \tag{3.4}$$

From Experiment HF-COM, the non-filtered force field was shown to be not learnable. In this section, I address whether the non-filtered field is perceivable by comparing results from six sets of experiments shown in Table 3.3. The fields are abbreviated to HFF (high frequency field), MFF (medium frequency field), LFF (low frequency field), OHFF (opposite high frequency field), IHFF (integrated high frequency field), and null (no force perturbation). The HFF, MFF, and LFF correspond to Fields 0, 5, and 18 respectively. The OHFF was the same random field as Field 0, but all force

Group #	*First Field*	*Second Field*	*Third Field*
1	HFF	HFF	HFF
2	LFF	LFF	LFF
3	LFF	MFF	HFF
4	LFF	MFF	null
5	LFF	MFF	OHFF
6	LFF	MFF	IHFF

Table 3.3: The groups tested with different frequency perturbation force field. HFF is high frequency field, MFF is medium frequency field, LFF is low frequency field, null is no force applied, OHFF is the opposite of HFF (same frequency, but the force direction is inverted), and IHFF is the integrated force field of the HFF.

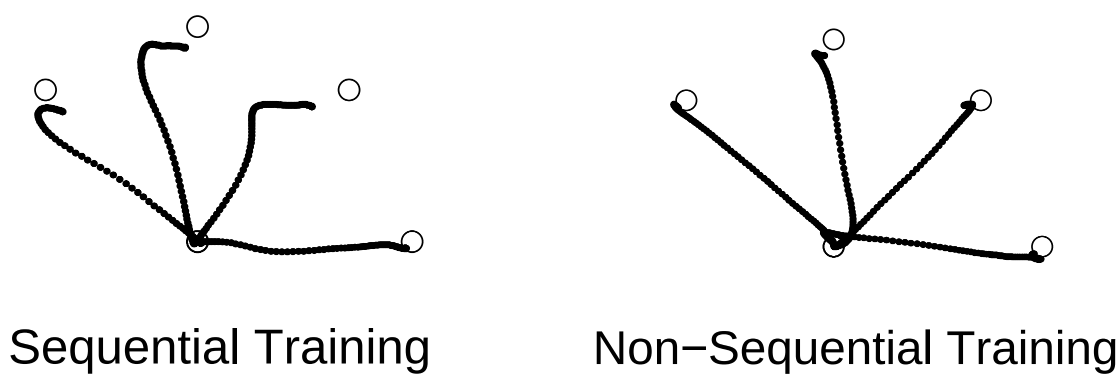

Figure 3-23: The aftereffect trajectories for Field 0. The left side shows the trajectories after sequentially exposed to Fields 18 and 5 prior to Field 0. The sequential experiment's aftereffect trajectories contain significantly more distortions.

directions were inverted, and the IHFF was a low frequency field with the force direction and the magnitude matching the integrated force of the HFF. After one baseline epoch, three force epochs with the force condition specified were conducted. At the end of the last force epoch, catch trials were conducted to observe the aftereffects.

Groups 1 and 2 are identical to the Experiment HF-COM Fields 0 and 18 experiments, where the results are illustrated in Figures 3-19 and 3-14. Group 3 is identical to Experiment HF-SEQ Group 1, and the aftereffects trajectories are re-illustrated in Figure 3-23 comparing the effects observed for Group 1. As shown, the aftereffect trajectories did not contain any high frequency information, but the trajectories observed for the sequential exposure (Group 3) contained a significant amount of distortion to the 180 degree direction compared to the non-sequential exposure to the same field (Group 1). This distortion corresponds to the aftereffects observed when subjects were exposed to the LFF alone as in Group 2 (Figure 3-14). This is

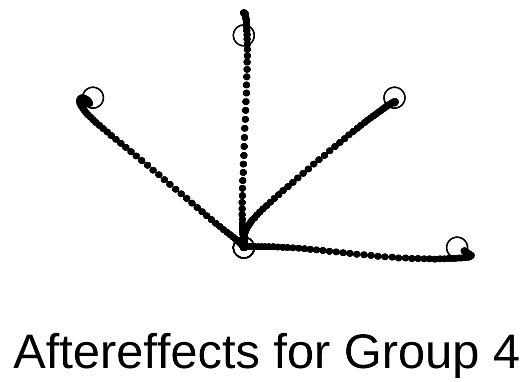

Figure 3-24: The aftereffect trajectories for Group 4 in Experiment HF-PER. If the null field was exposed to the subjects instead of the HFF as for Group 3, the effects from the previous fields are quickly erased.

surprising because the exposure to the HFF alone does not produce these aftereffect trajectories.

The results from the first two groups showed that an internal model can be built for the low frequency field but not for the high frequency field. When the subjects were exposed to three related different force fields, starting from the learnable field and finishing with the unlearnable field, the effect for the LFF was retained whereas no information about the HFF was learned.

For Group 4, no force field was applied during the last epoch. If the last epoch is trained without perturbation, instead of the HFF as in Group 3, the aftereffects for the previous fields were quickly erased, as shown in Figure 3-24. From this experiment, it can be concluded that the HFF has an effect on the internal model even though it is not learnable. There are two possible explanations for how the byproducts of the HFF are causing such an effect.

The first possibility is that any force perturbations with high frequency components can disturb the washout process. To determine if this statement is true, a field with the same frequency but a different force field was created (OHFF) and was applied to the subjects in Group 5 instead of the HFF during the last epoch of training. As shown in Figure 3-25, the distortions from previous fields were completely erased.

Another possibility for this phenomena is that the HFF random force directions are not completely random and the slight bias in the integrated force direction still contributes to the retention of the previous field information. Random directions were created by a random number generator in MATLAB and when the directions

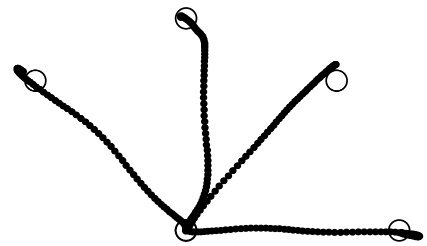

Aftereffects for Group 5

Figure 3-25: The aftereffect trajectories for Group 5 in Experiment HF-PER. If the unrelated high frequency force field is introduced instead of the related HFF, the distortions from previous fields were completely washed out.

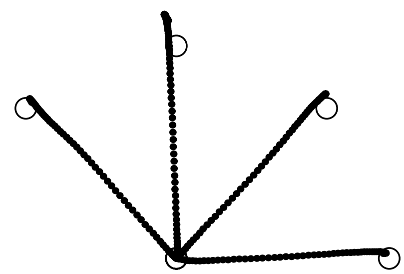

Aftereffects for Group 6

Figure 3-26: The aftereffect trajectories for Group 6 in Experiment HF-PER. If the integrated version of the HFF is introduced instead of the HFF, the distortions from previous fields were erased.

are integrated together, there is a slight bias to one direction as shown in Figure 3-21. Thus a field, IHFF, was designed to match the integrated forces of the HFF. If the force bias of the randomness in the HFF were causing the retention phenomena, this field should also have the same effect as the HFF. Group 6 was tested with the IHFF for last force epoch instead of the HFF, and the aftereffects were observed. As shown in Figure 3-26, the effect was again erased completely by exposure to the IHFF.

These results are remarkable because they show that when the force fields were related, the internal model built from the previous field was not erased. Together, the data suggested that a non-learnable high frequency field can affect the internal model thus perceived.

Parameter	*Human*	*Manipulandum*	*units*
link length (upper)	0.33	0.357	m
link length (lower)	0.34	0.337	m
COM link (upper)	0.165	0.179	m
COM link (lower)	0.170	0.169	m
Mass (upper)	1.92	0.024	Kg
Mass (lower)	1.52	0.024	Kg
Inertia (upper)	0.0141	0.0141	
Inertia (lower)	0.0188	0.0188	

Table 3.4: From Mussa-Ivaldi, et al. The parameters used for the simulation of the arm and the manipulandum.

3.7 Simulations

In the experiments with high frequency perturbations, distorted end point movements were observed under different frequencies. In order to verify the results, two levels of simulations were conducted. First, the movements executed under perturbations were simulated without the learning components. This simulation verifies whether the response to the high frequency perturbations is simply a mechanical response. If some neglected factors are significantly contributing to the generation of reaching movements, the simulation results should contradict the actual results. In addition, the model incorporated learning components to simulate the spatial generalization primitives defined in Chapter 2.

3.7.1 Parameter Calibration

The simulation was written in MATLAB. The model included a dynamic model of the manipulandum coupled with a dynamic model of a planar human arm with two degrees of freedom. Parameters such as inertia, mass, and length, were chosen from selected literature [Mussa-Ivaldi, et al., 1985] and are shown in Table 3.4. The code was written in a way that the Cartesian end point coordinates were converted to the robot and human joint coordinates first. Then the minimum jerk target trajectory was calculated with the assumption that the trajectory was a straight line from the origin to the target. The following equation was used to calculate the actual joint acceleration.

$$\ddot{\theta}_r = M_{tot}^{-1}((J_r^T(J_s^T)^{-1})(C - H_s\dot{\theta}_s - M_sQ) - H_r\dot{\theta}_r + \tau_{ext} + \tau_{int}) \qquad (3.5)$$

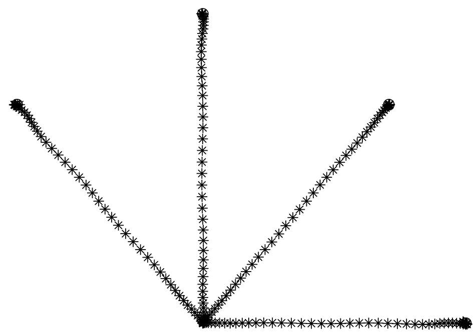

Figure 3-27: The simulated baseline trajectories.

where

$$M_{tot} = (M_r + J_r^T (J_s^T)^{-1} M_s J_s^{-1} J_r), \tag{3.6}$$

and

$$C = K(\theta_s^T - \theta_t^T) + B(\dot{\theta}_s - \dot{\theta}_t) + H_s\dot{\theta}_s + M_s\ddot{\theta}_s + (J_r^T(J_s^T)^{-1})^{-1}(M_r\ddot{\theta} + H_r\dot{\theta}_r), \tag{3.7}$$

where $\ddot{\theta}$ is the acceleration, $\dot{\theta}$ is the velocity, θ is the position, J is the Jacobian, M is the inertia matrix, H is the centrifugal and Coriolis matrix, Q is the torque and non-conservative forces, τ_{ext} is the externally applied forces, τ_{int} is the internal forces, K is the spring constant of the human arm, B is the damping constant of human arm, and the subscript s stands for subject, r for robot, and t for target. τ_{ext} was calculated by reading a direction matrix file and the equation,

$$\tau_{ext} = J_r^t F \tag{3.8}$$

where

$$F = Bv = BJ_r\dot{\theta}_r. \tag{3.9}$$

Finally the forward kinematics mapped the actual end point position into Cartesian coordinates.

First, the simulation was run without any external forces (Figure 3-27). The simulated trajectories were straight with a unimodal velocity profile as predicted. Second, external perturbation of the LFF was added as τ_{ext} in Equation 3.5, and the simulated trajectories are shown in Figure 3-28. It can be seen that the trajectories

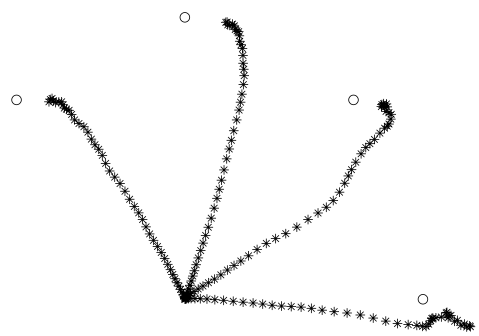

Figure 3-28: The simulated trajectory when the LFF was introduced.

were distorted in the direction of the forces. Parameters were calibrated to match the amplitude of the distortions observed during the experiments. The simulated trajectories can be compared to Figure 3-14.

When the HFF force perturbations were input as the external torque in the simulation, the simulated trajectories were distorted to multiple directions corresponding to the perturbation directions as shown in Figure 3-29. The simulated trajectories remarkably resembled the actual initial trajectories in the top row of Figure 3-19.

Finally, to simulate the trajectories of the subjects who showed evidence of co-contraction, the stiffness, K, was increased, as observed in the bottom row of Figure 3-19. As shown in Figure 3-30, as K increased the trajectory became straighter, corresponding to the behavior observed. The simulated trajectories under external force perturbation were qualitatively very similar to the initial trajectories observed for human subjects. Thus the theory is supported by the data.

3.7.2 Simulations of Spatial Generalization Primitives

In addition to the simulation described above, the learning process is simulated with the spatial generalization primitive defined in the last chapter. τ_{int} from Equation 3.5 signifies the torque change made within the nervous system to counterbalance the external torque. In the last section, τ_{int} was set to be 0 because the learning process was not included in the simulation.

The primitives were specified in the workspace with a fixed size in the direction and the location of the movement execution. The counterbalancing torque was updated at the end of every trial. For each primitive, a sensory error signal was calculated to

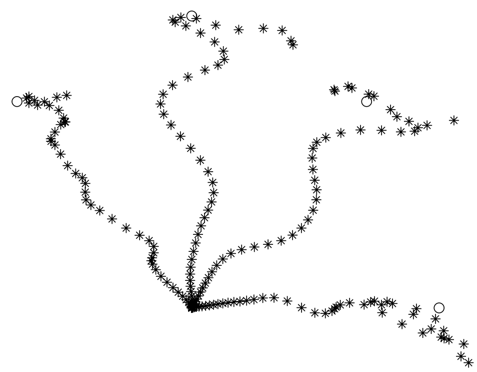

Figure 3-29: The simulated trajectory in the HFF. The trajectory is distorted significantly corresponding to the forces.

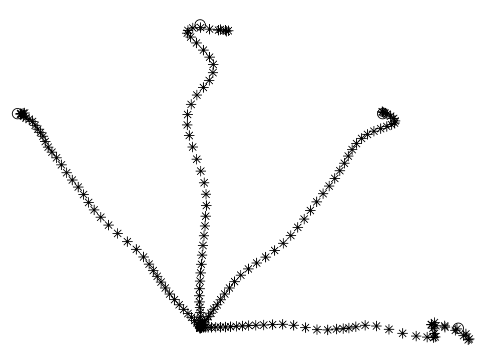

Figure 3-30: The simulated trajectory in the HFF with high K.

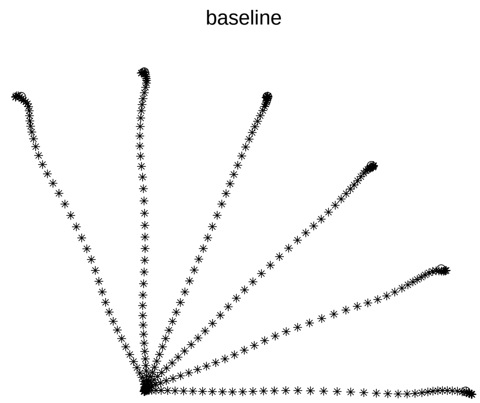

Figure 3-31: Six simulated baseline trajectories for Experiment DOM. They are 22.5 degrees away from each other.

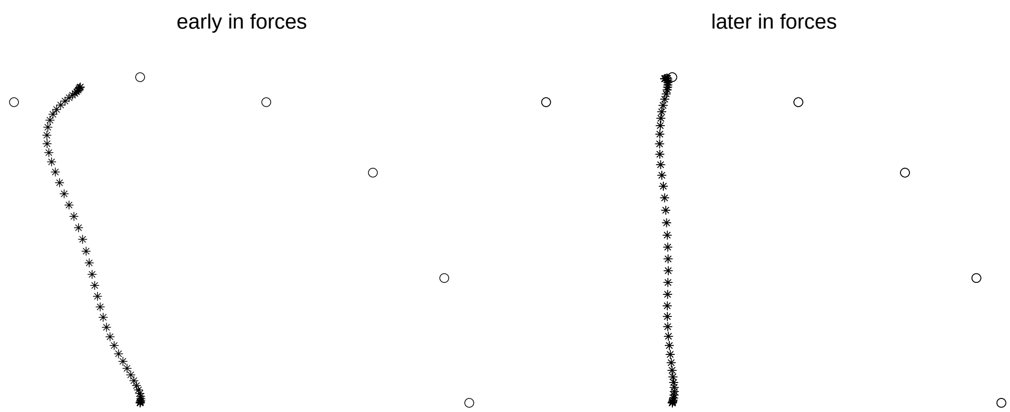

Figure 3-32: The simulated 90 degree movement was trained with the external forces to the left. Other trajectories were never trained. Initially the trajectory was distorted to the direction of the forces (left figure). After 100 iteration of training, the trajectory became straight (right figure).

make the correction for the next trial. The spatial error was calculated from the goal straight trajectory at 100Hz and multiplied with the weight which is determined by the primitive.

First, the experimental results from Experiment DOM is simulated. The simulation was done on six movements with the same origin. The movements were 22.5 degrees off from each other. The baseline trajectories are shown in Figure 3-31 The 90 degree movement was trained with the external forces while other trajectories were never trained under forces. The initial and the final trajectories in the forces are shown in Figure 3-32. With τ_{int} correction over time, the trajectory became straight again after 100 iterations.

To simulate the catch trials, the external torque, τ_{ext} was removed from Equation

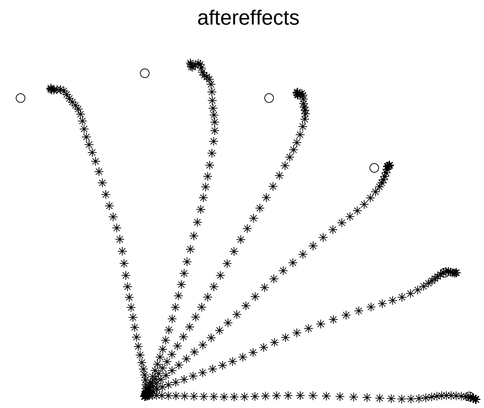

Figure 3-33: The simulated aftereffect movements. The trained movement contained the mirror image trajectory, while other trajectories also retained the effect from the 90 degree movement, but the effect decayed with distance.

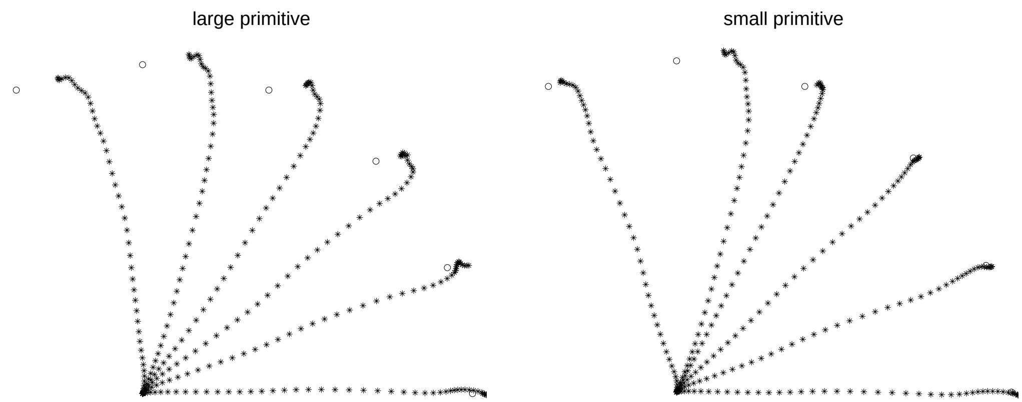

Figure 3-34: The simulated primitive size was varied to show different effects. When the primitive was large (left), the effect transferred more to other movements that were not trained. When the primitive was small (right), the transfer effect was not as significant.

3.5. As shown in Figure 3-33, the aftereffect for the 90 degree movement is an mirror image of the initial trajectory in the forces. Other five trajectories were also simulated after training. These trajectories also contained the effects from the 90 degree movement but the effect decayed smoothly with distance. This is the effect of the primitive designed.

In addition, the primitive size was varied to estimate the actual size observed in the experiment. When the primitive was set up too large or too small, as shown in Figure 3-34, the distance the effect transferred changed accordingly. After calibration, the primitive size was set to $\sigma = 19 degrees$.

When two primitives were introduced next to each other in Experiment DG-A,

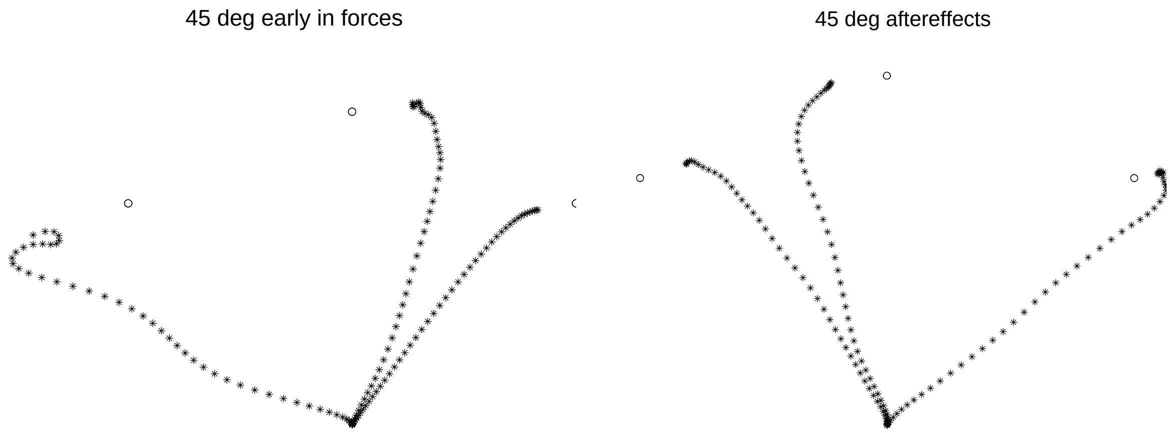

Figure 3-35: Simulated trajectories with 45 degree interference. The initial trajectories in forces and the aftereffects. All forces were learned separately.

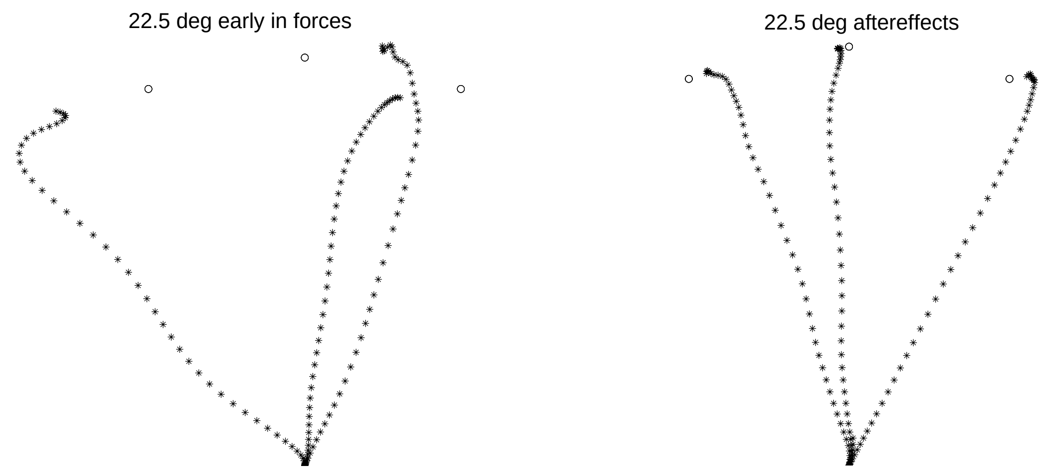

Figure 3-36: Simulated trajectories with 22.5 degree interference. The initial trajectories in forces and the aftereffects. The interference effect is observed.

the effects from both primitives were observed to sum. For the simulation, the effects were designed to be added linearly when they were overlapped. Using the fixed size primitives defined above, the 45, 22.5, and 7.5 degree interference trajectories were simulated and trained. The 90 degree movement was perturbed to the right while other trajectories were perturbed to the left. The initial trajectories in the forces and the aftereffects are shown in Figures 3-35, 3-36, and 3-37. All the forces were learned separately when the interference trajectories were set at 45 degrees. However, with decrease in the angle, the overlap of the primitives disturbed the adaptation for each force. When the interference angle was 7.5 degrees, the 90 degree trajectory contained small aftereffect matching the opposite forces from the ones experienced at the location. These effects simulated were comparable to the actual data shown in

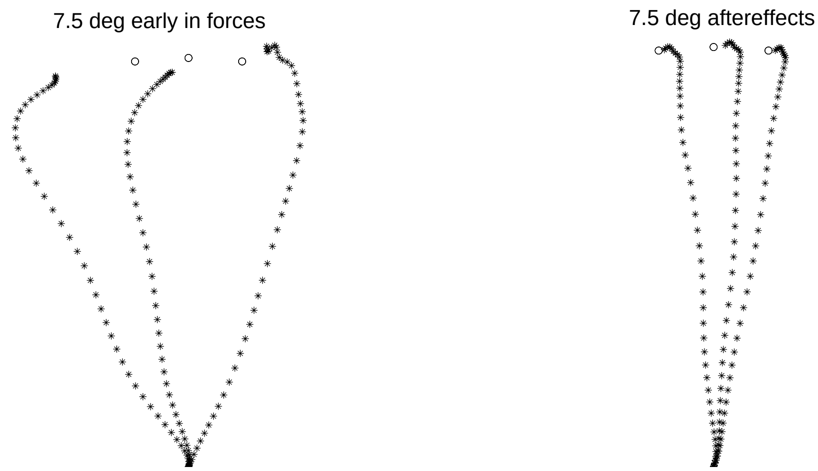

Figure 3-37: Simulated trajectories with 7.5 degree interference. The initial trajectories in forces and the aftereffects. The interference is so large that the 90 degree movement inherited the effect from the other trajectories.

Chapter 2.

3.8 Conclusion

In this chapter, the generalization effect for one continuous movement was investigated. Spatially high frequency force fields were designed to perturb the hand in multiple directions while subjects performed reaching movement. The results indicated that it is possible to learn multiple directional forces, but when the frequency of the perturbations was increased, the forces were unlearnable. When the frequency of the force field was higher than what is learnable, the integrated force direction was learned instead of the actual environment.

Chapter 4

Temporal Processes of Spatial Learning and Unlearning

4.1 Introduction

When a specific reaching task is mastered, humans can execute movements to an object every time without failure. When these mastered movements are analyzed, their hand paths are not consistent from one to the other. On the other hand, if a robot is to learn a reaching task, after the task is mastered, the end-effector takes an identical path every time. This is due to the fact that robot's movements are heavily driven by the inverse kinematics operation, which determines the exact path that should be taken. Thus it would be more calculation intensive to execute movements with different hand paths to achieve the same target every time for robots. From this observation, it is apparent that the learning scheme used for robots is not the scheme used for humans.

To understand humans' learning scheme for voluntary reaching movements, we must have a strategy to quantify adaptation. In this chapter, various components of the hand's paths are evaluated as a way to quantify adaptation. In addition, these quantified results are utilized to model the temporal process of learning.

When conflicting external forces are introduced, the previously learned information is erased [Brashers-Krug, et al., 1996]. This erasing effect can be considered as *un*learning of an environment. The unlearning process is equally crucial to understand as is the learning process in the nervous system, yet, it has not been investigated thoroughly in the past. Thus, the process of unlearning is quantified and analyzed in addition to the process of learning in this chapter. Furthermore, as discussed in the proceeding chapters, unlearning is necessary to perform contextual level adaptation.

4.2 Background

For multi-joint arm movements, the hand trajectory is first planned in visual coordinates and the hand moves approximately straight with a bell-shaped speed profile regardless of the intrinsic coordinates [Morasso, 1981]. When the goal path is curved, the hand path appears to be composed of a series of gently curved segments and the speed profile contains multiple peaks [Abend, et al., 1982].

Flash and Hogan [1985] proposed that voluntary arm movements are executed with the objective of minimizing the square of the magnitude of jerk,

$$C = \frac{1}{2}\int_0^t \left(\left(\frac{d^3x}{dt^3} \right)^2 + \left(\frac{d^3y}{dt^3} \right)^2 \right) dt. \tag{4.1}$$

This hypothesis is called "minimum jerk model." This model is based solely on the kinematics of the movement ignoring the dynamics of the musculo-skeletal system.

On the other hand, Uno, et al. [1989] proposed "minimum torque-change model" in which they hypothesized that the objective of the movement is to minimize the square of the rate of change of torque integrated over the entire movement,

$$C = \frac{1}{2}\int_0^t \sum_{i=1}^{n} \left(\frac{dz_i}{dt} \right)^2 dt, \tag{4.2}$$

where z_i is the torque command for the i-th muscle. This model incorporates the dynamical quantities such as arm length, payload, motor command, torque and external forces, which were ignored in the minimum jerk model.

The first model is shown to fit simple movements such as one continuous movements used so far in this thesis, while the latter model is shown to fit more complex movements.

Motor learning can be quantified as minimizing errors of motor parameters. In order to establish these errors, the baseline parameter values need to be identified. As a result, with an introduction to a new environment, some of the baseline values would be perturbed and would contain errors. Over extended exposure to the same environment, these errors may be minimized and the values would return to the baseline.

As one of the parameters, velocity profiles were analyzed previously [Shadmehr and Mussa-Ivaldi, 1994a,Gandolfo, et al., 1996]. This method was chosen because the velocity profiles are reasonably consistent for movements that are already learned. Many other movement components contain errors following introduction to a new environment. Using the experimental results from Chapter 3, various temporal and spatial components are evaluated in this chapter.

4.3 Temporal Variables as Learning Components

In this section, three temporal variables of the hand paths were investigated in an attempt to quantify adaptation. All the variables were analyzed with results from Experiments HF-COM, HF-SEQ and HF-PER from Chapter 3.

4.3.1 Velocity Profile Correlations

First, the velocity correlation method used by Shadmehr and Mussa-Ivaldi [1993] and Gandolfo [1996] was revisited.

The basic idea is to correlate the velocity profile of each trajectory under force perturbation to a desired or goal velocity profile. The desired velocity profile was assumed to be the most typical profile from the baseline epoch. To identify the most typical profile, each profile within the baseline epoch was correlated with all other baseline profiles. The profile with the highest correlation was chosen as the typical profile. The baseline epoch consisted of 192 movements and movements were usually similar from one to another.

To evaluate the errors, in order to produce a learning curve, the velocity profile of each trajectory executed with perturbation was compared to the typical profile. If the profile was identical to the typical profile, the correlation was 1. The similarity of two profiles was calculated by taking the inner product of the profiles. Given v_{base} is the typical baseline velocity vector and v_n is the velocity vector for movement number n with force perturbation, the similarity measurement was expressed as follows:

$$\rho_n = \frac{Cov(v_{base}, v_n)}{\sigma(v_{base})\sigma(v_n)} \tag{4.3}$$

for each n, where,

$$\sigma(v) = \|v - \bar{v}\| \tag{4.4}$$

$$Cov(v_1, v_2) = \langle v_1 - \bar{v}_1, v_2 - \bar{v}_2 \rangle \tag{4.5}$$

$$\langle v_1, v_2 \rangle = \sum_i v_{1i} \circ v_{2i} \tag{4.6}$$

where i is the index for each time step within one trajectory, and

$$\bar{v} = \langle v, v \rangle. \tag{4.7}$$

The similarity measure with the baseline, ρ_n, is called the correlation coefficient for trajectory n.

In Experiment HF-COM from Chapter 3, various high frequency force fields were imposed on the subjects' hand movements. The highest frequency field (HFF) was filtered multiple times to create related lower frequency fields. The low frequency field (LFF) was defined to be the field that was filtered 18 times.

Four directional movements were executed during the experiment. All the velocity coefficients were separated directionally to isolate habits that may have existed for one direction but not for the other directions. Thus, the velocity profiles were correlated with the typical profile of the same movement direction. Catch trial trajectories and the movement immediately after the catch trials were eliminated and the correlation coefficients were averaged with blocks of eight movements.

The velocity profile correlation analysis was conducted for the LFF and the HFF perturbations, and the results are shown in Figure 4-1. Both curves are an average of seven subjects trained. For the LFF, the curve increased rapidly at the beginning passing the mean value of the correlation coefficient after 8% of the training session. The total gain of the coefficient was 0.18, and the curve saturated at the end of training. The final coefficient value was 0.87, showing a significant amount of correlation with the baseline trajectories. In contrast, the HFF curve did not increase significantly with practice and the total gain in the correlation coefficient was 0.03 compared to 0.18 for the LFF.

In addition, learning curves for various other frequencies trained during Experiment HF-COM were examined. As the first analysis, the initial and the final coefficients are plotted in Figure 4-2. The frequency of the perturbation increases from the left to the right. Within one field, the left bar represents the initial value and the right represents the final value. Initially, the velocity profiles contain more errors for the lower frequency fields. This is not trivial because the higher frequency trajectories appear to have many more curves introducing multiple peaks in one velocity profile. Figure 4-3 shows the typical baseline profile, the initial LFF profile and the initial HFF profile. The correlation coefficient for the LFF curve is 0.65, while it is 0.88 for the HFF. These plots indicate that the global shape of the velocity profile is more perturbed with lower frequency force fields. At the end of the training session,

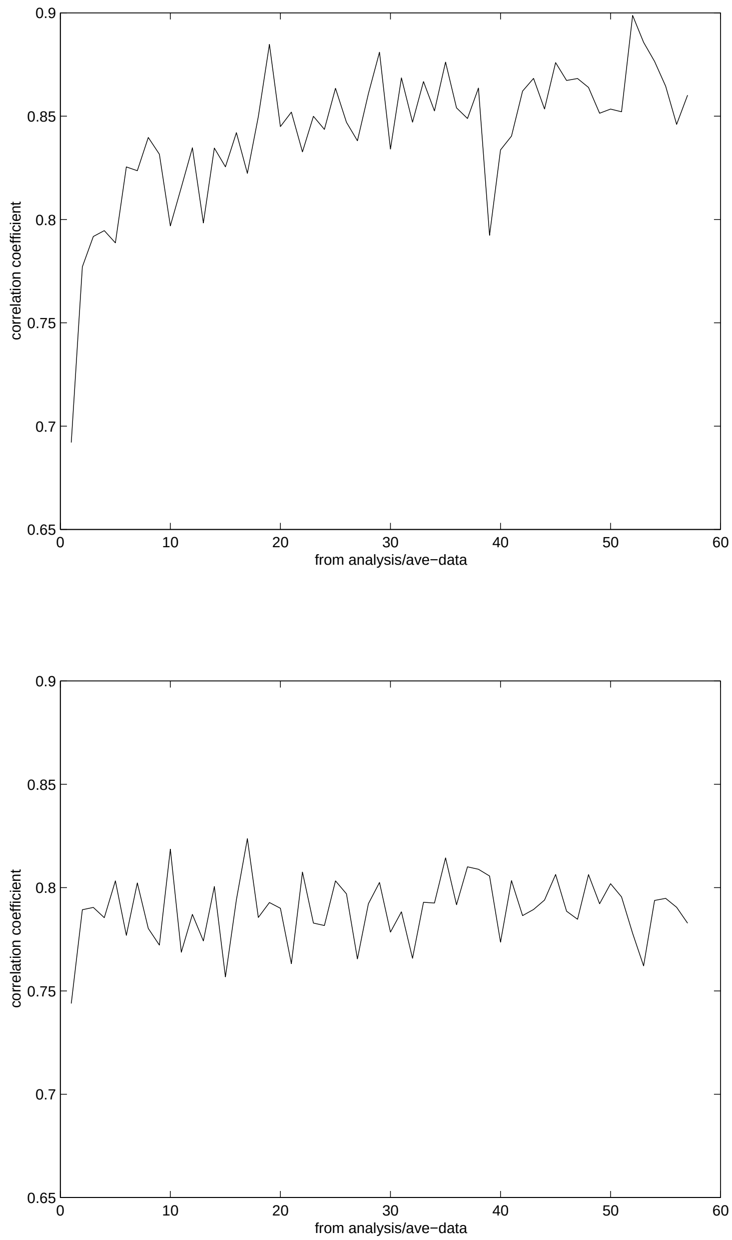

Figure 4-1: The LFF (top) and the HFF (bottom) learning curves of velocity profile correlation coefficient. The curves are an average of seven subjects who were trained in the LFF and the HFF. The x-axis represents the time (eight movements per unit) and the y-axis represents the velocity correlation coefficient.

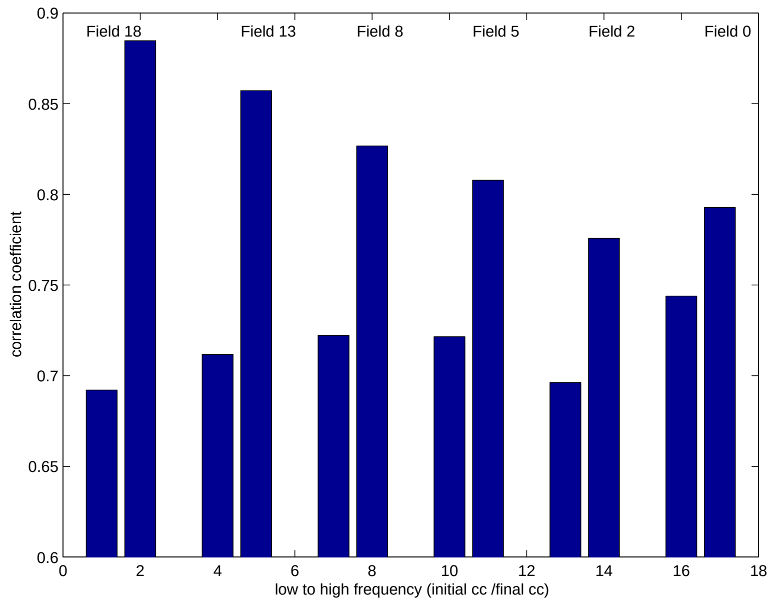

Figure 4-2: The initial and the final coefficients for various frequencies tested in Experiment HF-COM. The frequency of the perturbation increases from the left to the right. Within one field, the left bar represents the initial value and the right represents the final value. The initial values are higher for the higher frequency fields, and the final values are higher for the lower frequency fields.

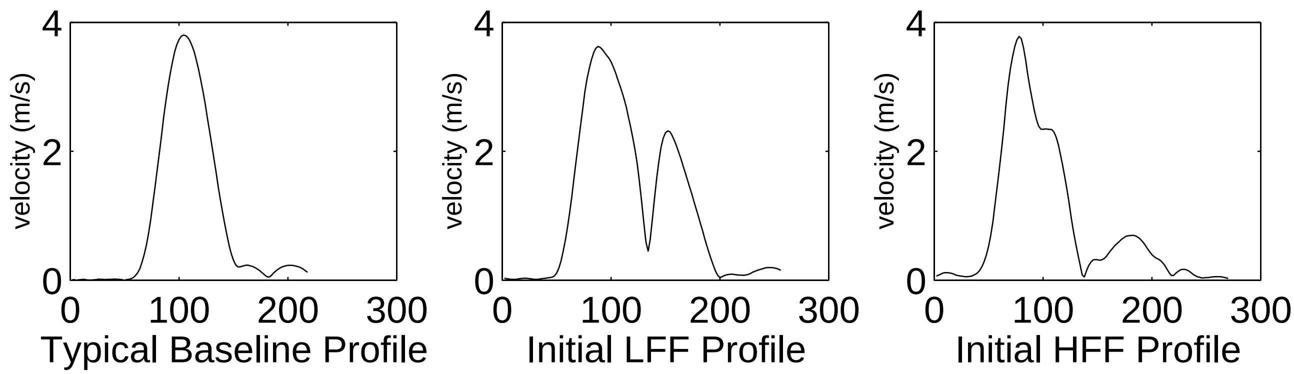

Figure 4-3: The example profiles for the typical baseline movement and the initial movements in the LFF and the HFF. The correlation coefficient for the LFF is 0.65 and 0.88 for the HFF.

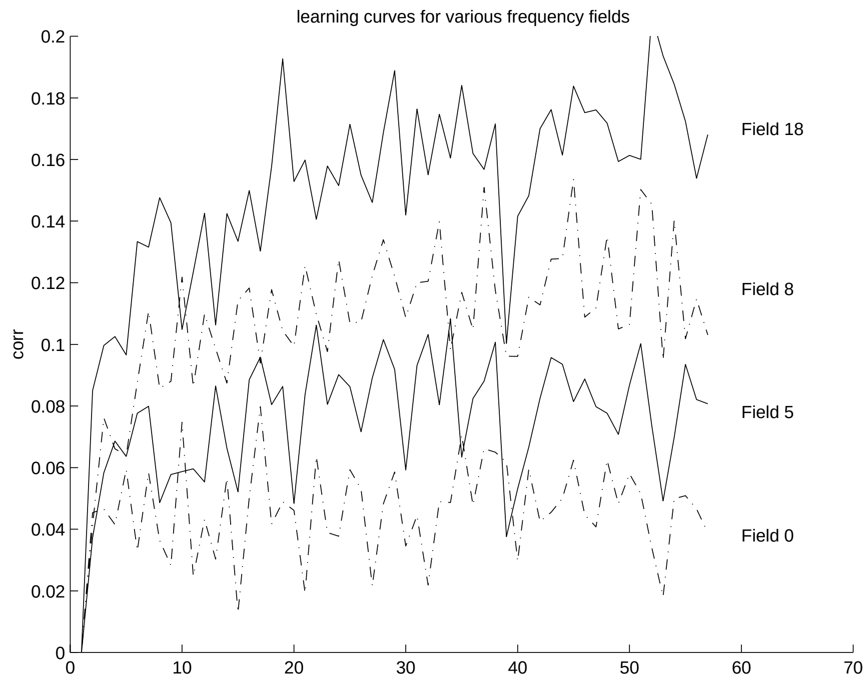

Figure 4-4: The velocity profile correlation coefficient learning curves for various frequency fields. They are aligned by the initial value of the coefficient to compare the quantity of learning. The curves are ordered in the order of the perturbation frequency.

the lower frequency fields have the highest values indicating that the movement is more similar to the baseline movements than the ones trained under higher frequency perturbations.

Figure 4-4 shows learning curves for Fields 0, 5, 8 and 18 aligned at their initial values. The initial value was determined by averaging the first three coefficients for all matrices. This is equivalent to the first 24 trajectories. As the figure shows, the curves are ordered in increasing order of frequency.

One additional analysis was conducted using the velocity profile correlation coefficient for Experiment HF-SEQ. In sequential experiments, different frequency fields were introduced to the subjects, one right after another. When the learning curve is plotted, there are drops in the curve observed when a new frequency is introduced as shown in Figure 4-5. The magnitude of these drops may be correlated to the difference in the force fields that were introduced next to each other.

The difference between various frequency fields can be quantified by finding a correlation between two force fields, $ff1$ and $ff2$. There were 16 x 13 force directions, F_d, assigned for the workspace of the manipulandum. The field correlation coefficient

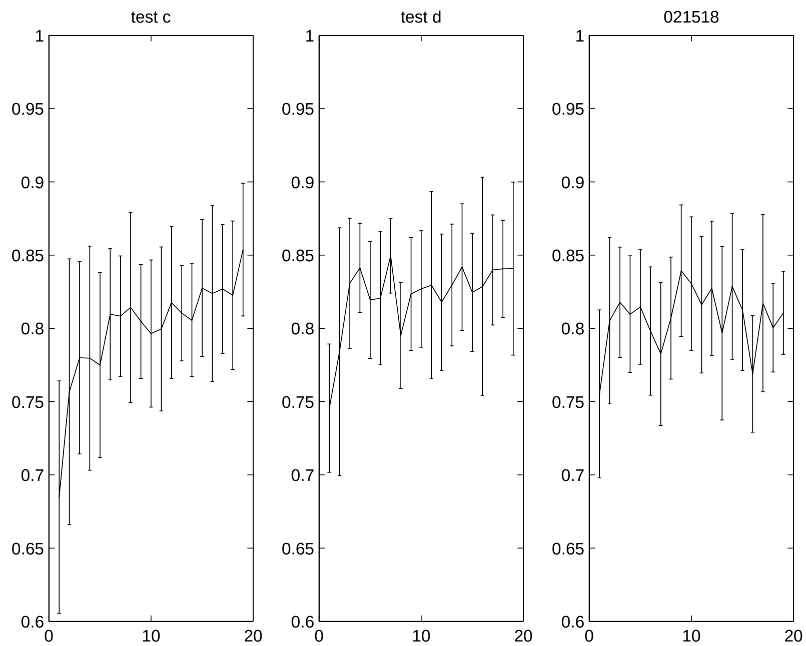

Figure 4-5: The typical velocity profile learning curve observed during the sequential learning paradigm. The field introduced were Fields 18, 5 and 2. Drops in the curve between two different fields are observed.

can be defined by taking an inner product of the angles:

$$\zeta(ff1, ff2) = \frac{1}{n}\sum_{i=1}^{n}\langle A(F_{d_i}^{ff1}), A(F_{d_i}^{ff2})\rangle \tag{4.8}$$

where

$$A(F_{d_i}^{ff}) = (cos(F_{d_i}^{ff}), sin(F_{d_i}^{ff})) \tag{4.9}$$

for the i-th force direction in force field, ff. The correlation, $\zeta(ff1, ff2)$, is called the frequency correlation coefficient (FCC) for fields $ff1$ and $ff2$. For example, if two identical force fields are compared, the FCC is 1, whereas if one field is completely the opposite of the other the FCC would be -1.

There were many different sequences of force fields that were imposed on the subjects during Experiments HF-SEQ and HF-PER. The magnitude of the drops in velocity profile correlation coefficient is plotted against the FCC in Figure 4-6. As the figure indicates the amount of drops has a monotonic relationship with the force direction difference in two fields. The amount of drop in the learning curve indicates the interference effect for individual force directions assigned throughout the

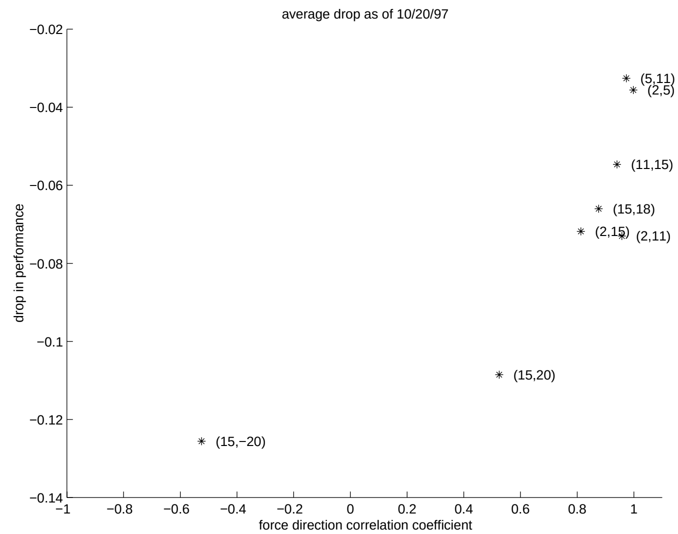

Figure 4-6: The magnitude of the drops in velocity profile correlation coefficient is plotted against the FCC for various combination of frequencies. The drops have a monotonic relationship with the FCC.

workspace. This result confirms the results shown by Brashers-Krug, et al. [1996], that if an opposite force field was imposed consecutively after subjects learned a force field, the distortion of the hand trajectory would be larger than the distortion observed without the exposure to the prior field.

Quantifying adaptation with velocity profiles has been shown to be robust from previous experiments for low frequency fields [Shadmehr, et al., 1993].

4.3.2 Velocity Peaks: Amplitude and Timing

In the analysis of shapes of the velocity profiles, the profiles were aligned at the peak and were scaled. Therefore, the peak amplitude and its timing were ignored. In this section, these two variables are investigated as learning components using the results from the LFF and the HFF in Experiment HF-COM.

To quantify learning using the amplitude of the peak velocity, the baseline value was determined by taking an average of all the baseline trajectories. When there were multiple peaks in the profile, the highest peak was chosen. Figure 4-7 shows the velocity amplitude change during learning the LFF and the HFF. The dotted line indicates the baseline peak amplitude. During training, the hand velocity increased with the forces were turned on. Despite training, the velocity peak amplitude does not seem to change very much throughout the whole training session for both low

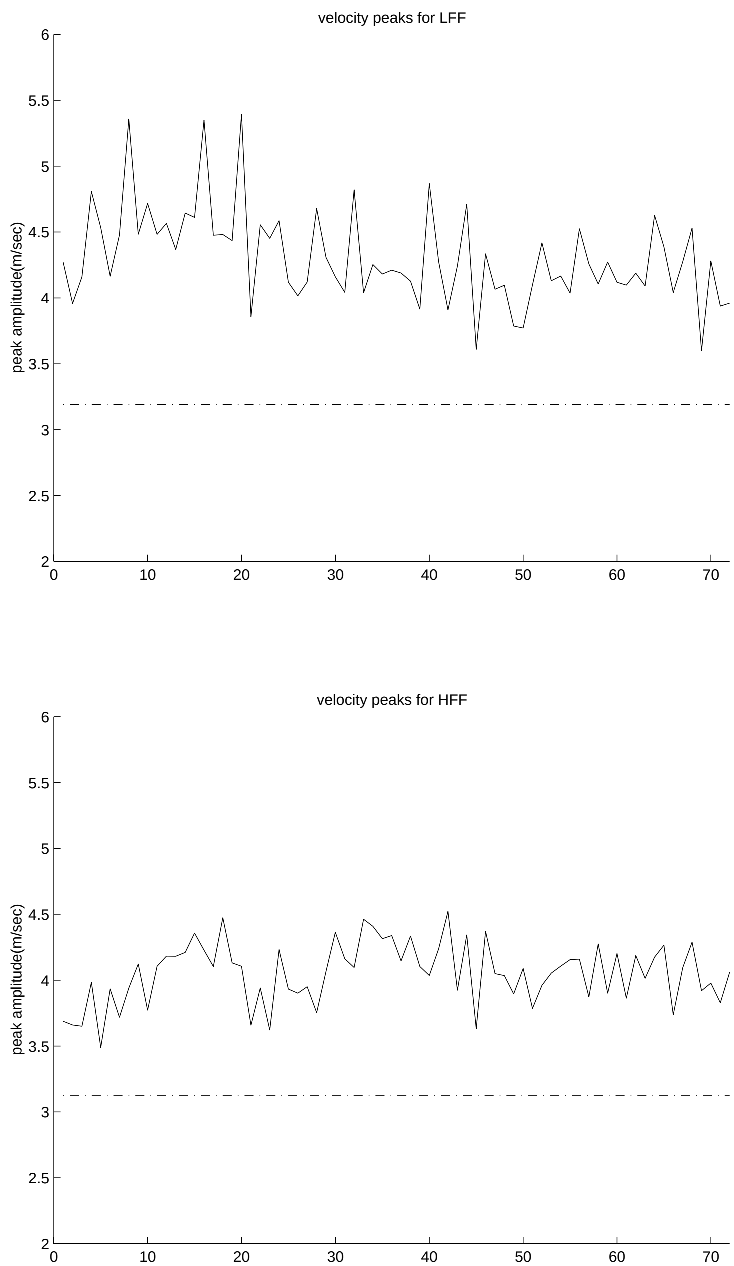

Figure 4-7: The velocity amplitude change during learning the LFF (top) and the HFF (bottom) from Experiment HF-COM. The dotted line indicates the base peak amplitude from the baseline epoch. The curve is an average of seven subjects. The x-axis represents the time course of training. One unit is an average of eight trajectories.

and high frequency fields. When the forces were removed after the force epochs, the peak amplitudes returned to the original values.

The same analysis was conducted for the timing of the movement. In order to investigate the timing, the hand location where the peak velocity was reached is identified for all movements. The hand location was quantified as the distance from where the movement started. The base number was obtained from taking the average distance of the baseline epoch. The average location were the peak velocity was reached was at 46 mm from the origin of the movement. Because the movements were 10 cm long, the peak velocity was shown to have reached slightly before the half way point.

The results for the LFF and the HFF are illustrated in Figure 4-8. The dotted lines represent the baseline average values. As shown, neither plot displayed any statistically significant changes in the errors from training. The values for the HFF was approximately the same as the baseline value. However, it is interesting to note that the peak velocity was reached after the 50 mm point in the movement consistently for the LFF.

In the analysis of the velocity profiles for the LFF, the errors were shown to decrease with training. However, the velocity peak amplitude and its location did not change from training. It can be hypothesized that the specific parameter chosen is not used as the variable for executing movements. Thus the difference in the value induced by the exposure to the new environment did not matter in terms of adaptation. Alternatively, it can be hypothesized that these consistent differences in the parameter values are strategies. These strategies are used as long as the movements are executed within the same environment.

4.3.3 Acceleration Change (Jerk)

In order to assess a parameter that is already hypothesized to be minimized during movement execution, the acceleration change (jerk) was investigated as a learning component. If it is a goal to minimize the jerk during one movement, it should be also minimized while one adapts to a new environment.

The jerk for the whole movement was calculated as

$$J = \sum_{i=0}^{n} \sqrt{\left(\frac{d^3 x_i}{dt^3}\right)^2 + \left(\frac{d^3 y_i}{dt^3}\right)^2}. \tag{4.10}$$

The baseline value was the average jerk of the baseline epoch. As soon as the force

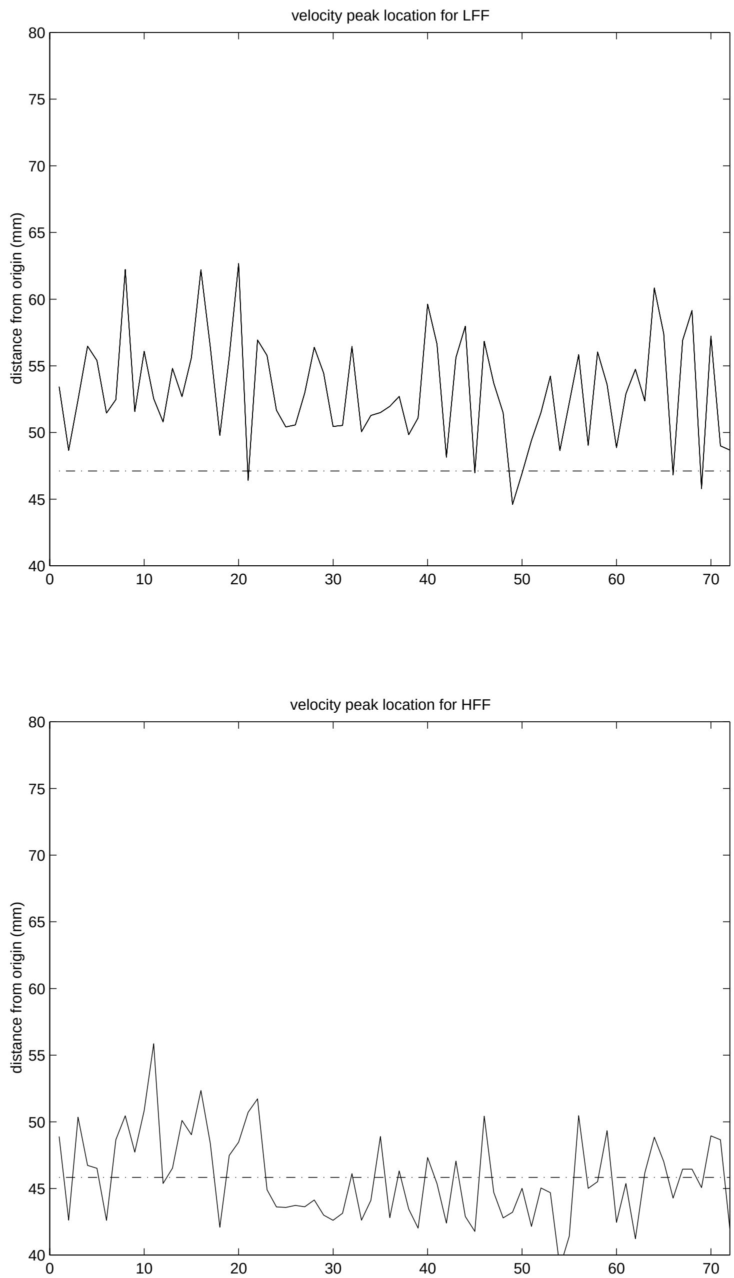

Figure 4-8: The velocity timing change during learning the LFF (top) and the HFF (bottom). from Experiment HF-COM. The dotted lines indicate the baseline values. The curves are the average of seven subjects. For the LFF, the mean of the curve was 53 mm while the mean was 45 mm for the HFF. The x-axis represents the time course of training. One unit is an average of eight trajectories.

perturbation was turned on, the jerk value jumped up, showing disturbance in the control of the movement. The whole course of learning session for the LFF and the HFF are shown in Figure 4-9. The curve for the LFF displayed the converging effect to the baseline value as predicted. However, the jerk for the HFF was much higher than the values for the LFF, did not decrease with training, and exhibited high standard deviation. Using the jerk as a learning component, the LFF is a learnable environment, but the HFF is not. This result is consistent with the velocity profile correlation.

4.4 Spatial Variables as Learning Components

As Morasso [1981] pointed out first, hand trajectory planning is heavily linked with visual coordinates. Therefore, the visual components in hand trajectories are crucial in adaptation. Three different components are analyzed in spatial coordinates to further quantify adaptation during reaching movements.

4.4.1 Spatial Error Integration

For most perturbation learning experiments in the past, the term aftereffect was used to determine whether the task has been learned [Wolpert, et al., 1995, Ghahramani, et al., 1996, Shadmehr, et al., 1993, Lackner and Dizio, 1994, Gandolfo, et al., 1996]. The analysis of the aftereffect trajectories were simply to detect spatial distortion from a straight trajectory made during the baseline epoch. Even though the spatial error of the movement has been emphasized, it has never been quantitatively analyzed because it is not trivial to quantify the spatial error of a hand trajectory.

The spatial error cannot be simply integrated. For example, Figure 4-10 shows some trajectories observed that are difficult to analyze. Trajectories often do not end at the target and contain loops and hooks. Thus the spatial integration strategy must be able to incorporate these situations properly.

Out of various strategies tried, the perpendicular distance strategy worked best. The perpendicular distance strategy is illustrated in Figure 4-11. From a straight trajectory line, a perpendicular distance to the actual hand trajectory, d_i, was measured every 1 mm and the integrated spatial error, ise, was calculated to be

$$ise = \sum_{i=0}^{n} d_i. \tag{4.11}$$

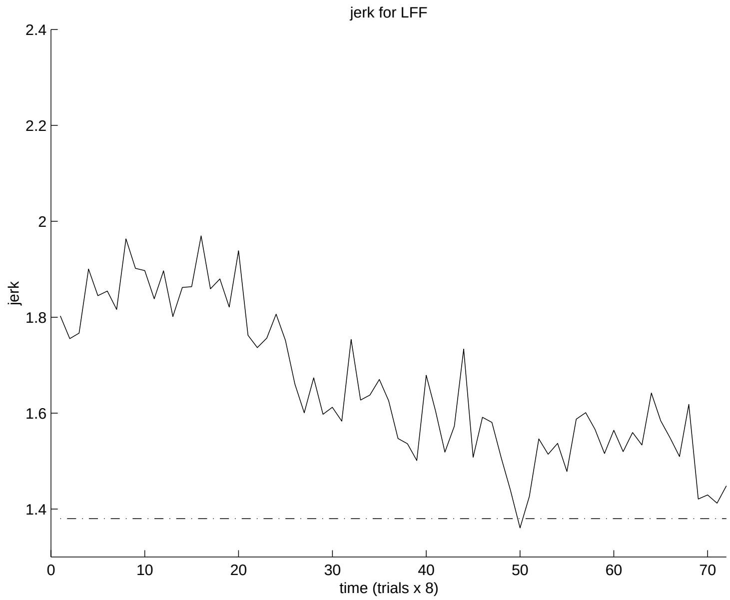

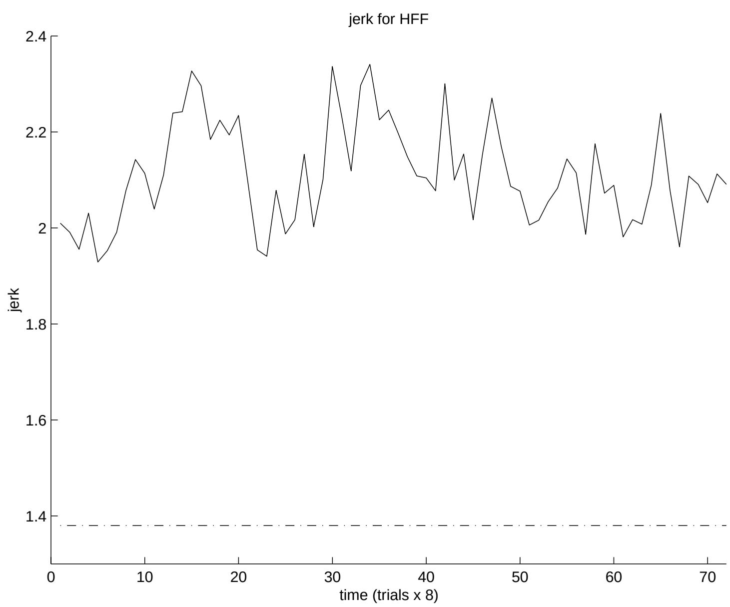

Figure 4-9: The jerk during learning the LFF (top) and the HFF (bottom) from Experiment HF-COM. The dotted lines indicate the average jerk for the baseline epoch. The curves are the average of seven subjects. The x-axis represents the time course of training. One unit is an average of eight trajectories.

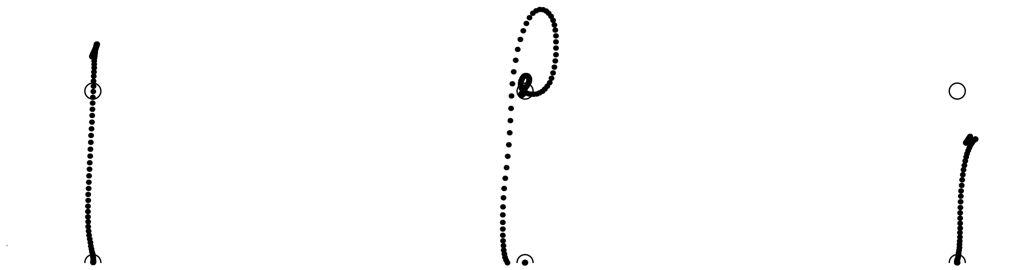

Figure 4-10: Some example trajectories from other literature. It is not trivial to take an integral of the spatial error.

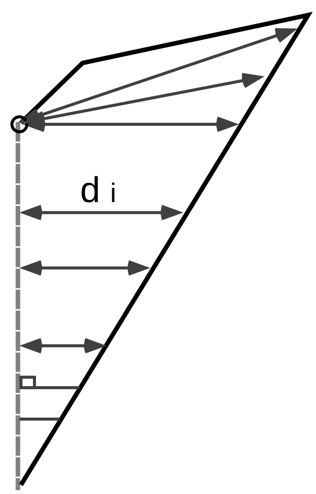

Figure 4-11: The perpendicular distance strategy used to take the spatial integration of hand trajectories. From a straight trajectory line, a perpendicular distance to the hand trajectory, d_i, was measured every 1 mm, and all d_i were added. If the trajectory passed the perpendicular line multiple times, the furthest point was chosen and taken as the distance. When the trajectory overshot, the distance to the target was measured for every 1mm of vertical displacement. If the trajectory undershot, the distance from the end of the trajectory to the perpendicular line was measured for every 1 mm up to the target.

If the hand trajectory overlapped and crossed the perpendicular point multiple times, the furthest point was taken for the distance and the rest were ignored. If the trajectory overshot, the distance from the target was measured for every 1 mm of vertical displacement. If the trajectory undershot, the distance from the end of the trajectory to the perpendicular line was measured for every 1 mm up to the target.

The base number is an average of the *ise* for all the baseline movements. The trajectories for the LFF and the HFF from Experiment HF-COM were analyzed and their results are shown in Figure 4-12. The *ise* was significantly larger for the LFF than the HFF at the initial exposure to the forces because the force direction was more uniform. When the forces push to the left and then to the right, the second force can contribute to reducing the integral of spatial error. With training, both curves showed decrease in the error, mostly within the first 120 trials[1] When the catch trials are included within the analysis the error can be plotted as in Figure 4-13. The *ise* during the catch trials are large, indicating that this spatial error analysis is a good approach to quantifying aftereffects assessed qualitatively in the past.

4.4.2 Distance of Furthest Deviation

When the spatial error was visually inspected, the actual integrated spatial error for the whole movement may not correspond to the perceived error. For example, when the two illustrations in Figure 4-14 are qualitatively analyzed, the left trajectory seems to be more closely correlated to the desired trajectory than the right trajectory. However, when these two trajectories are analyzed with the integrated spatial error strategy, both have the same values.

Todorov and Gandolfo [from personal communications] investigated what kind of trajectories subjects think contain more errors. They concluded that the perceived spatial error is more correlated with the distance of the furthest point away from the straight desired trajectory than the actual integrated spatial error. Thus, the analysis conducted in this section takes the furthest deviation point on the hand trajectory from the straight trajectory. The distance is determined by taking a perpendicular distance as shown in the last analysis, but instead of accumulating all d_i, the largest value of d_i is chosen as the value as

$$dfd = \max_{i=0}^{n} d_i. \tag{4.12}$$

[1]The graphs plot the average of eight movements, so 120 trials are showing as 0 to 15 on the x-axis of the graphs.

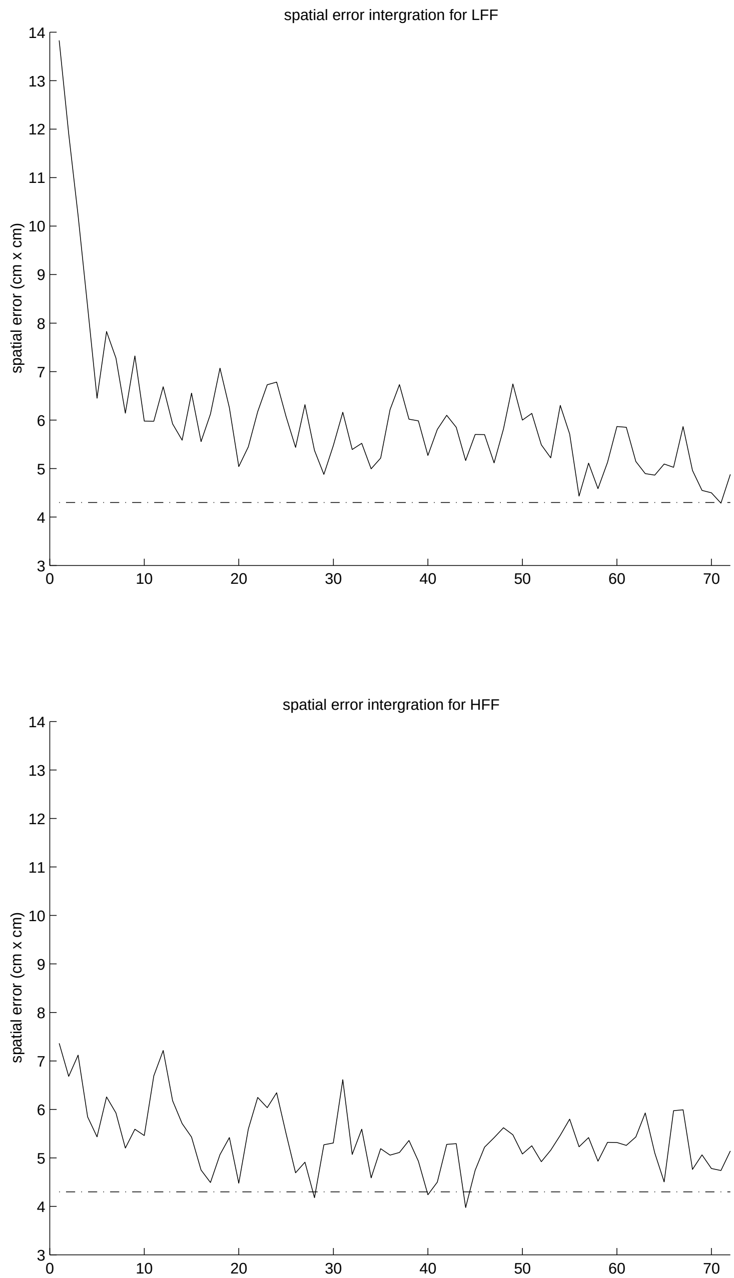

Figure 4-12: The spatial error integration learning curves for the LFF (top) and the HFF (bottom) from Experiment HF-COM. The LFF curve showed a significant amount of errors initially. The errors decreased over time for both curves. The x-axis represents the time course of training. One unit is an average of eight trajectories.

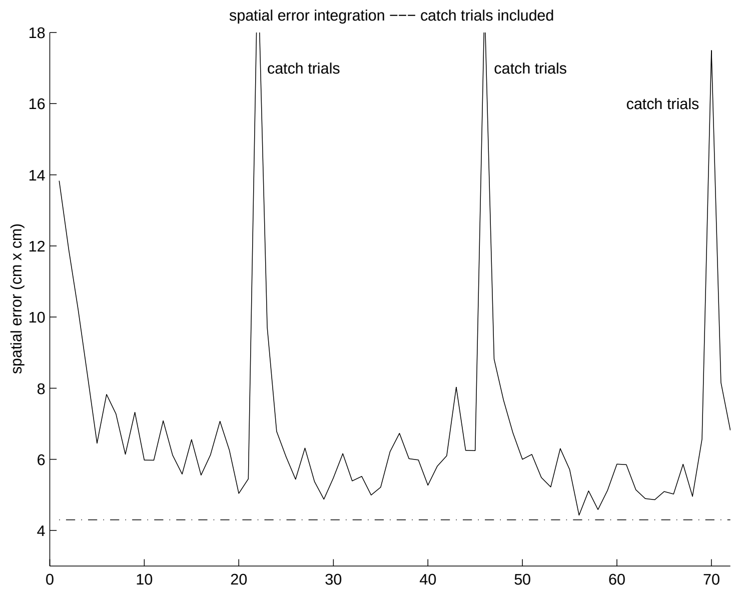

Figure 4-13: The integrated spatial error learning curves for the LFF with catch trials. The x-axis represents the time course of training. One unit is an average of eight trajectories.

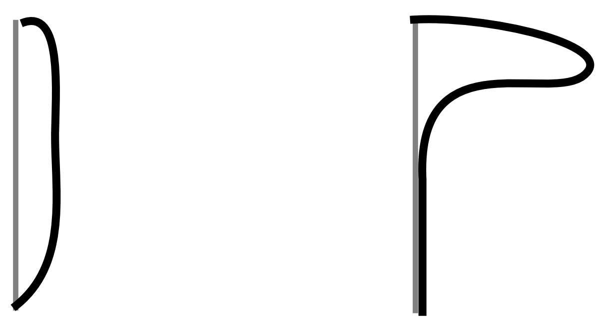

Figure 4-14: Two trajectories with the same integrated spatial errors. However, the right trajectory is visually perceived to contain more error than the left trajectory.

The results for the LFF and the HFF experiments are shown in Figure 4-15. The curves were similar to the integrated spatial error analysis in that the LFF curve contained significantly more error at the initial exposure to the forces than the HFF. For the HFF, the error value did not change significantly opposed to what was observed for the *ise* analysis. When subjects were asked if they perceived the HFF to be harder than the LFF, they consistently answered that they perceived the HFF to be easier. As the learning curves show the HFF contained less errors at the beginning of the training session matching the subjects' perception. Thus this analysis is a good measurement for quantifying learning at the perceptual level.

4.4.3 Initial Direction Angle

When a movement is planned, the components of the planned movement from the CNS should be most evident at the beginning of the movement before the sensory feedback occurs. For this reason, the initial angle direction of the movement was analyzed. The angle difference was measured from the straight desired trajectory line, as illustrated in Figure 4-16. The movement angle was measured every 10 msec from the location of the hand to origin of the movement. The angles were measured until the first peak in the velocity profile was detected. To determine the initial direction angle for the whole movement, id_n, all the angles were averaged as

$$id = \frac{1}{n}\sum_{j=1}^{n}\theta_j. \tag{4.13}$$

The baseline value was an average of all movements during the baseline epoch. The initial direction angle learning curve for the LFF is plotted in Figure 4-17. The learning curve showed improvement over time. The curve corresponds to only for one epoch of forces, and the curve is based on an average of 26 subjects who were tested for one epoch of the LFF.

From observing the catch trial trajectories, it seems that the planned movement was straight with the offset for the LFF in the movement direction. The movement direction is determined by the total predicted external forces. Thus the amount of the initial angle deviation seemed to reflect the internal model built for the environment.

These analyses indicated that many components converge toward the values of the baseline movements while the perturbation is applied. However, in parallel, many parameters alter their values with exposure to perturbations, but do not change their values over time with training. There were two hypotheses proposed for this

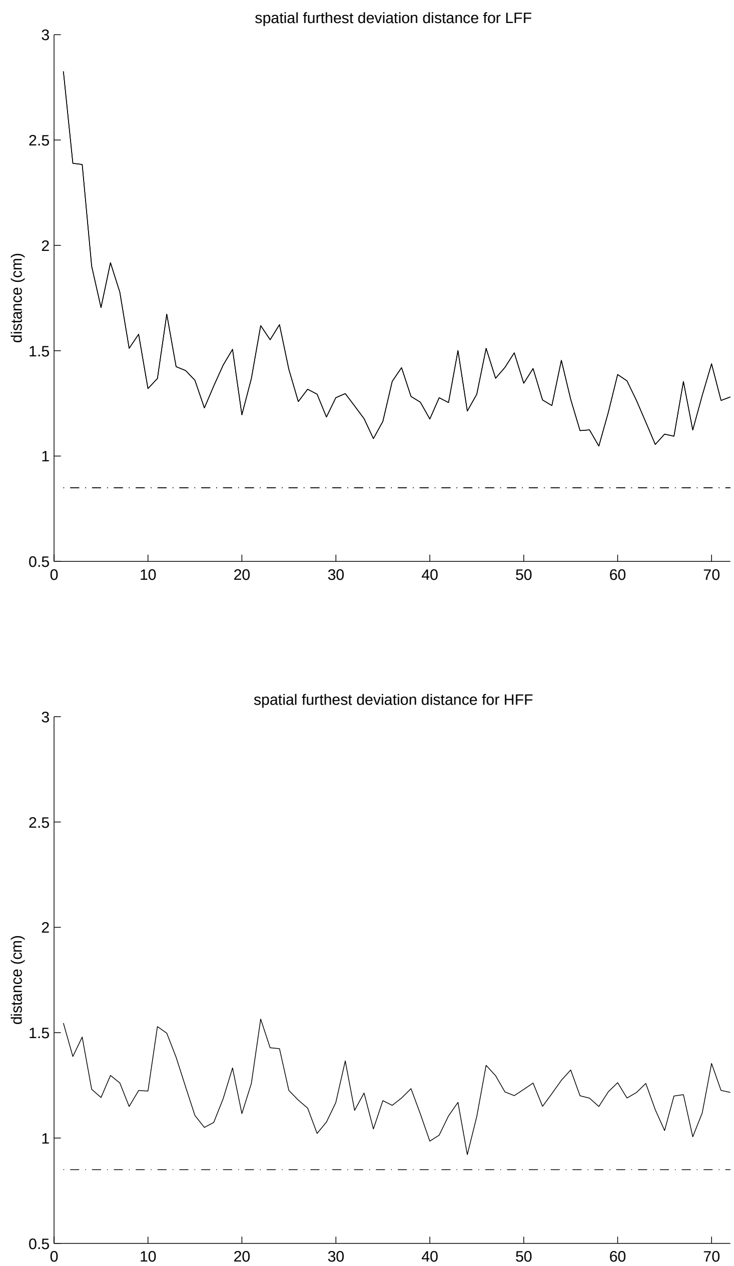

Figure 4-15: The furthest deviation distance learning curves for the LFF (top) and the HFF (bottom) experiment from Experiment HF-COM. The dotted lines indicate the baseline average. Both curves converged with the desired values. The x-axis represents the time course of training. One unit is an average of eight trajectories.

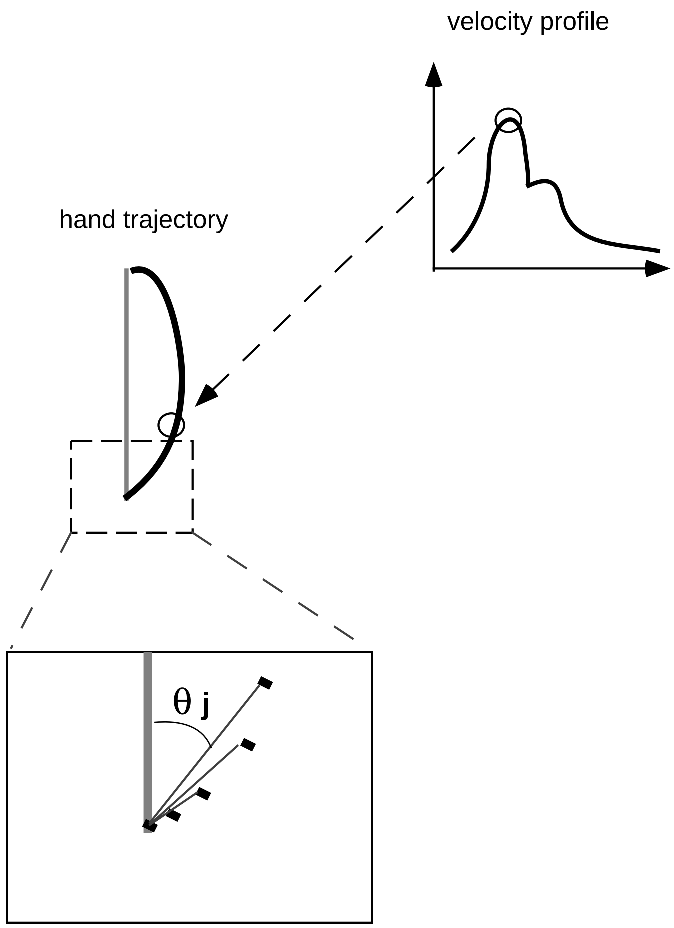

Figure 4-16: The initial directional angle of the movement is measured from the straight trajectory line. All the points to the first velocity profile peak are taken. A line is drawn from each point to origin to measure the angle. All the angles are averaged to get the initial direction angle for the whole movement.

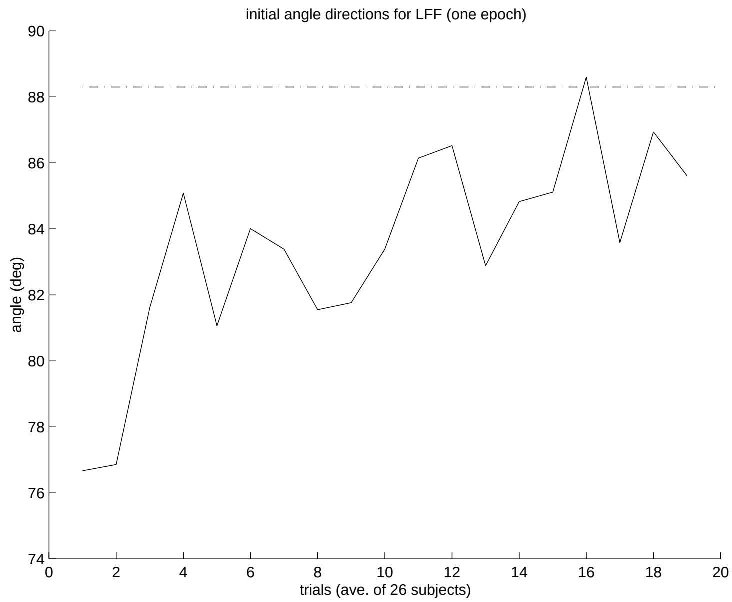

Figure 4-17: The initial direction angle learning curves for the LFF from Experiment HF-COM. The dotted line indicates the baseline average.

condition. The first hypothesis claimed that the parameter chosen is not a variable for the movement control. The other hypothesis claimed that the environment presented is too difficult to learn. From these analysis, the LFF can be categorized as learnable because a majority of the parameters that contained errors due to the perturbation were minimized with training. Therefore, we can hypothesize that the parameters which did not change their values from practice, such as velocity peak amplitude and locations, were not minimized during movement control. Rather, they can be treated as strategies for a specific environment. In the next section, the learning curves are analyzed in detail to quantify the learning and unlearning processes.

4.5 Temporal Learning Process

To analyze the process of learning in detail, the initial direction angle analysis and the jerk analysis were used. These analyses are good representatives of learning because the initial direction angles have the most correlations to the internal model built, and the jerk is hypothesized to have a strong link with a fundamental law of control. With these components, the temporal effect in adaptation is quantified in this section. The results from Experiment TDP in Chapter 3 are revisited for the analysis.

Movement in one direction was tested throughout the training session. Two epochs of 192 movements were tested, and all the movements were to the 90 degree direction

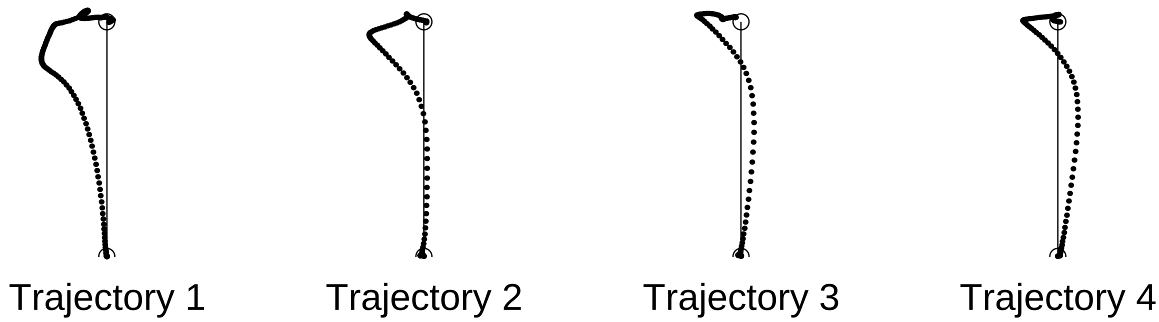

Figure 4-18: Partial perturbation experiment from Experiment TDP. To illustrate the rate of change in the initial angle of the movement, the first four 90 degree movements of the training are shown. The angle changed dramatically within the first few movements.

Trajectory #	*1*	*2*	*3*	*4*
Initial Angle	95.6	88.1	81.6	78.7

Table 4.1: The initial angles of the trajectories for the first four movements are quantified and tabulated.

and -90 degree direction returning to the starting point. Thus the 90 degree movement was trained for 96 trials. The first epoch was with no perturbation for baseline training, then forces were applied for the second epoch. The forces were applied for the last 12 cm of the 20 cm movement with gradual increase in the gain as showing in Equation 3.1. The last 20 trajectories were interleaved with catch trials.

To observe the change in more detail than shown in Figure 3-4, Figure 4-18 shows the first four movements after the perturbation was turned on. The initial angle was almost straight toward the target only for the first movement. Even within the first four movements, the initial direction angle was changed significantly. The angle correction increased with time, but the rate of increase decreased with time. The angles were quantified using the technique described in section 4.4.3 and the results of the first four movements are presented in Table 4.1.

To assess the whole course of the training session, trajectories from various times are displayed in Figure 4-19. Trajectories 8 and 15 are from earlier in the training session. The initial angles are similar to Trajectory 4 in Figure 4-18, however the magnitude of the corrective motion at the end of the movement still decreases over time. The trajectories observed after Trajectory 50 were almost identical from one trajectory to another and from one subject to another. This demonstrates the robustness of the data.

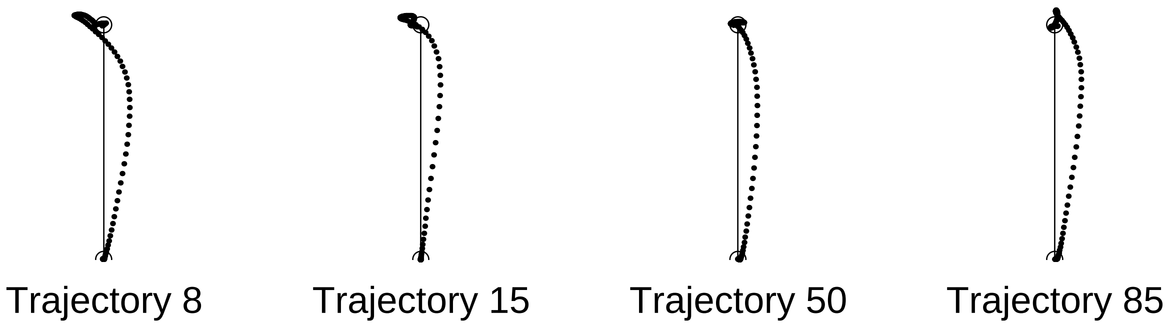

Figure 4-19: The trajectories from various times of the training are plotted. They are Trajectory number 8, 15, 50, and 85. These are a total of 96 trajectories trained. The initial angles are not changing significantly later in the training session.

When the initial direction angles of all the movements are plotted as shown in Figure 4-20, it shows that most of the initial direction angle change occured very early in the training session. However, the jerk of the movement, as plotted in Figure 4-21 shows decrease for the entire duration of training. This may be contributed to by the correction made at the end of the movements. However, these corrective movements disappeared midway through the force epoch, whereas the jerk continued to decrease even after Trajectory 50, as seen in Figure 4-21.

It seems that the initial angle of the movement was adjusted within the movement planning stage using the knowledge gained from previous experience. This adjustment occured rapidly. In addition to this knowledge-based learning, the adjustment at the end of the trajectory seems to be made using the sensory information that fed back from the beginning of the movement. This fine tuning of the movement using the immediate sensory feedback occurs for a longer period of time. This concept is shown schematically in Figure 4-22. Combining these two learning curves, a mathematical model for the temporal aspect of learning, TL, can be expressed

$$TL(T) = A\Psi(r_{lk}, T) + B\Psi(r_{lf}, T) \quad \text{for } T \geq 0 \tag{4.14}$$

with the rate of knowledge based learning, r_{lk}, and the rate of feedback based learning, r_{lf}, where

$$r_{lk} \gg r_{lf} \tag{4.15}$$

and

$$A + B = 1. \tag{4.16}$$

$\Psi(r, T)$ is a learning curve determined by the rate of learning, r. When the rate is

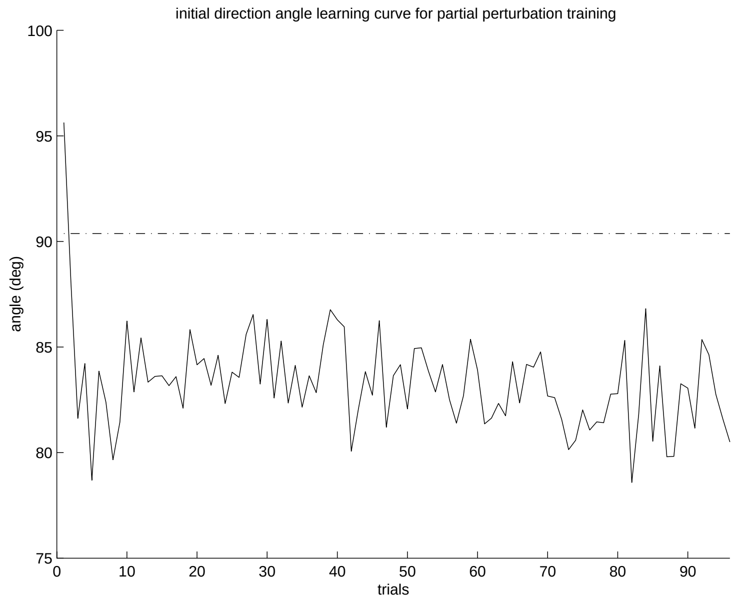

Figure 4-20: The initial direction angle change is plotted for the whole course of training. Most of the change occured very early in the training. The dotted line shows the baseline average. The x-axis represents the time course of training. One unit is an average of eight trajectories.

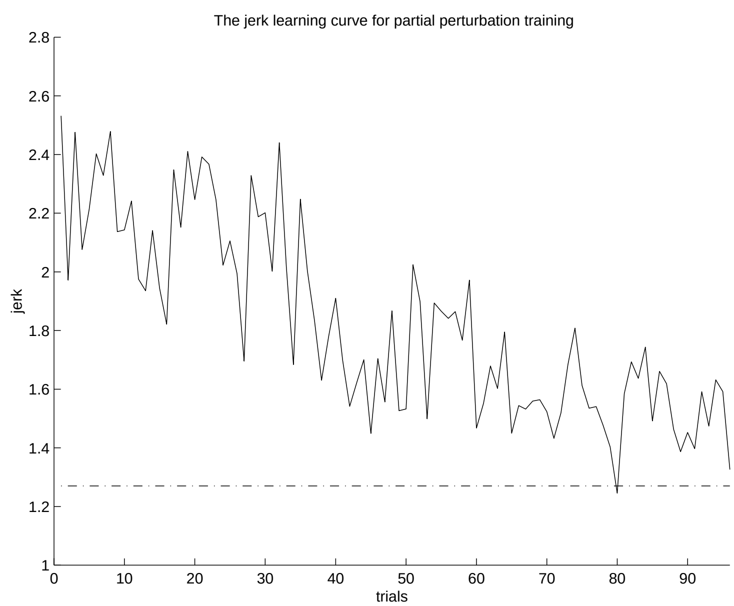

Figure 4-21: The jerk of the movements are plotted for the whole course of training. The jerk learning curve does not saturate for much longer than for the initial direction angles. The dotted line shows the baseline average. The x-axis represents the time course of training. One unit is an average of eight trajectories.

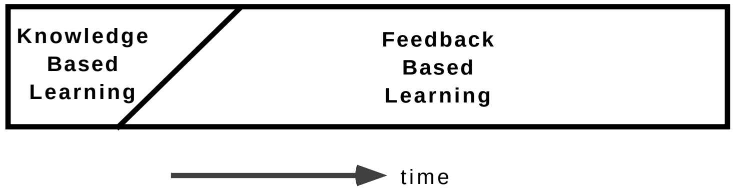

Figure 4-22: The time course of adaptation to a new task. Initially, the change made by the knowledge from previous experience dominates the adaptation. This process occurs very quickly. In addition, the fine tuning based on the immediate sensory feedback takes place. The duration for this process is much longer than the knowledge based learning.

higher, the learning occurs faster. Depending on the task, A, B, r_{lk}, and r_{lf} vary. When one movement is executed, the discrete time, T, increases by one.

To show an example where the task is more difficult than the partial perturbation environment, the opposite force perturbation was added at the beginning of the movements. This experiment was conducted in Experiment TDP and the results are shown in Figure 3-9. The initial direction angle and the jerk curves are plotted in Figures 4-23 and 4-24. Because the task is more difficult, the learning rate for

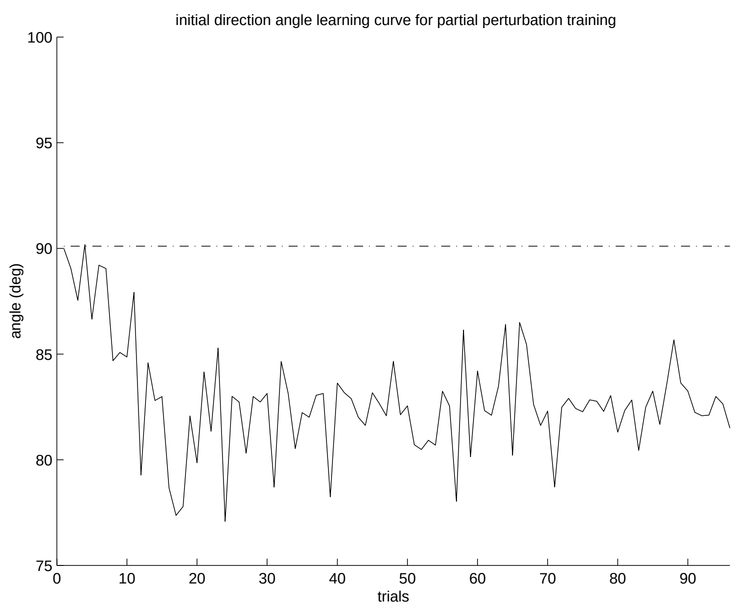

Figure 4-23: The initial direction angle learning curve for Experiment TDP with two opposing forces. The curve has a slower learning rate than the partial perturbation experiment because it is more difficult to learn.

both initial angle and jerk are smaller than for the partial perturbation curves. The variation of A and B are discussed in Chapter 6.

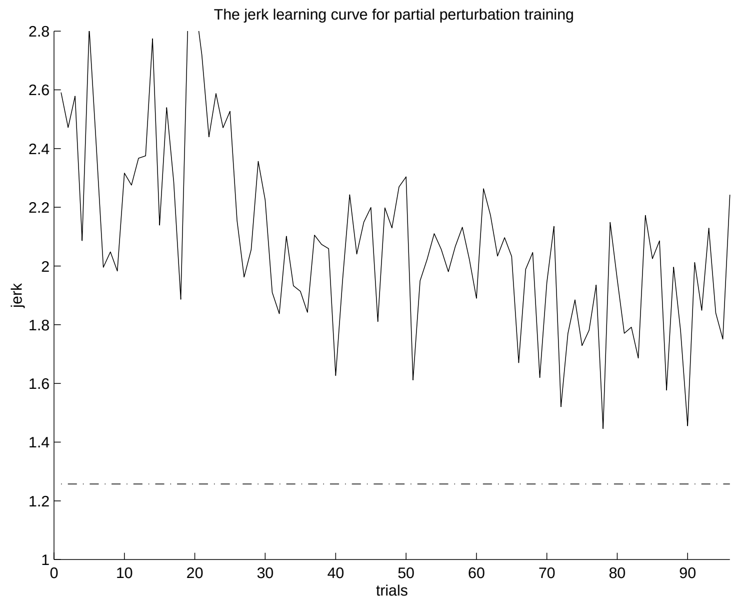

Figure 4-24: The jerk learning curve for Experiment TDP with two opposing forces. The curve has a slower learning rate than the partial perturbation experiment because it is more difficult to learn.

4.6 Temporal Unlearning Process

When a task is learned and no interference is introduced following the adaptation, the information learned is retained and consolidated. However, in most situations in everyday life, some conflicting information is introduced and the learned information is gradually erased. This erasing process can be called "unlearning." The process of unlearning is important to understand because the rate and the ability to learn a new task may be heavily dependent on the simultaneous unlearning of another skill. Indeed, this conflicting effect was observed during the analysis of velocity profile correlation coefficient drops at the beginning of this chapter.

The unlearning process is difficult to analyze because the only way to observe the effect is by forcing another task to be learned. Thus teasing from unlearning effect out of the learning effect is challenging.

To remain constant with previous studies of the learning process, the partial perturbation experiment was used again as an example. This time, in addition to one epoch of force training, 100 movements[2] were executed, with no forces immediately following the force training. The last movement in the forces and three unlearning trajectories are shown in Figure 4-25. The initial angle error diminished very quickly.

[2]Because every other movement is a -90 degree movement, a total of 50, 90 degree movements were executed without forces.

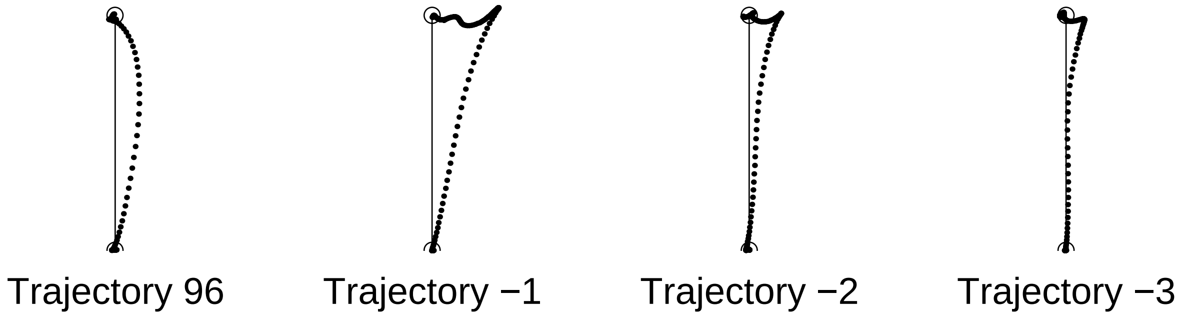

Figure 4-25: Trajectories 96, -1, -2 and -3 during unlearning the partial perturbation. Trajectory 96 shows the final trajectory under perturbation. Trajectories -1, -2, and -3 are the first three trajectories after the forces were turned off.

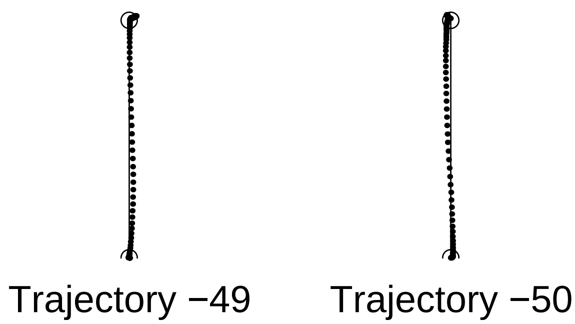

Figure 4-26: Trajectories -49 and -50 during unlearning the partial perturbation. They do not contain any information about the forces corresponding to the baseline movements.

In addition, Trajectory -49 and -50 are shown in Figure 4-26. These trajectories were equivalent to the baseline trajectories.

Because learning the movements in a null field was a very fast process, the learning part of this process had to be subtracted from the unlearning effect above. In order to do so, the movements from the baseline session are analyzed. The initial direction angle and the jerk change curves for the baseline session were subtracted from the unlearning results and plotted in Figure 4-27. The initial direction angle unlearning curve shows that the knowledge-based unlearning happens very quickly. The rate of knowledge-based unlearning, r_{uk}, is equivalent to the learning rate, r_{lk}. However, observing the jerk change unlearning curve, the effect does not seem to be unlearned as quickly as learning occurs. Thus the rate of feedback based unlearning, r_{uf}, must be less than the learning rate, r_{lf}. The temporal unlearning process can be expressed as

$$TU(T) = C\theta(r_{uk}, T) + D\theta(r_{uf}, T) \text{for } T \geq 0 \tag{4.17}$$

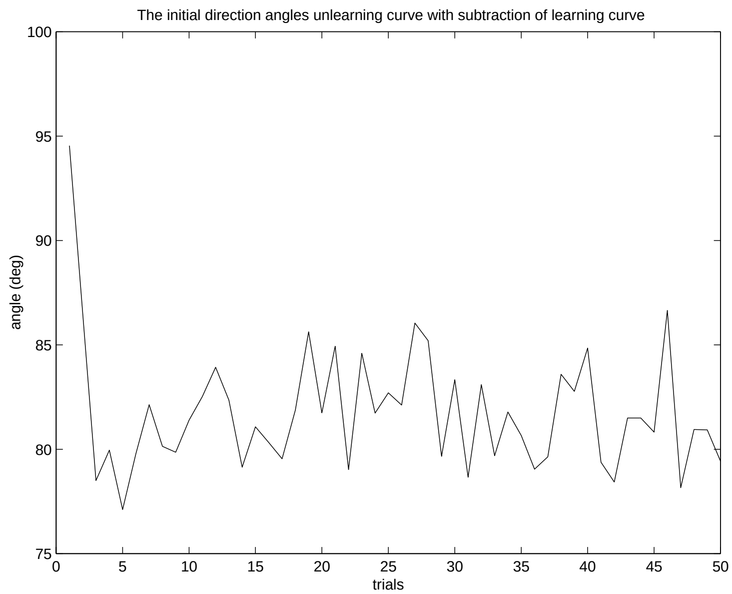

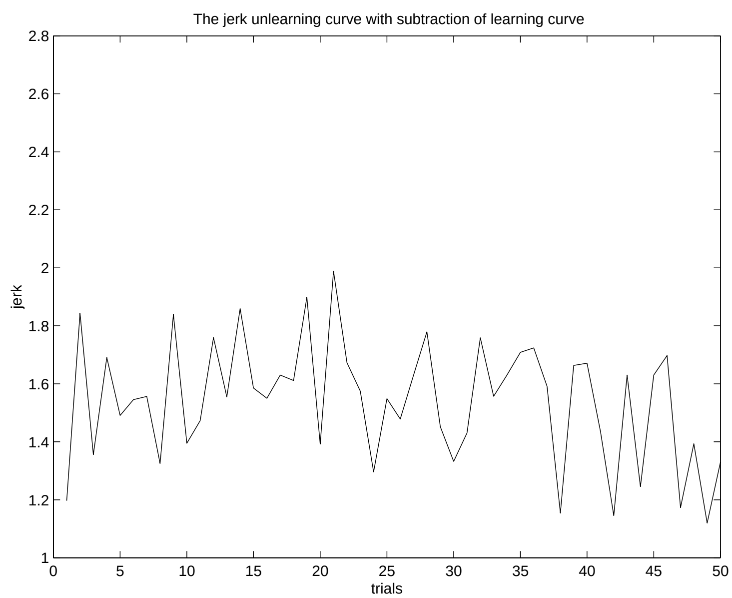

Figure 4-27: Unlearning curves for the initial direction angles and the jerk for the partial perturbation experiment. The initial angle curve is equivalent to the learning curve, but the jerk curve seems to decay slower.

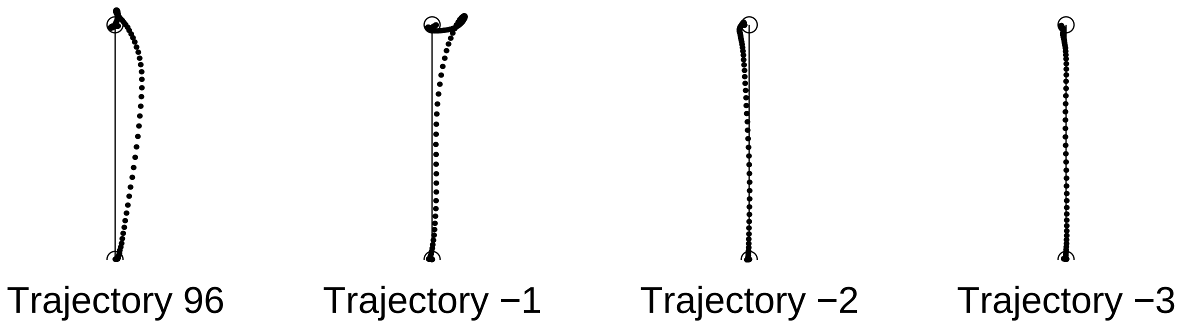

Figure 4-28: Trajectories for partial perturbation training during unlearning with prior knowledge about when the force perturbation is turned off. Trajectory 96 shows the final trajectory under perturbation. Trajectories -1, -2 and -3 are the first three trajectories after the forces were off. The unlearning process is significantly quicker with knowledge of the environment.

where

$$r_{uk} \gg r_{uf}, \tag{4.18}$$

and

$$C + D = 1. \tag{4.19}$$

As stated above,

$$r_{lk} \approx r_{uk} \tag{4.20}$$

and

$$r_{lf} > r_{uf}. \tag{4.21}$$

However, unlearning is normally combined with other learning components, thus the actual rates cannot be observed directly.

In order to show that the r_{uk} is truly knowledge based, two subjects were informed verbally when the force perturbation was removed. Their trajectories are shown in Figure 4-28 and indicate that the initial direction change was observed at the first movement when the forces were turned off. Thus if subjects were given prior knowledge of the environment,

$$r_{uk} \to \infty \tag{4.22}$$

making the global rate of unlearning faster. The same statement should be true for the leaning rate.

4.7 Conclusion

In this chapter, the human learning scheme for voluntary reaching movements was investigated by quantifying various components that changed their value when a new environment was introduced. Both learning and unlearning effects were mathematically analyzed to have two different rates: knowledge-based and feedback-based rates. The knowledge-based learning and unlearning rates can be changed cognitively, adding another dimension to the adaptation of motor skill.

Part II

Context Generalization

Overview

In Part One, spatial generalization was investigated for one continuous movement while the movements were executed under a given condition or context. In Part Two, I discuss the generalization effect as it pertains to the execution of a given movement under multiple contexts.

The same intrinsic coordinate movements are executed for various tasks every day. It is not practical to have all movements generalized completely by their spatial coordinates. It is also impossible to have a representation in our nervous system for each task or object that is encountered over a life time. Thus, we must not only generalize movements spatially, but also by the context of the situation. In the next three chapters, the structure of context-level generalization is explored.

Chapter 5 reveals how originally spatially generalized movements can be separated and generalized contextually with training. Experiments are presented to show that such separations are possible by varying components such as location of the targets, velocity of the movement, sequence of the movements, and the amount of a priori knowledge given about the movements.

Chapter 6 explores how these different models are created, modified or selected within one state space. As discussed in Chapter 5, when two interfering environments are presented in an interleaved fashion, multiple models can be established. However, when these environments are introduced separately, without temporal consolidation, internal models for both environments cannot be developed simultaneously due to the interference effect. Therefore, the sequence of exposure to multiple environments is critical and Chapter 6 explores models of the process of retaining multiple models.

Finally, Chapter 7 investigates various strategies used during the learning of context dependent movements. When learning to deal with a given situation particularly challenging, various strategies may be exploited in order to cope with the environment rather than to actually learn to respond for individual forces applied. These strategies are utilized frequently and give subjects the perception of mastering the tasks, thus such strategies are studied as a part of the learning process.

Chapter 5

Separation of Spatial Generalization by Context

5.1 Introduction

Many movements are executed to accomplish tasks everyday. Most of these movements are already learned from prior experience and are executed without much thought. Thus this movement information must be stored within the CNS. Because it is not plausible to hypothesize that our CNS has a representation for each task, previous chapters investigated the organization of the motor system. From the reaching experiments, the movements were shown to be learned and generalized according to the direction and the intrinsic coordinates of the movements. If a movement was learned, the acquired information transferred to other movements that were directionally and spatially close. Furthermore, two conflicting perturbations could not be learned at the same time if the movements were directionally and spatially identical. Therefore, the representation within the motor system must be organized according to the direction and the location of the movements executed.

However, multiple tasks are executed within the same state space everyday without much interference. For example, if there are two doors with the same appearance that are encountered frequently, and the one by the principal's office is heavier than the other by the biology classroom, the amount of force exerted to open the doors is adjusted accordingly for each door. Eventually these movements become learned and automatic. Thus, two motions that are the same intrinsically can be executed using different models of the environment hypothetically based on context.

In this chapter, I show that multiple movements, within a give spatial location, can be distinguished according to relevant contextual information. Experiments were conducted with force perturbations during planar reaching movements. Two conflicting perturbations with different context were imposed for movements in the same

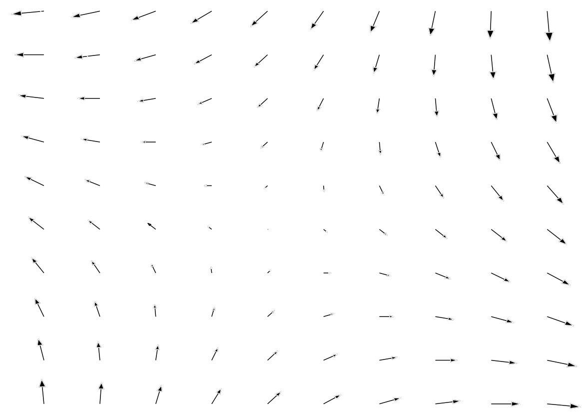

Figure 5-1: From Gandolfo [1996]. Force perturbations used during training the reaching task. Forces are designed to accentuate the distortion of circle drawing movements.

direction and space in order to demonstrate that they can be learned if the context of the tasks is varied.

5.2 Background

Various researchers have argued against the idea that movements can be generalized by context. They hypothesized that if an internal model was built for one task in some intrinsic coordinates, the effect of the model is transferred to other tasks in the same coordinates.

For example, Gandolfo and Conditt [1996] explored whether there was any transfer of aftereffects from a "reaching task" to a "circle drawing task" under force perturbations shown in Figure 5-1. Subjects were asked to make circular drawing movements and were trained with no perturbations until they could produce these circles consistently (Figure 5-2.A). Subjects were then asked to make reaching movements from one target to another (Figure 5-2.B). Force perturbation was turned on during the execution of reaching movements. After these perturbations are learned for the reaching task, the subjects were asked to draw circles again under no force perturbations. As shown in Figure 5-2.C, the circle drawing movements were distorted to the opposite direction of the forces applied for the reaching task. The aftereffect observed after training only the circle drawing task (Figure 5-2.E) is very comparable to the aftereffects displayed after training reaching movements. Thus, the effect indeed transferred to another task.

Concurrently, there exist other experimental results that suggest that contextual

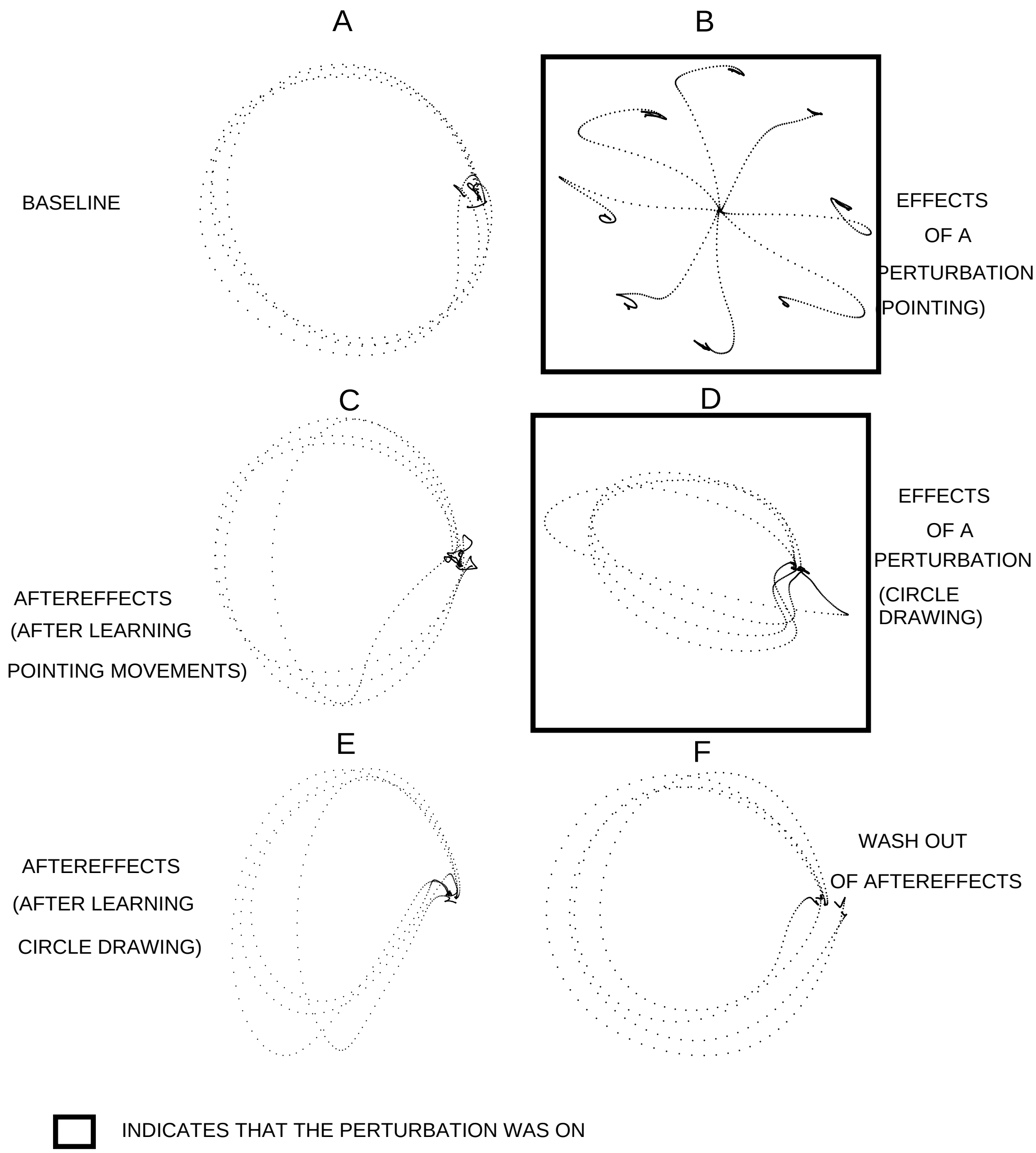

Figure 5-2: From Gandolfo [1996]. A: Circle drawing movements made as baseline before the perturbations were on. B: Training under perturbations for reaching task. Notice that the movements are distorted to the direction of the perturbations. C: After training only the reaching task under perturbations, circle drawing movements are made under no forces. It displayed distortion even though it was never trained under perturbations. D: Circle drawing movements under perturbation forces. E: After learning circle drawing task with forces, perturbations are removed to observe the aftereffect without any forces. The effect shown here is similar to the aftereffects in C. F: The learned effect washed out after experiencing no forces for over 50 trials.

discrimination is not possible for movements in the same state space. Gandolfo [1996] altered visual cues by varying the color of the training room's lighting in conjunction with the force perturbation directions during reaching movements. After training, the movements were not distorted. Gandolfo also modified the proprioceptive cues by asking the subjects to use two different thumb postures in association with two different force directions. The overall posture of the arm was not altered by moving the thumb. As with the visual cue experiment, subjects could not learn to distinguish the forces.

As indicated above, movement adaptation is strongly generalized according to the intrinsic coordinates of the limb. Simple cues associated with external force perturbations do not necessarily cause our nervous system to create multiple internal models. Since previous experiments do not supply any evidence of contextual level distinction and generalization, further investigation was required to understand our ability to acquire multiple movements within one state space.

5.3 Summary of Experiments

In this chapter, the contextual level differentiation in motor control is investigated and results from the human psychophysical experiments are presented. In the experiments, a manipulandum was used again to induce force perturbations to the subject's arm during reaching movements. The specifications and setup of the manipulandum are described in Chapter 1.

To review the basic phenomena of movement generalization, three control experiments were conducted. Following these, contextual variations were applied over the space used for the control experiments. These experiments explored the generalization characteristics of our nervous system under situations when multiple tasks need to be accomplished using the same movement. The summary of all the experiments conducted in this chapter are tabulated in Table 5.1. The contextual differences were imposed by varying components such as location of the targets, velocity of the movement, segments of the movements, and the amount of knowledge given about the movements.

One training session consisted of three epochs of 192 reaching movements. The first epoch was assigned to be the baseline epoch without any perturbation. The following two epochs were trained with force perturbations. To prevent anticipatory movements, a holding time of one second was enforced between the time the target was displayed on the screen and the time the subjects were allowed to begin a movement.

Exp.	*#*	*Movement* *(deg)*	*(cm)*	*(cm)*	*Perturbation* *(deg)*	*Interval* *(+/- 0.05 sec)*	*Investigate:*
CE	1	90	20	0	180	0.50	Generalization of movements with different magnitudes.
		90	10	0	no training	0.50	
		90	10	v10	no training	0.50	
	2	90	20	0	no training	0.50	
		90	10	0	180	0.50	
		90	10	v10	no training	0.50	
	3	90	20	0	0	0.50	
		90	20	0	180	0.50	
SIZ	1	90	20	0	180	0.50	Separation of generalization with different magnitude of movements.
		90	10	0	0	0.50	
		90	10	v10	no training	0.50	
	2	90	20	0	180	0.50	
		90	10	0	no training	0.50	
		90	10	v10	0	0.50	
	3	90	20	0	no training	0.50	
		90	10	0	180	0.50	
		90	10	v10	0	0.50	
SEG	1	90 → 180	10 → 10	0	no training	1.0	Separation of generalization with various segmentation.
		90	10	0	0	0.50	
	2	90 → 180	10 → 10	0	180	1.0	
		90	10	0	0	0.50	
	3	180 → 90	10 → 10	h10	no training	1.0	
		90	10	0	0	0.50	
	4	180 → 90	10 → 10	h10	180	1.0	
		90	10	0	0	0.50	
	5	90 → 180	10 → 10	0	0	1.0	
		90	10	0	180	0.50	
VEL	1	90	20	0	0	0.45	Sep. of gen. with velocity variance.
		90	20	0	180	0.75	
KNO	1	90	20	0	0	0.60	Same stimuli as VEL, with no velocity var.
		90	20	0	180	0.60	
	2	90	20	0	0	0.60	Same stimuli as VEL, with sequence var.
		90	20	0	180	0.60	
	3	90	20	0	0	0.60	Same stimuli as VEL, with known sequence var.
		90	20	0	180	0.60	

Table 5.1: The road map for experiments in Chapter 5. Three numbers in the "Movement" column are directions, the lengths of the movements, and the starting point deviation. Two segmented movements are specified with → for the first and second segments. The "Perturbation" column specifies the direction of the forces. The "Interval" column specifies the time interval that the movements must be completed in to receive a reward. The intervals are +/- 0.05 seconds from the specified time. In the KNO experiment, the variance is specified in the "Investigate:" column.

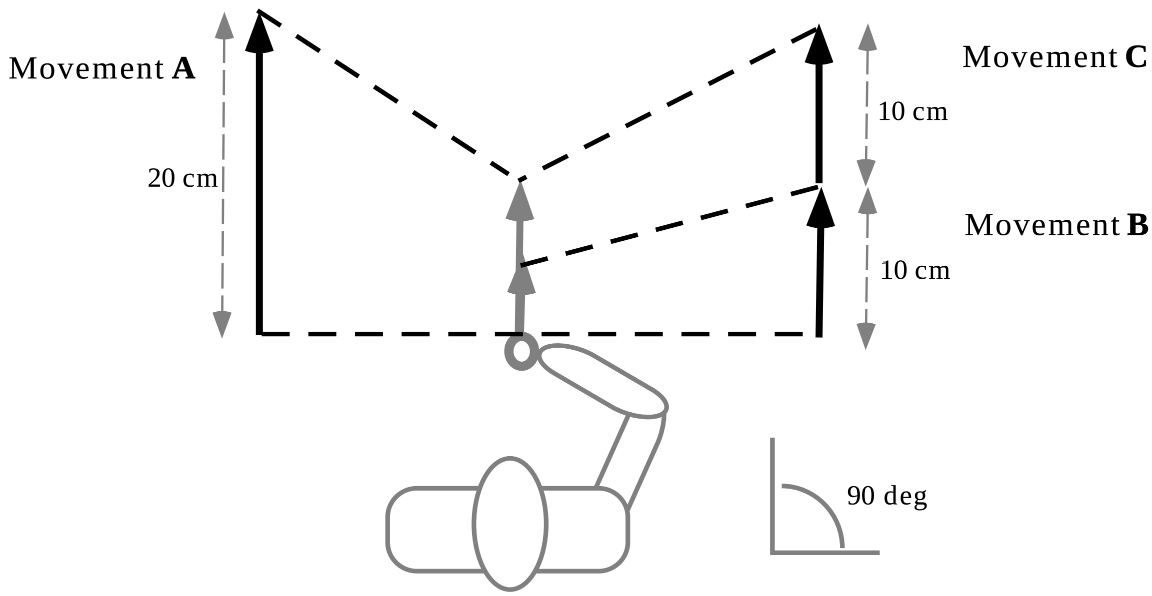

Figure 5-3: Three movements, A, B, and C were introduced. All the movements were made in the 90 degree direction, and are in the same state space of the arm. Movement A is 20 cm long, and Movements B and C are 10 cm long. Movements A and B share the same starting point, and Movement B's end point is the starting point for Movement C.

This starting time was indicated by a beep. The total movement had to be executed within the specified interval.

5.4 Experiment CE: Control Experiments

As control experiments, we demonstrate how an internal model built for one task can be generalized for tasks that are similar or the same in the state space of the arm.

Subjects were asked to make one continuous movement from one target to another in a specified time interval while holding the manipulandum end effector. Subjects were rewarded when the movements were executed within 0.5 +/- 0.05 seconds.

The three different movements used for the following experiments are illustrated in Figure 5-3. All movements were made to the 90 degree direction, away from the body. Movement A was a 20 cm long movement. Movement B was a 10 cm long movement sharing the same starting point as Movement A. Movement C was also a 10 cm movement whose end point was the same as that of Movement A. The starting point of this movement was the target point of Movement B. This setup was used for all three experiments.

Training Movement A Only

All the movements were trained without forces during the baseline epoch, as indicated in Figure 5-4.1. Next, force perturbation was applied only to Movement A (Figure 5-4.2). Movements B and C were not trained during the force epochs. Initially, the trajectories of the hand were distorted toward the direction of the forces; as seen previously, the subjects started making straight trajectories with training. Following the force epochs, the force field was removed to observe aftereffects for all three movements. These results are shown in Figure 5-4.5.

As predicted, Movement A exhibited a large aftereffect towards the direction opposite to the forces. In addition, Movements B and C both exhibited significant aftereffects in the same direction as Movement A. These results showed that the internal model built for Movement A transferred to Movements B and C. This statement seems intuitive since these smaller movements are subsets of the state space visited by the large movement, Movement A.

Training Movement B Only

The second experiment was conducted with the same setup as the previous experiment, but this time only Movement B was trained under perturbation. The results of this experiment are shown in Figure 5-5. After training, forces were removed to observe the aftereffects for all three movements. As shown in Figure 5-5.5, the effect learned for Movement B transferred to Movements A and C without training, showing that the internal model built for Movement B was generalized for Movement A and C. Even though the state spaces used for Movements A and C are not the subset of Movement B, these movements are intrinsically similar. Thus, it is not surprising that the learned effect from Movement B transferred to the other movements, if the nervous system generalizes motor information in intrinsic coordinates.

Training Movement A with Two Different Forces

So far we have shown that if force perturbations were applied to one movement, the learned effect is not only observable for the movement that was trained but also for the movements that are not trained if they are intrinsically similar.

As shown by Brashers-Krug, et al. [1996], opposite perturbations cannot be learned within close spatial areas. In the third control experiment, this interfering phenomenon is demonstrated under the setup used for this chapter.

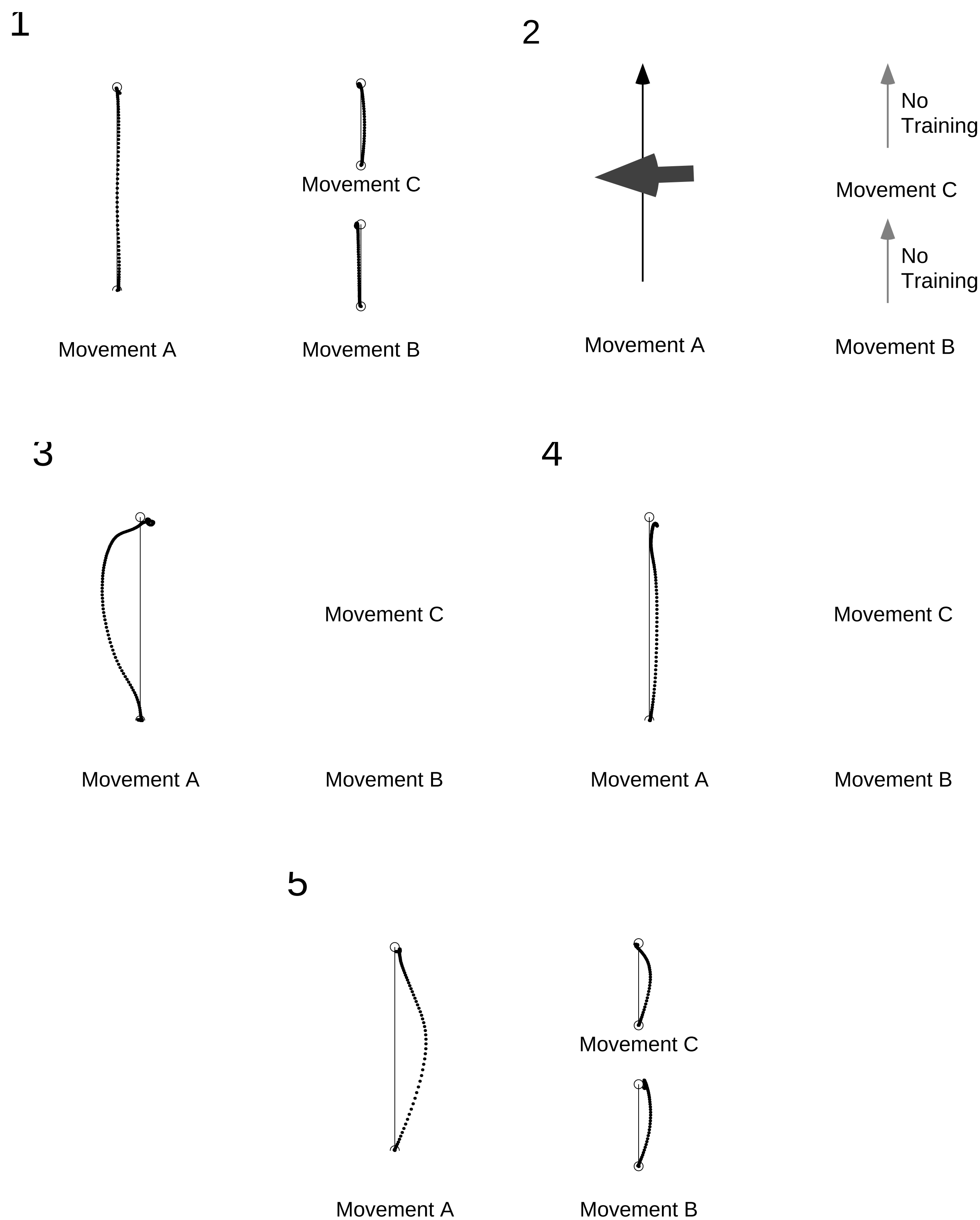

Figure 5-4: 1: Movements A, B, and C were trained without perturbations to establish baseline performance. The movements were straight to the targets. 2: The force applied during force epochs. 3: A trajectory early in the training session under perturbations. The movement was distorted to the direction of the forces. 4: A trajectory later in the training session under perturbations. The movement is again straight like the baseline movements. 5: The aftereffects were observed for all three movements. The distortion observed for Movement A was also seen in Movements B and C.

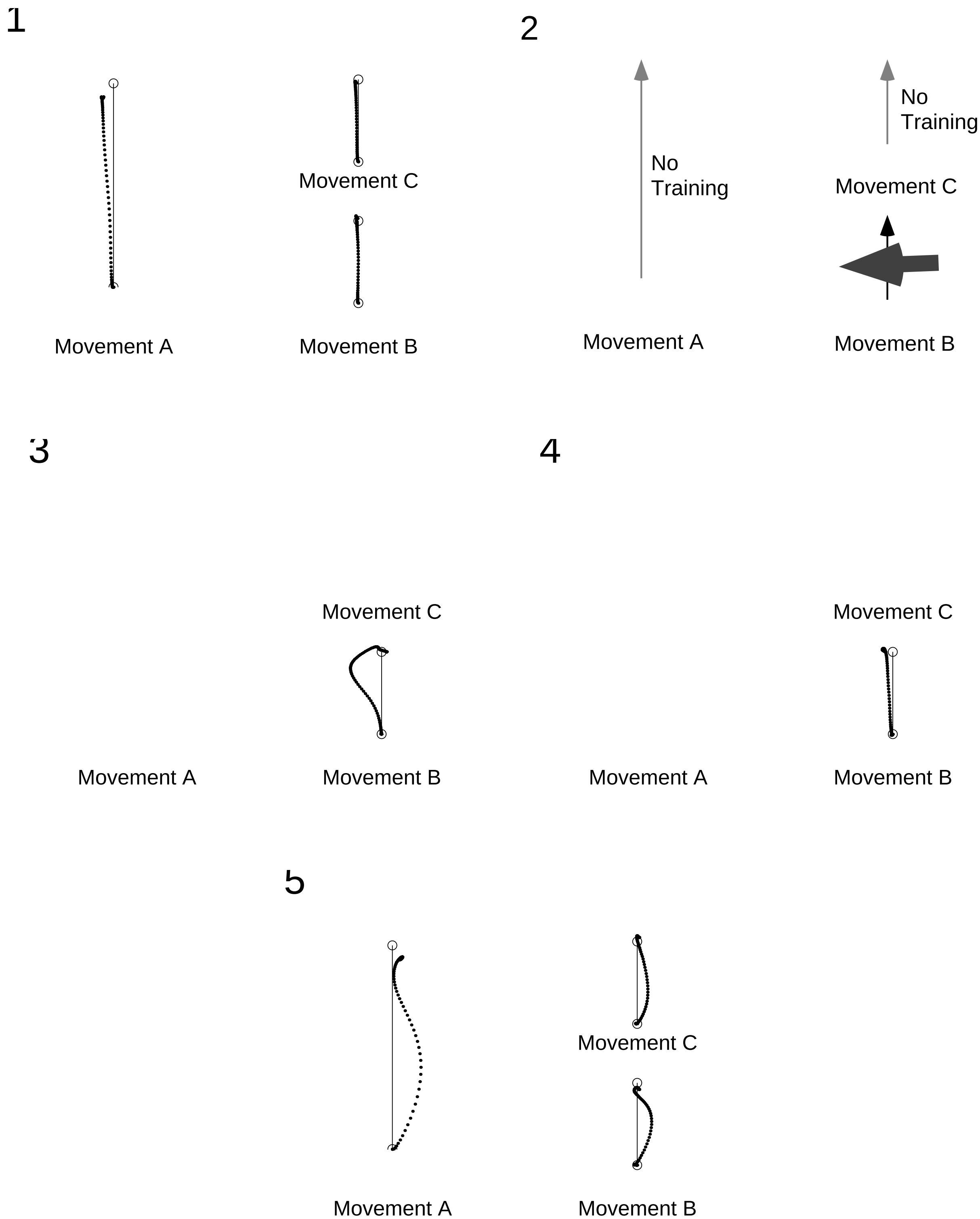

Figure 5-5: 1: Movements A, B, and C were trained without perturbations to establish baseline performance. 2: The force applied during force epochs. 3: A trajectory early in the training session under perturbations. The movement is distorted to the direction of the forces. 4: A trajectory later in the training session under perturbations. The movement is again straight like the baseline movements. 5: The aftereffects were observed for all three movements. The distortion observed for Movement B was also seen in Movements A and C.

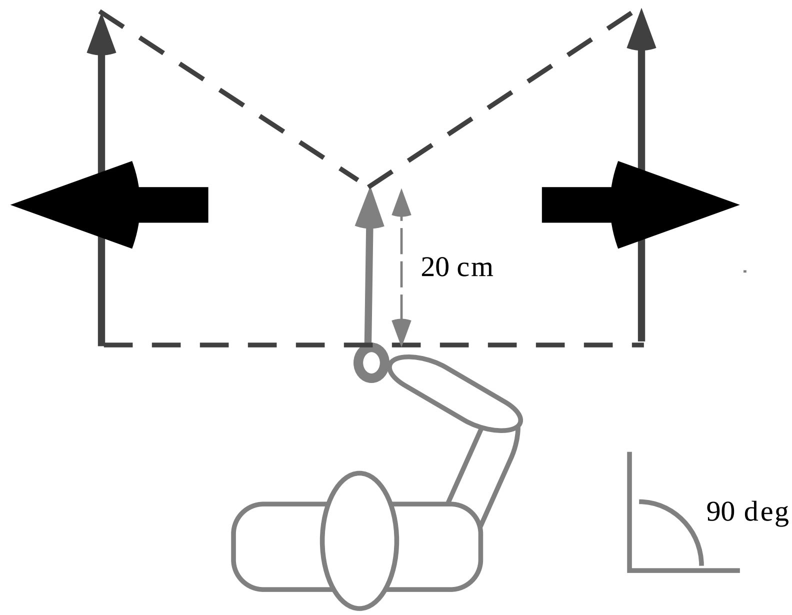

Figure 5-6: Two opposite force perturbations are designed to be applied for the same movement during Experiment CE. These two forces were applied interleavingly in a random order.

All the movements trained were identical; 20 cm long 90 degree reaching movements. The movement time was specified to be 0.5 +/- 0.05 seconds. The baseline movements were established without perturbations. The force perturbations were designed to apply two opposite forces in a random order. The two forces were 180 degree (to the left) and 0 degree (to the right) forces as shown in Figure 5-6. Before the movement was begun, subjects could not know which forces would be applied. They were trained for two epochs of 192 trajectories under force perturbations. In the force field, the hand trajectories did not become straight even after two full epochs of force training as shown in Figure 5-7.3. When the forces were removed, there was no distortion in the hand movements specifically matching either force field (Figure 5-7.4). Thus if movements in the same direction and magnitude are executed in the same workspace and each movement is subjected to opposite perturbations, neither perturbation can be learned to the same degree as before. This implies that the internal model for this task was not altered by the perturbations.

These results lead to the hypothesis that there is only one internal model for each state space. The next four experiments address whether two conflicting perturbations can be learned in the same state space if they are presented through different contexts. To explore this issue, contextual information such as size, velocity, sequence and knowledge of the movements were varied.

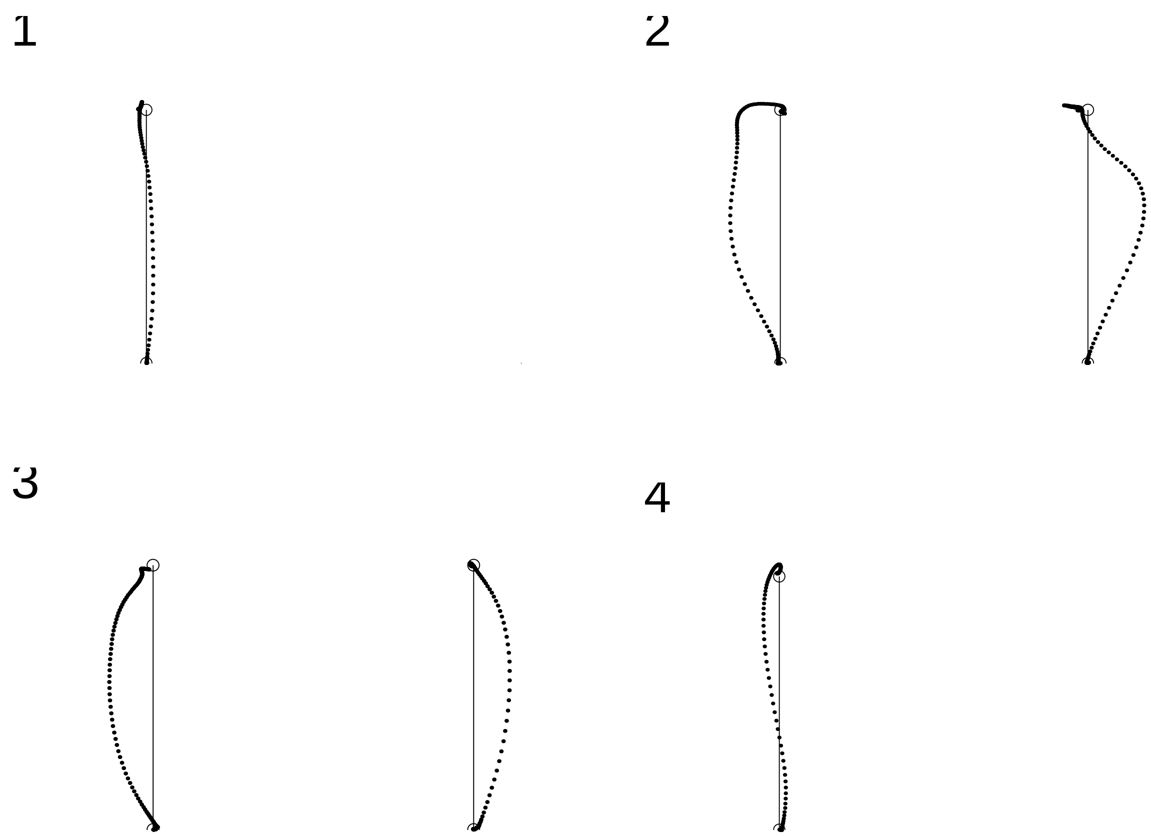

Figure 5-7: 1: A typical baseline trajectory without perturbations. 2: Initial trajectories under forces. The trajectory on the left had the forces to the left and the other to the right. 3: Later trajectories under forces. The trajectories are still distorted to the direction of the forces. 4: Aftereffects observed after training. The movements were not distorted to the specific direction of forces.

Group #	*Trajectory with 180 degree force field*	*Trajectory with 0 degree force field*
1	A	B
2	A	C
3	B	C

Table 5.2: Trajectories trained under perturbations in Experiment SIZ.

5.5 Experiment SIZ: Size Variance in Reaching Task

In this section, opposite forces were introduced for movements in the same workspace and direction. The setup shown in Figure 5-3 was used again for this experiment. There were three movements, A, B, and C, each corresponding to 20 cm movement, 10 cm movement with the same starting position as Movement A, and 10 cm movement with the same end position as Movement A. Instead of training only one trajectory, two trajectories were trained with opposite forces. Aftereffects were observed for all three trajectories.

Table 5.2 shows the combinations of trajectories trained with corresponding perturbation force directions for the next three experiments. Two epochs with force perturbation followed the baseline epoch. The last 30 trajectories in the forces were interleaved with catch trials to observe aftereffects.

Training Movements A and B with Opposite Forces

The first group from Table 5.2 was tested for two movements that shared the same initial hand location and direction, but were of different magnitudes; 10 cm and 20 cm. As shown in Figure 5-8.1, two opposite forces were applied for each movement. Initial trajectories were distorted in the directions of the forces as shown in Figure 5-8.2. With training, the distortions diminished. During catch trials, Movement A and B were distorted in two different directions (Figure 5-8.4) matching the forces that these movements had been trained under. This is surprising because distinguishing two different force perturbations for the same state space of the arm had been assumed to be impossible. As shown in Figure 5-4 and 5-5, two movements executed in the same location are usually generalized together. However, in this experiment these movements were disassociated.

Moreover, the catch trials for Movement C, which was not trained under perturbations, exhibited aftereffects in the same direction as seen for Movement A. Since the only time these states for Movement C were visited was during Movement A, it is

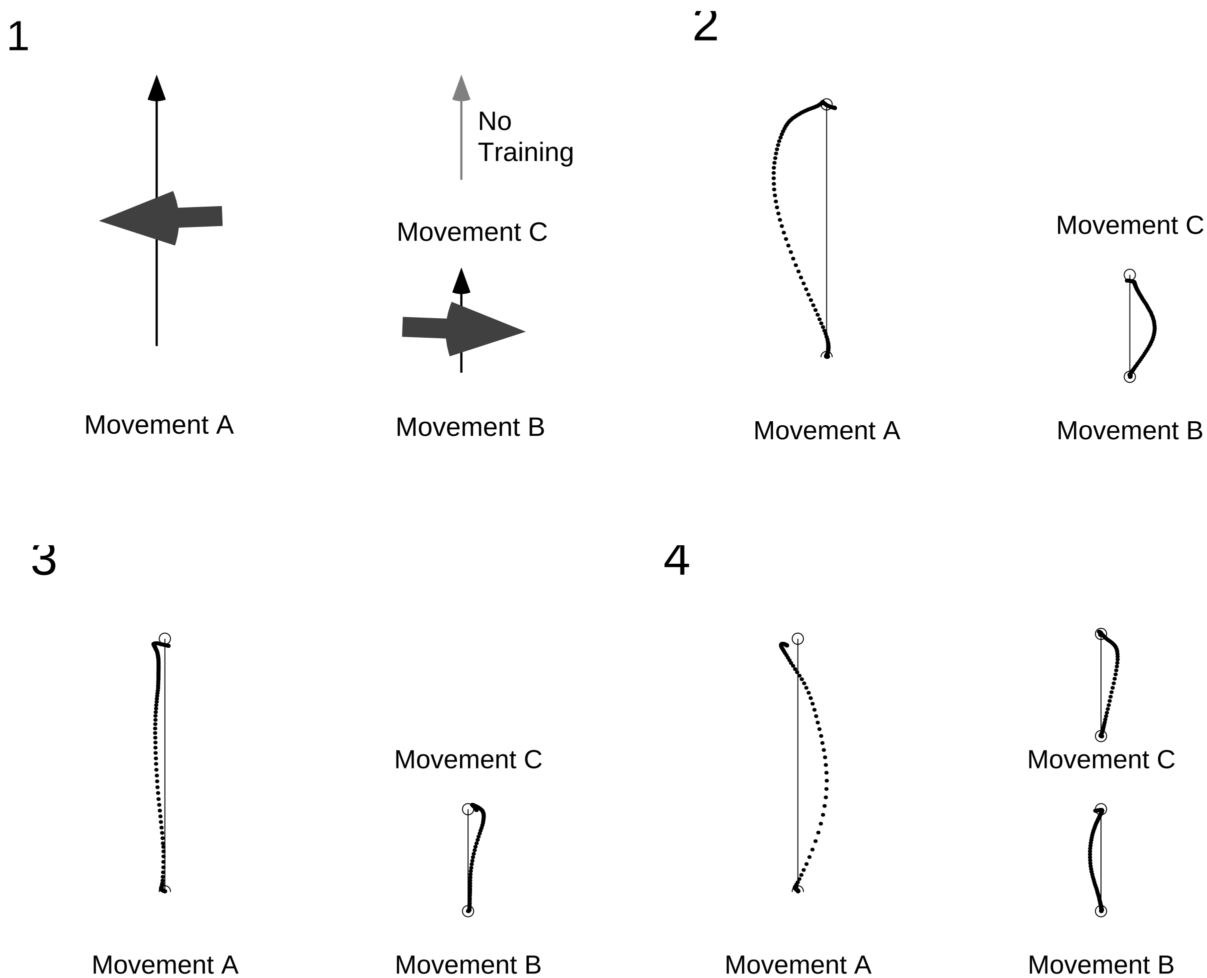

Figure 5-8: 1: The perturbation force directions applied during training sessions. Movement A to the left and Movement B to the right. 2: Initial trajectories during training. The movements are distorted in the direction of the forces. 3: Trajectories later in training. The distortions seen initially are decreased. 4: Interleaved catch trial trajectories without perturbations. Movements A and B display separate aftereffects showing separate generalization. Movement C had the same directional distortion as Movement A.

reasonable that the learned effect was generalized. These results are consistent with the control experiments, but it is still intriguing that the effect did not transfer from Movement B which was of the same magnitude and velocity.

This experiment was tested on six subjects. Out of these six, two did not learn the two opposite perturbations separately; instead, all of their movements showed aftereffects toward the same direction. This phenomenon is addressed in Chapter 7.

Training Movements A and C with Opposite Forces

Next, the second group from Table 5.2 was tested. For this group, Movements A and C were trained with opposite forces, as shown in Figure 5-9.1. These two movements had different starting points but shared the same target position. If in the first group the reason for the disassociation was the difference in visual stimulus (location of the target shown on the screen), this experiment should show that these two reaching movements are not distinguishable. Contrary to this prediction, the movements in the same workspace were learned separately as shown in Figure 5-9.4. In this experiment, only one of the six subjects adapted to a different strategy. Consistently from the previous experiment, the trajectory not trained exhibited aftereffects similar to those for Movement A.

Training Movements B and C with Opposite Forces

In Experiment ST-1, Movements B and C were shown to be separatable. However, the effect of the combined movement, Movement A, which was not trained, was not observed. For this group, as in Experiment ST-1, Movements B and C were trained with opposite forces, but the forces were removed intermittently for all three movements to check for aftereffects. Consistent with previous results, the aftereffects of Movements B and C were opposites, matching the corresponding forces experienced as shown in Figure 5-10. The aftereffect for Movement A appeared as if those for Movements B and C were combined. This result is quite interesting because it shows that two internal models may be combined to create a movement that does not necessarily have a model of its own.

If a specific perturbation was introduced for Movement A in addition to the training above, an aftereffect matching the applied force could be obtained. In addition to the left and right forces for Movements B and C, Movement A was perturbed to the left, as shown in Figure 5-11.1. After training, forces were removed to measure aftereffects. As shown in Figure 5-11.2, all three trajectories showed aftereffects matching

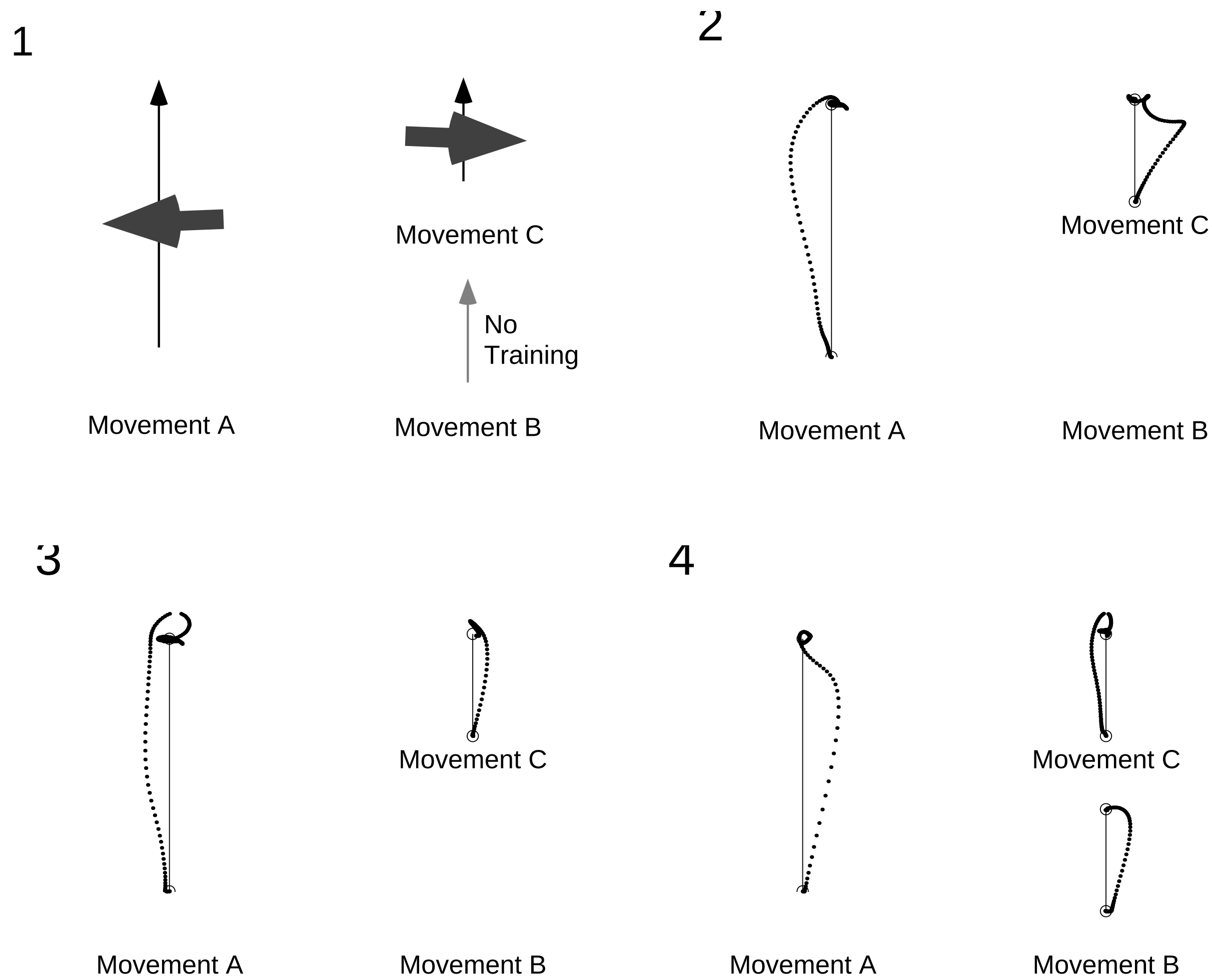

Figure 5-9: 1: The perturbation force directions applied during training sessions. Movement A to the left and Movement C to the right. 2: Initial trajectories during training. The movements were distorted to the direction of the forces. 3: Trajectories later in training. The distortions seen initially were decreased but they were still observable. 4: Interleaved catch trial trajectories without perturbations. Movements A and C displayed separate aftereffects showing separate generalization. Movement B had the same directional distortion as Movement A.

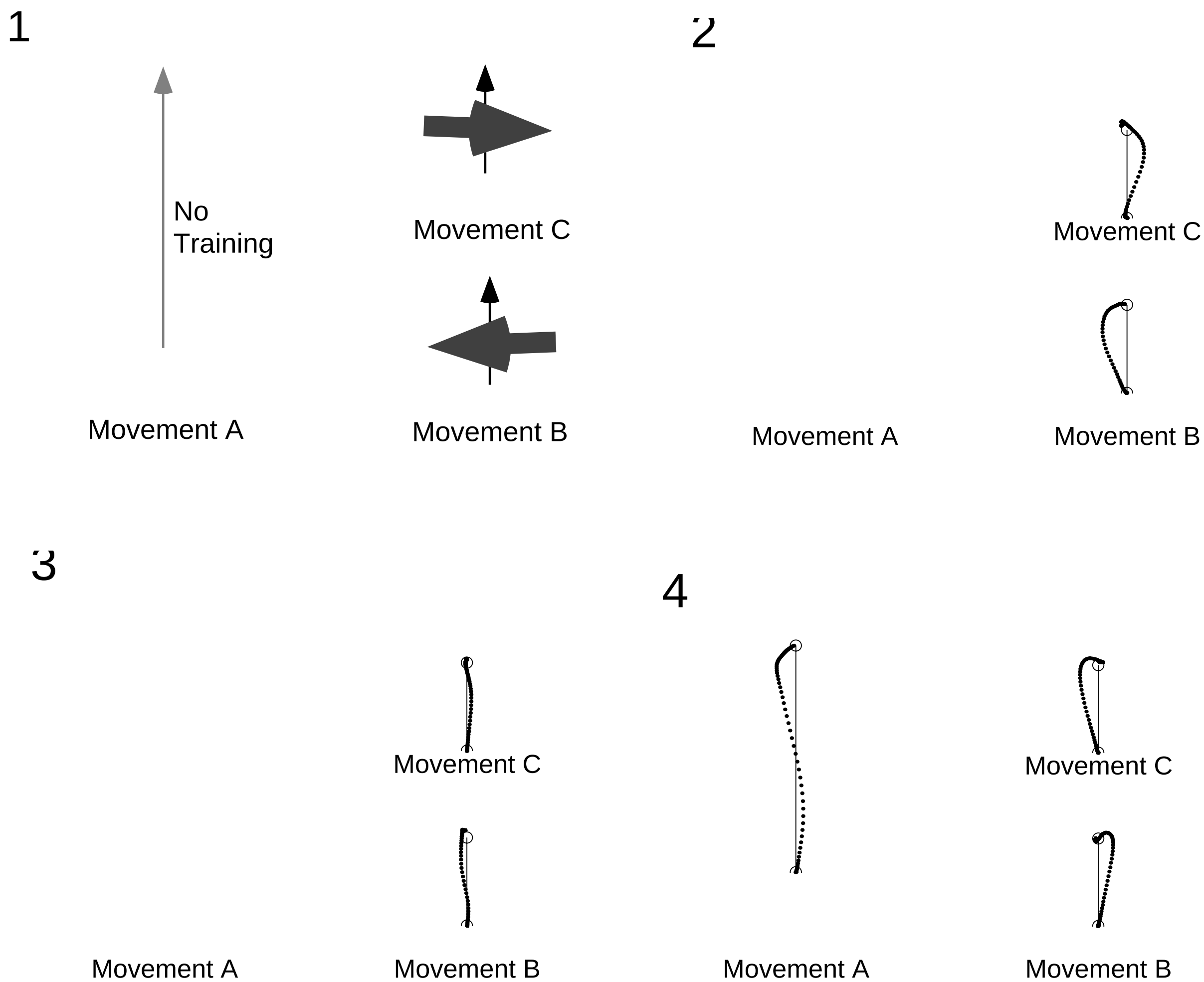

Figure 5-10: 1: The perturbation force directions applied during training sessions. Movement B to the left and Movement C to the right. 2: Initial trajectories during training. The movements were distorted to the direction of the forces. 3: Trajectories later in training. The distortions seen initially diminished. 4: Interleaved catch trial trajectories without perturbations. Movements B and C displayed separate aftereffects showing separate generalization. Movement A looked as if the effects from Movements B and C were combined.

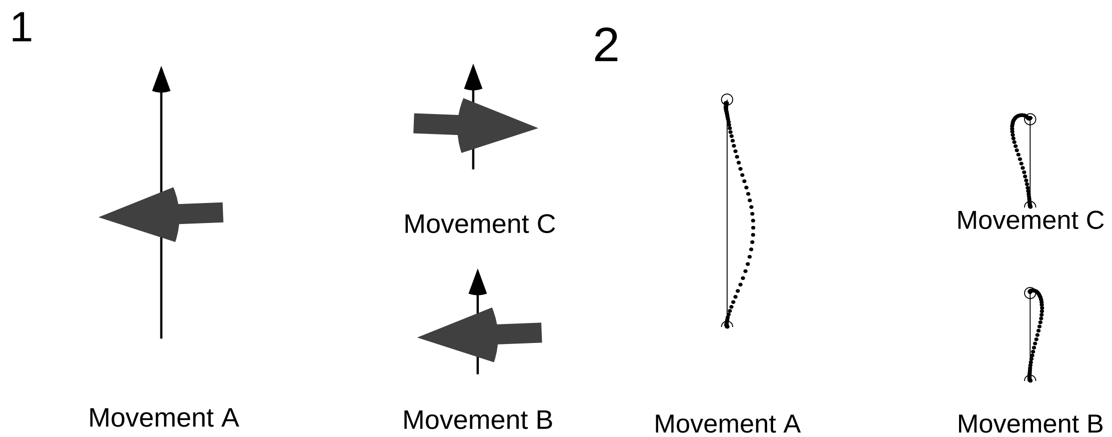

Figure 5-11: 1: Perturbation force directions for all movements. 2: Aftereffects observed after training was over. Each trajectory exhibited distortion toward the opposite direction of the forces experienced.

the forces experienced specific to each trajectory. Thus, movements that share the same spatial location and direction can be separately associated with different internal models if the magnitudes of the movements are different.

5.6 Experiment SEG: Segment Variance in Reaching Task

In the last section, it was shown that multiple independent models could be obtained for the same state space of the arm while the movement size was varied. By varying the size of reaching movements, other parameters were also altered as a consequence. For example, the velocity of the hand movements had to be larger for longer movements because the desired movement time to the target was set to be the same for all movements. The location of the hand when the peak velocity was reached was also different.

In this section, a new experiment was proposed to ensure consistent velocity and size of the reaching movements by changing the reaching task into a "via point" reaching task. The experiment was designed to have seven 10 cm reaching segments arranged as shown in Figure 5-12. One reaching task consisted of either one or two segments. The two segmented movements were "L" shaped movements with a via point at the turning point. These movements are interleaved randomly with single segment movements. The trajectory investigated for this experiment was the 90 degree movement executed at the middle of the workspace as highlighted in Figure

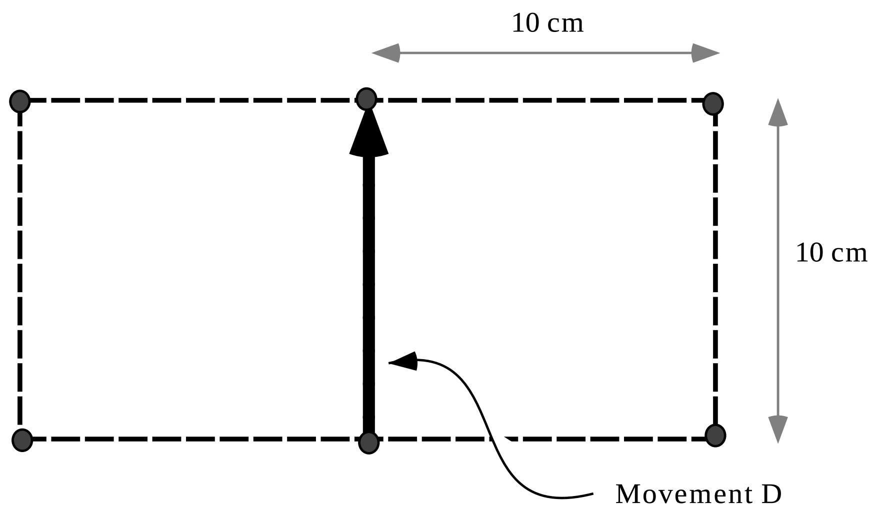

Figure 5-12: Seven 10 cm segments are used for "via point" experiment. One reaching task had either one or two segments. If two segments were used, the end of the first segment was used as a via point. The trajectory investigated for this experiment is highlighted. The movement that used the highlighted segment without any via point is denoted as Movement D.

5-12. The highlighted segment movement is denoted as Movement D.

Using the results from Experiment DOM and ST1, all movements that may interfere or contribute to learning Movement D were eliminated from the training set. For example, the movements shown in Figure 5-13 interfered with learning Movement D. If the force direction for these movements was opposite to the training force direction for Movement D, it had an unlearning effect, as shown in Experiment ST1. In parallel, if these movements were trained with the same force direction as the training direction, these movements would result in contributing to learning Movement D. Thus, any movements that were combined with these movements were eliminated. Even though the -90 degree movements may have shared the same spatial locations, they appeared to have no effect on learning 90 degree movements, as shown in Experiment DOM. Therefore they were included in the training set.

The targets were 4 x 4 mm and blue, via points were 2 x 2 mm and yellow, and the hand cursor was 2 x 2 mm and white. The movement criteria for the "L" movements was to pass through the via point by making two continuous movements as if they were separate, individual movements. The subjects were rewarded only if the hand cursor directly passed over the via point within a 0.5 +/- 0.05 second interval and the overall reaching time was 1.0 +/- 0.1 seconds.

As shown in Figure 5-14, two different "L" movements contained the 90 degree segment were executed (Movement D). Movement E contained the 90 degree movement

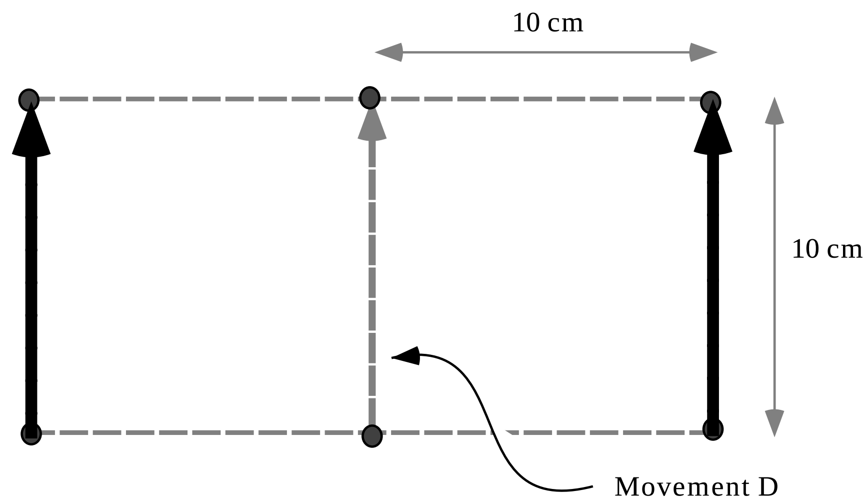

Figure 5-13: Movements that contain the segments shown are excluded because of their influence to the learning ability for Movement D. If these movements are perturbed to the opposite direction from Movement D's perturbations, they interfere with learning Movement D; whereas if these movements are perturbed to the same direction, they contribute to learning Movement D.

as its first segment and Movement F contained it as its second segment.

Five groups of people were tested under this experimental setup. Subjects from all groups were trained with one baseline epoch, and two training epochs with perturbations. The second training epoch contained randomly interleaved catch trials with no forces for the last 30 movements. The testing conditions for the five groups are presented in Table 5.3.

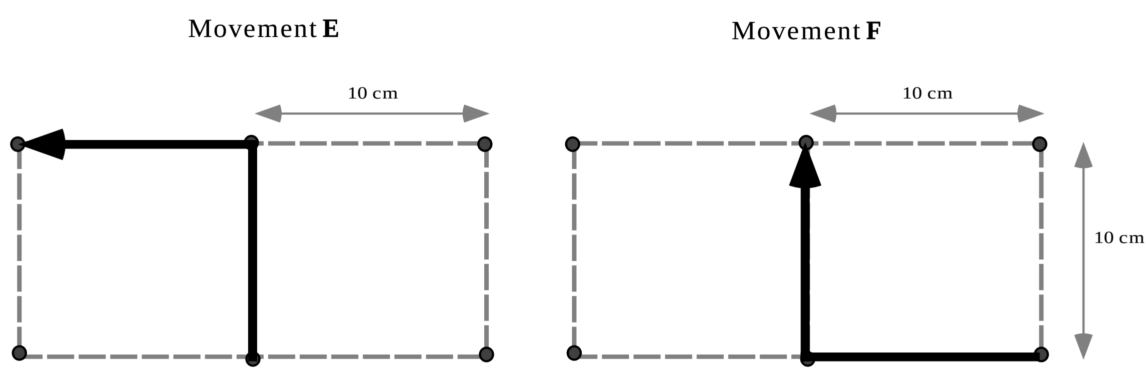

Figure 5-14: Two "L" movements tested for Experiment SEG. Movement E uses the 90 degree segment (Movement D) as the first segment, and Movement F uses it as the second segment.

Group #	*with 0 degree field*	*with 180 degree field*	*# of subjects*	*aftereffects observed for*
1	D		2	D, E
2	D	E	6	D, E
3	D		2	D, F
4	D	F	6	D, F
5	E	D	6	D, E

Table 5.3: Five groups of subjects were tested for Experiment SEG. While Groups 1 and 3 tested the generalization properties by training only Movement D, Groups 2 and 4 applied opposite forces to Movement D from the "L" movements to observe the effect in adaptation. Groups 1 and 3 contained two subjects and Groups 2 and 4 contained six subjects.

Training Movement D Only

The goal of this paradigm was to observe if the learned effect for Movement D would be generalized to Movement E, which contains the trained movement. The baseline epoch and the catch trials included both Movements D and E. However, during training with forces, only Movement D was executed.

The results for both subjects were consistent, and they are shown in Figure 5-15. The perturbations imposed on Movement D were learned as the distortion toward the force direction diminished. When the forces were removed, both Movement D and E were distorted in the direction opposite to the forces experienced for Movement D. This result was expected for the movements made in the same spatial location and in the same direction.

Training Movements D and E with Opposite Forces

As shown in Figure 5-16.1, both Movements D and E were trained, each perturbed with opposing forces, for the second group. Movement D was perturbed to the right and Movement E was perturbed to the left. Even after two training epochs, the distortion of the hand trajectories was not minimized, as seen in Figure 5-16.3. For all subjects, the aftereffects observed during catch trials did not match the corresponding forces (Figure 5-16.4). Four of six subjects did not display significant spatial distortions during catch trials. In contrast, the other two subjects adopted a different strategy for learning these forces: for both Movements D and E, their hand movements were significantly distorted in the same direction. This strategy is discussed in Chapter 6.

This result shows that it is more difficult to distinguish two movements as separate tasks when the magnitude and velocity of the movements were the same. To further

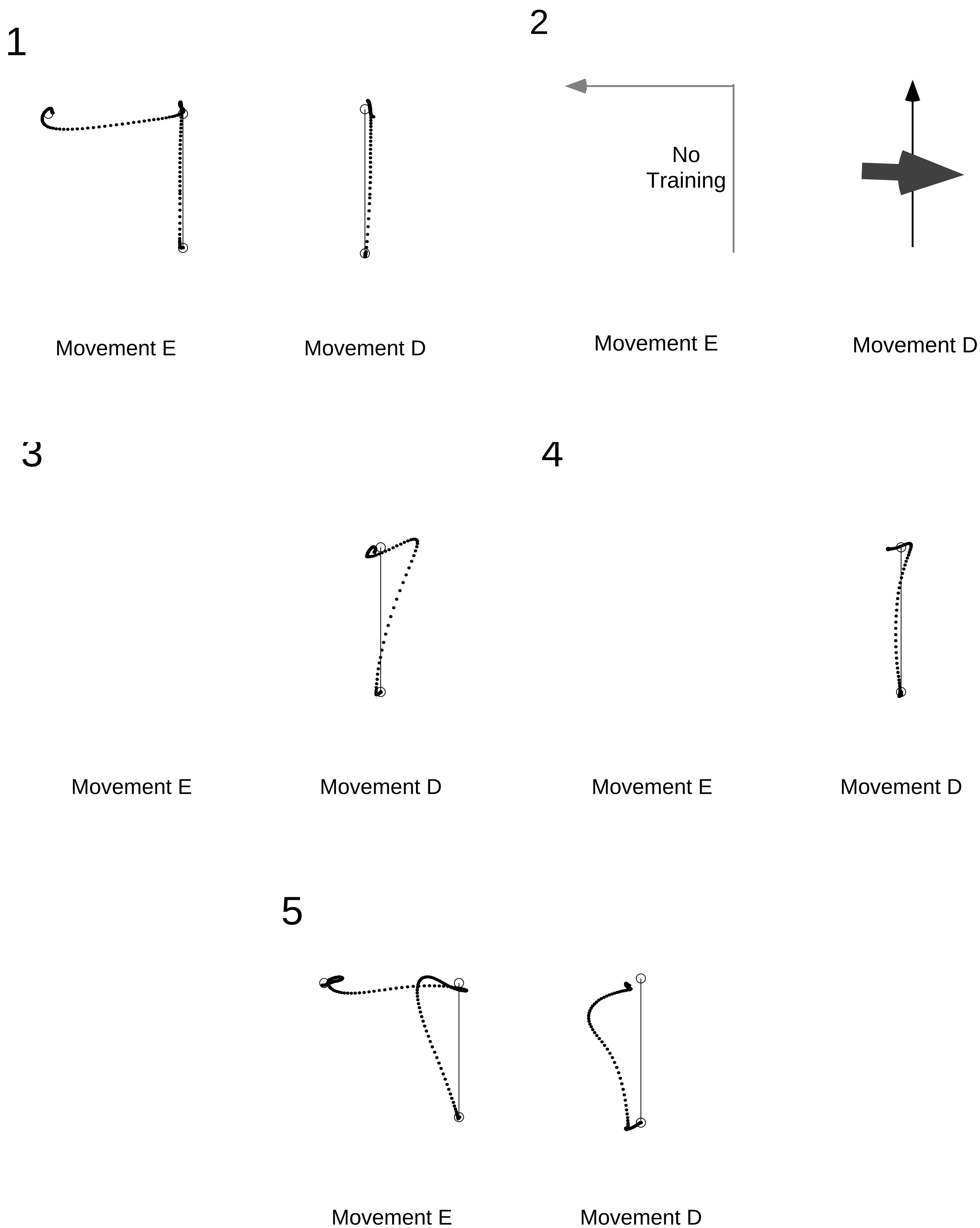

Figure 5-15: Results for training Movement D only. 1: Baseline movements for Movements D and E. 2: Perturbation force direction assigned for Movement D. 3: Initial trajectory under perturbations. The distortion observed is to the direction of the forces. 4: Trajectory for Movement D later in training. The distortion has diminished. 5: The aftereffects during catch trials for Movements D and E. The effect learned for Movement D transferred to Movement E.

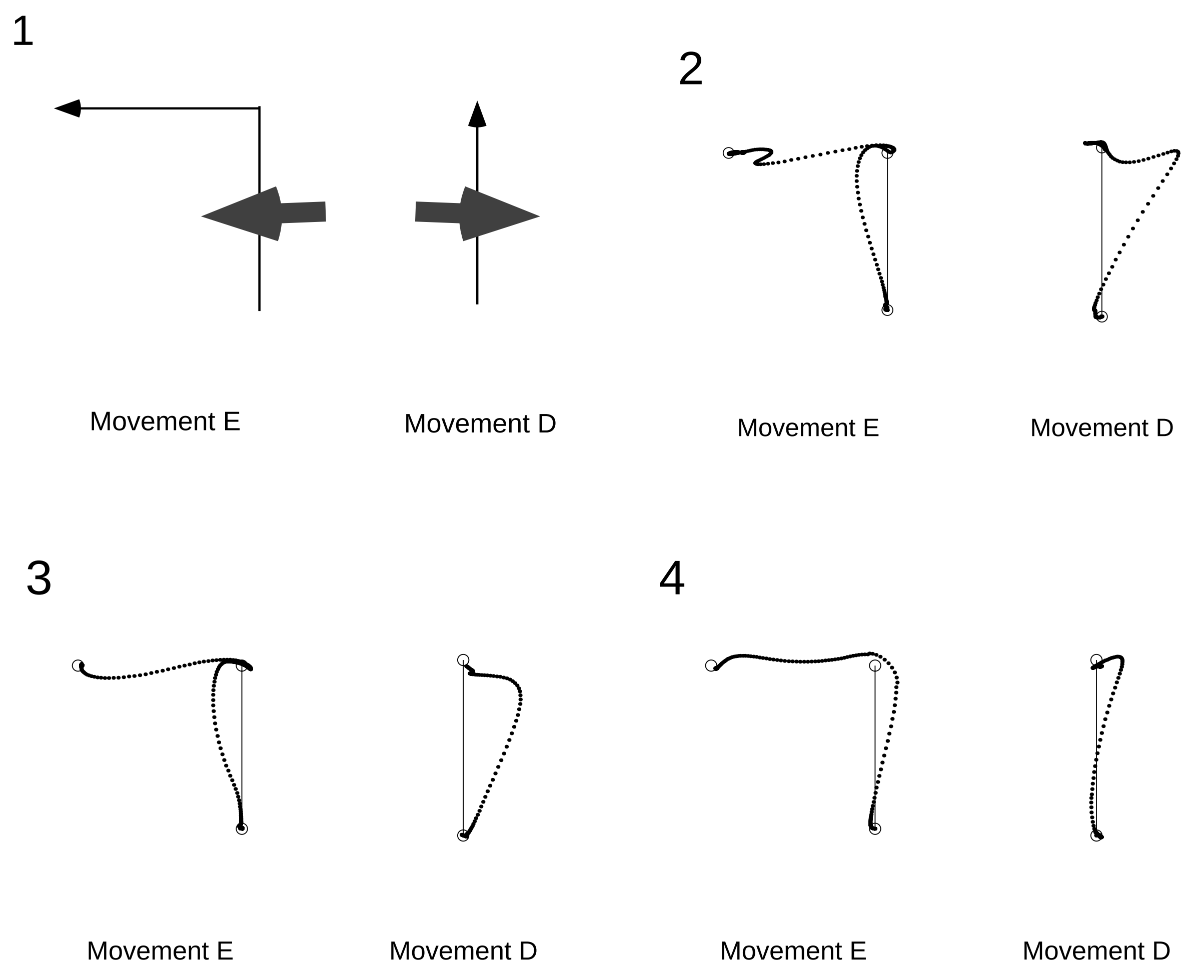

Figure 5-16: Results for training Movements D and E without forces. 1: Perturbation force directions assigned for Movements D and E. 2: Typical initial trajectories under perturbations. The distortions observed are to the directions of the forces. 3: Typical trajectories later under perturbations. The distortions are still observable. 4: The aftereffects during catch trials for Movements D and E did not show distortions that represent learning of the perturbations.

analyze this result, another "L" movement was investigated for the next two groups.

Training Movement D Only

This group was tested for the same condition as the first group except that Movement F shown in Figure 5-14 was used in place of Movement E. Movement F contained the segment of interest as the second segment of the movement. Movements D and F had different starting points but the same target points. Aside from Movements D and F, no trajectories passed through the middle 90 degree trajectory.

The baseline was established for both Movements D and F before forces were turned on, as indicated in Figure 5-17.1. The perturbations were applied only to Movement D, and Movement F was never required during force epochs. After training, both Movements D and F were executed under no force perturbations. As predicted, the learned effects from Movement D indeed transferred to Movement F for both subjects as shown in Figure 5-17.5.

Training Movements D and F with Opposite Forces

For this experiment, Movement F was perturbed to the opposite direction of the perturbations for Movement D. Movement D was exposed to a rightward force and movement F was exposed leftward force, as shown in Figure 5-18.1. After training with these forces, the perturbations were removed to observe the effects learned. Surprisingly, four out of six subjects retained two separate aftereffects corresponding to the directions of the forces as shown in Figure 5-18.4. The other two subjects used another strategy to cope with the situation and did not seem to develop two separate models of the perturbations. Despite the fact that not all the subjects learned two models, it is clear that it is possible to retain two models of the environment for the same movement executed under different contexts.

It is interesting to notice that the results from groups 2 and 4 from Table 5.3 were different. To confirm that these results were not perturbation direction dependent, the Movements D and E were trained again, but with the forces opposite to those in the previous experiment.

Training Movements D and E: revisited

The experiment for this group was conducted simply to check whether the perturbation force directions contribute to the contextual ability to separate two models. The

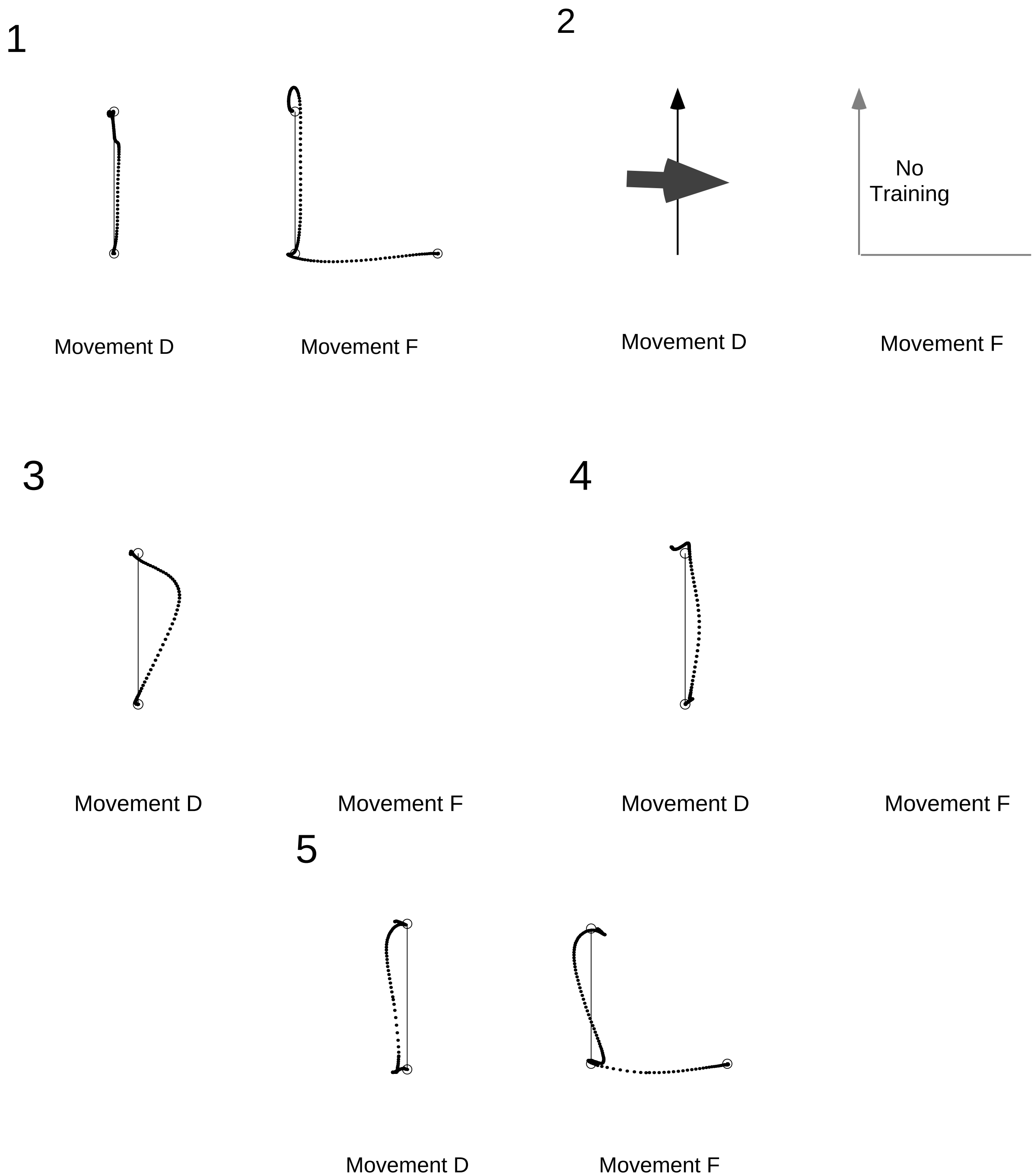

Figure 5-17: Results for training Movement D only. 1: Baseline movements for Movements D and F. 2: Perturbation force direction assigned for Movement D. 3: Initial trajectory under perturbations. The distortion observed is to the direction of the forces. 4: Trajectory for Movement D later in training. The distortion has diminished. 5: The aftereffects during catch trials for Movements D and F. The effect learned for Movement D transferred to Movement F.

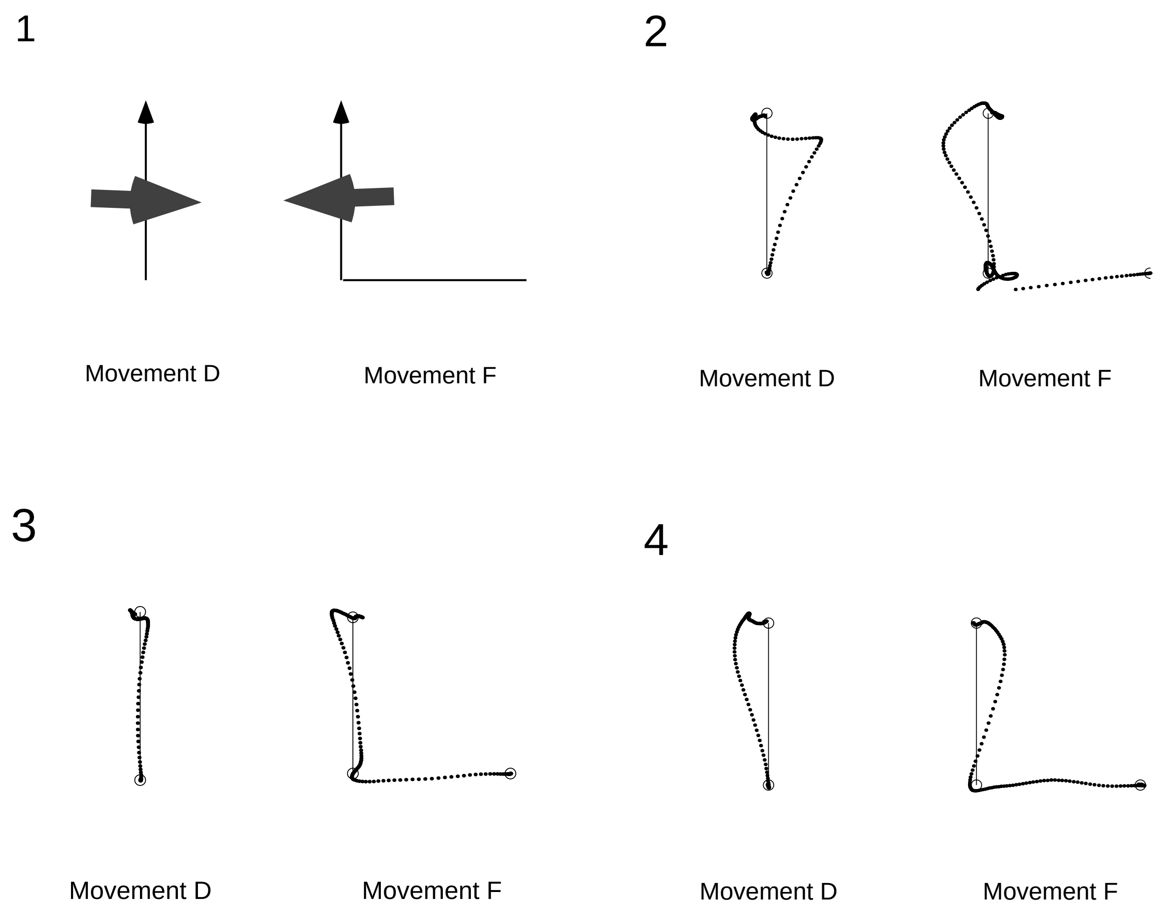

Figure 5-18: Results for training Movements D and F with opposite forces for four out of six subjects tested. 1: Perturbation force directions assigned for Movements D and F. 2: Typical initial trajectories under perturbations. The distortions observed are to the directions of the forces. 3: Typical trajectories later under perturbations. 4: The aftereffects during catch trials for Movements D and F. Both movements were distorted to the directions of the forces showing that two separate models were learned for Movements D and F.

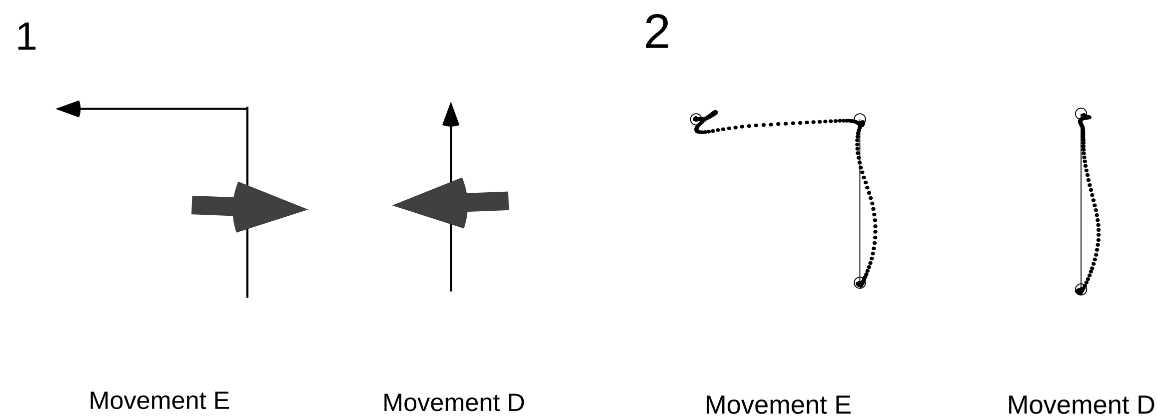

Figure 5-19: Results for training Movements D and E with opposite forces from the second group. 1: Perturbation force directions. 2: The aftereffects did not contain opposite distortions.

experiment was set up exactly as for the second group but with the force directions flipped 180 degrees as shown in Figure 5-19.1. For all six subjects tested under this condition, the aftereffects for Movements D and E were not distinguished (Figure 5-19.2). This result was consistent with the second group. Thus, for the fourth group, the direction of the perturbation forces did not contribute to the learning of multiple models.

There are various differences between Movements E and F. For example, the starting point of the movements are at different locations. If the movement planning for the first and the second segments are different in our nervous systems, or dependent on starting location, we can learn Movements D and F separately but not so for Movements D and E.

These experiments were conducted at the edge of learnability for humans. Thus from these experimental results, it is difficult to determine whether it is impossible to learn Movements D and E separately. However, over 50% of the fourth group's subjects appeared to be able to obtain two separate internal models for the same movements. It might be hoped that even Movement E can be learned separately from Movement D if the experiment consisted of more trials or if stricter criteria were imposed during training.

5.7 Experiment VEL: Velocity Variance in Reaching Task

From Experiments SIZ and SEG, it is clear that movements made in the same intrinsic space are not strictly generalized together. These experiments varied the movement trajectories themselves. In Experiments VEL and KNO, the movement trajectories were assigned consistently while other variables were changed. In Experiment VEL, an experiment was conducted to verify whether velocity variance for the same movement would allow the construction of multi-layered internal models.

All the movements used for this experiment were identical: 20 cm long 90 degree reaching movement. The speed assigned was displayed as "FAST" and "SLOW" on the left corner of the screen. The color of the targets were varied to magenta and green to correspond to the speed assigned. The fast (magenta) movement time was assigned to be 0.45 +/- 0.05 seconds while the slow (green) reaching time was assigned to be 0.75 +/- 0.05 seconds. Subjects received a quacking reward sound if the target was reached within the interval. This color coding allowed the subjects to calibrate their movements during the baseline training.

Six subjects were tested for this experiment, and they were tested for one baseline and two force epochs. All epochs consisted of randomly interleaved slow and fast reaching movements. In the baseline epoch, all subjects learned to make two distinct velocity movements without any force perturbations (Figure 5-20).

Depending on the speed of the hand movements, two different force perturbations were applied during the training session. The forces pushed the hand to the right for fast movements and to the left for slow movements. The last thirty trajectories of the force epoch were interleaved with catch trials to measure the aftereffects. As shown in Figure 5-21.3, for three of six subjects, when no forces were experienced during catch trials, the movements were distorted to the opposite direction of the forces depending on the speed of the movements. Therefore, it appears possible to obtain two separate internal models in the nervous system for exactly the same path if the velocity is varied. In Experiment CE, the same experiment was conducted without velocity variations. The results showed that neither forces were learned. Thus, velocity differences appear crucial to differentiating the internal models.

After training, subjects were asked whether they used the word on the corner or the color of the target to determine the speed of the next movement. All subjects stated that they initially used the spelled-out speed but eventually learned to associate speed with the color of the targets.

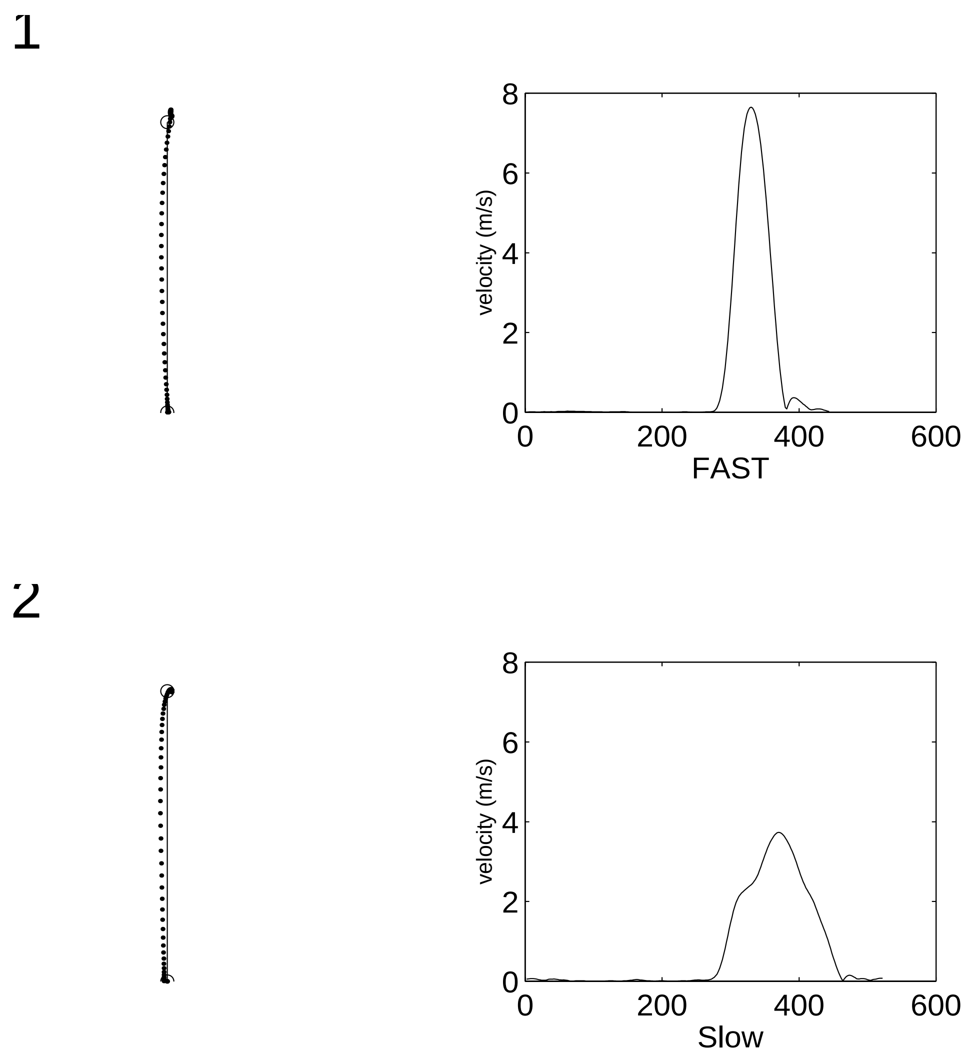

Figure 5-20: The baseline hand paths and their velocity profiles for fast and slow movements. 1: fast. 2: slow.

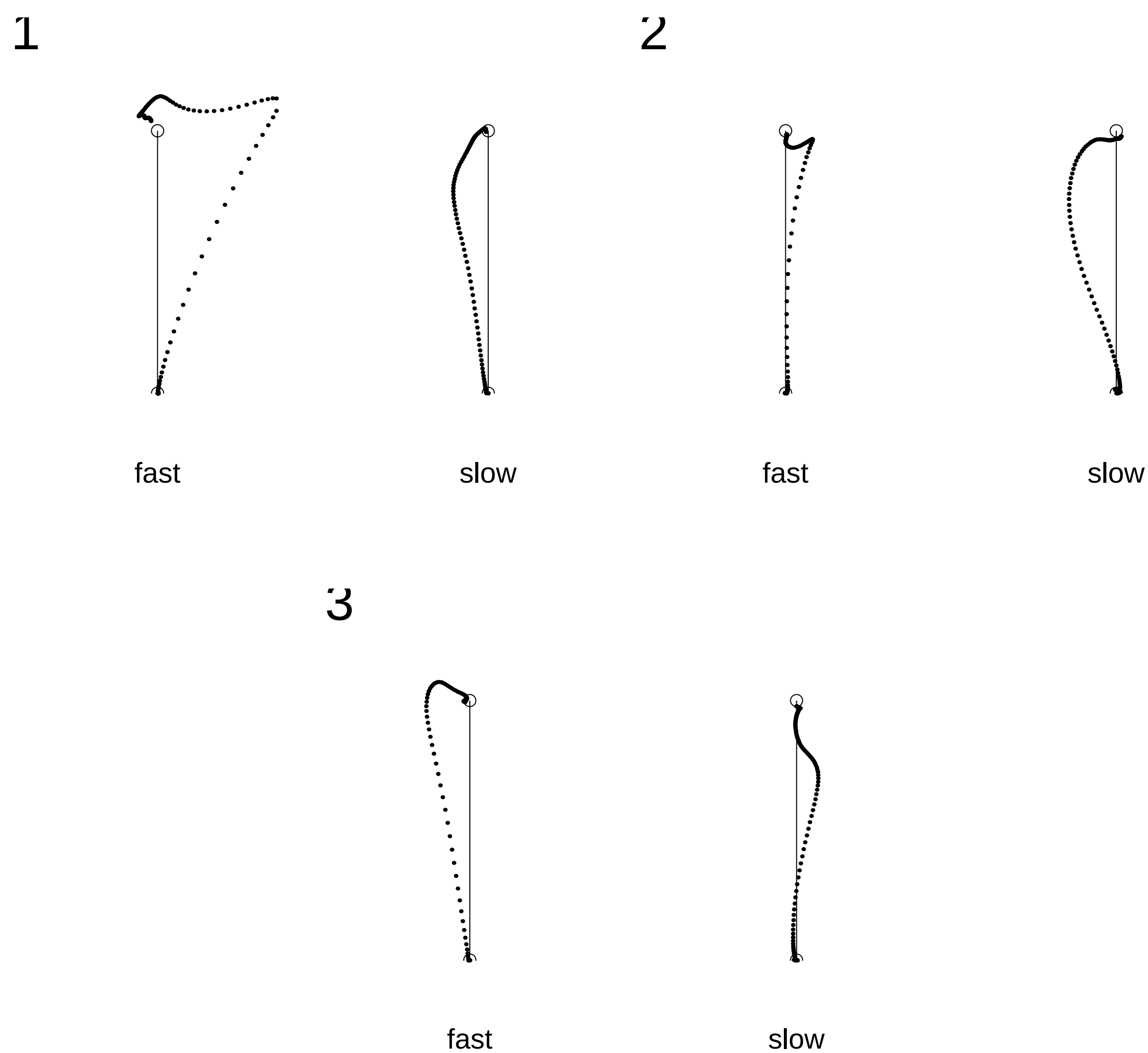

Figure 5-21: Results for Experiment VEL. 1: Typical trajectories at the beginning of training sessions. Distortions are observed to the direction of perturbations. 2: Trajectories seen later in training. 3: Aftereffects observed during catch trials. They show two separate directional responses corresponding to the direction of the forces.

Can the extra stimuli applied to change the velocity behavior itself create such behavioral adjustment? In the next section, I specifically vary knowledge or cognitive level parameters in for the exploration of this issue.

5.8 Experiment KNO: Knowledge Variance in Reaching Task

In order to determine if multiple internal models can be built for the same state space, various kinematic properties such as velocity, size and the shape of the movements were varied for the experiments presented above. The results showed that varying these properties indeed had an affect on obtaining multiple representations for the same internal state. The experiments described in this section were conducted with constant kinematic properties but with varied in the amount of information given to the subjects.

It was shown that subjects were able to retain two separate models for two different colors of targets when the velocity was varied. It is possible that subjects were simply learning the color association with different force direction instead of associating the velocity to the force direction. Thus, the first experiment here examined the same protocol as Experiment VEL, but with no velocity variation.

Target Color Variance with No Velocity Variance

The first experiment displayed exactly the same visual cues as Experiment VEL. The speed was displayed on the corner of the screen as “SLOW” and “FAST” and the color of the targets and the force directions was varied accordingly. However, for this experiment, the beeping reward sound was given only when the movements were made within the interval 0.6 +/- 0.05 seconds for both movements. Thus subjects had to execute all the movements with identical speed.

All six subjects learned to make consistent movements during the baseline epoch, and were trained under forces for two consecutive epochs. Aftereffect trajectories were recorded during catch trials at the end of the second force epoch, and the results are shown in Figure 5-22. Five out of six subjects displayed no distortions in their hand trajectories during catch trials showing that they did not learn either force directions. As in Experiment VEL, one subject adopted a strategy to learn one of the forces but did not build two separate internal models. Therefore, none of the visual stimuli from Experiment VEL contributed to creating multiple internal models in one state space,

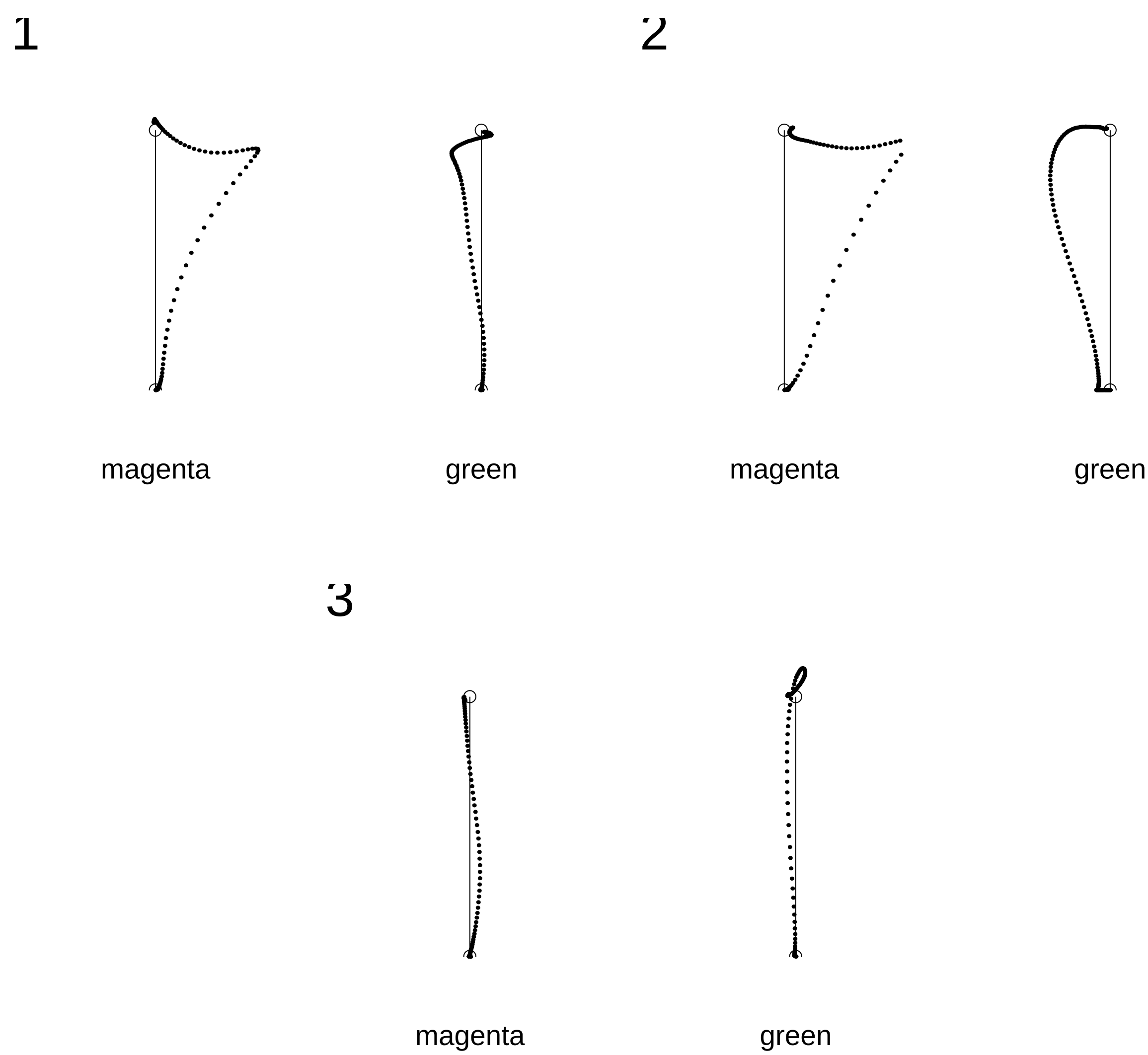

Figure 5-22: Results for target color and words variance with no velocity variance. When the target was green the forces were to the left, and to the right for magenta. 1: Trajectories at the beginning of training sessions. The left trajectory is under forces to the left and the right trajectory is under forces to the right. 2: Trajectories toward the end of training under perturbations. 3: Typical trajectory observed during catch trials. No distortion was observed.

showing the importance of variation of velocity.

Colored Target Sequence Variance: No Knowledge

For this experiment, a structure in the introduction of the targets was imposed to test whether a certain sequence of targets can assist learning the task. To do so, the colors of the targets were interleaved in groups of four; four green targets followed by four magenta targets. Subjects were not informed about the sequence of targets, nor the force directions assigned. As in the previous experiment, when the target was green, the hand was perturbed to the left, and when the target was magenta, the hand was perturbed to the right. After training with perturbations, the forces were removed intermittently in order to observe aftereffects. As shown in Figure 5-23, even when the colors were varied systematically, none of the subjects learned to distinguish the movements.

Colored Target Sequence Variance: No Knowledge

To explore whether knowing more about the environment helps in learning it, the experiment above was modified to allow more information to be supplied to subjects.

This time, subjects were informed about the sequence of the targets and the force directions matching the color of targets. Six subjects were tested for this experiment and aftereffects were observed during catch trials as shown in Figure 5-24. Three out of six subjects were able to separate the two different movements. The other three subjects displayed no distortions in their aftereffects, as observed for the last group in Figure 5-23.

These experimental results show that if significant amounts of contextual information is given to the subjects, they are capable of creating multiple internal models for a given state space.

5.9 Multiple Internal Models for One State Space

In the previous section, experimental results were presented to prove that, through training, one internal model can be split into multiple models. Using these data, a computational model of such a structure is proposed in this section.

Within one state space, there is normally one internal model representing the movement action,

$$A = f(\overline{S}) \tag{5.1}$$

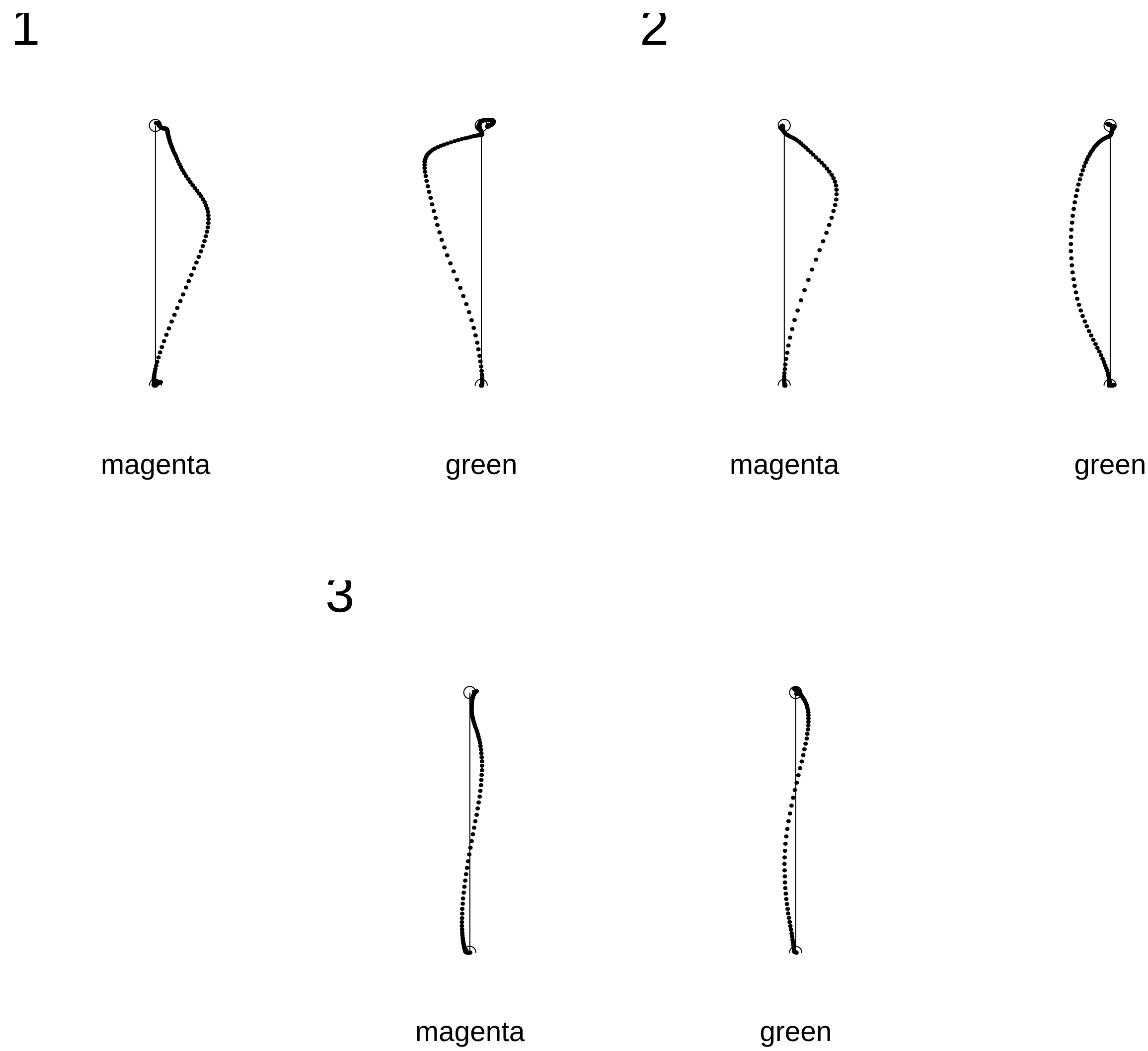

Figure 5-23: Results for patterned sequences with no knowledge. 1: Trajectories at the beginning of training sessions. The green target trajectory is perturbed to the left and the magenta target trajectory is perturbed to the right. 2: Trajectories toward the end of training under perturbations. 3: Typical trajectory observed during catch trials. No distortion was observed.

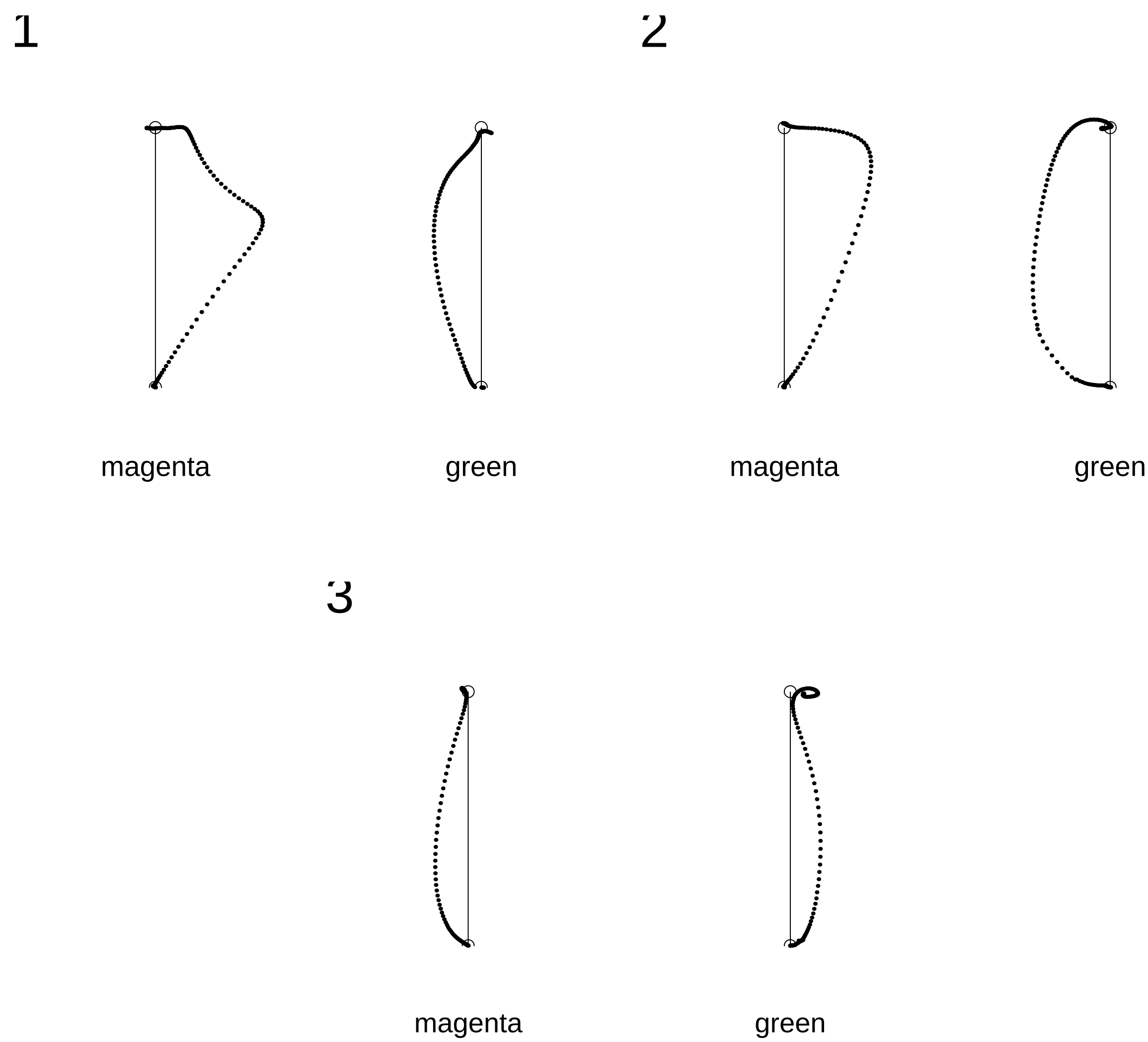

Figure 5-24: Results for patterned sequences with knowledge. 1: Trajectories at the beginning of training sessions. The green target trajectory is perturbed to the left and the magenta target trajectory is perturbed to the right. 2: Trajectories toward the end of training under perturbations. 3: Typical trajectory observed during catch trials. Two out of four subjects displayed learned response for both perturbations.

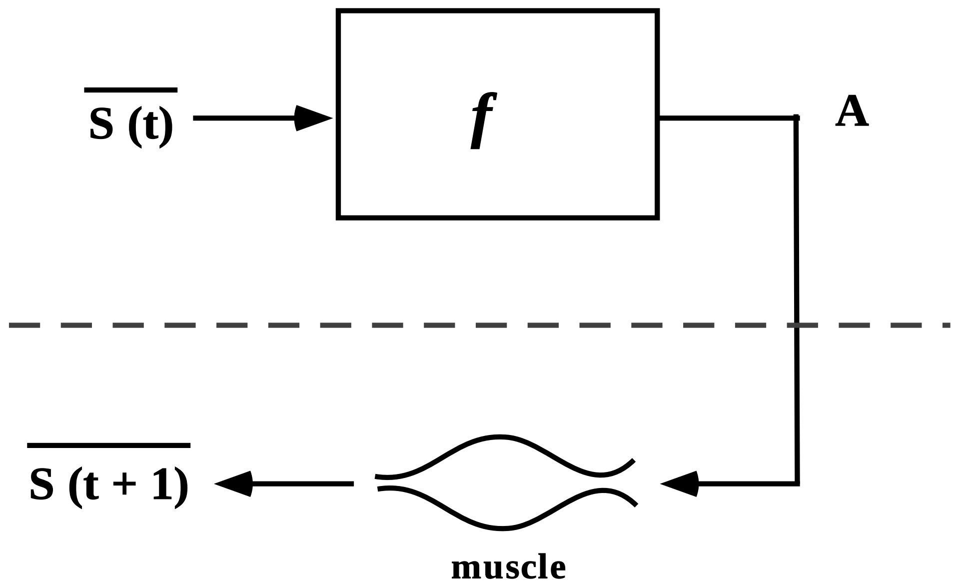

Figure 5-25: A block diagram of an internal model built for one environment for a state, $\overline{S}$. For $\overline{S}$, A is chosen as the next action according to the model built from training.

where A is a chosen next action and $\overline{S}$ is a vector of the state space of the arm configuration. $\overline{S}$ contains the position of the joints, but not the angular velocity about the joints. It also contains external environment parameters such as the torque applied and the direction of the torque. This function is continuous and smooth for the spatial and temporal neighboring states. This hypothesis is illustrated in Figure 5-25.

In order to incorporate the ability to learn multiple representations for one intrinsic space of the arm, two plausible models can be considered. The simple way to represent the experimental results is to simply increase the dimension of state variables. Thus there is still only one model built per state. For example, $\overline{S}$ would not only contain the information about the arm configurations but would also contain velocity, size and shape, and prior knowledge of the movements. This is a reasonable assumption since many connections exist from the somato-sensory cortex [Castro-Alamancos, et al., 1995] and hippocampus [Squire, 1991] to the motor cortex. In the same way that near by states were influenced spatially (as discussed in Chapter 2), when velocity, size, shape, and other state parameters are close, the learned information transfers and decays smoothly with distance in state space.

The phenomena of strong generalization during training under one condition for the same intrinsic space and separation for multiple conditions can be explained by the distance in state space across which the learned information must transfer. This

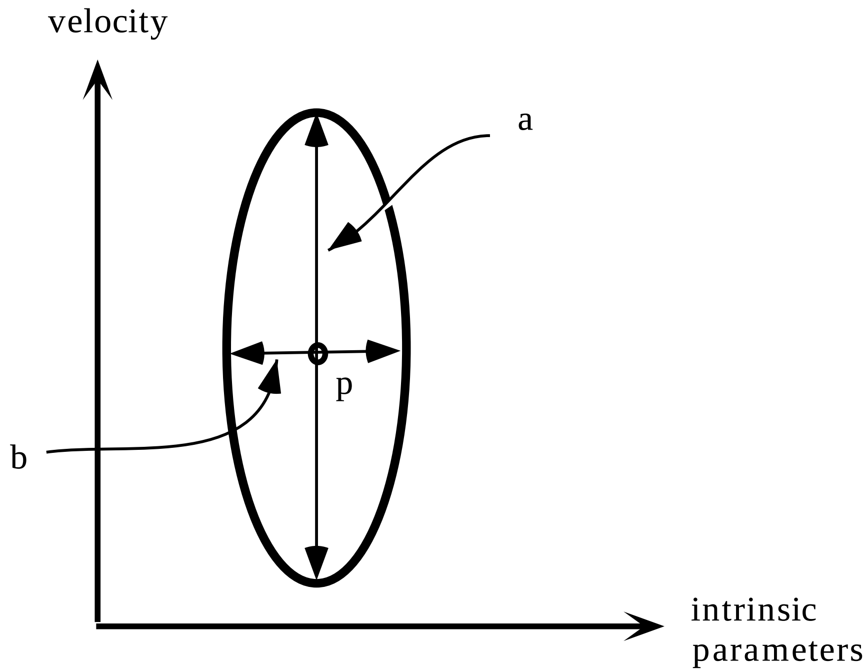

Figure 5-26: A simplified $\overline{S}$ where the x-axis represents all intrinsic parameters, and the y-axis represents the velocity of the hand movement. Point P is where the training occured and the ellipse is the areas where the learned effects are generalized. The ellipse boundary is called "generalization boundary" and a and b are "generalization distance" for velocity and intrinsic parameters.

distance is denoted as "generalization distance". For example, the generalization distance for the intrinsic parameters are much smaller than the one for velocity of the hand movement. Figure 5-26 illustrates a simplified $\overline{S}$ space to show the generalization boundary. All intrinsic parameters are compressed into the x-axis, and the y-axis represents the velocity of the hand movement. The ellipse represents the generalization boundary for when training occured at point P. For the same intrinsic coordinates, the learned information transferred over much greater range of velocity because the generalization distance for velocity is much larger than those for intrinsic parameters.

However, from our experimental results, it is not clear if $\overline{S}$ parameters other than the intrinsic information have limits. In order to test these points, extreme measures of velocity, size, and knowledge of movements need to be examined. Due to the limitation of our movements due to the mechanics and the inertia of the limbs, it is difficult to characterize such limits, or even determine their existence. Thus, another model is proposed to explain the results from the experiments.

This model expands the dimension of the internal model layer instead of $\overline{S}$ space.

When a single environment is presented for a specific state, a function can be established as its internal model as shown in Equation 5.1. When multiple environments are presented, the function can be divided to be multiple functions, building multiple models. Equation 5.1 can be vectorized to express multiple models as:

$$A_1 = f_1(\overline{S}) \tag{5.2}$$

$$A_2 = f_2(\overline{S}) \tag{5.3}$$

$$..... \tag{5.4}$$

$$A_n = f_n(\overline{S}) \tag{5.5}$$

for the same state space. For example, Experiment SIZ showed that large and small movements can have different internal models for the same state space; one function is assigned for large movements and another is assigned for small movements. Depending on the target location, different functions are applied to decide on the next action. If an appropriate model for the specific task does not exist, a new model is created. A simple algorithm can be written as

```
If similar, then MODIFY,
else COPY or COMBINE and learn
```

This algorithm is expanded and simulated in the proceeding chapters. In order to explain these interactions of the functions, a new computational module is created as shown in Figure 5-27. This new module is called the "Function Decider" (FD). FD takes not only the motor sensory feedback but also the internal inputs such as memory and cognitive states. The functionality of this module is discussed in the next chapter.

5.10 Conclusion

In this chapter, experiments were conducted to prove that multiple internal models can be built for one state space representation. Experiments were presented to show that such creations are possible by varying components such as location of the targets, velocity of the movement, sequence of the movements, and the amount of a priori knowledge given about the movements.

Previous experiments had focused on the fact that movements are learned in intrinsic space and had not demonstrated that multiple models can be attained for one such space. As discussed in the experimental section, it is quite difficult to

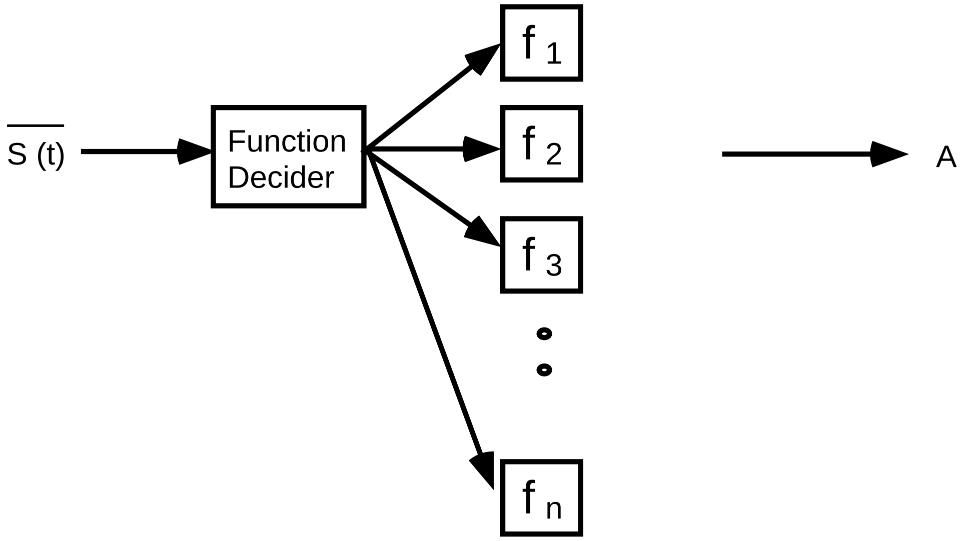

Figure 5-27: Multiple internal models can be built for the same intrinsic coordinates according to the decision made by "function decider."

separate one internal model into multiple models and not all subjects learned to divide within the given amount of time. Two plausible models were built to explain the experimental results: by expanding the state space itself, and by making multiple copies of the internal models themselves. In addition, by using a strategy, many subjects avoided learning another model. These strategies can be chosen within the Function Decider module and these phenomena are investigated further in the next chapter.

Chapter 6

Sequential Learning of Context

6.1 Introduction

Internal models for motor control take the current intrinsic state as their input. For each intrinsic state, there is a different representation of the environment, and it has previously been assumed that there is only one representation allowed per state. However, the experimental results from the previous chapter indicated that it is possible to obtain multiple representations for the same intrinsic space of the limb. In order to create multiple models, there must be a mechanism to determine what should be learned according to the sensory and contextual cues.

Brashers-Krug et al. [1996] demonstrated that immediate exposure to opposite force perturbation erased the internal model built for previously learned perturbations. This phenomena is called interference. However, it was also shown by the authors that if the opposite forces were introduced 4 hours after the previous learning session, subjects could retain both force fields. When the learned information is no longer erasable by exposure to other forces, the information is considered to be consolidated. By temporally sequencing two conflicting environments with sufficient intermissions, multiple internal models should be created for the same state space.

Concurrently, experiments from the previous chapter provided evidence that two conflicting environments can be learned at the same time. However, this was only possible when presentations of the two interfering perturbations were alternated. Thus, it is evident the "sequence" of the exposure to interfering force fields plays a key role in obtaining internal models for both force fields within the same state space.

In this chapter, various sequences for learning two conflicting perturbations are explored to understand the mechanism for developing multiple models within one state space. In addition, experiments were conducted to confirm the hypotheses that all the models within one state are influenced by the sensory cues, whereas the motor command is an output of only one of the models.

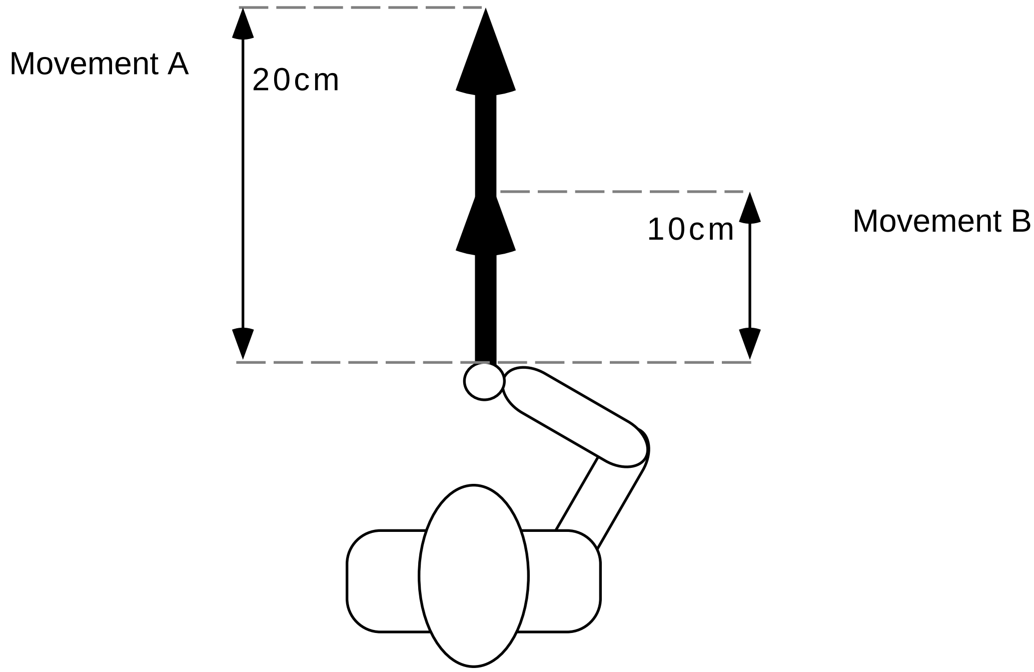

Figure 6-1: Movements A and B were 90 degree movements away from the body and were executed in the same state space of the arm. Movement A was 20 cm long, and Movements B was 10 cm long. They were perturbed in opposite directions, and when these two movements were interleaved randomly during training, both environments could be learned separately.

6.2 Experiment LBS: Large Block Size with Movement Size Variation

When two opposite force perturbations were alternatively imposed on movements of differing magnitude, as observed in Experiment SIZ, both forces could be learned separately. For example, Movements A and B shown in Figure 6-1 could be generalized separately when the right perturbation was applied to Movement B and the left perturbation was applied to Movement A. The results are illustrated in Figure 5-8.

Conversely, these movements are generalized together if two environments were not separately imposed on each movement, as shown in Experiment CE from Chapter 5. Thus it is reasonable to predict that if one movement is learned and then a second movement, perturbed with an opposite force field, is trained, the learned information from the first movement would be erased.

In order to test this hypothesis, an experiment was set up to train Movements A and B in blocks of 48 trials as shown in Figure 6-2. Out of 48 trajectories, half were

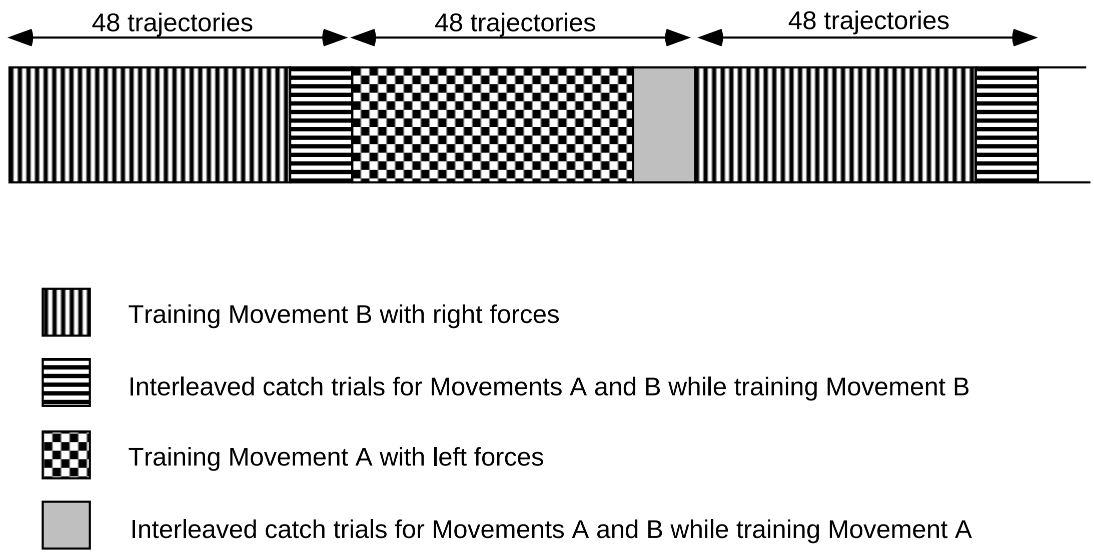

Figure 6-2: The setup for Experiment LBS. Movements A and B were trained in blocks and each block contained 48 trajectories. A total of 16 blocks are trained for each subject.

ones in which the subject moved back to the starting point, thus only 24 movements were trained in total. Out of these 24 movements, two movements were used for Movement A catch trials and two movements were used for Movement B catch trials. Therefore, within each block, 20 movements were trained under forces. The training condition was identical to Experiment SIZ in that subjects were asked to make one continuous movement from one target to another under a specified time constraint (0.5 +/- 0.05 seconds). At the end of each block, catch trials were inserted to assess aftereffects. Four subjects were tested in this experiment, and all of them were trained over a total of 16 blocks of trials.

Figure 6-3 shows the catch trial trajectories from the first four blocks of training. For each block, the most recent training seemed to overwrite the information learned for both Movements A and B during the previous blocks. As shown in Figure 6-4, even after 16 blocks of training, the aftereffects still showed that the previously obtained internal model was erased completely. Therefore, as predicted, experiencing two opposite forces in large blocks caused interference, and both sets of information could not be retained at the same time regardless of the repetition.

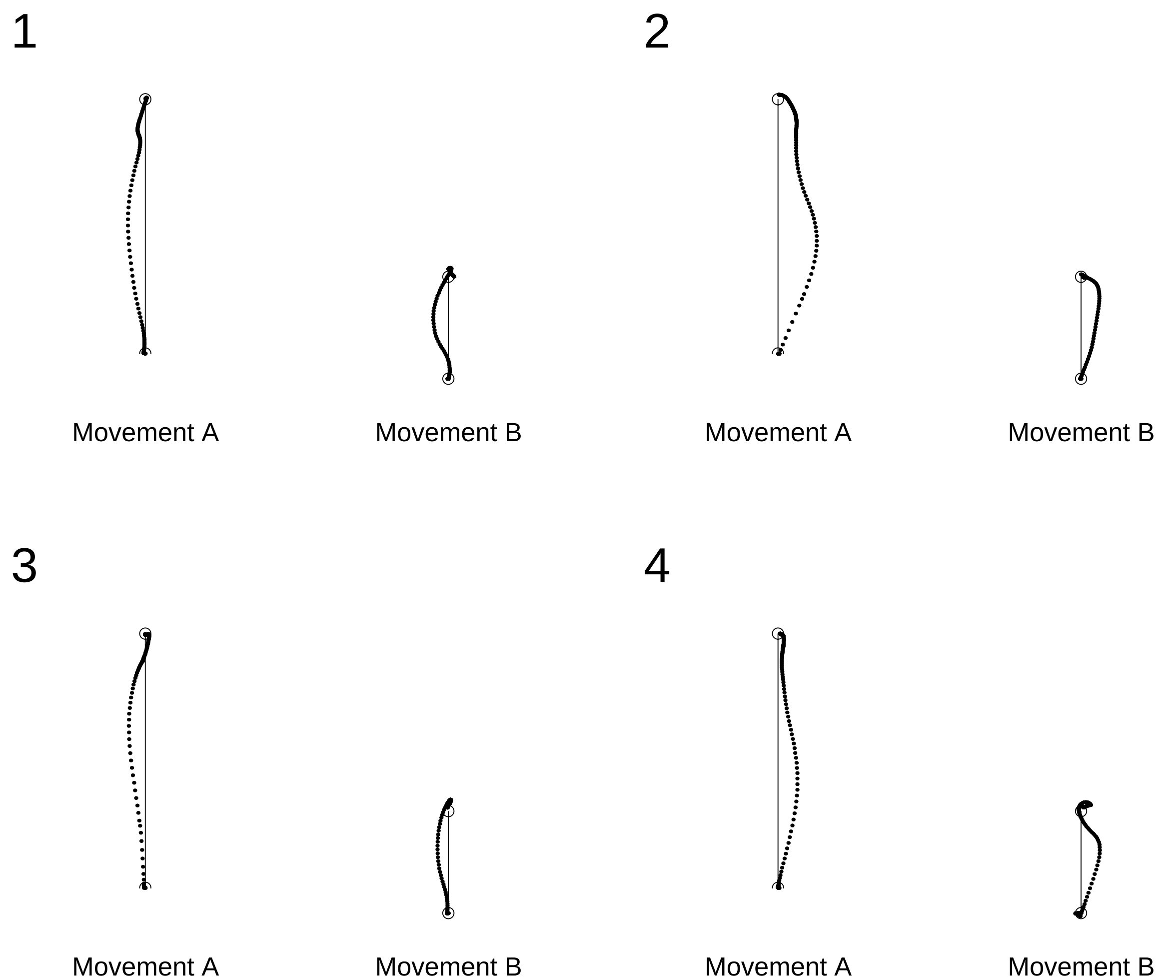

Figure 6-3: The aftereffect trajectories for Experiment LBS for the first four blocks. Blocks 1 and 3: Movement B was trained with right forces. Blocks 2 and 4: Movement A was trained with left forces. For each block, the aftereffects for both Movements A and B corresponded to the most recent training erasing the previously learned effects.

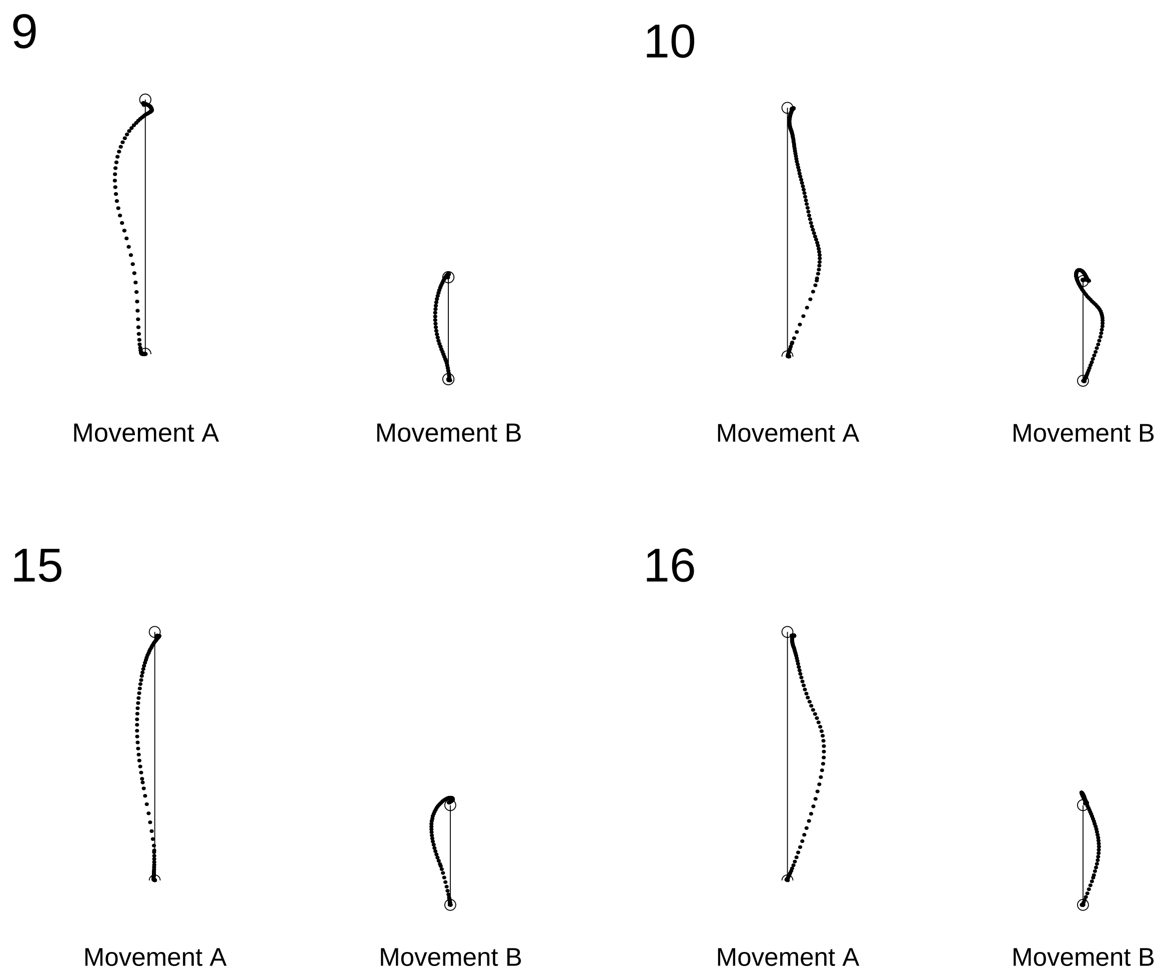

Figure 6-4: The aftereffect trajectories for Experiment LBS for two middle blocks, 9th and 10th, and the last two blocks, 15th and 16th. Blocks 9 and 15: Movement B was trained with right forces. Blocks 10 and 16: Movement A was trained with left forces. Even after 16 iterations, old information was erased every time to learn the new perturbations.

6.3 Experiment SBS: Small Block Size with Movement Size Variation

As it was demonstrated in Experiment SIZ, When Movements A and B were interleaved randomly with the block size of 1 to 3, two separate internal models could be built. Thus as the block length gets short enough, it is possible to obtain two separate internal models. For this experiment, the block length was cut in half to 24 trajectories and all subjects were trained for 32 blocks total. As a result, the total amount of reaching movements executed was the same as the previous experiment. Out of 24 trajectories, half of them were used to go back to the starting point, thus only 12 movements were trained in total. Out of these 12 movements, two movements were used for Movement A catch trials and two movements were used for Movement B catch trials. Therefore, only 8 movements were trained under forces within each block. Typical performance in the first 4 blocks is shown in Figure 6-5. At the beginning of the training session, the aftereffect distortions corresponded to the most recent perturbation, as seen in Experiment LBS. However, as shown in Figure 6-6, as the training progressed, the effects did not necessarily correspond to the most recent perturbations. Of four subjects, two did not produce distorted trajectories during catch trials, and the other two subjects learned one of the perturbations and never adapted to the other.

As the block size decreased, adaptation for each block seemed to become impossible. Instead, subjects learned only one perturbation well at the cost of poor performance for the other, or they did not learn either of the forces. In either case, two separate internal models were not constructed. Thus the sequence of training must play a significant role in simultaneously obtaining multiple internal models. These characteristics are simulated later in this chapter.

6.4 Experiment PS: Learning with Patterned Sequence

In the next two experiments, another aspect of sequential learning was investigated. Instead of investigating the length of blocks, the patterns of force field introduction was varied to observe the effect on building multiple models. All the movements executed for these experiments were 20 cm 90 degree movements. In both Experiments PS and RS, forces were applied to only selected movements. In Experiment PS, the

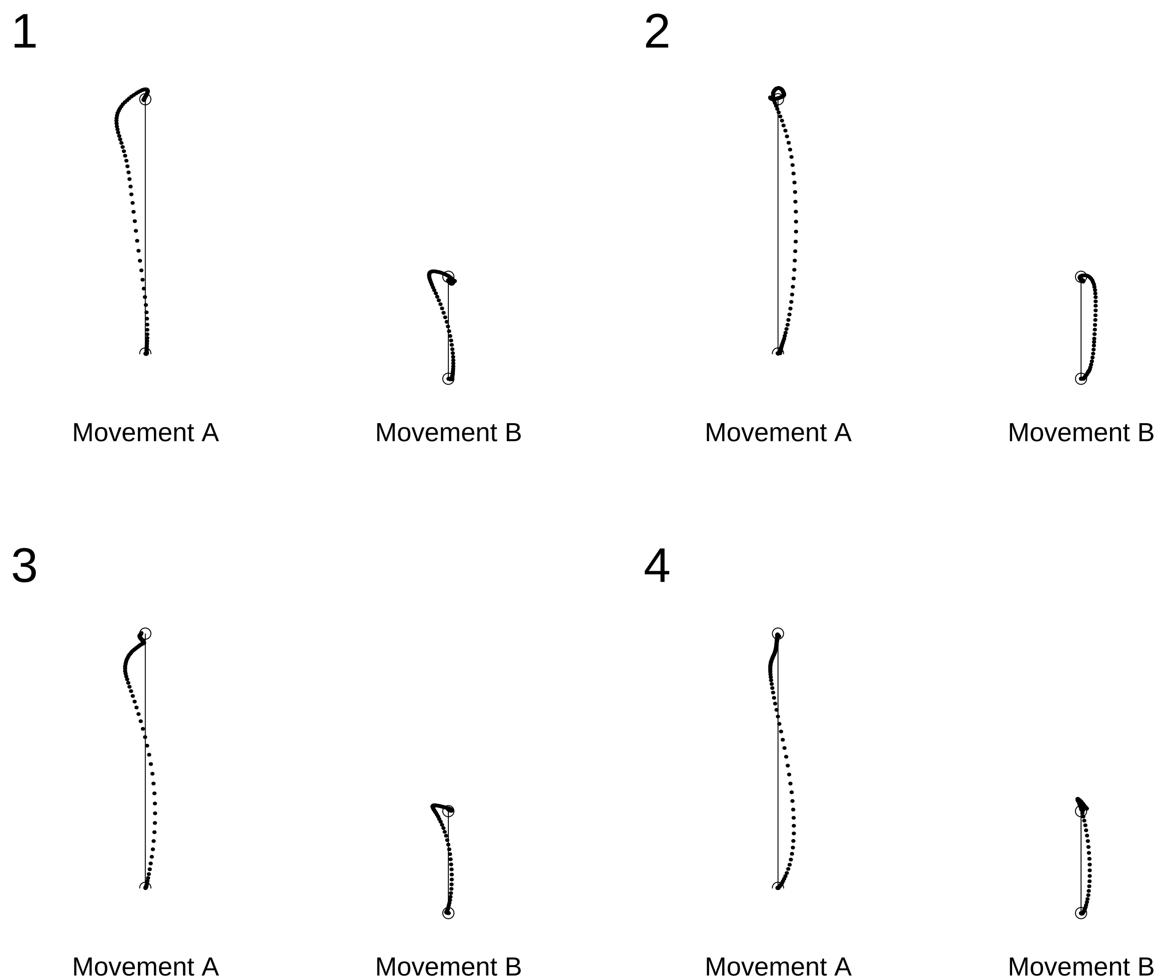

Figure 6-5: The aftereffect trajectories for Experiment SBS for the first four blocks. Blocks 1 and 3: Movement B was trained with right forces. Blocks 2 and 4: Movement A was trained with left forces. Initially, the distortions matched the most recent forces exposed. However, these effects became less defined as the training proceeded.

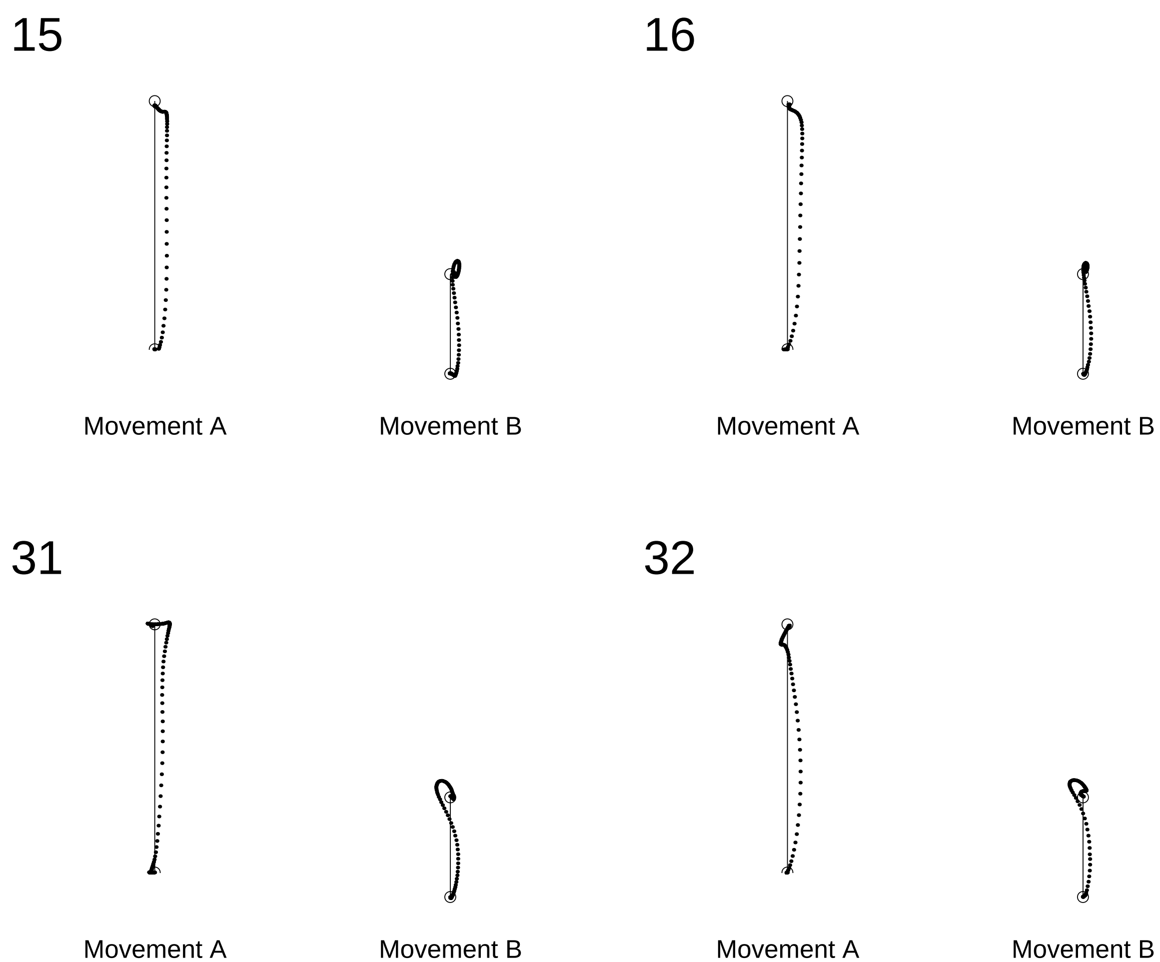

Figure 6-6: The aftereffect trajectories for Experiment SBS as the training progressed. Blocks 15 and 31: Movement B was trained with right forces. Blocks 16 and 32: Movement A was trained with left forces. The aftereffect trajectories no longer contained distortion corresponding to the most recent perturbations. Instead, this subject had a slight bias toward the forces to the left causing distortions to the right for all movements.

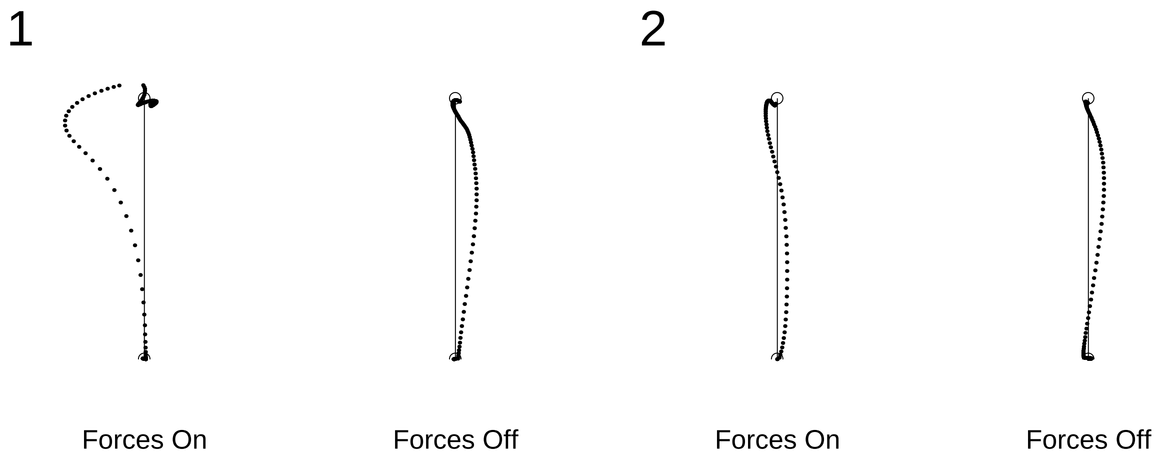

Figure 6-7: Typical movements executed in Experiment PS. 1: Initial trajectories in forces. Movements with force perturbations were distorted toward the direction of the forces. The movements without perturbations are slightly distorted in the opposite direction of the forces displaying some interference. 2: Later trajectories in forces. Both distortions became smaller.

left forces were applied to alternate movements and the subjects were informed of the sequence.

Four subjects were tested under this condition. Figure 6-7 shows the typical movements executed during training. As expected, when the forces were turned on initially (Figure 6-7.1), the movements were distorted in the direction of the forces. In addition, the movements that were not perturbed were slightly distorted to the opposite direction from the forces. This phenomena indicates some interference between these two conditions. As the training progressed, the amount of distortion decreased for both movements (Figure 6-7.2).

To determine whether two different environments had been learned, catch trials were incorporated, again by removing the forces from the trajectories when the perturbation was expected. Figure 6-8 illustrates movements made during catch trials, along with the movements before and after the catch trials. The trajectories in the first and third rows are the ones before and after catch trial movements. The second row trajectories are the movements made during catch trials. It is evident that the distortions were more prominent for the movements made during catch trials. To confirm the above qualitative analysis, the angles of the initial direction of movement were analyzed. The mean angle for the catch trial movements was 16.8 degrees away from the straight movement, whereas the mean of all other non-perturbed movements was 10.4 degrees with the standard deviation of 2.1 degrees. Thus, they seemed to have been clearly distinguished at the motion planning stage, providing evidence of

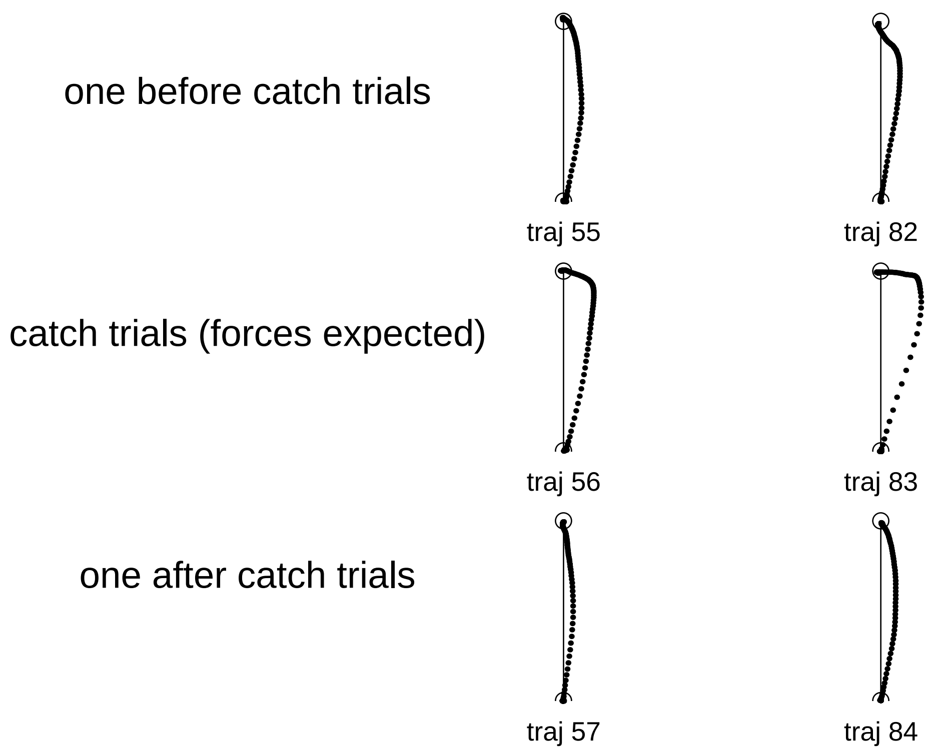

Figure 6-8: The movements on the first row are one trajectory before the catch trials. The second row trajectories are catch trial movements where perturbations were normally expected. The third row trajectories are one movement after the catch trials. The second row trajectories are distorted more than other trajectories.

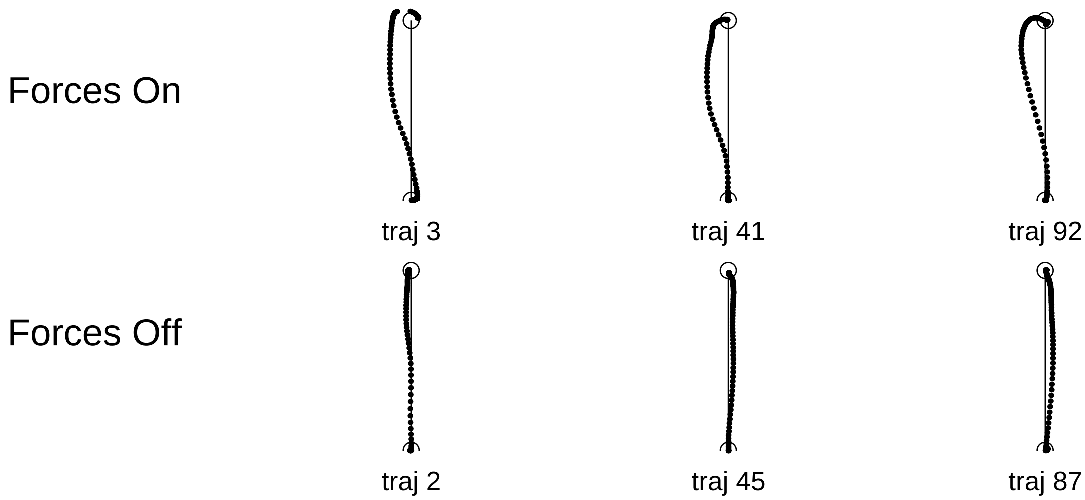

Figure 6-9: Typical movements made during training in Experiment RS. The trajectories in the first row shows the movements under perturbations and the second row shows the movements without perturbations. From left to right, the time progress is shown. The distortions in the movements under forces never decreased.

the existence of two separate internal models.

6.5 Experiment RS: Learning with Random Sequence

In the previous experiment, the subjects were informed of the pattern of the perturbations and they were predictable to the subjects. This allowed the subjects to have confidence in determining which model to use, thus permitting the separation of two different internal models.

For Experiment RS, the same setup was used except that the perturbations were imposed in a random order. Four subjects were tested under this condition and their typical trajectories during the training session are shown in Figure 6-9. The trajectories in the first row are the movements executed under perturbations and the second row movements are executed without any perturbations. In the figure, training time progresses from left to right. Contrary to the results from Experiment PS, in Experiment RS, the movement distortions observed at the beginning of the training session did not decrease with training; the average distortion in initial angle for the first ten force trajectories was 9.9 degrees while the average for the last ten trajectories was 9.7 degrees. Moreover, the movements executed without forces were never distorted over 3.7 degrees. These results indicate that the forces were never learned, and only one internal model was developed to cope with both environments.

6.6 Structure of Function Decider

In Chapter 5, evidence for the existence of multiple internal models for one intrinsic state was presented. The module, Function Decider (FD) in Figure 5-27 allowed the co-existence of multiple functions within one possible state. This multiple function management mechanism is explored in this section.

Narendra and Balakrishnon [1997] have proposed that multiple models can be built depending on the environment, but only one model can be active at any given time. Conversely, Wolpert and Kawato [1998] stated, "In (Narendra's) approach ..... only one controller could be active at any given time as opposed to the blending approach we have chosen and which we believe is a fundamental component of skilled motor control." Their model is based on the responsibility estimator, which determines the weight of each module. This weight effects the output from all the controllers, which are then summed to produce the actual motor command.

If Narendra's model is correct, then only one model can be trained at a time. Thus learning a task under a different context should not interfere with the original task execution. For example, if two contextually different tasks are interleaved during training, both tasks should be learned as well as if they were trained independently. However, when two conflicting environments are introduced as in Experiment SEG, the effect from learning one environment influences the motor output of the other task significantly, and the overall learning for both tasks was slower than if these tasks were learned separately. Therefore, multiple modules seemed to be affected simultaneously.

However, at the same time, if Wolpert and Kawato's model is correct, the linear summation of context must be possible. For example, assume that the right perturbation was learned during reaching for a door knob, and the left perturbation was learned during reaching for a coffee mug. Under their hypothesis, there should be context which is a linear summation of these two contexts. When a reaching movement is executed under this context, the linear sum of the effects learned should be observed. However, it is not clear how to measure context in a continuous scale.

Furthermore, the results for Experiments LBS and SBS would have been identical if either of these models was used. In both experiments, both the shorter and the longer movements were trained for the same number of trials. Thus the output motor command would be the same for both Experiments LBS and SBS, contradicting the

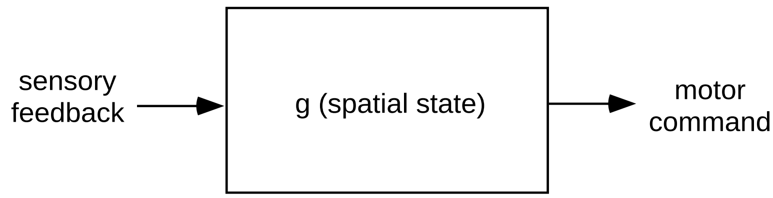

Figure 6-10: The illustration of one state with an assumption that only one model can be obtained within one state space. It takes the sensory feedback and calculates the motor command according to its spatial state.

experimental results.

To model the psychophysical data, I propose a new approach. It is clear that multiple functions exist for one state space (Chapter 5), and that multiple functions for various contexts are influenced during training for one task (Experiments SIZ, PS, SEG, etc.). At the same time, the overall amount of training per context does not correlate linearly with the amount of information changed (Experiments LBS and SBS). Furthermore, the role of interference and unlearning must be important in obtaining multiple functions within one state space. Finally, it must be possible to switch from one contextually dependent output to another, one right after another, if both are learned and can be distinguished (Experiments PS and SIZ).

Thus, my new model has the following capabilities:

1. Multiple functions are affected simultaneously by training for one task.

2. The effect on the functions is *not* linearly correlated with the amount of exposure to a task, but correlated with the temporal learning and *un*learning curves defined in Chapter 4.

3. The overall motor command is an output of only one of the functions and is decided by the context.

The original representation allowing only one internal model for each state space can be represented as shown in Figure 6-10. The sensory feedback is used to calculate the motor command as the controller's output. With the knowledge that multiple models of the environment can be learned within one state space, the illustration can be expanded to Figure 6-11, then to Figure 6-12. The spatial state can be expressed with multiple functions of context. In addition to the sensory feedback, it also takes the context signal as the controller's input. The connections of the inputs and the output to each function are described in the next sections.

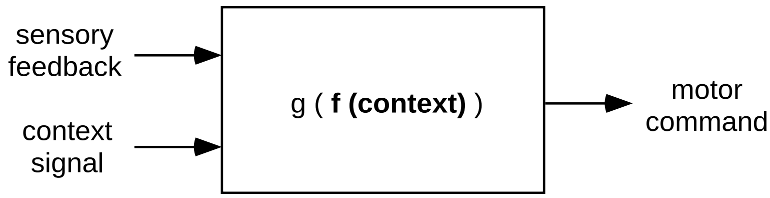

Figure 6-11: The illustration of one state with multiple context dependent internal models. Now the spatial state can be expressed with multiple functions of context. In addition to the sensory feedback, The controller takes the context signal as its input.

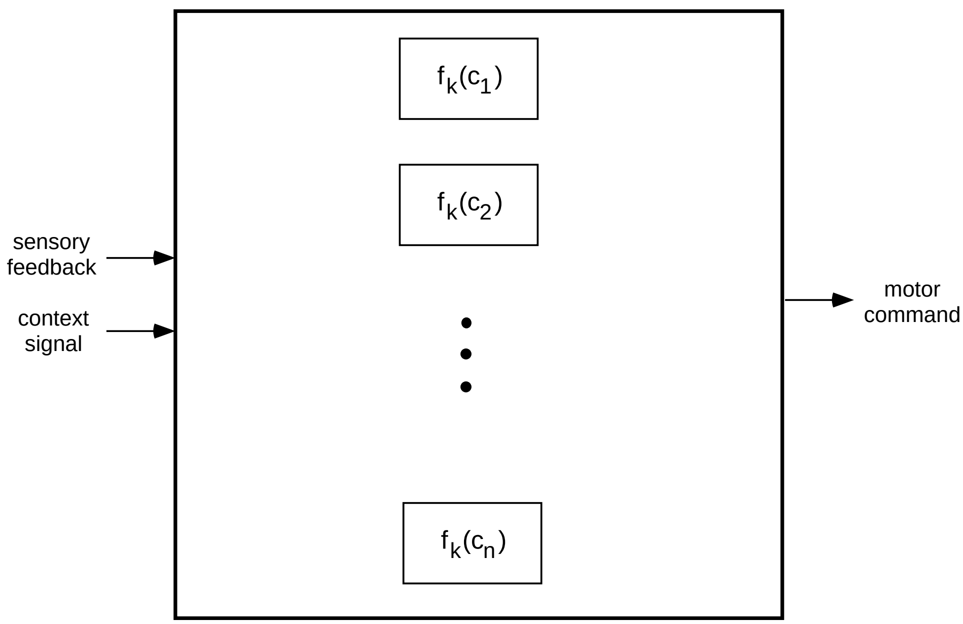

Figure 6-12: The expansion of Figure 6-11 for specific spatial state k for contexts, c_1 to c_n.

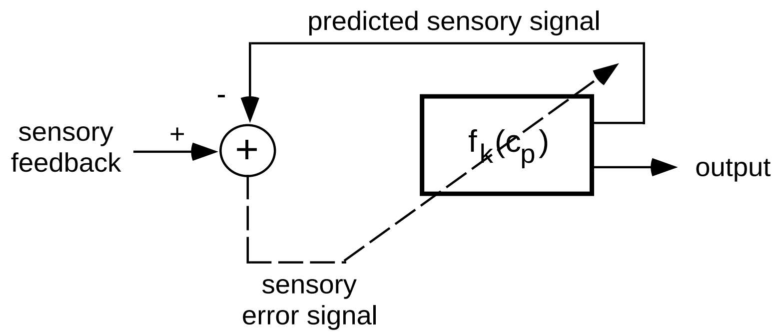

Figure 6-13: The predicted sensory signal is calculated within each function. The predicted signal is compared to the actual sensory feedback to get the error signal. The error signal is used to determine the weight for learning the specific function.

6.6.1 Learning Functions with Sensory Feedback

In this section, the effect of the sensory feedback is discussed. Within each function, there is a forward model of the motor output. The utilization of a forward model is indicated by the fact that the movements seemed to be determined prior to movement onset. The forward model also takes the current motor command and predicts the sensory signal. As shown in Figure 6-13, each set of sensory feedback is compared to the predicted sensory signal and the sensory error signal is calculated. The error signal is used for correction of each function. To show that the sensory feedback influences multiple functions, the following experiment was conducted.

This experiment added four trials to the design of Experiment SIZ group 1. After obtaining two separate aftereffects for Movements A and B as in Experiment SIZ, Movement B was trained with no forces for four movements. This should have resulted in washing out the effect learned for Movement B. If the effect learned for Movement A also washes out, then training under one contextual condition must affect multiple functions. Figure 6-14 illustrates the aftereffects obtained from the previous training trials (1), additional training condition (2), and the movements observed after the additional training (3). As shown, the effects observed for Movement A was also washed out from training Movement B with no forces. In addition, the amount of washout that occured seems to be equivalent for Movements A and B. This phenomenon was also observed during Experiments PS and SEG. Therefore, I hypothesize that all the functions within one state are affected equally by the sensory feedback. When the sensory error causes the negative directional correction in the movement, it is considered as "unlearning" of the function.

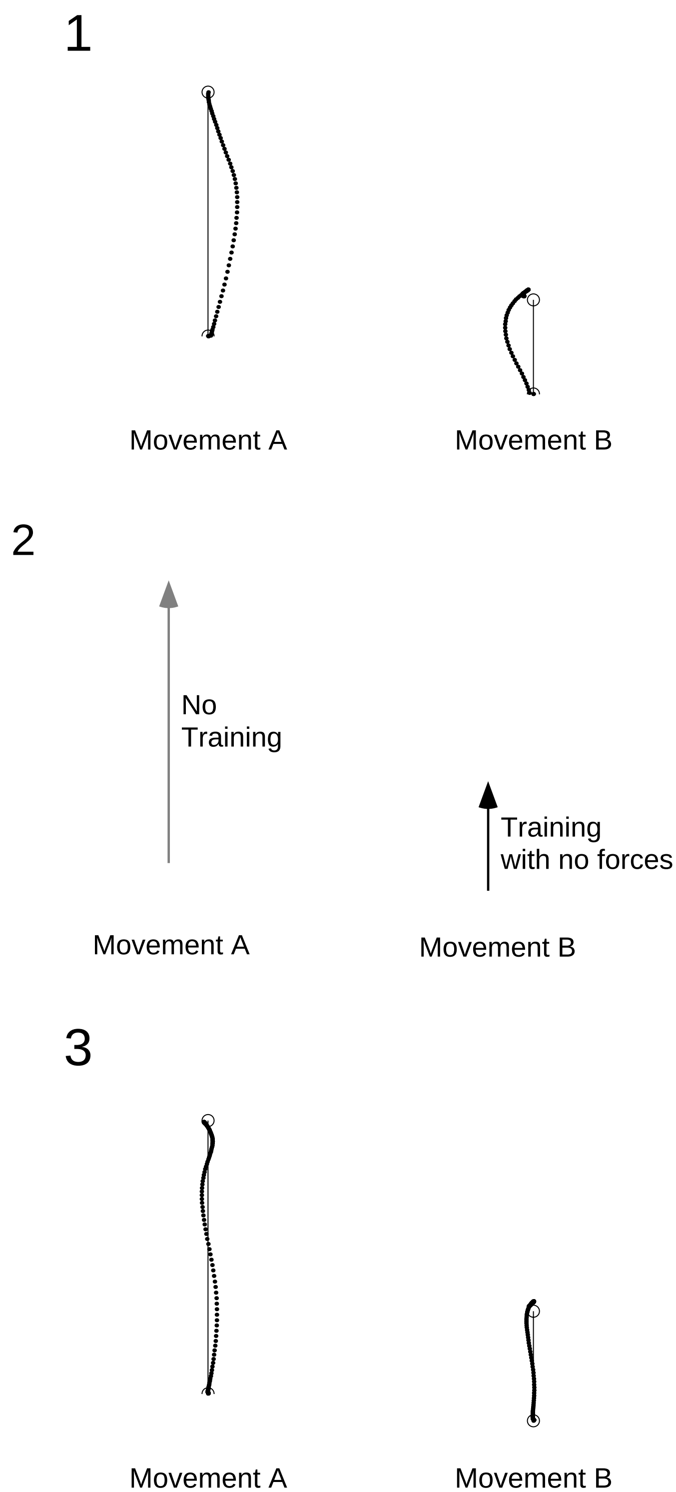

Figure 6-14: 1: The aftereffects from the previous training. Movement A was perturbed to the left and Movement B was perturbed to the right. Two separate aftereffects were observed. 2: Training condition for the next four movements. Movement B was trained with no perturbation. 3: The effects observed after the additional training. Both effects were washed out even though Movement A was not trained after the force epoch.

6.6.2 Choosing Motor Command with Context Signal

For the multiple function model, the input includes the context signal. The current context signal, c_T, can be compared to all the existing contexts, $C = [c_1, c_2, c_3, ..., c_n]$, for all functions in the state. This contextual error signal, C_{err} can be used to determine the output motor command.

There are two hypotheses of how the context error signal is used to determine the motor output for the state. The first hypothesis uses the probabilistic method. The context space can be treated continuously and assign the C_{err} to be from 0 to 1 depending on the similarity. Then the equation,

$$w_p = \frac{1 - e^{-(c_p - c_T)^2/\sigma^2}}{\sum_{i=1}^{n} \left(1 - e^{-(c_i - c_T)^2/\sigma^2}\right)} \tag{6.1}$$

can be used to determine the weight for function, f_p. The total output at time T is a weighted sum of all the functions,

$$O(T) = \sum_{i=1}^{n} w_i o_i, \tag{6.2}$$

where o_i is the output of function, f_i.

The second hypothesis treats the context space discretely and defines the error signal, C_{err} to be 0 except for the most similar context. The similarity is not mathematically defined, but it depends heavily on the perception of the task. Thus the overall output is simply the output of the function, whose context is most similar to the current context.

To test these hypotheses, a new experiment was conducted. In Experiment SIZ group 1, a 20cm and a 10cm movements were executed at the same location and were trained with opposite forces. In addition, for the new experiment, a 15cm long movement was introduced at the same location. This movement is labeled as Movement Z and it was intended to simulate a condition that is between Movements A and B. If contexts exist in a continuous space, then the contexts for Movements A and B should be able to sum to create the context for Movement Z, such that $A + B = Z$. Even if the context space does not linearly correspond to the spatial space, the context Z can still be expressed as

$$c_1 A + c_2 B = Z \tag{6.3}$$

where constants $c_1 > 0$ and $c_2 > 0$, if the first hypothesis is valid. Of course, one can

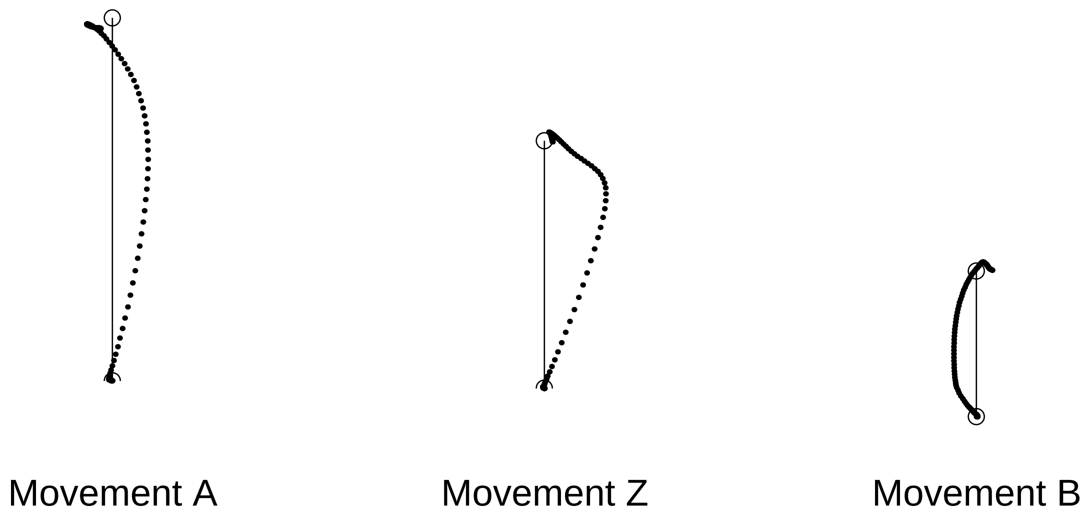

Figure 6-15: The aftereffects for Movements A, B, and Z after training Movement A with the left forces and Movement B with the right forces. Movement Z was never trained with forces. As shown two out of three subjects displayed the aftereffect corresponding to the effect for Movement A for Movement Z.

argue that these two hypotheses would produce the same result if $c_1 \approx 1$ and $c_2 \approx 0$. However, if it is always the case that one constant dominates the other, the second hypothesis describes the effect better than the probabilistic method.

All movements, A, B, and Z were trained during the baseline epoch. Following the baseline epoch, two sessions of force epochs were conducted. During the force training, only Movements A and B were trained. Movement A was perturbed to the left and Movement B was perturbed to the right. At the end of the force training, catch trials were introduced for Movements A, B, and Z. Figures 6-15 and 6-16 illustrate the aftereffects for all movements. Movements A and B retained separate aftereffects corresponding to the forces applied for each movement. Out of three subjects, two subjects showed aftereffect corresponding to the effect for Movement A for Movement Z. The third subject displayed the opposite effect matching the effect for Movement B as shown in Figure 6-16.

From these results, the probabilistic method does not seem plausible. None of the subjects produced aftereffects for Movement Z that were a linear sum of the effects from Movements A and B. All three subjects showed effects corresponding either for Movement A or B. Furthermore, the effect obtained for one subject was completely opposite of the other two subjects. This is possible only if the 15cm movement was perceived discretely.

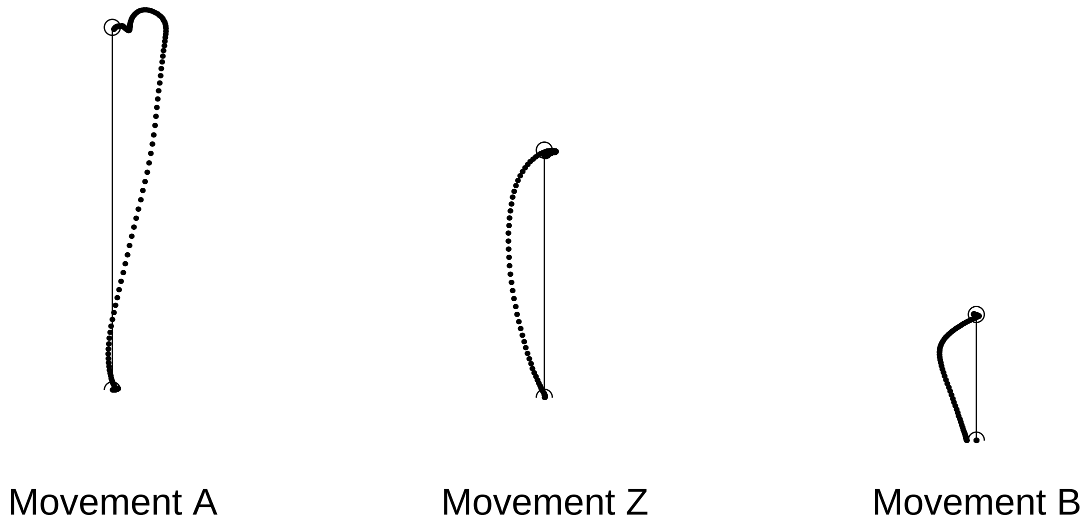

Figure 6-16: The aftereffects for Movements A, B, and Z after training Movement A with the left forces and Movement B with the right forces. Movement Z was never trained with forces. One of three subjects displayed the effect opposite from others for Movement Z, corresponding to the effect for Movement B.

Based on these hypotheses, the overall system of the multiple Function Decider can be illustrated as shown in Figure 6-17. Each function takes the sensory error to make a correction for the learning process. If the correction is to the positive direction, even if the current context is not the context for the function, the function minimizes the error of the function. Instead if the correction is to the negative direction, the function unlearns the specific task. In addition, the output motor command is determined by the context signal. Instead of summing the outputs from all the functions, only one output is activated and chosen as the global output.

6.7 Simulations

With the model proposed above, the simulation from Chapter 3 is expanded to include multiple contexts within one state space. Using the current context signal, the motor command is executed. After the execution of the movement, the sensory feedback returns to the nervous system and learning occurs.

A new function must be created when the task is introduced often, and erased if it is not used for some time. A context is considered to be new if in the discrete scale, it is determined to be different from all the other contexts already in the model. If the current context is similar to one of the contexts in the model, it may not be

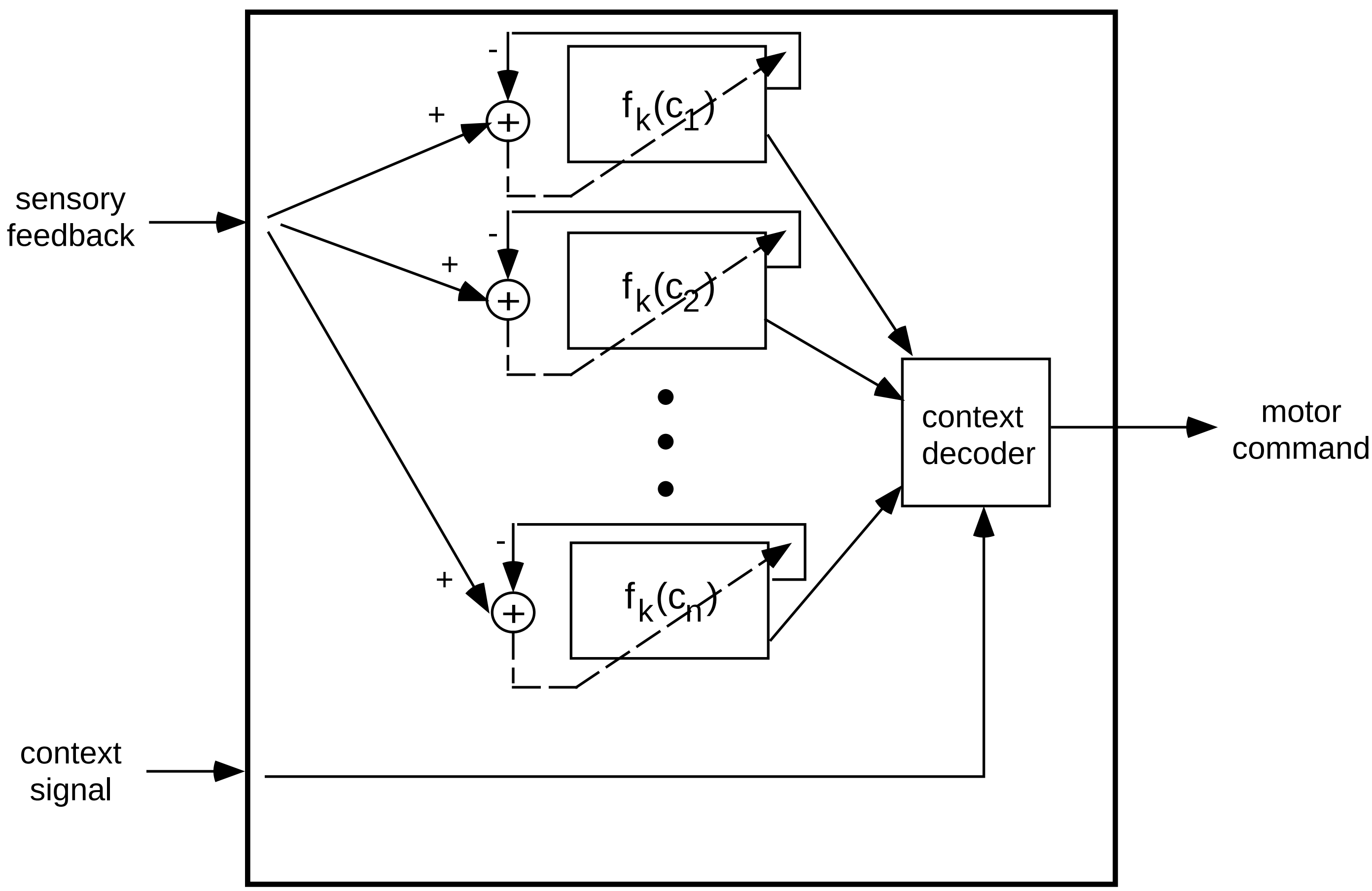

Figure 6-17: A block diagram of the multiple Function Decider which accommodates the experimental results. All functions learn with respect to the sensory error determined for each function. The context signal is used to determine the function that is for the most similar context. The motor command is the output of the function chosen by the context signal.

recognized as a separate context. When the current context is determined to be new, a new function is created immediately. A new function is created by copying the most recently activated function of that state. Each function is designed with variables, A, B, C, D, r_{lk}, r_{lf}, r_{uk}, and r_{uf} from Equations 4.14 and 4.17 in Chapter 4. These variables change with training. When a function is not used for a while, the function does not hold any unique characteristic for the specific context and it can be eliminated.

For this simulation, context signals are represented with discrete numbers (i.e. "1" for 20cm movement, "2" for 10cm movement etc.) and were used as one of the inputs for each movement. When the current context signal did not match any existing contexts in the model, a new function was created. If the contexts in the model were not being used for 12 trajectories, then the function was removed to speed up the simulation.

To determine the weight for learning the sensory information, the learning and unlearning rates defined in Chapter 4 were used. When a function was chosen as the outputting function, the "learning" rates were used. Otherwise the "unlearning" rates were used. The discrete time, T in Equations 4.14 and 4.17 was relative to the point where the specific series of learning or unlearning started. For example, if f_p was chosen as the outputting function for movements 1, 2, 6 and 7, then T for movements 1 through 7 would be 1, 2, 1, 2, 3, 4, 1 ,2. If the function had been learned or unlearned for a long time, the weight approaches to 0 because the learning and unlearning curves saturate over time.

Because r_{lf} is larger than r_{uf}, if multiple contexts were interleaved with small block size, they could be learned simultaneously. In addition, over time, the knowledge dependent learning rates increase if the specific context was introduced frequently. Thus learning becomes even quicker compared to the unlearning process, contributing to obtain multiple functions simultaneously.

The rest of the simulation was straight forward. For each step, τ_{int} from Equation 3.5 was updated for all functions. If the function, f_p, was chosen as the outputting function, then the τ_{int}^p was used to calculate the actual command. The resulting trajectory was investigated spatially as in Chapter 3 to evaluate the sensory error.

As the first simulation, Experiment SIZ group 1 was simulated. Movement A was assigned as context 1 and Movement B was assigned as context 2. These movements were introduced with the same sequence as in the experiment. The baseline trajectories for both movements are illustrated in Figure 6-18. When the forces were introduced, the initial trajectories were distorted to the direction of forces as shown

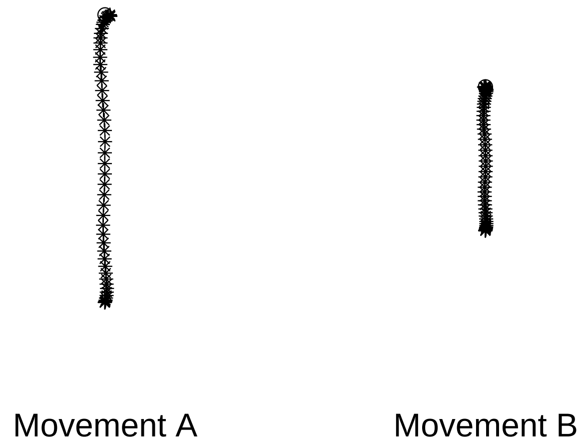

Figure 6-18: Simulated baseline trajectories for Movements A and B from Experiment SIZ group 1.

in Figure 6-19 (left). Movement A was perturbed to the left and Movement B was perturbed to the right. After 200 iterations, both movements became more straight as shown in Figure 6-19 (right). The aftereffect trajectories were simulated by removing τ_{ext} and they are illustrated in Figure 6-20. As shown, both movements exhibited aftereffects matching the forces experienced. This result indicates that two functions were established within one state space.

In addition, Experiments LBS and SBS were simulated. In Experiment LBS, one block of training consisted of 20 movements with forces and four movements of catch trials. Within one block, only one of the movements was trained. For example, for the Movement B training block, there were twenty trials of Movement B with forces, while two catch trials of Movement B and two catch trials of Movement A were interleaved within the last part of the block.

If the function was not used for more than 12 trajectories, it was erased. If Movement B was being trained for 20 trajectories within one block without training Movement A, the function for Movement A was erased. When Movement A was tested during catch trials, because there was no longer any function for the relevant context, a new function was created for Movement A by copying the function for Movement B. This amount to the same thing as using the function for Movement B to execute Movement A for the catch trials. As shown in Figure 6-21, both movements showed aftereffects matching the forces experienced most recently. Regardless of the duration of the training, the results did not change at all. These simulated results match the actual experimental results from Figures 6-3 and 6-4.

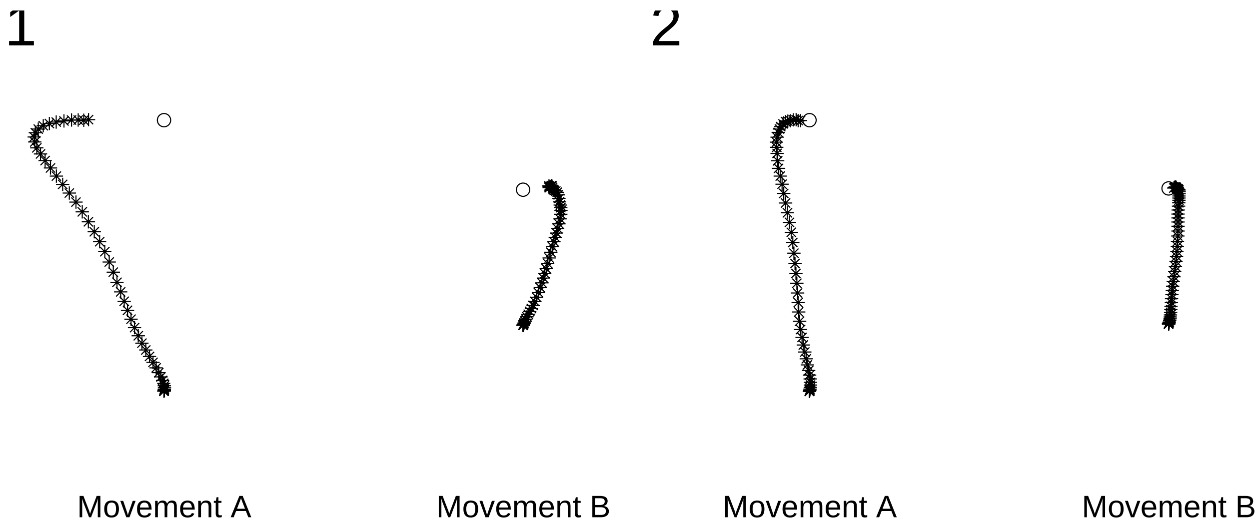

Figure 6-19: Simulated initial (left) and final (right) trajectories for Movements A and B from Experiment SIZ group 1. Movement A was perturbed to the left and Movement B was perturbed to the right. After 200 trajectories of training, the trajectories for both Movements A and B became straight.

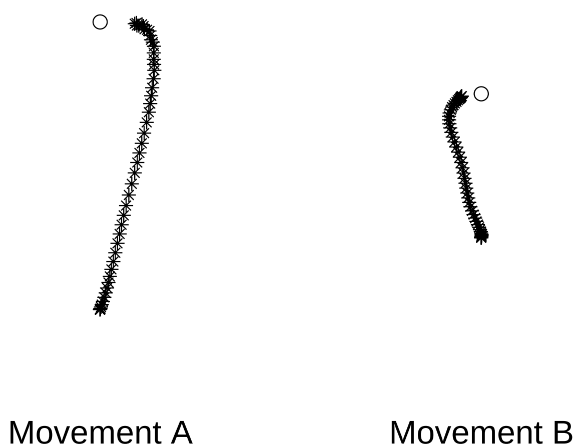

Figure 6-20: Simulated aftereffect trajectories for Movements A and B from Experiment SIZ group 1. They contain separate distortions showing multiple functions were established within one state space.

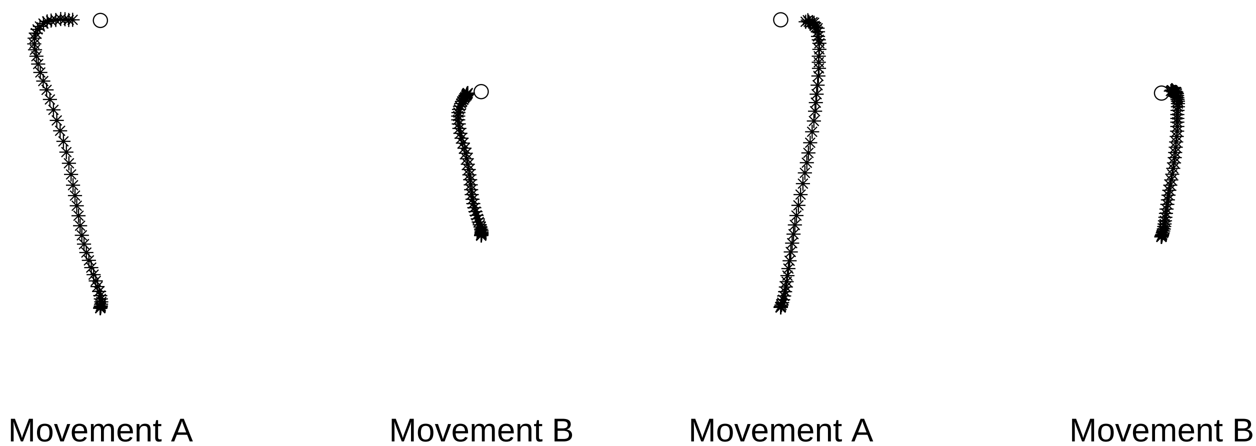

Figure 6-21: Simulated aftereffect trajectories for Movements A and B from Experiment LBS after the Movement B block (left) and after the Movement A block (right). They contain the same aftereffects matching the forces that were experienced more recently.

For Experiment SBS, one block of training consisted of eight movements with forces and two catch trials for each movement. When this condition was simulated, the results changed with the duration of training. The aftereffects from blocks 1, 2, 3, and 4 were shown in Figure 6-22. Initially, the aftereffects were similar to the long block simulation; the forces from the most recent training affected both movements. The experimental data in Figure 6-5 showed the same trend at the beginning the training. However, as the simulation continued, it seems that each movement obtained its own aftereffect. The separate effects were more pronounced in the 31st and 32nd blocks as shown in Figure 6-23. In the actual experiment, none of the subjects were able to obtain two separate effects (Figure 6-6). Instead, some learned neither forces, and some learned only one of them.

Variations of the learning rates did not reproduce the experimental results observed. I hypothesize that in addition to these mechanisms, subjects incorporate different strategies to accomplish the task. Strategies incorporated during learning multiple contexts are discussed in Chapter 7.

6.8 Conclusion

In this chapter, the mechanism of multiple function management within one state space was discussed. Previously, multiple-module, context-dependent models had been proposed, but without any experimental support. The model proposed in this

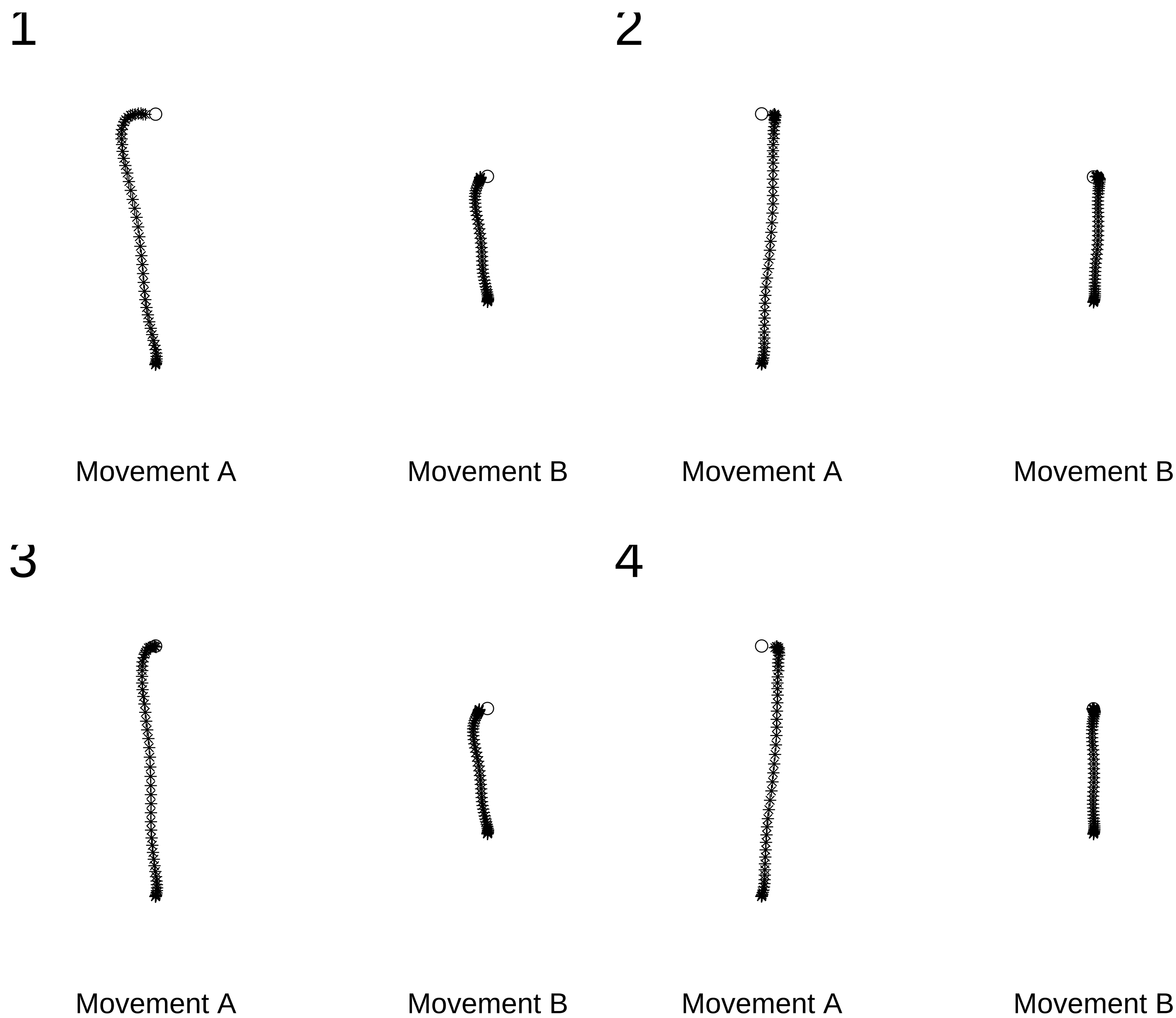

Figure 6-22: Simulated aftereffect trajectories for Movements A and B from Experiment SBS for blocks 1, 2, 3, and 4. The effects were similar to the experimental data at the beginning of training.

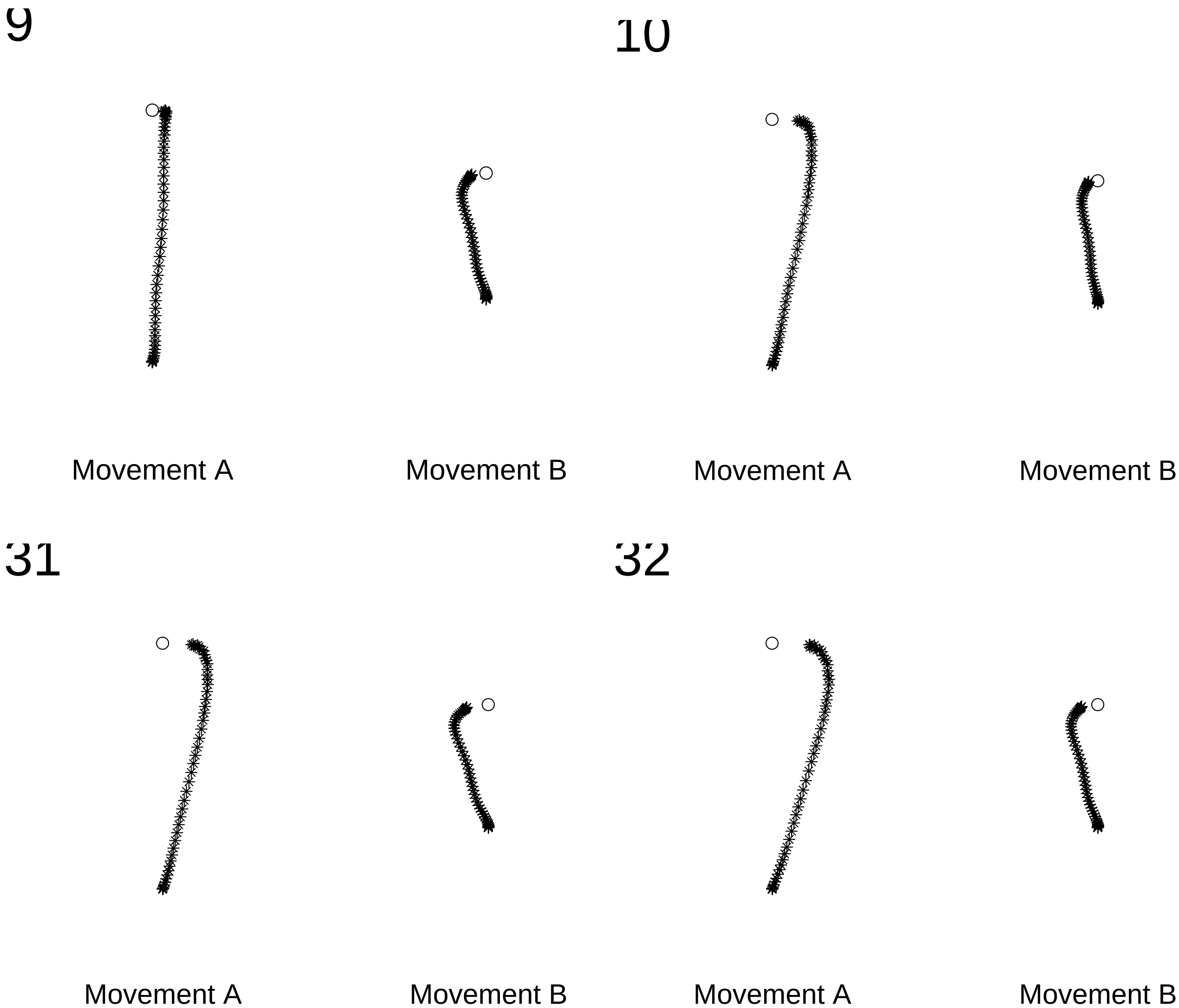

Figure 6-23: Simulated aftereffect trajectories for Movements A and B from Experiment SBS for blocks 9, 10, 31 and 32. With time, Movements A and B obtained their own aftereffects.

chapter allows multiple functions to be affected by a single experience; however, the output is selected from only one of these functions. This model simulates the actual results closely.

Despite the agreement between the experimental data and the results of the simulation of this model, there are other strategies that subjects were seen to have used in coping with a difficult task, as indicated in Chapters 5 and 6. In the next chapter, such strategies are explored.

Chapter 7

Strategies in Context Generalization

7.1 Introduction

In Chapters 5 and 6, the ability to acquire multiple models within one intrinsic state space was investigated and modeled. However, during the adaptation process, some subjects did not acquire two separate internal models for two contextually different environments. Instead, they seemed to employ a strategy which allowed them to cope with the situation that was difficult to adapt to. In addition, this coping strategy seemed to give the subjects the perception that they had mastered the task even though their performance was not optimal. Thus, such strategies should be investigated as a part of the learning process.

In this chapter, two strategies used mainly while learning context-dependent movements are investigated. The two strategies were "winner-take-all" and "block-out" strategies. Following an analysis of these two strategies, they are integrated as a part of the multiple function model from Chapter 6.

7.2 Winner-Take-All Strategy

Winner-take-all strategy was observed during Experiments SIZ, SEG, VEL, and KNO. As an example, the results from Experiment SIZ are discussed in this section.

Experiment SIZ Revisited

Experiment SIZ was chosen for re-investigation because it clearly provided a learnable experimental setup. Specifically, the scenario with Movements A and B is explored in detail here.

The experimental setup is illustrated in Figure 5-3. Movements A and B were of different magnitudes and were perturbed with different directional forces. Even though these two movements were executed in the same spatial areas, four out of six subjects were able to learn two different perturbations separately, as shown in Figure 5-8. However, the other two subjects did not learn to separate these two movements. Instead, both of them displayed the behavior shown in Figure 7-1. When the forces were initially applied, their hand trajectories were distorted in the direction of the forces as observed for the other subjects. However, as training progressed Movement A showed less distortion under the forces, while the distortion became more prominent for Movement B. When the force field was removed, all the hand trajectories were observed to be distorted to the right.

Because the effects for all the movements were in the same direction regardless of the direction of the perturbation applied to each movement, this may be called a "winner-take-all" strategy. The winner-take-all strategy seemed to be used for various other tasks from Chapter 5.

The trajectories observed later in the forces from Figure 7-1 showed that Movement B's performance was even worse than when the training started. However, the subjects stated that they believed they have learned to compensate for the perturbations for all movements. At the same time, when the subjects were asked if they knew that they had picked one force to adapt to and ignored the other, none of the subjects were aware of such behavior. Thus it seems that the winner-take-all strategy is automatic. and is not consciously decided on by the subjects.

Both subjects adapted for the forces applied to Movement A rather than for Movement B. To investigate whether larger movements are preferred exclusively, another experiment was conducted with opposite forces. This time, Movement A was perturbed to the right and Movement B was perturbed to the left. Eight subjects were tested under this condition, and three subjects learned with the winner-take-all strategy. One subject learned and contained aftereffect distortions to the right and the other two subjects' trajectories contained distortions to the left. The effects are shown in Figure 7-2. There seems to be a tendency to pick the larger movement forces as the "winner" forces. The forces for Movement A were experienced over more spatial areas, thus they may be considered to be the dominant forces. However, the non-dominant forces were also chosen as the winner forces occasionally.

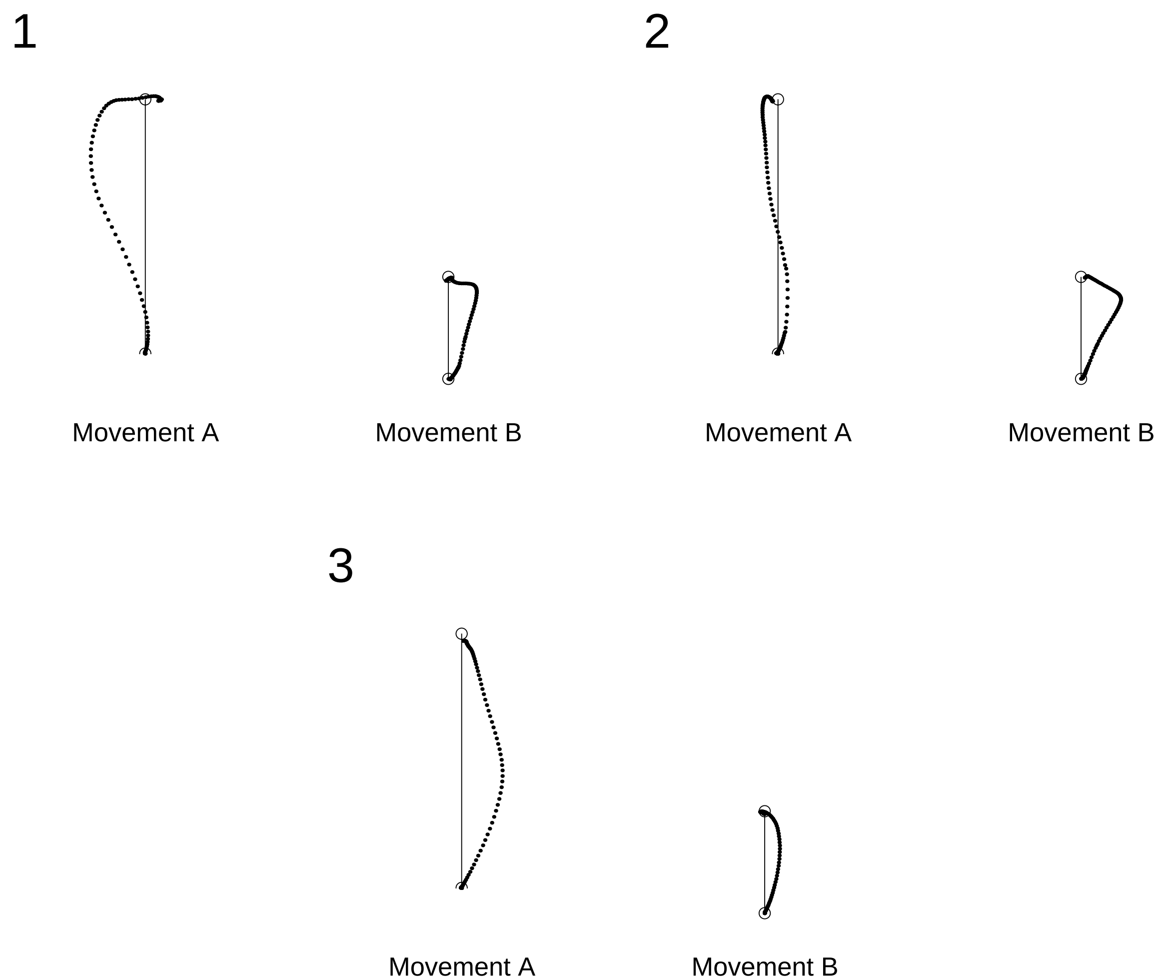

Figure 7-1: The results from Experiment SIZ with the winner-take-all strategy. 1: Initial trajectories during training. The movements are distorted to the direction of the forces. 2: Trajectories later in training. The distortion was decreased for Movement A, but the performance for Movement B was not improved over time. 3: Interleaved catch trial trajectories without perturbations. All movements were distorted in the 0 degree direction, not matching the perturbation force directions.

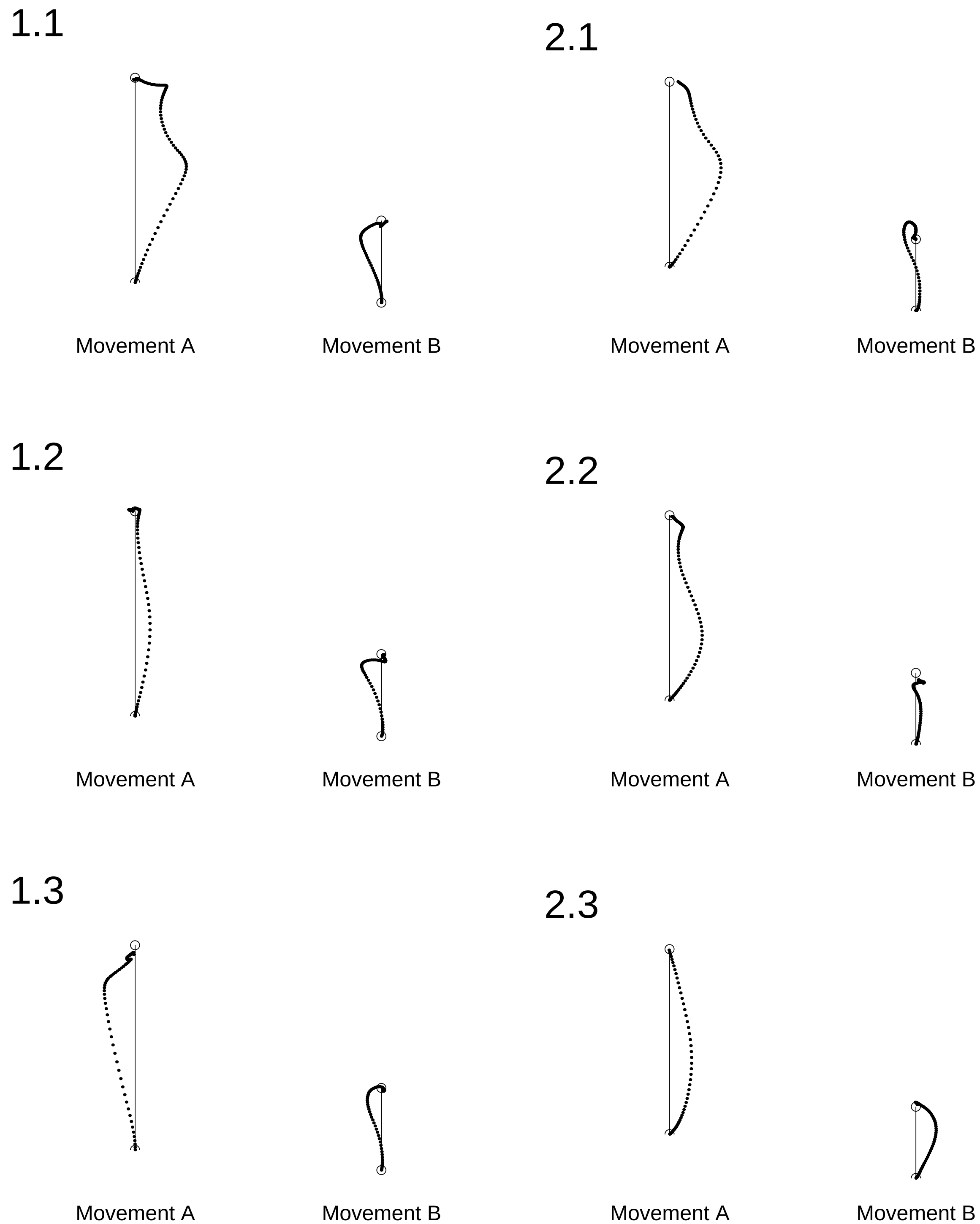

Figure 7-2: Movements observed for two subjects who adapted to the task with the winner-take-all strategy (subject 1 on the left column and subject 2 on the right column). The perturbation force directions were flipped from the previous experiment. The directions were to the right for Movement A and to the left for Movement B. 1: Initial trajectories during training. The movements are distorted in the direction of the forces. 2: Trajectories later in training. 3: Interleaved catch trial trajectories without perturbations. All movements were distorted to the 180 degree direction again for the first subject, whereas the second subject's movements were distorted to the 0 direction.

Extended Experiment SIZ

Can both perturbations be learned after a task has been learned with the winner-take-all strategy? An extended experiment of Experiment SIZ was setup to investigate this problem.

The experimental design was set up to interact with the subjects' aftereffects, as detected in catch trials. The first two training epochs were identical to Experiment SIZ. If the subject learned both perturbations separately, then the experiment was terminated. If the subject adapted to the task with winner-take-all strategy, the subjects were tested for two more epochs of training with force perturbation.

The experiment was designed to increase the number of trials of training for the movement that was not learned. For example, if the aftereffect distortion was in the 0 degree direction corresponding to Movement A with the 180 degree perturbation, then Movement B with the 0 directional perturbation was reinforced. For the first two epochs, both Movements A and B were trained for an equal amount. For the third epoch, the movements that were not learned in the first epoch were trained 75% of the time, and 87% for the fourth epoch.

There were three subjects who retained aftereffects in the 0 degree direction at the end of the second epoch. The extended training was conducted and the aftereffect trajectories were observed at the end of the fourth epoch. One of the subjects showed aftereffect distortions to the left for both movements. This makes sense because 87 % of the forces experienced were to the right. However, two subjects persistently practiced with the model that was learned in the first two epochs, and their aftereffect trajectories at the end of the fourth epoch are shown in Figure 7-3. As a result, the distortion at the end of the fourth epoch is still in the same direction as the one from the second epoch. This strategy seems to be a very unreasonable one to use for this task because 87% of the movements contained the perturbations that fought against their movements. Their hand trajectories for Movement B were distorted significantly during the training session, giving no sign of adaptation.

As a control experiment, six subjects were trained with only the fourth training epoch. After training solely with the epoch containing Movement B with the right perturbation 87% of the time, aftereffects were assessed and are shown in Figure 7-4. For both Movements A and B, all six subjects showed aftereffects to the direction matching the forces for Movement B.

From these experiments, the winner-take-all strategy was shown to have a very strong influence on what was learned. Different results can be obtained when the history of the training sequence is varied.

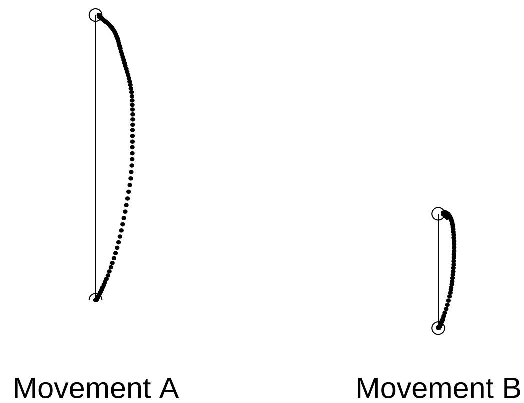

Figure 7-3: Movements observed for the subjects who qualified for the extended experiment SIZ. All subjects retained the effects in the 0 direction at the end of the second epoch. Two out of four subjects persistently performed with the bias for Movement A.

7.3 Block-Out Strategy

During a course of context learning experiments, another strategy was observed. Subjects were exposed to two different environments and the aftereffects showed no distortions for either environment. This strategy is called the "block-out" strategy and is investigated in this section.

Experiment VEL revisited

In Experiment VEL, two different velocities were tested for the same movement with visual cues. The two different velocity trajectories were interleaved randomly. The hand trajectories during catch trials were not distorted for three out of six subjects tested under this condition. When these subjects' movements were analyzed in detail as shown in Figure 7-5, there were some changes in the shape of the trajectories during training. When the forces were initially introduced, the trajectories were significantly distorted in the direction of the forces. However, with time, the influence of the forces on the hand movements was decreased even though there were no significant distortions observed during catch trials.

In order to decrease the amount of distortions in the movement while the forces are pushing the hand to the right, the forces exerted by the muscles must increase to the left direction. In parallel, decreasing the distortion to the left, the exerted force to the right must be increased. Without changing the overall outcome of the movement during catch trials, the forces exerted for both right and left directions

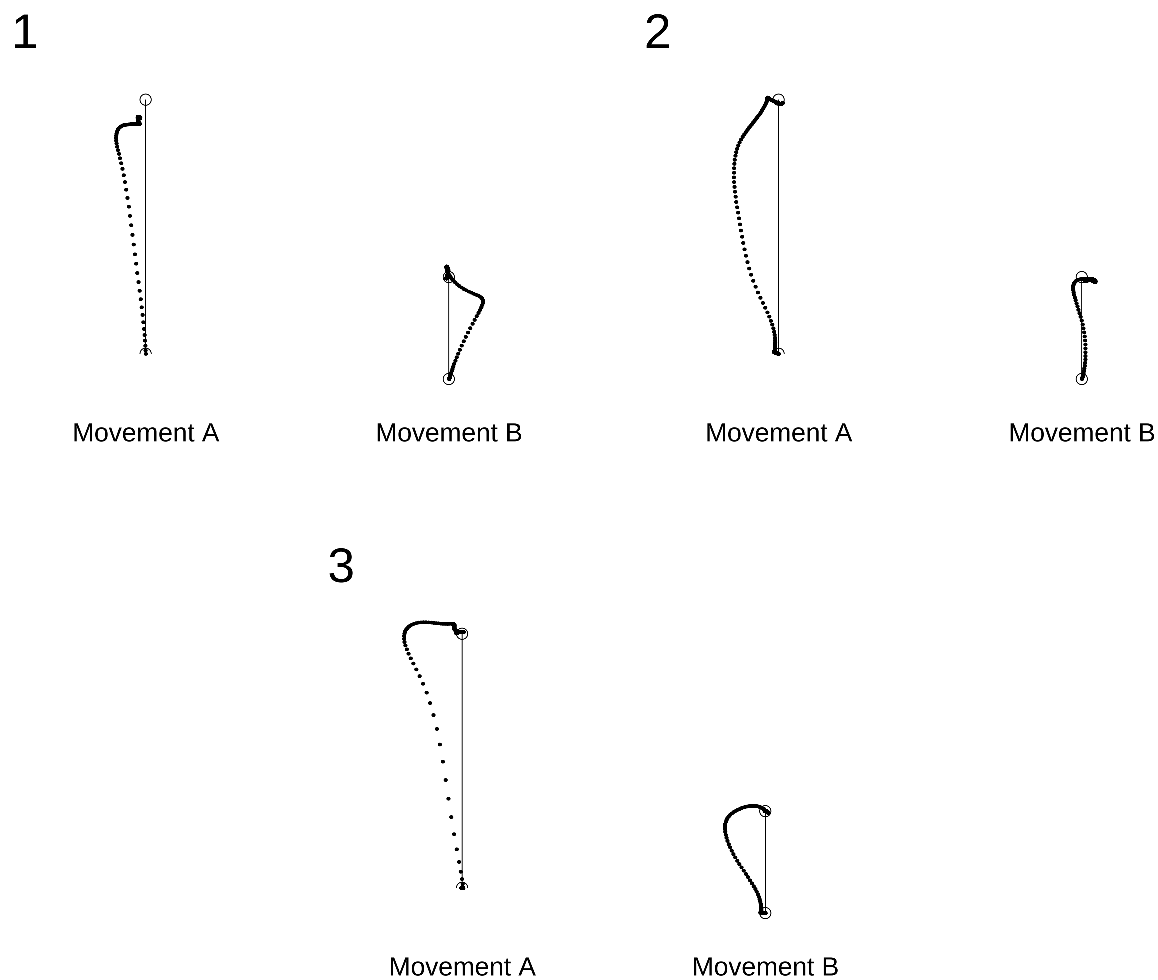

Figure 7-4: The fourth session alone was tested on six subjects. 87% of the movements were Movement B with perturbation to the right. All subjects showed aftereffects in the direction matching the forces for Movement B.

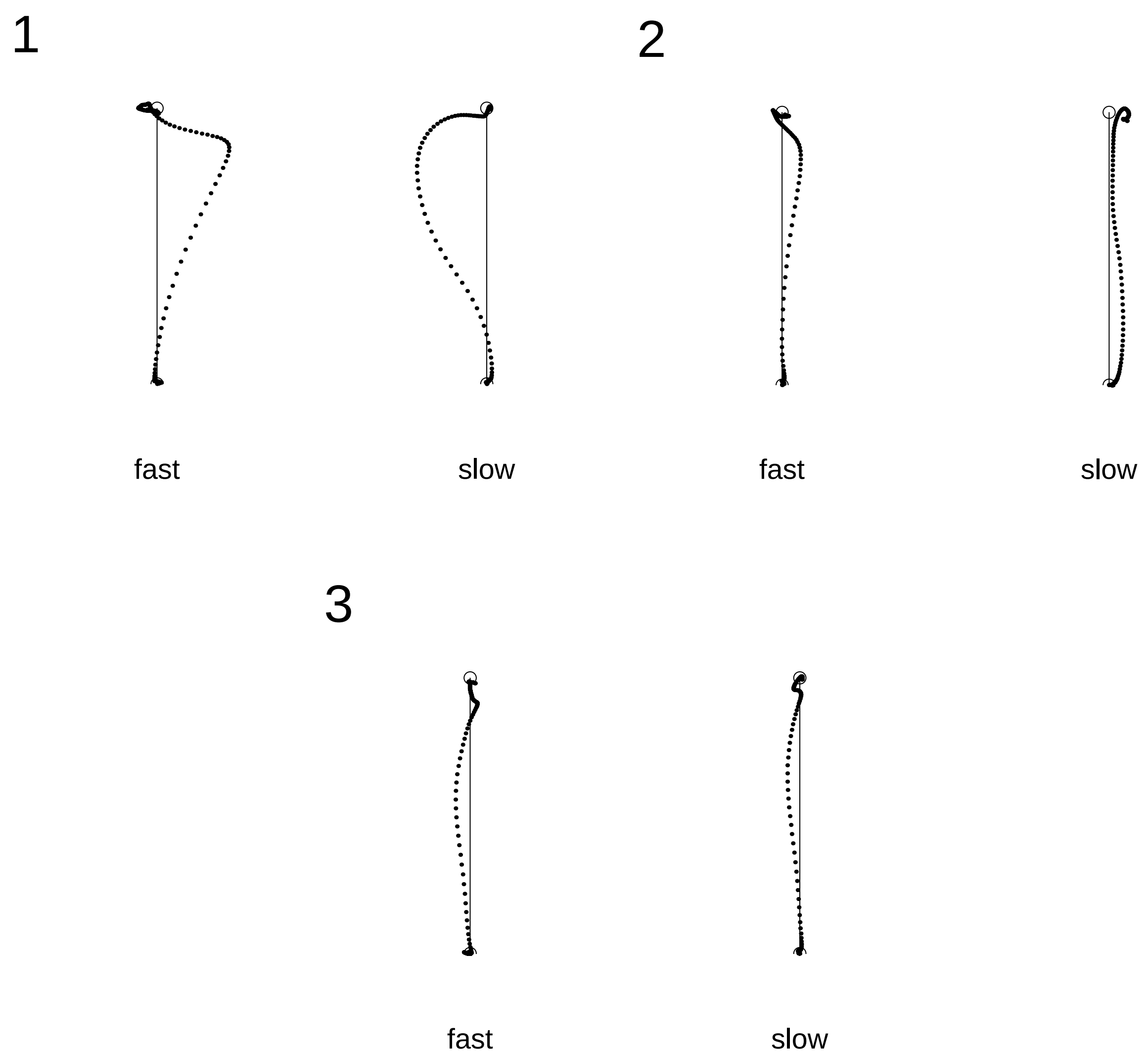

Figure 7-5: The trajectories observed during the training of Experiment VEL. The distortions in their hand movements decreased over time even though there was no significant distortions observed during catch trials.

must be large enough to have the external force negligible. Thus the arm muscles must be co-contracted to cope with the situation. This co-contracting behavior was also observed during performing other difficult spatial tasks, such as Experiment HF-COM.

The activation of both flexor and extensor muscles increases the arm stiffness. This behavior was observed for most of the subjects at the beginning of force training epochs and some co-contract throughout the whole training session. Thus co-contraction must be treated as a non-task-specific strategy. In the next section, this non-task-specific block-out strategy and the winner-take-all strategy are incorporated within the multiple function model introduced in the previous chapter.

7.4 Multiple Function Model with Strategies

The multiple function model was introduced and simulated in the last chapter. In this section, the winner-take-all and block-out strategies are incorporated within the model and simulated.

For the winner-take-all strategy, one context is chosen to be learned at all times regardless of the sensory inputs. The winner function is determined with a bias toward the dominate forces. Once the winner function is chosen, it dominates regardless of the contextual inputs. When the context signal does not match the winner context, the sensory signal does not influence the functions at all. As shown shown from the results in the extended Experiment SIZ, the winner function is very difficult to disengage once it is chosen.

For the block-out strategy, co-contraction is used. The contextually dependent signals are completely ignored because co-contracting the arm muscles is not a task-specific strategy. To simulate co-contraction, the stiffness of the arm is increased. Furthermore, the stiffness itself is adjusted according to the sensory inputs, and no other parameters are changed. In addition, none of the functions are changed because when the sensory information is blocked out, no learning can take a place.

Based on these criteria, Experiment SIZ was simulated with these new strategies. Because strategies were not used for all subjects, they were introduced to the simulation only 25% of the time: 18% winner-take-all and 7% block-out strategies. It may be the case that some sensory parameters trigger such strategies to be incorporated, but for the simulation, random sessions of the execution were chosen to be simulated with strategies.

For the winner-take-all strategy, the context with the largest total external torque over the space was chosen as the dominant context. The dominant context was chosen as the winner context 85% of the time in the simulation. If multiple contexts' external torque were of the same strength, the winner context is randomly chosen. When the input context signal matched the winner context, the sensory information was learned. Otherwise, the inputs were completely ignored.

With these strategies, 25 runs of the simulation were conducted, simulating running 25 subjects. Out of 25 runs, 5 runs used the winner-take-all strategy and 2 runs used the block-out strategy. The resulting trajectories using the winner-take-all strategy are illustrated in Figure 7-6. As the training proceeded, the distortion of Movement A became smaller while the distortions of Movement B became larger. When the external forces were removed, both movements contained the effect matching the forces for Movement A. This result closely matched the experimental data.

In addition, the trajectories corresponding with the block-out strategy are illustrated in Figure 7-7. When the stiffness was increased to reduce the spatial error, the stiffness value increased to more than twice its original value. As a result, when the forces were removed, the movements were still executed without much distortion. As shown in Figure 7-5, these simulated trajectories were similar to experimental results observed.

7.5 Conclusion

In this chapter, two coping strategies used during contextual learning were investigated and simulated. When these strategies were employed, the task was perceived as having been learned even though the correct context-dependent responses were not being performed.

In the literature, these strategies have largely been ignored even though they are a significant part of motor learning because of its complexity and its involvement of cognitive-level processes. Therefore, in the future, motor learning should be studied in a manner that includes cognition and sensory perception.

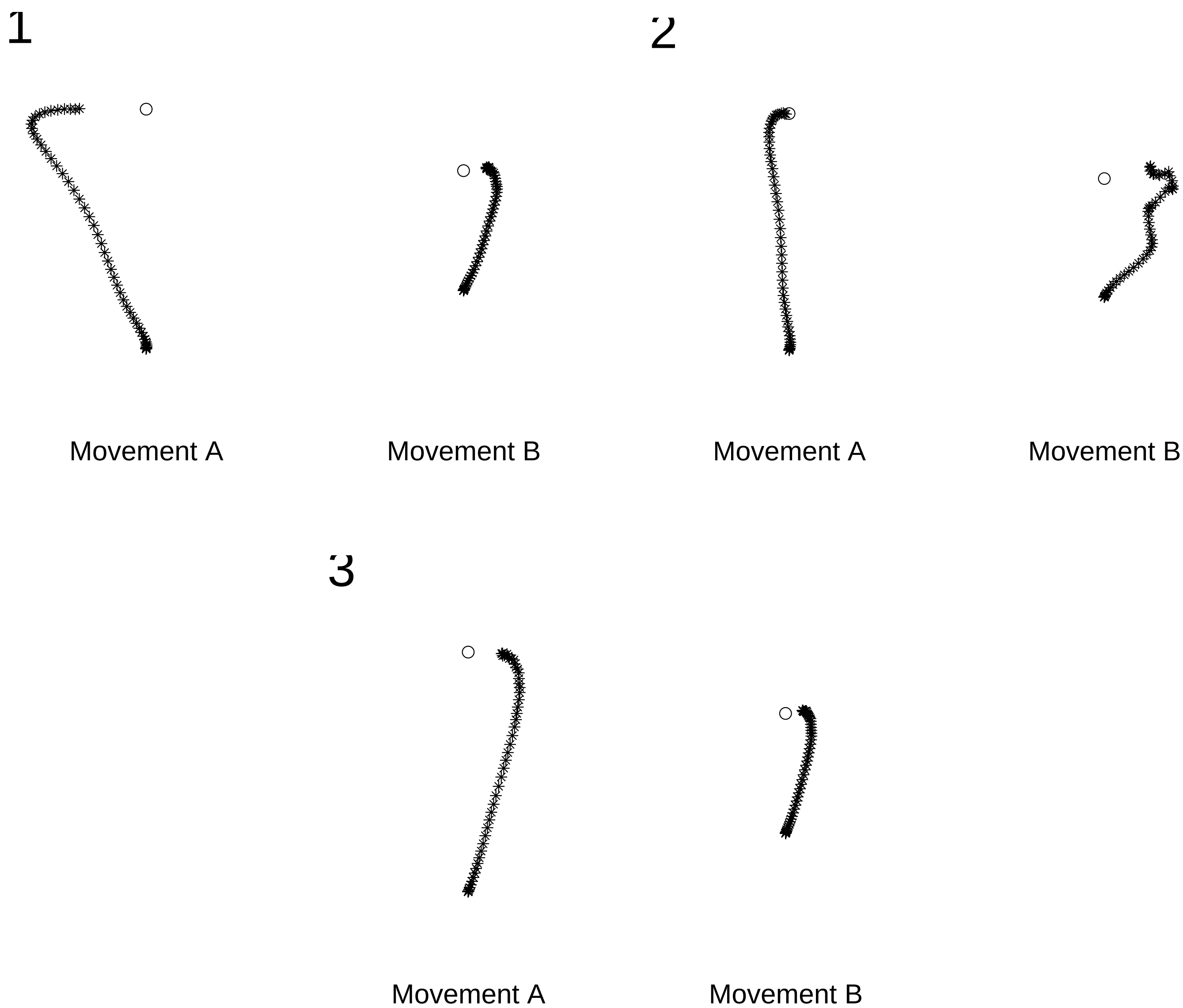

Figure 7-6: The simulated trajectories with winner-take-all strategy. 1: Initial trajectories in forces. 2: Trajectories later in forces. The distortion for Movement B is larger than the initial trajectory. 3: Aftereffect trajectories. Both movements obtained the same effect showing the result of the strategy.

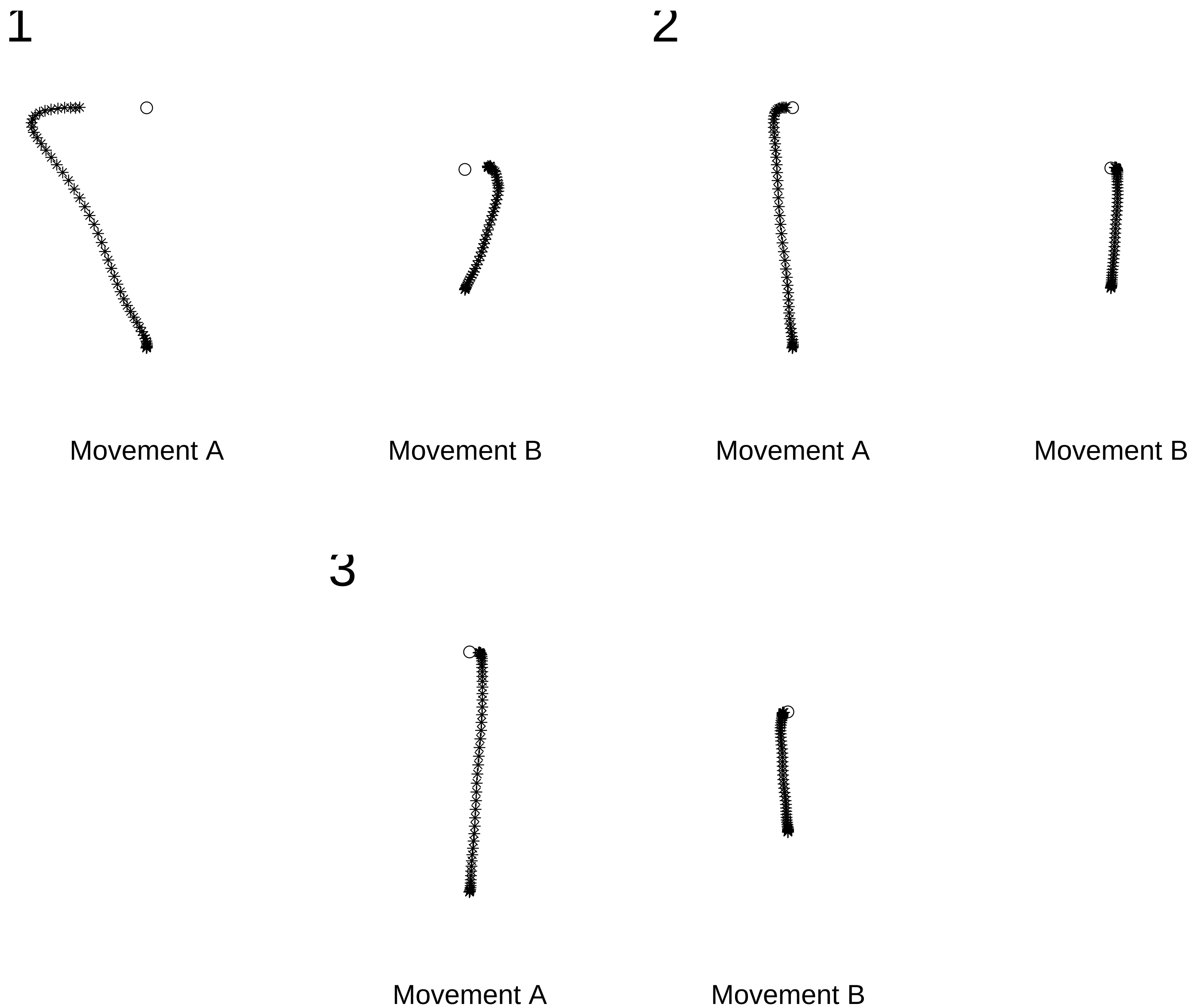

Figure 7-7: The simulated trajectories with block-out strategy. 1: Initial trajectories in forces. 2: Trajectories later in forces. The distortions for both movements were diminished. 3: Aftereffect trajectories. Both movements did not contain much distortions.

Chapter 8

Conclusion

This thesis investigated the CNS's ability to generalize a learned motor skill throughout surrounding spatial locations and its ability to divide this spatial generalization through the variation of context. As well, models were proposed suggesting how these generalizations might be implemented.

The investigation involved human psychophysics and simulations. The experimental paradigm was to study human neuromuscular adaptation to viscous force perturbation. When external perturbations were applied to the hand during a reaching task, the movement became distorted. This distortion motivated the CNS to produce counterbalancing forces, which resulted in the modification of the internal model for the task.

Experimental results indicated that the introduction of interfering perturbations near the trained location disturbed the learned skill. In addition, if the same movement was perturbed in two opposite directions in sequence, neither of the forces were learned.

Conversely, the adaptation to two opposite forces was possible within the same space when the forces were applied to two contextually distinguished movements. This was possible only when these movements were interleaved fairly regularly.

During adaptation to a difficult task, such as contextual distinction in the same spatial location, humans often used other strategies to avoid learning the actual paradigm. These strategies allowed subjects to perform the task without changing their internal models appropriately, and these strategies were also investigated as a part of the learning process.

Finally, a multiple function model was constructed which allowed multiple contextually dependent functions to co-exist within one state space. The sensory feedback affected all functions; however, only one function was active to output a motor command. Simulations based on this model matched well with the experimental data observed.

If a human-like robot was programmed with spatial and contextual generalization components, the versatility of the robot should be expected to be enhanced. When robots are built to be more versatile, their tasks do not have to be severely limited, as is the case with currently available robots.

The human CNS has superb capabilities for acquiring motor skills. In fact, motor skills are known to improve simply from visualization of the task without physical training [Abernethy, 1995]. Movement control is not only governed by actual sensory feedback: perception and cognition are also involved heavily in the execution and learning of movements. Therefore, motor control should be investigated without neglecting these aspects in the future.

Bibliography

[Abend, et al., 1982] Abend, W., Bizzi, E. and Morasso, P. (1985) Human arm trajectory formation, *Brain*, Vol.105, pp.331–348.

[Abernethy, 1995] Abernethy, B. (1995) Training the visual-perceptual skills of athletes: Insights from the study of motor expertise. *Congress Proceedings of Third IOC World Congress on Sport Sciences*, September.

[Adams, 1971] Adams, J. A. (1971) A closed-loop theory of motor behavior. *Journal of Motor Behavior*, Vol. 3, pp.111–149.

[Ahissar and Hochstein, 1997] Ahissar, M., Hochstein, S. (1997) Task difficulty and the specificity of perceptual learning. *Nature*, 387, pp.401.

[Ashe and Georgopoulos, 1993] Ashe, J. and Georgopoulos, A.P. (1993) Spatiotemporal motor processing *Cerebral Cortex*, Vol. 6.

[Bernstein, 1967] Bernstein, N. (1967) The co-ordination and regulation of movements. Pergamon Press, Oxford.

[Bizzi, et al., 1984] Bizzi, E., Accornero, N. Chapple, W., and Hogan, N. (1984) Posture control and trajectory formation during arm movement. *Journal of Neuroscience*, 4, pp.2738–2744.

[Bizzi, et al., 1991] Bizzi, E., Mussa-Ivaldi, F.A., and Giszter, S.F. (1991) Computations underlying the execution of movement: A biological perspective. *Science*, 253, pp.287–291.

[Bizzi, et al., 1992a] Bizzi, E., Hogan, N., Mussa-Ivaldi, F.A., and Giszter, S.F. (1992) Does the nervous system use equilibrium-point control to guide single and multiple joint movements? *The Behavioral and Brain Sciences*, 15(4), pp.603–613.

[Bizzi, et al., 1992b] Bizzi, E., Hogan, N., Mussa-Ivaldi, F.A., and Giszter, S.F. (1992) The equilibrium-point framework: A point of departure. *The Behavioral and Brain Sciences*, 15(4), pp.808–814.

[Brashers-Krug, 1995] Brashers-Krug, T. (1995) Consolidation in human motor memory. PhD thesis, Massachusetts Institute of Technology.

[Brashers-Krug, et al., 1995] Brashers-Krug, T., Shadmehr, R., Todorov, E. (1995) Catastrophic interference in human motor learning. *Advances in Neural Information Processing*, 7.

[Brashers-Krug, et al., 1996] Brashers-Krug, T., Shadmehr, R., Bizzi, E. (1996) Consolidation in human motor memory. *Nature*, 382, pp.252.

[Broadmann, 1909] Broadmann, K. (1909) Vergleichende Localizationslehre der Grosshirnrinde in ihren Prinzipien dargestellt auf Grund des Zeelenbaues, Barth, Lipzig.

[Brooks and Stein, 1994] Brooks, R. A., and Stein, L. A. (1994) Building Brains for Bodies. *Autonomous Robots*, 1, pp.7–25.

[Buekers, et al., 1994] Buekers, M.J., Magill, R.A., and Sneyers, K.M. (1994) Resolving a conflict between sensory feedback and knowledge of results, while learning a motor skill. *Journal of Motor Behavior*, Volume 26, No. 1, pp.27–35.

[Caminiti et al., 1990] Caminiti, R., Johnson, P.B. and Urbano, A., (1990) Making arm movements within Different parts of space: Dynamic aspects in the primate motor cortex. *Journal of Neuroscience*, Vol. 10, No. 7, pp.2039.

[Caminiti et al., 1991] Caminiti, R., Johnson, P.B. Galli, C., Ferraina, S., and Burnod, Y. (1991) Making arm movements within different parts of space: The premotor and motor cortical representation of a coordinate system for reaching to visual targets. *Journal of Neuroscience*, Vol. 11. Number 5, pp.1182 – 1197.

[Castro-Alamancos, et al., 1995] Castro-Alamancos, M.A., Donoghue, J.P. and Connors, B.W. (1995) Different forms of synaptic plasticity in somato-sensory and motor areas of the neocortex, *Journal of Neuroscience*, Volume 15, No. 7, pp.5324-5333.

[Camberlin and Magill, 1992] Chamberlin, C. J., and Magill, R. A., (1992) A Note on Schema and Exemplar Approaches to Motor Skill Representation in Memory, *Journal of Motor Behavior*, Vol. 24, No. 2, pp.221–224.

[Contreras-Vidal, et al., 1997] Contreras-Vidal, J.L., Grossberg, S., and Bullock, D. (1997) A neuronal model of cerebellar learning for arm movement control: Cortico-spino-cerebellar dynamics. *Learning and Memory*, 3, pp.475–502.

[Durbin, et al., 1989] Durbin, R., Miall, C., and Mitchison, G., (1989) The Computing Neuron, Addison-Wesley Publishing Company.

[Franklin, et al., 1991] Franklin, G. F., Powell, J. D., and Emami-Naeini, A., (1991) Feedback Control of Dynamic Systems, Addison Wesley Publishing Company.

[Flanagan and Rao, 1995] Flanagan, J. R., and Rao, A. K. (1995) Trajectory adaptation to a nonlinear visuomotor transformation: Evidence of motion planning in visually perceived space.

[Flash and Hogan, 1985] Flash, T., Hogan, N. (1985) The coordination of arm movements: An experimentally confirmed mathematical model. *Journal of Neuroscience*, 5:7, pp.1688–1703.

[Flash, 1987] Flash, T., (1987) The control of hand equilibrium trajectories in multijoint arm movements. *Biological Cybernetics*, Vol. 57, pp.257 – 274.

[Flash and Gurevich, 1991] Flash, T. and Gurevich, I., (1991) Human motor adaptation to external loads. *Annual International Conference of the IEEE Engineering in Medicine and Biology Society*, Vol. 13, pp.885 – 886.

[Fiorentini and Berardi, 1980] Fiorentini, A., Berardi, N. (1980) Perceptual learning specific for orientation and spatial frequency. *Nature*, 28.

[Gandolfo, 1996] Gandolfo, F. (1996) The role of motor primitives in the control of movement and learning. PhD thesis, Massachusetts Institute of Technology.

[Gandolfo, et al., 1996] Gandolfo, F., Mussa-Ivaldi, F.A. and Bizzi, E. (1996) Motor Learning by Field Approximation, *Proc. Natl. Acad. Sci.*, 93.

[Georgopoulos, et al., 1982] Georgopoulos, A.P., Kalaska, J.F., Caminiti, R., Massey, J.T. (1982) On the relation between the direction of two-dimensional arm movements and cell discharge in primate motor cortex. *Journal of Neuroscience* 2 pp.1527–1537.

[Georgopoulos, et al., 1983] Georgopoulos, A.P., Caminiti, R., Kalaska, J.F., Massey, J.T. (1983) Spatial coding of movement: a hypothesis concerning the coding of movement by motor cortical populations. *Experimental Brain Research* 7 pp.327–336.

[Georgopoulos et al., 1992] Georgopoulos, A.P., Ashe, J., Smyrnis, N., Taira M. (1992) The Motor Cortex and the Coding of Force, *Science* Vol. 256, 19 June.

[Georgopoulos et al., 1993] Georgopoulos, A.P., Taira, M., Lukashin, A. (1993) Cognitive Neurophysiology of the Motor Cortex, *Science*, Vol. 260, 2 April.

[Georgopoulos, 1994] Georgopoulos, A.P. (1994) New Concepts in Generation of Movement, *Neuron*, Vol. 13.

[Georgopoulos, 1995] Georgopoulos, A.P. (1995) Current issues in directional motor control, *TINS*, Vol. 18, No. 11.

[Ghahramani, et al., 1996] Ghahramani Z., Wolpert, D. M., and Jordan M. I. (1996) Generalization to local remapping of the visuo-motor coordinate transformation. *Journal of Neuroscience*

[Ghez, 1991] Ghez, C. (1991) *Principles of neural science. Voluntary Movement*, chapter 40, pp 609–625. Elsevier, third edition.

[Goldman-Rakic, et al., 1992] Goldman-Rakic, P.S., Bates, J.F., and Chafee, M.V. (1992) The prefrontal cortex and internally generated motor acts *Current Opinion in Neurobiology* Vol.2, pp.830–835.

[Gomi and Kawato, 1996] Gomi, H., Kawato, M. (1996) Equilibrium-point control hypothesis examined by measured arm stiffness during multijoint movement. *Science*, Vol. 272, 5 April.

[Gorinevsky, 1993] Gorinevsky, D. M., (1993) Modelling of direct motor program learning in fast human arm motions. *Biological Cybernetics*, Vol. 69, pp.219 – 228.

[Graybiel, 1995] Graybiel, A.M. (1995) Building action repertoires: memory and learning functions of the basal ganglia. *Current Opinion in Neurobiology* Vol.5, pp.733–741.

[Held, 1962] Held, R., (1962) Adaptation to rearrangement and visual-spatial aftereffects. *Psychologische Beitraege* Vol. 6, pp. 439–450.

[Hocherman and Wise, 1991] Hocherman, S., Wise, S.P. (1991) Effects of hand movement path on motor cortical activity in awake, behaving rhesus monkeys, *Experimental Brain Research*, Vol. 83, pp.285–302.

[Hoff and Arbib, 1993] Hoff, B. and Arbib, M.A. (1993) Models of trajectory formation and temporal interaction of reach and grasp. *Journal of Motor Behavior*, Volume 25, No. 3, pp.175–192.

[Hogan, 1984] Hogan, N., (1984) An organizing principle for a class of voluntary movements. *Journal of Neuroscience*, Vol. 4, No. 11, pp.2745 – 2754.

[Hogan, 1987] Hogan, N., (1987) The mechanics of multi-joint posture and movement control. *Biological Cybernetics*, Vol. 52, pp.315 – 331.

[Horak, 1992] Horak, M. (1992) The utility of Connectionism for motor learning: A reinterpretation of contextual interference in movement schemas. *Journal of Motor Behavior* 24:1 pp.58.

[Jackson, 1932] Jackson, J. H. (1932) Selected Writings of John Hughlings Jackson. J. Taylor ed, London.

[Jerkins, et al., 1994] Jenkins, I.H., Brooks, D.J., Nixon, P.D., Frackowiak, R.S.J. and Passingham R.E. (1994) Motor sequence learning: A study with positron emission topology. *The Journal of Neuroscience*, Volume 14, Number 6, pp.3775–3790.

[Jordan and Rumelhart, 1991] Jordan, M. I. and Rumelhart, D. E. (1991) Internal world models and supervised learning. *Machine Learning: Proceedings of the Eighth International Workshop*, San Mateo, CA.

[Jordan and Rumelhart, 1992] Jordan, M. I. and Rumelhart, D. E. (1992) Forward models: Supervised learning with distal teacher. *Cognitive Science*, Vol. 16, pp.307–354.

[Jordan, et al., 1994] Jordan M. I. Wolpert, D. M.; Ghahramani, Z. (1994) Perceptual distortion contributes to the curvature of human reaching movements. *Experimental brain research.*, 98:1, pp.153.

[Karni and Sagi, 1993] Karni, A. and Sagi, D. (1993) The time course of learning a visual skill. *Science*, Vol.365, No. 6443, pp.250.

[Katayama and Kawato, 1993] Katayama, M., Kawato, M., (1993) Virtual trajectory and stiffness ellipse during multijoint arm movement predicted by neural inverse models. *Biological Cybernetics*, Vol. 69, pp.353 – 362.

[Kawato and Gomi, 1992] Kawato, M. and Gomi, H. (1992) The cerebellum and VOR/OKR learning models. *TINS*, 15:11, pp.445.

[Lackner and Dizio, 1994] Lackner, J. R., Dizio, P. (1994) Rapid adaptation to Coriolis force perturbations of arm trajectory. *Journal of Neurophysiology* Vol. 72.

[Lloyd, 1946] Lloyd, D. P. C. (1946) Integrative pattern of excitation and inhibition in two-neuron reflex arcs, *Journal of Neurophysiology*, Vol.9, pp.439–444.

[Lukashin and Georgopoulos, 1994] Lukashin A.V., Georgopoulos, A.P., (1994) A Neural Network for Coding of Trajectories by Time Series of Neuronal Population Vectors, *Neural Computation*, Vol. 6.

[Lukashin, et al., 1996] Lukashin A.V., Amirikian, B. R., Georgopoulos, A.P., (1996) Neural computations underlying the exertion of force: A model *Biological Cybernetics*, Vol. 74, Number 5, pp.469.

[Mazzoni, et al., 1991] Mazzoni, P., Andersen, R.A., Jordan, M.I. (1991) A more biologically plausible learning rule for neural networks *Proc. Natl. Acad. Sci.*, 88, pp.4433–4437.

[McIntyre, et al., 1996] McIntyre, J., Mussa-Ivaldi, F. A., and Bizzi, E. (1996) The control of stable postures in the multijoint arm. *Experimental Brain Research* Vol.110, Number 2, pp.248.

[Morasso, 1981] Morasso, P. (1981) Spatial control or arm movement, *Experimental Brain Research*, 42, pp.223–227.

[Mussa-Ivaldi, et al., 1985] Mussa-Ivaldi, F.A., Hogan, N., and Bizzi, E. (1985) Neural, mechanical and geometrical factors sub-serving arm posture in humans. *Journal of Neuroscience*, 5, pp.2732–2743.

[Mussa-Ivaldi, 1988] Mussa-Ivaldi, F.A. (1988) Do neurons in the motor cortex encode movement direction? An alternative hypothesis, *Neuroscience Letters*, Vol. 91.

[Mussa-Ivaldi and Hogan, 1991] Mussa-Ivaldi, F.A. and Hogan, N. (1991) Integrable solutions of kinematic redundancy via impedance control. *The International Journal of Robotics Research*, 10, pp.481–491.

[Mussa-Ivaldi, 1992] Mussa-Ivaldi, F. A. (1992) From basis functions to basis fields: Vector field approximation from sparse data. *Biological Cybernetics* Vol. 67, pp.479.

[Mussa-Ivaldi and Giszter, 1992] Mussa-Ivaldi, F.A. and Giszter, S.F. (1992) Vector field approximation: A computational paradigm for motor control and learning. *Biological Cybernetics* Vol. 67, pp.491 – 500.

[Narendra and Mukhopadhyay, 1991] Narendra, K. S., and Mukhopadhyay, S., (1991) Intelligent Control Using Neural Networks, *American Control Conference*, Boston, MA.

[Narendra and Balakrishnon, 1997] Narendra, K. S., and Balakrishnon, J (1997) Adaptive control using multiple models *IEEE transactions on automatic control*, Vol.42, No.2, pp. 171.

[Paulignan, et al., 1991a] Paulignan, Y., MacKenzie, C. Marteniuk, R. and Jeannerod, M. (1991) Selective perturbation of visual input during prehension movements, 1. The effects of changing object position. *Experimental Brain Research*, Vol. 83, pp.502–512.

[Paulignan, et al., 1991b] Paulignan, Y., Jeannerod, M., MacKenzie, C. and Marteniuk, R. (1991) Selective perturbation of visual input during prehension movements, 2. The effects of changing object size. *Experimental Brain Research*, Vol. 87, pp.407–420.

[Penfield and Rasmussen, 1950] Penfield, W. and Rasmussen T. (1950) The cerebral cortex of man: A clinical study of localization of function. Macmillan.

[Peters, 1994] Peters, M. (1994) When can attention not be divided? *Journal of Motor Behavior*, Volume 26, No.2, pp.196–199.

[Poggio, 1990] Poggio, T. and Girosi, F. (1990) A theory of networks for learning. *Science*, Vol. 247, pp.978–982.

[Poggio, et al., 1992] Poggio, T., Fahle, M., Edelman, S. (1992) Fast perceptual learning in visual hyperacuity. *Science*, Vol. 256, pp.1018–1020.

[Roby-Brami and Burnod, 1995] Roby-Brami, A. and Burnod, Y. (1995) Learning a new visuo-motor transformation: Error correction and generalization. *Cognitive Brain Research*, Vol. 2, pp.229–242.

[Rosenblatt, 1958] Rosenblatt, F., (1958) The Perceptron: A probabilistic model for information storage and organization in the brain, *Psychological Review* 65, pp.386–408.

[Russel and Norvig, 1995] Russel, S. J. and Norvig, P. (1995) Artificial Intelligence, A modern approach.

[Sainburg, et al., 1995] Sainburg, R. L, Ghilardi, M. F., Poizner, H. and Ghez, C. (1995) Control of limb dynamics in normal subjects and patients without proprioception.

[Sanger, 1993a] Sanger, T.D. (1993) Theoretical considerations for the analysis of population coding in motor cortex. *Neural Computation* 6 pp.29–37.

[Sanger, 1993b] Sanger, T.D. (1993) A practice strategy for robot learning control. *Advances in neural information processing systems* Vol. 5 pp.335–341.

[Sanger, 1996] Sanger, T.D. (1996) Probability Density Estimation for the Interpretation of Neural Population Codes, *Journal of Neurophysiology* Vol. 76, No. 4.

[Schmidt, 1975] Schmidt, R.A. (1975) A schema theory of discrete motor skill learning. *Psychological Review*, 82, pp.225–260.

[Scott and Kalaska 1995] Scott, S.H. and Kalaska, J.F. (1995) Changes in motor cortex activity during reaching movements with similar hand paths but different arm postures. *Journal of Neurophysiology*, Vol. 73, pp.2563.

[Shadmehr and Arbib, 1992] Shadmehr, R., and Arbib, M. A. (1992) A mathematical analysis of the force-stiffness characteristics of muscles in control of a single joint system. *Biological Cybernetics* Vol. 66, pp.463 – 477.

[Shadmehr, et al., 1993] Shadmehr, R., Mussa-Ivaldi, F. A. and Bizzi, E. (1993) Postural force fields of the human arm and their role in generating multijoint movements. *Journal of Neuroscience*, Vol. 13, pp.45.

[Shadmehr and Mussa-Ivaldi, 1993] Shadmehr, R. and Mussa-Ivaldi, F.A. (1993) Geometric structure of the adaptive controller of the human arm. *A.I. Memo No. 1437, C.B.C.L. Memo No. 82*.

[Shadmehr, 1993] Shadmehr, R. (1993) Control of Equilibrium Position and Stiffness Through Postural Modules. *Journal of Motor Behavior*, Vol. 25, No. 3, pp.228–241.

[Shadmehr and Mussa-Ivaldi, 1994a] Shadmehr R. and Mussa-Ivaldi, F.A. (1994) Computational elements of the adaptive controller of the human arm. *Advances in neural information processing systems.*, 6, pp.1077

[Shadmehr and Mussa-Ivaldi, 1994b] Shadmehr R. and Mussa-Ivaldi, F.A. (1994) Adaptive Representation of Dynamics During Learning of a Motor Task. *Journal of Neuroscience*, 14:5.

[Shadmehr, et al., 1995] Shadmehr, R., Brashers-Krug, T., Mussa-Ivaldi, F. (1995) Interference in learning internal models of inverse dynamics in humans. *Advances in neural information processing systems* Vol. 7, pp.1117.

[Squire, 1991] Squire, L. R. (1991) Memory and the hippocampus.

[Todorov, et al., 1997] Todorov, E., Shadmehr, R., Bizzi, E. (1997) Augmented feedback presented in a virtual environment accelerates learning of a difficult motor task. *Journal of Motor Behavior* 29:2 pp.147–158.

[Uno, et al., 1989] Uno, Y., Kawato, M., Suzuki, R. (1989) Formation and control of optimal trajectory in human multijoint arm movement *Biological Cybernetics* Vol. 61, pp.89 – 101.

[von Hofsten, 1991] von Hofsten, C., (1991) Structuring of Early Reaching Movements: A Longitudinal Study, *Journal of Motor Behavior*, Vol. 23, No. 4, pp.280–292.

[Wolpert, et al., 1995] Wolpert D M; Ghahramani Z; Jordan M I. (1995) Are arm trajectories planned in kinematic or dynamic coordinates? an adaptation study. *Experimental brain research.*, 103:3, pp.460.

[Wolpert and Kawato, 1998] Wolpert D. M., and Kawato, M. (1998) Multiple paired forward and inverse models for motor control *Neural Networks*, submitted.

[Woodworth, 1899] Woodworth, R. S. (1899) The accuracy of voluntary movement. *Psychological Review*, Vol. 3 pp.1–114.

[Yessis, 1995] Yessis, M. (1995) Muscle Synergy *Joe Weider's Muscle and Fitness*, Vol.56, No.1, pp.116.

[Young and Schmidt, 1992] Young, D.E. and Schmidt, R.A. (1992) Augmented kinematic feedback for motor leaning, *Journal of Motor Behavior* Volume 24, No. 3, pp.261–273.